Mutual Coupling Suppression in Multiple Microstrip Antennas for Wireless Applications

By :

ALAA H. RADHI THUWAINI

A Thesis Submitted in Fulfilment of the Requirements for the Award of the Degree of **Doctor of Philosophy (Ph.D.)** in Communications

Department of Electronic and Computer Engineering,

Collage of Engineering, Design and Physical Sciences

Brunel University London

London, United Kingdom

September 2018

Abstract

Mutual Coupling (MC) is the exchange of energy between multiple antennas when placed on the same PCB, it being one of the critical parameters and a significant issue to be considered when designing MIMO antennas. It appears significantly where multiple antennas are placed very close to each other, with a high coupling affecting the performance of the array, in terms radiation patterns, the reflection coefficient, and influencing the input impedance. Moreover; it degrades the designed efficiency and gain since part of the power that could have been radiated becomes absorbed by other adjacent antennas' elements. The coupling mechanism between multiple antenna elements is identified as being mainly through three different paths or channels: surface wave propagation, space (direct) radiation and reactive near-field coupling.

In this thesis, various coupling reduction approaches that are commonly employed in the literature are categorised based on these mechanisms. Furthermore, a new comparative study involving four different array types (PIFA, patch, monopole, and slot), is explained in detail. This thesis primarily focuses on three interconnected research topics for mutual coupling reduction based on new isolation approaches for different wireless applications (i.e. Narrow-band, Ultra-wide-band and Multi-band).

First, a new Fractal based Electromagnetic Band Gap (FEBG) decoupling structure between PIFAs is proposed and investigated for a narrowband application. Excellent isolation of more than 27 dB (Z-X plane) and 40 dB (Z-Y plane) is obtained without much degradation of the radiation characteristics. It is found that the fractal structures can provide a band-stop effect, because of their self-similarity features for a particular frequency band.

Second, new UWB-MIMO antennas are presented with high isolation characteristics. Wideband isolation ($\geq$ 31 dB) is achieved through the entire UWB band (3.1-10.6 GHz) by etching a novel compact planar decoupling structure inserted between these multiple UWB antennas.

Finally, new planar MIMO antennas are presented for multi-band (quad bands) applications.

A significant isolation improvement over the reference ($\geq$ 17 dB) is achieved in each band by etching a hybrid solution.

All the designs reported in this thesis have been fabricated and measured, with the simulated and measured results agreeing well in most cases.

Table of Contents

Chapter 3: Survey of coupling suppression techniques for different wireless applications

Chapter 4: Development of Multiple Antennas with High Isolation for Narrowband Applications

---

List of Figures

List of Tables

List of Abbreviations

Abbreviation:	Definition
1D:	One Dimensional
2D:	Two Dimensional
3D:	Three Dimensional
3G:	Third Generation
3GPP:	Third Generation Partnership Project
4G:	Fourth Generation
5G:	Five Generation
AUT:	Antenna Under Test
BW:	Bandwidth
CLL:	Close Loop Lines
CPW:	Coplanar Wave Guide
CLS:	Current Localisation Structure
CST:	Computer Simulation Technology
DCS:	Digital Cellular System
DF:	Degradation factor
DG:	Diversity Gain
DGS:	Defect Ground Structure
DMN:	Decoupling Matching Networks
DR:	Dielectric Resonator
DWS:	Decoupling Wall Structure
E field:	Electric field
EBG:	Electromagnetic Band Gab
ECC:	Envelope Correlation Coefficient
EDG:	Effective Diversity Gain
EM:	Electromagnetic
FCC:	Federal Communications Commission
FDTD:	Finite Different Time Domain
FEM:	Finite Element Method
FEBG:	Fractal Electromagnetic Band Gab
FIT:	Finite Integral Technique
GPS:	Global Position System
GSM:	Global System for Mobile Communications
H field:	Magnetic field
HFSS:	High Frequency Structure Simulator
IEEE:	Institute of Electrical and Electronics Engineers
IFA:	Inverted-F Antenna
ILA:	Inverted-L Antenna
LAN:	Local Area Network
LHCP:	Left Hand Circular Polarization
LTE:	Long Term Evolution
MA:	Monopole Antenna
MC:	Mutual Coupling
MEG:	Mean Effective Gain
MEMS:	Micro Electro Mechanical Systems
MIMO:	Multi Input Multi Output
MOM:	Moment of Method
MTMs:	Meta-Material structures

N/A:	Not Applicable
N/P:	Not Presented
NL:	Neutralisation Line
NMHA:	Normal Mode Helix Antenna
PBC:	Periodic Boundary Conditions
PCB:	Printed Circuit Board
PCS:	Personal Communication Service
PDA:	Personal Digital Assistant
PDC:	Personal Digital Cellular
PD:	Polarisation Diversity
PEC:	Perfect Electric Conductor
PMA:	Planar Monopole Antenna
PMC:	Perfect Magnetic Conductor
PML:	Perfect Matched Layer
PSD:	Power Spectrum Density
RF:	Radio Frequency
RHCP:	Right Hand Circular Polarization
PIFA:	Planar Inverted F Antenna
RLC:	Resistance, Inductance and Capacitance
SAR:	Specific Absorption Rate
SISO:	Single Input Single Output
SMA:	Sub-Miniature version A
SRR:	Split Ring Resonator
SNR:	Signal to Noise Ratio
TE:	Transverse Electric Propagation Mode
TEM:	Transverse Electromagnetic Propagation Mode
TL:	Transmission Line
TM:	Transverse Magnetic Propagation Mode
UMTS:	Universal Mobile Telecommunications System
UWB:	Ultra-Wideband
VNA:	Vector Network Analyser
VSWR:	Voltage Standing Wave Ratio
WAN:	Wide Area Network
WCDMA:	Wide band Code Division Multiple Access
Wi-Fi:	Wireless Fidelity
WiBro:	Wireless Broadband
WiMAX:	Worldwide Interoperability for Microwave Access
WLAN:	Wireless Local Area Network
WMAN:	Wireless Metropolitan Area Networks
W/O:	Without
XPR:	Cross-Polarisation Power Ratio
XPD:	Cross-Polarisation discrimination

List of Symbols

Notation:	Definition
λ_0	Wavelength in free space (mm)
λ_g	Guided Wavelength inside substrate (mm)
Γ	Reflection coefficient
σ	Conductivity (S/m)
η_{rad}	Radiation efficiency
β	Bloch propagation constant
c	Speed of light in free space = 2.99792458×10^8 (m/s)
C	Capacitance (F)
dB	Decibel
ε_r	Dielectric constant (Dimensionless)
ε_{eff}	Effective dielectric constant (Dimensionless)
ε_0	Permittivity of free space = 8.854×10^{-12} (F/m)
E	Electric Field Strength (V/m)
D	Electric Flux density (C/m²)
D	Directivity
f_r	Resonance frequency (Hz)
f	Operating frequency (Hz)
f_c	Cut off frequency (Hz)
G	Gain
GHz	Gigahertz, 10^9 hertz
h	Thickness of the substrate (mm)
H	Magnetic Field Strength (A/m)
k	Wave vector
KHz	Kilohertz, 10^3 hertz
N	Iteration order
N_r	Number of receiving antennas
N_t	Number of transmitting antennas
MHz	Megahertz, 10^6 hertz
Q	Quality factor
R	Resistance (Ω)
S_{ij}	Scattering matrix elements
L	Inductance (H)
P_c	Complex cross-correlation coefficient
ρ_e	Envelope correlation coefficient
tan δ	Dielectric loss tangent
μ	Absolute permeability = $\mu_0.\mu_r$ (H/m)
μ_0	Permeability of free space = $4\pi \times 10^{-7}$ (H/m)
ω_0	Angular frequency = $2\pi f$ (rad/sec)
Z_c	Characteristic impedance (Ω)
Z_{in}	Input Impedance (Ω)

Author’s Declarations

I declare that all the material contained in this thesis is my work.

I declare that no material contained in the thesis has been used in any other submission for an academic award.

I declare that while registered as a candidate for the University's research degree, I have not been a registered candidate or an enrolled student for another award of the University or other academic or professional institution.

I confirm that I have undertaken the programme of related studies in connection with the programme of research following the requirements of my research degree registration.

Alaa Thuwaini
14/09/2018

Acknowledgements

First of all, All praise to GOD (**ALLAH**), the creator of our universe, profound thanks to my Lord, the most merciful for giving me the strength and wisdom to complete this research work, without his blessing and mercy this thesis would not have final shape.

I would like to express my appreciation and gratefulness to my sponsor ‘’ Higher Committee for Education Development (**HCED**) in Iraq ‘’ for awarding me a full scholarship covering all financial commitments for four years period to study Ph.D. degree in UK \ London.

I would also like to offer my sincere gratitude to my academic supervisor **Dr. Rajagopal Nilavalan** for providing me with the best supervision, guidance, and enthusiastic support that a Ph.D. student can wish for. His door was always open. He had been very supportive every time I faced a problem; this work would not have been possible without his help and unlimited support.

My special thanks goes to my second supervisor **Professor Hamed Al-Raweshidy** for his encouragement and useful advice. I am deeply grateful to **Dr. Yi Wang** and his student **Amira Ali** from Greenwich university, for the joint collaboration and providing the laboratory facilities.

I want to appreciate my dear wife (**Noora**) and my beloved kids (**Taif & Nawras**) for their moral support, love, inspiration and encouragement, thanks wife for patiently listening to all of my complaints throughout my Ph.D. and during the writing of this thesis. Without her love and sacrifices, this thesis would not be possible.

A special word of thanks goes my family (**Father & Mother**) for their utmost interest in my education. They are a source of inspiration for me in all my life. Thanks to my beloved brothers and relatives, for their constant love, support throughout the long years of my Ph.D. journey. I love you all.

Also, I value the role of my employer ‘’Ministry of Communications in Iraq (**MOC**)’’ for allowing me to complete my study further abroad.

Finally, I would also like to thank my colleagues, friends and lecturers in the faculty of Engineering\Electronic and Computer (ECE) Dept. for their encouragement throughout my Ph.D. study.

Alaa Thuwaini

Brunel University London, 2018

Chapter 1: Introduction and Fundamentals

1.1 Introduction

Microstrip antennas are typically metallic structures (transceivers) designed for radiating and receiving electromagnetic waves. They are essential components of any modern wireless communication system for converting radio frequency fields into induced currents or vice versa. That is, an antenna acts as a transitional structure between a guiding device (e.g. waveguide, transmission line) and free space [1]. Figure 1.1 shows a schematic antenna as a conversion device, where the arrows shown correspond to the lines of the electric field when the wave is transformed into free space.

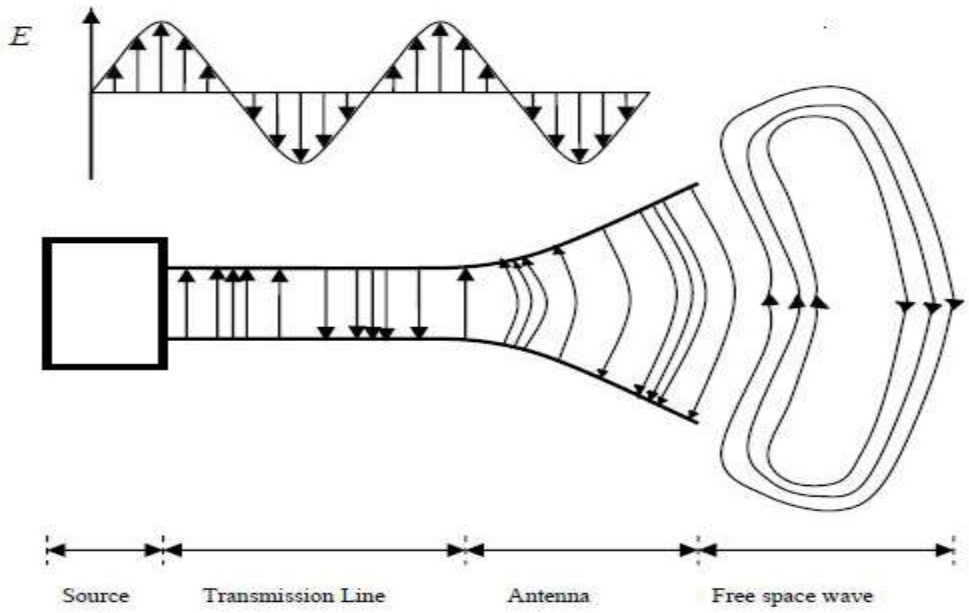

Figure 1.1: A schematic diagram of an antenna as a transition device [1]

In any wireless system, the performance of radio communications depends on the design of an efficient antenna [2]. Microstrip antennas are widely used for various applications, such as mobile and satellite communications, GPS reception, and radar applications. In mobile communication antenna design, the antenna has become an integral part of the mobile device, playing an important role in small mobile terminals. To achieve this goal, the antenna for mobile sets must be small, flexible, and highly efficient [3]. The antennas used for small mobile terminals have evolved from PIFAs, monopoles, and also other types of antennas have been used, such as Normal Mode Helix Antenna (NMHA), meander lines and Dielectric Resonators (DR) [4-5]. Moreover, there are different types of microstrip antennas for various

wireless applications. Some of the typical and commonly used antennas inside cellular handsets are briefly described in this section.

1.1.1 Patch Antennas

A patch Antenna consists of a metal patch on a substrate and a ground plane, as shown in Figure 1.2.

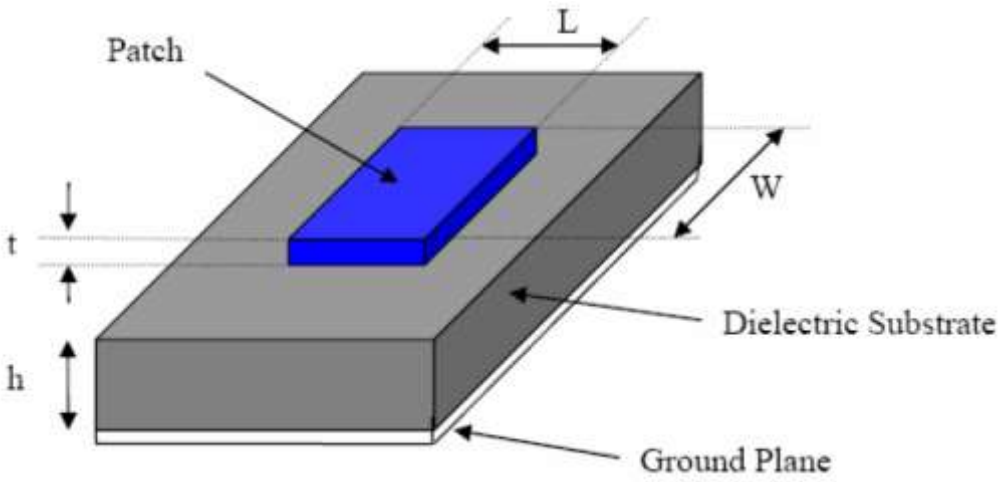

(a)

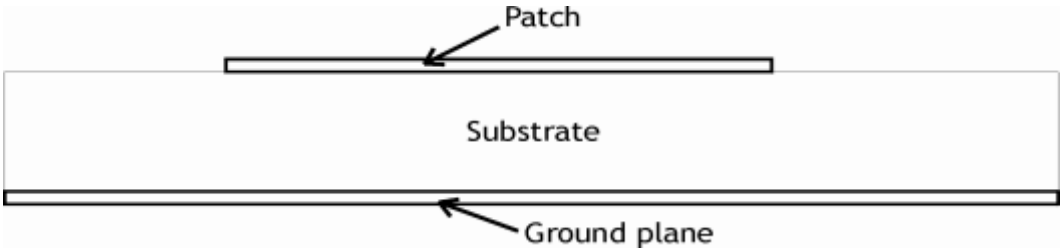

(b)

Figure 1.2: A schematic micro-strip patch (rectangular) antenna. **(a)** 3D view **(b)** side view

The length and width of a Microstrip Patch Antenna can be calculated using the following formulas:

$$L = \frac{\lambda_g}{2} = \frac{\lambda_0}{2\sqrt{\varepsilon_{eff}}} = \frac{c}{2\,fr\sqrt{\varepsilon_{eff}}} \qquad (1.1)$$

$$W = \frac{\lambda_0}{2\sqrt{\frac{\epsilon_{r+1}}{2}}} = \frac{c}{2\,fr\sqrt{\frac{\epsilon_{r+1}}{2}}} \qquad (1.2)$$

$$\lambda_g = \frac{\lambda_0}{\sqrt{\varepsilon_{eff}}}$$

Where, (λ_o) is the free space wavelength at operation frequency (*f*).

W = width of the patch antenna
L = length of the patch antenna
ε_r = dielectric constant

For W/h $\geq$ 1:

$$\varepsilon_{eff} = \frac{\varepsilon_r + 1}{2} + \frac{\varepsilon_r - 1}{2}\left(1 + 12\frac{h}{W}\right)^{-0.5} \qquad (1.3)$$

$$Z_c = \frac{\eta}{\sqrt{\varepsilon_{re}}}\left\{\frac{W}{h} + 1.393 + 0.677\ln\left(\frac{W}{h} + 1.444\right)\right\}^{-1} \qquad (1.4)$$

Where, Z_c = characteristics impedance of the patch antenna, $\eta = 120\pi$ Ω is the wave impedance in free space. The actual range of parameters for a patch is usually such that $0.25 \leq W/h \leq 2.75$;
$2.5 \leq \varepsilon_r \leq 25$

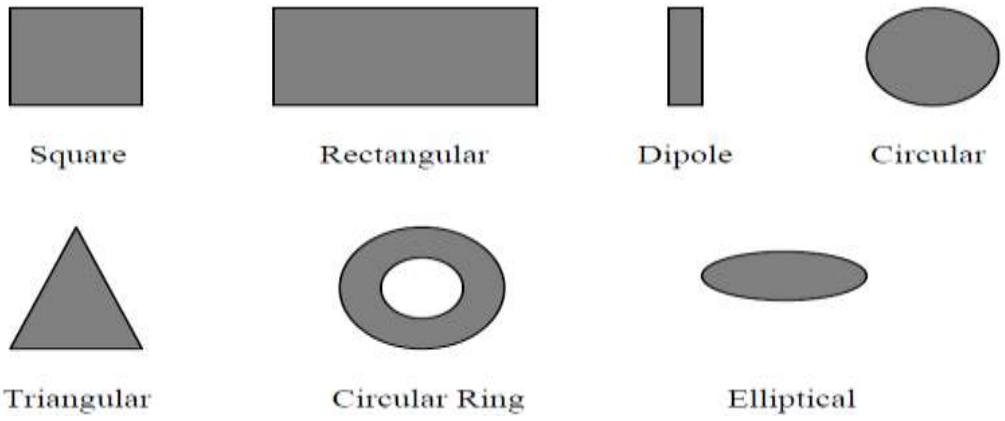

Figure 1.3: Common shapes of microstrip patch elements

To meet different design requirements and simplify performance analysis, the commercial microstrip patch can take the form of a range of shapes [1] (square, rectangular, circular, elliptical or triangular), as shown in Figure 1.3. The Microstrip Patch Antenna has a wide range of applications (both commercial and military) due to the reduction in size, price and power consumption that it can deliver. The advantages of patch antennas are [1]:

1- Low profile, if a thin substrate is used;

2- Reduced overall size of the portable terminals;

3- Linear and circular polarisation is possible, with a simple feed configuration;

4- Dual-frequency and dual-polarisation antennas can be easily instigated;

5- Low manufacturing cost;

6- Simple to produce and readily adaptable for mass production;

7- Feed lines and matching networks can be manufactured simultaneously with the antenna structure;

8- Can be easily integrated with other integrated microwave circuits;

9- Cavity support is not required.

Some of the disadvantages of patch antennas are:

1- Reduced efficiency and gain;

2- Narrow bandwidth and associated tolerance problems;

3- Surface wave excitation;

4- Low power handling and higher ohmic losses in the structure of an array feed;

5- Extraneous radiation from feeds and junctions;

6- Unacceptably high levels of coupling (in particular at high frequencies) within arrays;

7- Polarisation purity is difficult to achieve.

The patch antenna can be fed by a variety of methods, such as coaxial power and the microstrip line, as shown in Figure 1.4 [6].

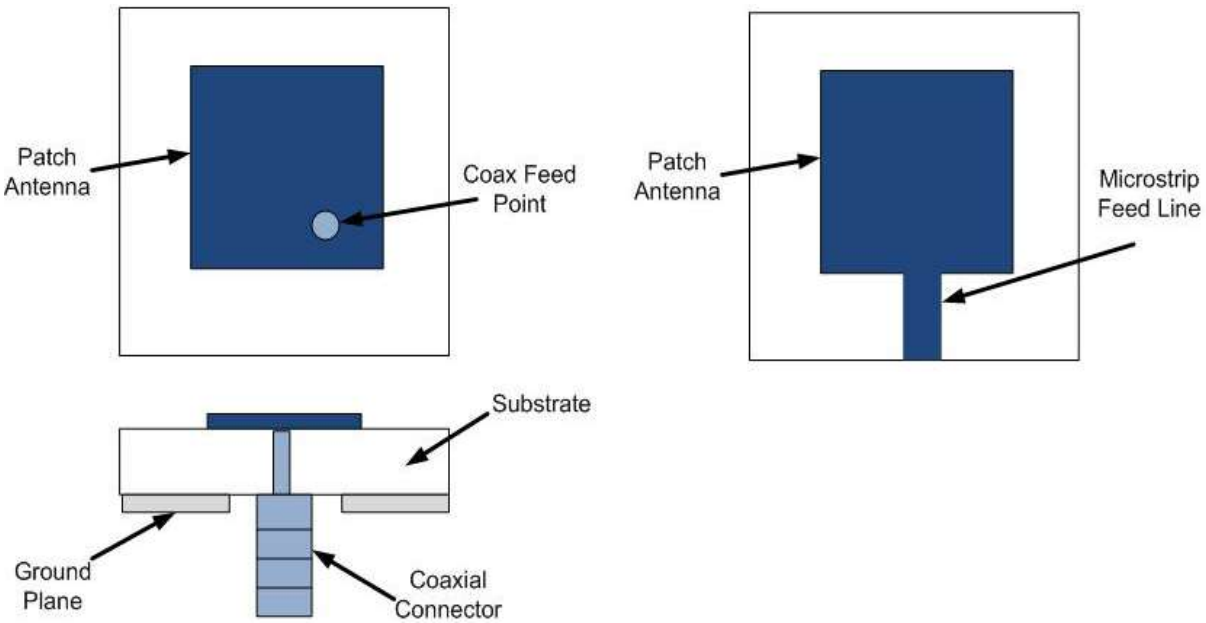

Figure 1.4: Different feed methods the can be used in patch antennas

1.1.2 Monopolies Antennas

Quarter-wave monopole antennas are the fundamental handset antennas, having the simplest structures [7], as shown in Figure 1.5.

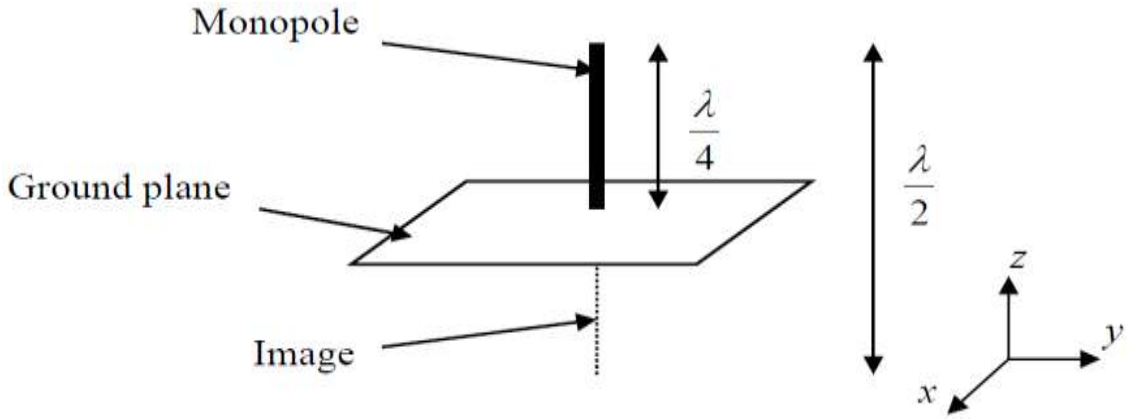

Figure 1.5: A quarter wavelength monopole antenna

This antenna distributes much larger currents in the terminal case than a half-wavelength monopolar antenna [2], for which the amplitude of the maximum current occurs around the centre of the monopole. As a result, the current magnitude around the feed point between the monopole and the terminal housing is very small and thus, little current flows into the terminal housing. Conversely, for a monopole of a quarter wavelength, the maximum amplitude of the current occurs around the feed point and large currents flow into the interior of the terminal housing.

Due to the leakage currents, the length of the terminal housing significantly modifies the radiation characteristics of an antenna. Monopoles are very useful in mobile applications where the conducting plane is the car's body or in the handset cases. The typical gain for quarter wavelength monopoles is between 2 and 6 dB, with bandwidth of about 10% [9]. Moreover, monopolar antennas with 3/8 or 5/8 wavelengths have been used in practice for mobile terminals. The radiation pattern for a monopole is shown below in Figure 1.6.

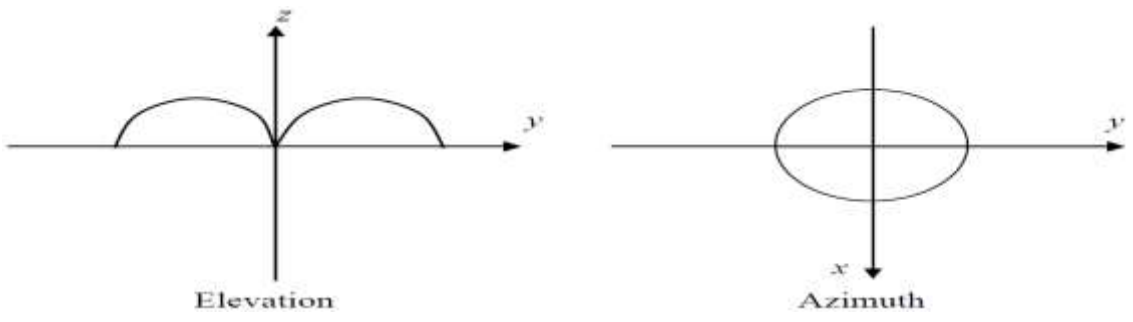

Figure 1.6: Radiation pattern for the monopole antenna

The advantages of monopolar antennas when used in handset phones are:

1) Low SAR;

2) High efficiency.

1.1.3 Planar Inverted-F Antennas (PIFAs)

Planar Inverted-F Antennas (PIFAs) are popular antennas for mobile phones due to their having many attractive features, such as low profile, lightweight, omnidirectional pattern, high radiation efficiency, easy integration and manufacturability [11]. PIFAs can be described as a modification of the IFA. This is achieved by replacing the radiating linear horizontal strip of an IFA with a planar plate that is often positioned parallel to the ground plane, as shown in Figure 1.7.

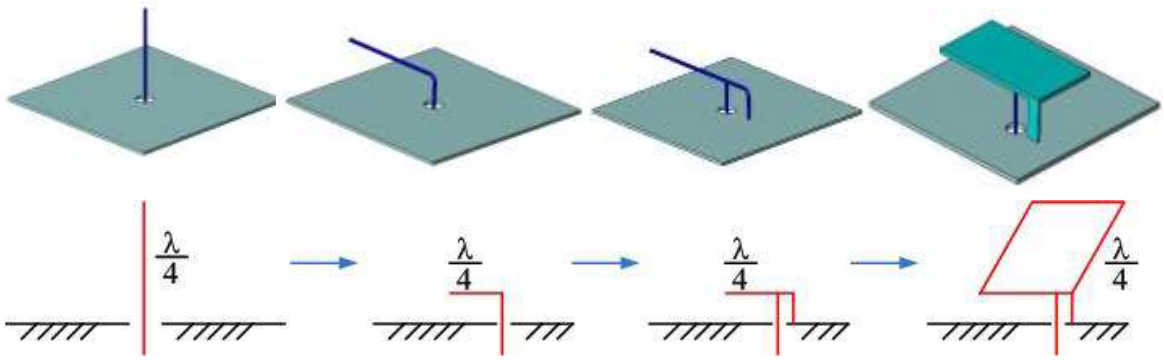

Figure 1.7: Evolution of a PIFA from a monopole antenna

A PIFA typically consists of a rectangular planar element located above a ground plane, a short circuiting plate or pin, and a feeding mechanism for the planar element [10].

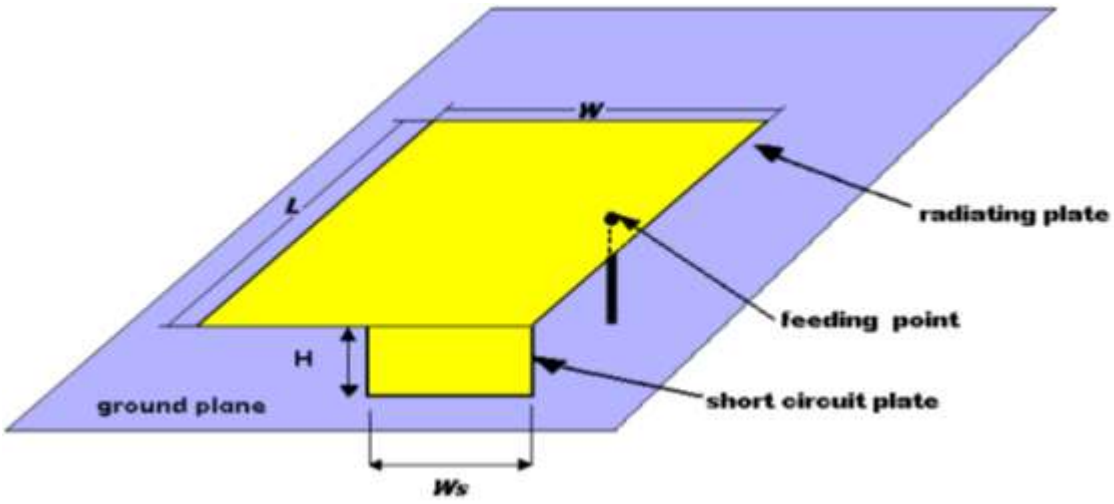

Figure 1.8: Basic layout of the Planar Inverted-F Antenna (PIFA)

Figure 1.8 shows the basic design of a PIFA, where *L* and *W* are the length and width of the planar radiant element (plate), respectively, whilst *Ws* is the width of the short-circuit plate [12]. The width of the PIFA short-circuit plate plays a vital role in the governing of its resonance frequency, whereby the narrower this width, the lower resonance frequency of the PIFA. Unlike microstrip antennas that are conventionally made at half wavelength, PIFAs are

constructed with a wavelength of just one-quarter resonance [13]. Normally, the resonance frequency f_r of a PIFA can be calculated by using equation 1.6:

$$\frac{\lambda_0}{4\sqrt{\varepsilon_{eff}}} = (L + H + W - W_s) \qquad (1.5)$$

$$fr = \frac{c}{4(L + H + W - W_s)\sqrt{\varepsilon_{eff}}} \qquad (1.6)$$

Where, L, W and H are the length, width and height of the PIFA radiator, respectively.

W_s is the width of the short-circuit strip.

In the case of $W = Ws$,

$$fr = \frac{c}{4(L + H)\sqrt{\varepsilon_{eff}}} \qquad (1.7)$$

In the case of $W_s \approx 0$, this means replacing the shorting plate with a shorting pin as a step to reduce the size of the antenna and the estimated resonant frequency can be determined by:

$$fr = \frac{c}{4(L + W + H)\sqrt{\varepsilon_{eff}}} \qquad (1.8)$$

Meanwhile, the shape and size the of the radiators, the height of the plate above the ground plane, the shape, size and position of the shorting pin or shorting plate, and the feed point location along the dielectric substrate, all of these parameters have a considerable impact on the frequency bands, impedance matching, bandwidth, gain and efficiency of the antennas. The table below summarises the effect of the different PIFA parameters, such as the height, width, length, location of feeding and the shorting pin on its characteristics [14].

Table 1.1: Effect of different PIFA parameters

Parameters	Effect
Height	controls BW
Width	controls impedance matching
Length	determine resonance frequency
Width of short strip	effect on the resonance and increases BW
Feed position from short strip	effect on the resonance frequency and BW

There are some advantages behind the use of PIFAs, as follows:

The first is compactness, whereby it can be hidden inside the handset phone case, which is not so for the other antenna types, such as rod/whip/helix; Second, they have considerable gains in the vertical and horizontal polarisation states. This feature is particularly advantageous in wireless communications, where the orientation of the antenna is not fixed and reflections are presented from the different corners of the environment [15]; Third, the backward radiation in the user's head is reduced, which minimises the SAR (Specific Absorption Rate) and improves the performance of the antenna. However, the narrow-band feature of PIFAs remains one of the significant limitations of its commercial application for wireless communication systems.

1.1.4 Slot Antennas

Slot antennas are popular because they can be cut out of whatever surface they are to be mounted on, and have radiation patterns that are roughly omni-directional.

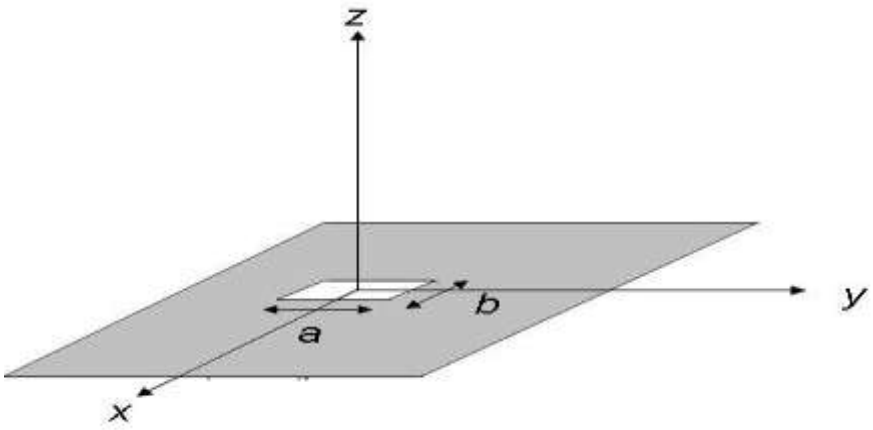

Figure 1.9: Schematic rectangular slot antenna with dimensions *a* and *b*

Moreover, the polarisation of the slot antennas is linear, whilst the slot size and shape offer design variables that can be used to tune performance. Printed slot antennas can be created by inserting a slot in the ground plane of a grounded substrate. The shape of the slot can take different forms or any shapes, as previously shown in Figure 1.3. Some basic slot shapes that have been well studied are the rectangular, annular, squire and tapered slots [16]. As with microstrip patch antennas, slot antennas are fed by microstrip lines or coplanar waveguides. In fact, slot antennas radiate on both sides of the slots, which has led to their being classified as bidirectional radiators. A brief table depicting a comparison regarding the different antenna types described above is provided below.

Table 1.2: A brief comparison of different microstrip antennas types

Characteristics	Patch	Monopole	PIFA	Slot
Radiation patterns	Directional	Omnidirectional	Omnidirectional	Roughly omnidirectional
Polarisation	Linear and circular	Linear	Linear	Linear
Gain	High	High	Moderate to high	Moderate
Modelling and fabrication	Easier to fabricate and model	Modelling is difficult	Easier in fabrication using PCB	Fabrication on PCB can be done easily.
Applications	Satellite Communication, GPS navigations and Aircrafts	Internal antennas of mobile phones and some network devices	Internal antennas of mobile phones	Rader, Cell phone base stations
Merits	Easy to surface mount and integration, Low cost, Low weight, simple to manufacture.	Low fabrication cost, large bandwidth support, Inside phone for more design freedom,	Reduced backward radiation for minimising SAR	Design simplicity, low SAR, not sensitive to external disturbances, radiation characteristics remain unchanged
Problems	Surface waves excitation, large profile, i.e. not applicable inside phones	High SAR in regions close to the antenna, requires more extended handsets	Narrow BW characteristics	Large size constraint for mobile handheld devices, single-band

1.2 Main Parameters of Antennas

There are several fundamental performance parameters that have a significant impact on the performance of microstrip antennas, which include scattering parameters, impedance bandwidth, radiation pattern, directivity, gain, and so on. In practice, these important parameters must be taken into account when designing different microstrip antennas, which is why certain critical parameters are discussed in this section.

1.2.1. Scattering parameters

The scattering-parameters (referred to as S-parameters) describe the behaviour of the antenna system. This is usually defined by measuring the voltage of the travelling waves between the multiple antenna ports, as shown in Figure 1.10. The S-parameter measurement is a very useful quantity since it is easily undertaken using a vector network analyser and is utilised to calculate return loss, isolation and VSWR between the multiple antenna ports. A dual ports network (as shown in Figure 1.10 (a)) is used as an example, where the dual fed probes are placed near each other; the equivalent of the dual-port circuit with S-parameters is shown in Figure 1.10 (b).

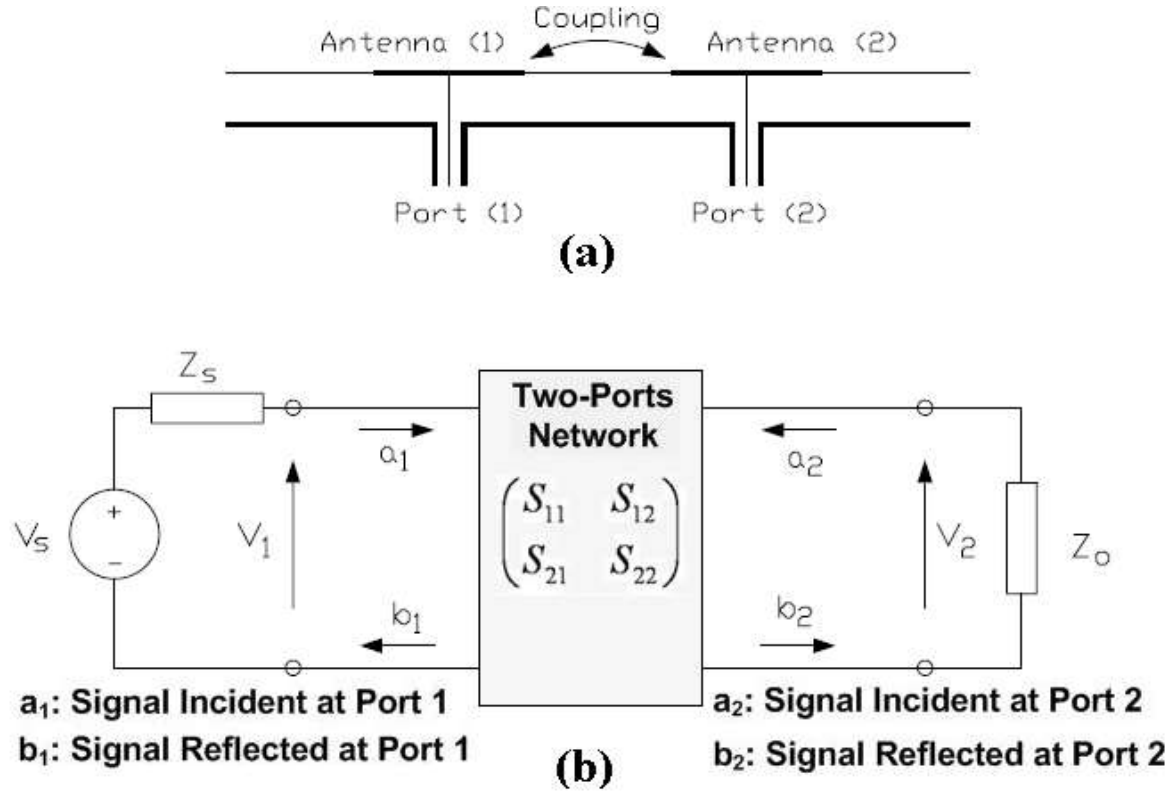

Figure 1.10: **(a)** Dual antennas coupled together but fed separately and **(b)** S-parameter equivalent circuit

The following equations describe the relationship between the dual ports regarding the incident and reflected waves (a_1, a_2, b_1, b_2):

$$b_1 = S_{11}\, a_1 + S_{21}\, a_2 \qquad (1.9)$$

$$b_2 = S_{21}\, a_1 + S_{22}\, a_2 \qquad (1.10)$$

Furthermore, for a 2×2 network, the S-Parameters can be defined as the following matrix:

$$\begin{bmatrix} b_1 \\ b_2 \end{bmatrix} = \begin{bmatrix} S_{11} & S_{12} \\ S_{21} & S_{22} \end{bmatrix} \times \begin{bmatrix} a_1 \\ a_2 \end{bmatrix} \quad (1.11)$$

If we assume that each port is terminated in impedance Z_0, the S-parameters of these ports can be defined and measured as shown in the following.

A) S_{11}: reflection coefficient on the input with 50 Ω terminated output, where a_1 and b_1 represent electric fields and the ratio between the two results in a reflection coefficient.

$S_{11} = b_1/a_1;\ a_2 = 0$ (1.12)

To measure S_{11}, a signal is injected at port -1- and port -2- is terminated with an impedance matched (50 Ω) to the characteristic impedance of the transmission line and then, its reflected signal is measured. As no signal is injected into port -2, then $a_2 = 0$.

B) S_{21}: forward transmission coefficient of 50 Ω terminated output.

$S_{21}=b_2/a_1;\ a_2 = 0$ (1.13)

To measure $S_{21,}$ a signal is injected at port -1- and port -2- is terminated with an impedance matched (50 Ω) to the characteristic impedance of the transmission line, then subsequently, the resulting signal exiting on port -2- is measured. No signal is injected into port -2- and hence, $a_2 = 0$.

C) S_{12}: reverse transmission coefficient of 50 ohm terminated input.

$S_{12}=b_1/a_2;\ a_1 = 0$ (1.14)

To measure $S_{12,}$ a signal is injected at port -2- and port -1- is terminated with an impedance matched (50 Ω) to the characteristic impedance of the transmission line, subsequent to which, the resulting signal on port -1- is measured. As no signal was injected into port -1-, then $a_1 = 0$.

D) S_{22}: reflection coefficient on the output with 50 ohm terminated input.

$S_{22}=b_2/a_2;\ a_1 = 0$ (1.15)

To measure $S_{22,}$ a signal is injected at port -2- and port -1- is terminated with an impedance matched (50 Ω) to the characteristic impedance of the transmission line, with its reflected signal being subsequently measured. No signal is injected into port -1- and hence, $a_1 = 0$.

In general, the return loss (S_{11}) and transmission losses of the antenna can be written as follows:

$$Return\ Loss = 10\log_{10}\left(\left|S_{11}\right|\right) \quad (1.16)$$

$$Transimssion\ loss = 10\log_{10}\left(\left|S_{21}\right|\right) \quad (1.17)$$

1.2.2 Antenna impedance

The law of maximum power transfer implies that the maximum amount of power will be transferred between a source and a load when the characteristic impedance of the source and the load are equal (matched) [17].

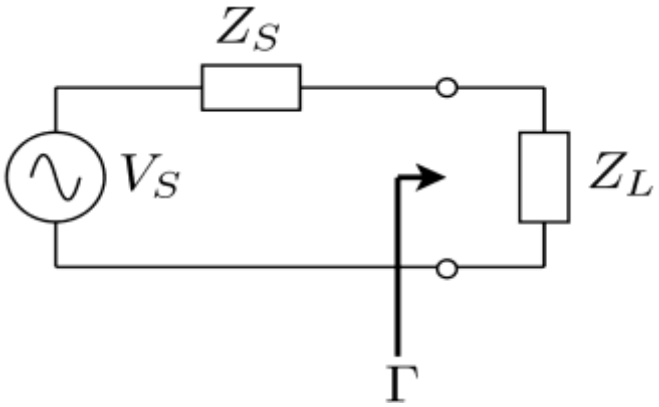

Figure 1.11: Sample circuit configuration depicting the source and load impedance

The components of the circuit in Figure 1.11 can also represent an antenna connected to a receiver system as follows:

• V_S is the signal received by the antenna

• Z_S is the characteristic impedance of the antenna

• Z_L is the load impedance of the receiver circuit

When the source and the load impedances are not matched, a maximum amount of power is not transferred to the load and consequently, it will be reflected back to the source. This is described by the reflection coefficient, which relates the incident signal with the reflected signal as follows:

$$reflection\ coefficient\ (\Gamma) = \frac{\text{reflected signal}}{\text{incident signal}}, \frac{V^-}{V^+} \quad (1.18)$$

As reflection is the direct result of a mismatch between the source and load impedance, the reflection coefficient can also be expressed in terms of the source and load characteristic impedances, which are denoted by Z_S and Z_L, respectively.

$$reflection\ coefficient\ (\Gamma) = \left| \frac{Z_L - Z_S}{Z_L + Z_S} \right| \leq -10dB \qquad (1.19)$$

This equation (1.19) shows that any variation in both the load and source impedance will change the amount of energy reflected from the load.

Moreover; an input impedance is influenced by all the voltages and currents induced on the antenna, including those that are induced due to mutual coupling effects.

For instance, in a dual antenna array, the input impedance on the first and second antenna element in an array environment can be written as the following equations:

$$Z_{in\ first} = Z_{11} + Z_{12} \frac{I_2}{I_1} \qquad (1.20)$$

$$Z_{in\ second} = Z_{22} + Z_{21} \frac{I_1}{I_2} \qquad (1.21)$$

Where, Z_{12} and Z_{21} are the impedance coupling terms

At the same time, the voltage standing wave ratio (VSWR) can be written as:

$$VSWR = \frac{1 + |\Gamma|}{1 - |\Gamma|} \qquad (1.22)$$

This is usually smaller than 2:1, which means that less than or equal to 10% input power is reflected.

1.2.3 Impedance Bandwidth (*BW*)

The impedance bandwidth (*BW*) of an antenna is the usable frequency range (in units of frequency) over which it operates and has acceptable losses due to the mismatch effects. Usually, this is taken as being less than -10 dB ($S_{11} \geq -10$) over its frequency bandwidth (As shown in Figure 1.12), often stated as the percentage bandwidth. However, for a narrow-band antenna, the bandwidth can be calculated using the following equation:

$$BW = \left[\frac{(f_H - f_L)}{f_C} \right] \times 100 \qquad (1.23)$$

Whilst for broadband antennas, the bandwidth is usually expressed as the ratio of the higher to the lower frequencies of an operation where the performance is acceptable, as presented in equation 1.24.

$$BW = \frac{f_H}{f_L} \qquad (1.24)$$

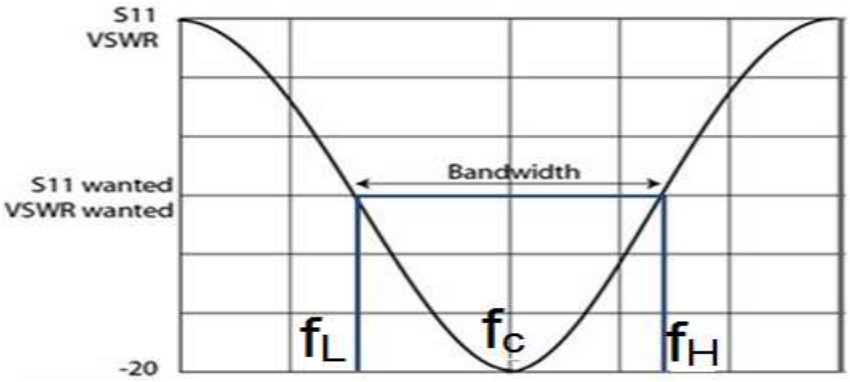

Figure 1.12: Measuring bandwidth from the plot of the reflection coefficient

Where, f_c is the centre frequency, whilst f_L and f_H are the lower and higher frequencies, respectively.

Impedance bandwidth is inversely proportional to the quality factor Q, which is defined for a resonator as:

$$Q = \frac{Energy\ stored}{Power\ lost} \qquad (1.25)$$

1.2.4 Radiation patterns

Radiation patterns are defined [1] as the graphical representation of the radiation properties of the antennas as a function of space coordinates, which are specified by both an elevation angle θ and an azimuth angle φ. In most cases, the radiation patterns are determined in the far-field region and represented as a function of the directional coordinates.

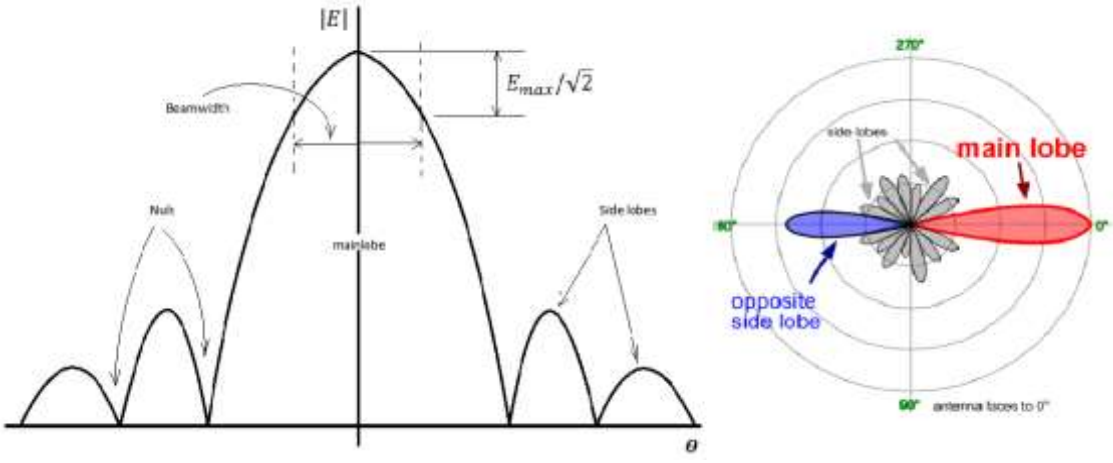

Figure 1.13: Antenna radiation pattern; cartesian (**left**) and polar diagram (**right**)

For a linearly polarised antenna, its performance is often described in terms of its principle *E*-plane and *H*-plane patterns.

• The *E*-plane is defined as the plane containing an electric field vector and the direction of maximum radiation.

• The *H*-plane is defined as the plane containing a magnetic field vector and the direction of maximum radiation [1].

Usually, the patterns describe normalised fields (either gain or power quantities values) with respect to the maximum values. In general, radiation properties include radiation intensity, power flux density, field strength, directivity, phase and/or polarisation.

Moreover, radiation patterns have main lobe, side lobes and back lobe, as shown in Figure1.13

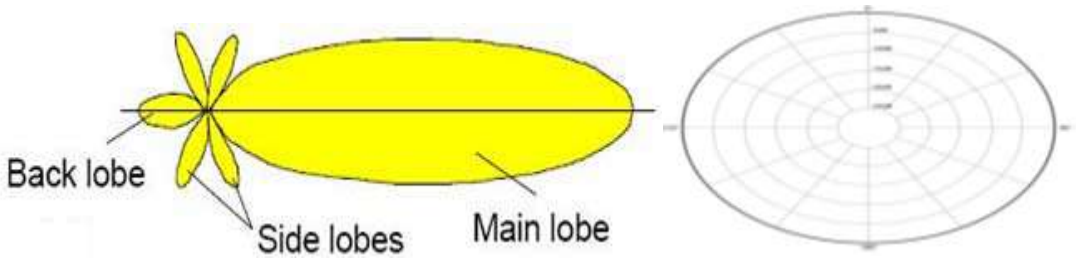

(a) **(b)**

Figure 1.14: (a) Directional radiation pattern and **(b)** Omnidirectional radiation pattern

Three common radiation patterns are used to describe an antenna's radiation property:

a) Isotropic – An antenna having equal radiation in all directions. It is only applicable for an ideal antenna (lossless) and is often taken as a reference for expressing the directive properties of actual antennas.

b) Directional – An antenna having the property of radiating or receiving electromagnetic waves more effectively in some directions than in others, as shown in Figure 1.14(a). These antennas are suitable for wireless applications, such as point to point applications, because they have a high gain as the power is channeled in one direction [18],

c) Omni-Directional - An antenna having an essentially non-directional pattern in a given plane and a directional pattern in an orthogonal plane, as shown in Figure 1.14(b). Omni-directional antennas tend to have a little gain, because the power radiates in all directions and thus, they suitable for many applications, including those of mobile phones [19].

1.2.5 Directivity (*D*)

The directivity is the ability of an antenna to focus energy in a particular direction. It is mainly defined as the ratio of radiation intensity in a given direction from an antenna to radiation intensity averaged over all directions [1]. It is a measure of how 'directional' an antenna's radiation pattern can be [20].

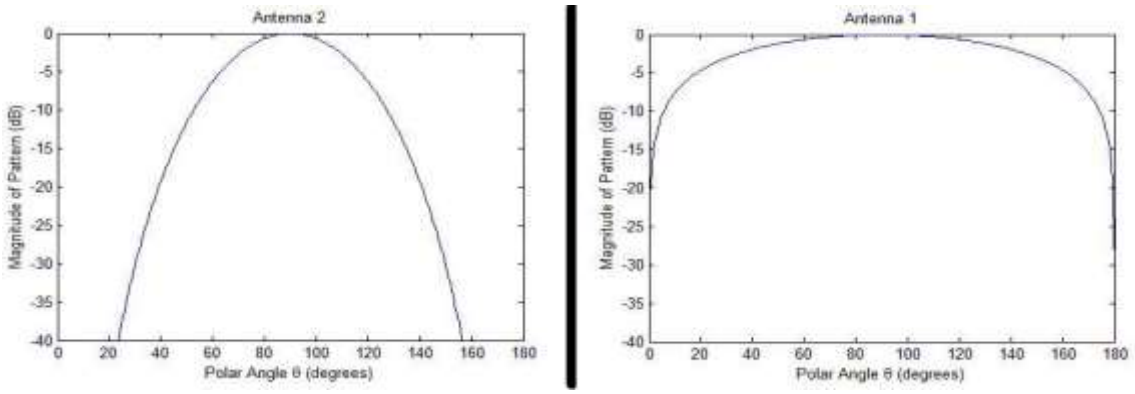

(a) **(b)**

Figure 1.15: Radiation patterns for antennas. **(a)** high directivity and **(b)** low directivity

Directivity is a dimensionless quantity, since it is the ratio of two radiation intensities. That of an antenna can be easily estimated from its radiation pattern characteristics. Moreover, an antenna that has a narrow main lobe will have better directivity, compared to one with a broad main lobe (As shown in Figure 1.15).

1.2.6 Gain (*G*)

Antenna gain is a parameter closely related to the directivity of the antennas. For a given antenna, this is defined as the ratio of the power radiated or received by it in a given direction, to the power radiated or received by an isotropic antenna, both being fed by the same power and measured in dBi. As above mentioned, the gain of an antenna is closely related to its directivity and hence, to find the former, the latter should be found. Equation (1.26) below is used to determine gain.

$$G(\theta,\varphi) = \eta_{rad} \times D(\theta,\varphi)\ ; \qquad (0 \le \eta_{rad} \le 1) \qquad (1.26)$$

Where, η is the efficiency of the antenna and D is the directivity. Gain is always less than directivity, because efficiency varies between 0 and 1. Both the value for the gain and directivity of an antenna are typically expressed with the unit dB. In antenna design, the calculated gain or directivity relative to an ideal isotropic radiator. Hence, it is generally expressed in dBi, but are generally just shortened to dB.

1.2.7 Radiation efficiency

The radiation efficiency is defined as the ratio of the power radiated or dissipated within the antenna to the total input power delivered or supplied to the antenna and is denoted by η_{rad} [17].

$$\text{Thus, } \eta_{rad} = \frac{P_{rad}}{P_{in}} \times 100\% \qquad (1.27)$$

Where, P_{rad} is the power radiated by the antenna, whilst P_{in} is that delivered by the antenna.

In terms of resistances, η_{rad} can be written as follows:

$$\eta_{rad} = [\frac{\frac{1}{2}|I^2|R_{res}}{(\frac{1}{2}|I^2|R_{ohm} + \frac{1}{2}|I^2|R_{res})}] \times 100 = \frac{R_{res}}{(R_{ohm} + R_{res})} \times 100 \qquad (1.28)$$

Where, R_{res} is radiation resistance and R_{ohm} the ohmic loss resistance of the antenna conductor. As an array represents a multi-port, it is essential to calculate the total radiation efficiency using the following formula:

$$\eta_{Total} = \eta_{rad}(1 - |S_{11}|^2 - |S_{12}|^2) \qquad (1.29)$$

However, the total efficiency of an antenna in its environment is reduced by some losses, including any ohmic losses, mismatch losses, feedline transmission losses, edge power losses and/or any external parasitic resonances. In general; a high-efficiency antenna has most of the power present at its input radiated away. A low-efficiency antenna has most of the power absorbed by losses within it or reflected away due to the impedance mismatch effect.

1.2.8 Polarisation

The polarisation of an antenna indicates the orientation of the *E* and *H* waves transmitted or received by the antenna [17]. Typically, this is defined the direction of maximum radiation.

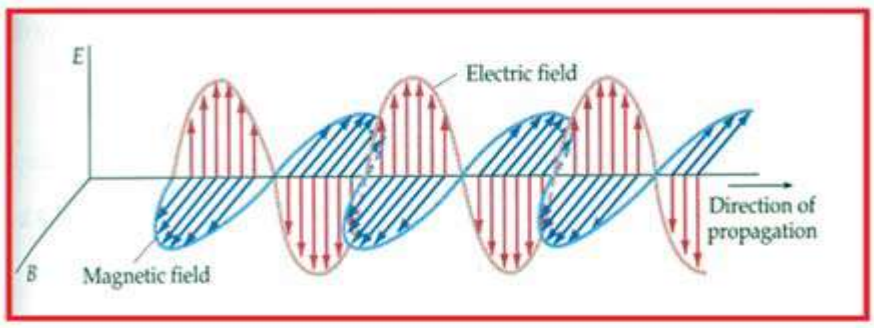

Figure 1.16: Polarisation of EM wave in free space

The most common types of polarisation are linear (horizontal or vertical) and circular (right hand or left hand), whilst there is an elliptical form. In fact, antennas will exhibit elliptical polarisation to some extent.

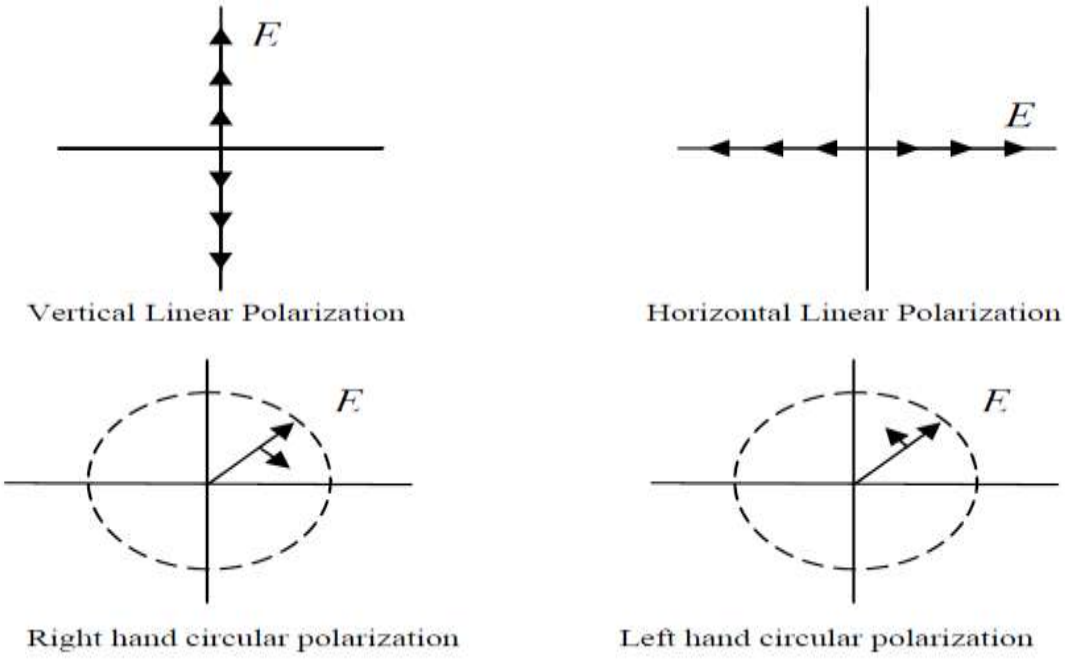

Figure 1.17: Commonly used antenna polarisation schemes

1.2.9 Antennas field regions

The electromagnetic field distribution of a radiated antenna changes with distance as the radiation moves away from it. Generally, the space surrounding it can be divided into three different regions of the radiating field (as shown in Figure 1.18) [2, 20].

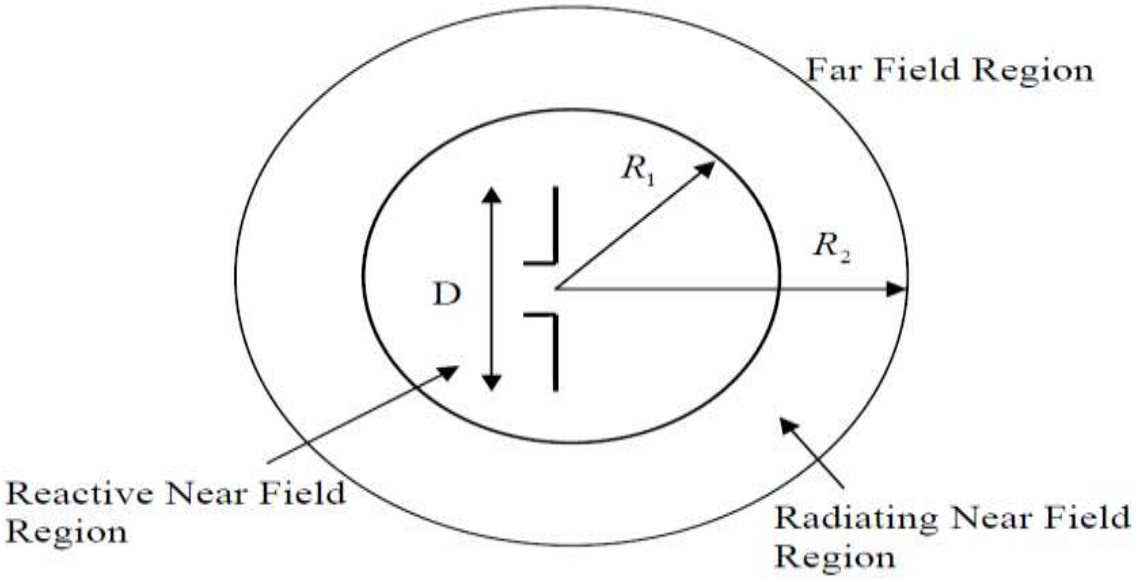

Figure 1.18: Antenna field regions

1) Reactive Near-Field

For the majority of antennas this region exists at:

$$R_1 \leq 0.62\sqrt{D^3/\lambda} \qquad (1.30)$$

Where, *R* is the radius and *D* is the largest linear dimension of the antenna.

2) For the Radiating Near-Field region (also called the Transition or Fresnel region), the boundaries are between:

$$0.62\sqrt{D^3/\lambda} \leq R_2 \leq 2D^2/\lambda \qquad (1.31)$$

In this region, energy is only stored and none is dissipated. However, if the antenna is very small compared to the wavelength, this region may not exist.

3) Far-Field region (also called the Fraunhofer region) is located at a radial distance of:

$$R \geq 2D^2/\lambda \qquad (1.32)$$

In this region, the wave-front becomes approximately planar [17].

1.3 Motivation

While the necessity of multiple-antenna (array) systems in modern wireless transceivers is irrefutable, the integration of these multiple radiating elements in close proximity gives rise to mutual coupling and signal correlation problems. Antenna coupling adversely affects (decreases) the performance of any multiple-antenna (array) system. In general, it degrades radiation efficiency and the designed peak gain due to the fact that part of the power that could have been radiated now being absorbed by other adjacent antennas' elements [21]. Antenna loading can also alter radiation patterns and introduce some unwanted side lobes [22]. Another downside of the coupling problem is the resulting on signal correlation. Optimum performance of any MIMO system relies on the uncorrelated received or transmitted signals. It is generally agreed that coupling between antennas can lead to higher channel correlation, which will limit the MIMO capacity of the system [23-25].

Isolating the antennas is not only of crucial importance for the improved performance of these multiple-antenna systems, for it also simplifies the system design due to creating close to stand-alone operating conditions (ideal) for individual antennas. The research presented in this thesis deals with different types of antenna for different wireless applications, which range from narrow-band to ultra-wideband and multi-band applications.

In this work, various multiple-antenna structures are designed for the specific requirements of these applications and novel coupling reduction techniques are developed for improving the performance of these systems.

The investigated antenna geometries include PIFAs (Planar inverted-F antennas) or monopole as well as slot and patch antennas that are integrated incorporation with new isolation methods and applicable coupling suppression techniques.

As has been noticed, despite a lot of research activities in the field of antenna coupling reduction, there remains a lack of systematic and coherent approaches to the identification of the different mechanisms that contribute to the coupling problem. To address this gap, in this thesis a comprehensive analysis of the coupling sources of antennas that occur between multiple-antenna systems in different wireless applications is provided. Moreover, there is a clear classification of the mechanisms that contribute to the mutual coupling problem between different antenna array systems.

Analysis of mutual coupling in different applications explored in this thesis clearly demonstrates that the choice of a proper coupling reduction approach is strongly tied to various parameters such as antenna geometry, operating frequency, bandwidth, integration platform, and the device form factor. This emphasizes the importance of the guidelines provided herein to identify the underlying coupling mechanism and to devise a proper coupling reduction approach for the considered application.

Whilst past studies have provided a wealth of information, most have had some limitations. In particular, there were many gaps in past studies regarding the coupling mitigation in different applications. In this study, the researcher has the aim of overcoming some of the limitations, especially filling the lacunae in knowledge regarding isolation enhancement in antenna arrays. Specifically, in this thesis, new antennas with novel isolation approaches are developed to be used in portable low profile wireless terminals for narrowband, ultra-wideband and multiband applications, thereby enhancing antenna systems capability.

Throughout the discussion, the designs are verified through experimental implementation. These new array antennas offer many outstanding characteristics, such as high isolation, geometric simplicity, compactness in size, in addition to excellent diversity performance. As a consequence, the proposed MIMO antennas in this thesis are good candidates for a range of different wireless communication applications.

1.4 Scope of the thesis

The aim of the research work presented in this thesis is to investigate, characterise, analyse, design and develop different antennas arrays with reduced mutual coupling in various wireless applications. This is achieved through a combination of numerical simulations and measurement processes.

In order to achieve the desired aim and after having defined the general research problem, the main objectives can now be formulated explicitly as follows:

1- A through literature review and fundamental investigation into the most recent developments of isolation techniques between different MIMO antennas in various wireless applications;
2- Theoretical knowledge of these isolation mechanisms, followed by the introduction of optimal integration of newly developed coupling reduction techniques between different MIMO antennas;
3- The implementation of these new applicable isolation techniques for different MIMO antennas, with the aid of simulation software programs for the purpose of antenna coupling suppression;
4- The use of conventional PCB technology for the fabrication of the developed MIMO antenna designs;
5- The use of circuit designer software programs and PCB prototyping machines for the conventional PCB fabrication technology;
6- The fabrication of the developed MIMO antenna designs;
7- The use of full-wave electromagnetic analysis and solvers for the development of different MIMO antenna designs;
8- The use of a network analyser for the measurement of the S-parameters of all the developed MIMO antenna designs;
9- The use of anechoic chambers for the measurement of the radiation patterns of the developed MIMO antenna designs;
10- The presentation and comparisons of the simulations and measurements of all the developed MIMO antenna designs;
11- In-depth study of the results obtained, including the return and transmission losses, surface currents density and distribution, radiation patterns, peak gain as well as radiation efficiency, of all the developed MIMO antenna designs.

1.5 Research Contributions

The research presented in this thesis has made significant contributions to knowledge, which are summarised in the respective chapters as follows:

Comparative study on the diversity of performance between different microstrip antenna arrays (Chapter 2)

For the first time, a systematic comparative study involving four different microstrip antenna array types (PIFA, patch, monopole, and slot) is studied and presented, based on the diversity of performance (mutual coupling effects and correction). All these different microstrip antennas have been designed and printed on a thin and cheap FR_4 substrate, suitable for wireless PCS applications. The findings of this study could prove beneficial for antenna designers or RF engineers selecting a microstrip antenna type when designing antenna arrays at frequency 1.9 GHz for wireless PCS applications. The salient contents of this work were published as a full-length conference paper presented at the Loughborough Antennas and Propagation Conference (LAPC 2017) [R5].

Survey of coupling suppression techniques for different wireless applications (Chapter 3)

A unique coherent survey, including various mutual coupling reduction approaches commonly employed in the literature is presented. These techniques are categorised based on the coupling mechanisms that they target for more efficient suppression of antenna coupling. The chapter provides a summarised overview of previous methodologies as subsections under the main classifications. In these subsections, three major wireless applications that are central to this research work are defined and discussed, these being: narrowband, multiband and ultra-wide-band (UWB). Moreover, this survey includes a precise classification of the mechanisms that contribute to the coupling problem and their suppression approaches based on these mechanisms for different antenna arrays. The survey will be helpful for any antenna designer/researcher regarding finding an apt solution that easily will fit with his / her specific application restrictions (the survey work is presented in detail in chapter three of this thesis).

Design of multiple antennas with high isolation for narrow-band applications (Chapter 4)

An applicable isolation technique is introduced to reduce the mutual coupling between two closely-placed antenna elements. In addition, a new decoupling approach based on the utilisation of fractals with EBG corporation is proposed and investigated for narrow-band applications. Further, a novel and compact MIMO antennas (PIFAs) design is proposed and realised. The analysis results (theoretically and practically) show that the proposed MIMO antennas guarantee a high coupling reduction being obtained between the antennas, without much degradation of the radiation characteristics. The important contents of this work were published as a full-length journal paper in IET Microwave Antenna and Propagation [R1] and also as a full-length conference paper in Loughborough Antennas & Propagation Conference (LAPC 2016) [R6].

Design of multiple antennas with high isolation for UWB applications (Chapter 5)

A novel MIMO antenna with high isolation characteristics is designed and developed for UWB application. Mutual coupling reduction is achieved by adding a new effective decoupling structure. In addition, a simple but highly efficient isolation technique is proposed.

The proposed MIMO (UWB disc monopolies) antennas are simple in design, small in size and easy to manufacture (fabrication). Moreover, the analysis results (theoretically and practically) show that the proposed UWB-MIMO antenna guarantees the entire UWB operation with high isolation and sustained satisfactory (nearly omnidirectional) radiation performance, which makes it very suitable for the future UWB applications. The key contents of this work were published as a full-length journal paper in the International Journal of Microwave and Wireless Technologies (JMWT) [R2] and also as a full-length conference paper for IEEE MTT-S International Microwave Workshop Series on Advanced Materials and Processes for RF and THz Applications (2017 IMWS-AMP) [R4].

Design of multiple antennas with high isolation for multi-band applications (Chapter 6)

A new high isolation quad-band MIMO (slots) antenna design is presented, with mutual coupling reduction being achieved by adding a hybrid decoupling solution. The MIMO antennas can be used to serve most mobile and wireless applications, including DCS mobile communication, Higher GSM band (1.7 - 1.8 GHz), LTE band (2.55 -2.7 GHz), WiMAX band (3.3 - 3.5 GHz), intended HiperLAN (4.8 - 5.2 GHz) and many more. A combination of isolation enhancement mechanisms has been proposed for reducing the mutual coupling effects between the closely packed antenna elements, which is relatively straightforward and easy to implement. A good agreement is observed between the measured and the simulated results that demonstrates the success of the suggested design topology. The main contents of this work were published as a full-length conference paper for the European Conference on Antennas and Propagation (EuCAP 2018) [R3].

1.6 List of Author's Publications and Novel Works

The work presented in this thesis has led to the following publications:

Journal papers

[R1] A. H. Radhi, R. Nilavalan, Y. Wang, H. S. Al-Raweshidy, A. A. Eltokhy, and N. A. Aziz, "Mutual Coupling Reduction with a Novel Fractal Electromagnetic Band Gap Structure," IET Microwaves Antennas & Propagation, October 2018. **(Published in October 2018).**

[R2] A. H. Radhi, R. Nilavalan, Y. Wang, H. S. Al-Raweshidy, A. A. Eltokhy, and N. A. Aziz, "Mutual coupling reduction with a wideband planar decoupling structure for UWB–MIMO antennas," International Journal of Microwave and Wireless Technologies, pp. 1–12, April 2018. **(Published in July 2018).**

Conference papers

[R3] A. H. Radhi, R. Nilavalan, H. Al-Raweshidy, and N. A. Aziz, "A New Quad-band Diversity Antenna with High Isolation," Proceedings of 12th European Conference on Antennas and Propagation (EuCAP 2018), April 2018, ExCeL London, United Kingdom.

[R4] A. H. Radhi, R. Nilavalan, H. S. Al-Raweshidy, and N. A. Aziz, "High isolation planar UWB antennas for wireless application," 2017 IEEE MTT-S International Microwave Workshop Series on Advanced Materials and Processes for RF and THz Applications (IMWS-AMP), September 2017, Pavia, Italy.

[R5] A. H. Radhi, R. Nilavalan, H. Al-Raweshidy, and N. A. Aziz, "Comparative Study on the Diversity Performance between Different Microstrip Antenna Arrays," 2017 Loughborough Antennas & Propagation Conference (LAPC 2017), November 2017, United Kingdom.

[R6] A. H. Radhi, N. A. Aziz, R. Nilavalan, and H. S. Al-Raweshidy, "Mutual coupling reduction between two PIFA using uni-planar fractal based EBG for MIMO application," 2016 Loughborough Antennas & Propagation Conference (LAPC 2016), November 2016, United Kingdom.

[R7] N. A. Aziz, **A. H. Radhi**, and R. Nilavalan, "A reconfigurable radiation pattern annular slot antenna," 2016 Loughborough Antennas & Propagation Conference (LAPC 2016), November 2016, United Kingdom.

1.7 Thesis Organisation

This thesis consists of seven chapters including this introductory chapter (**Chapter 1**), as presented above. This chapter has covered the basic theory of microstrip antennas, whilst also providing a brief description of the primary fundamental parameters of these microstrip antennas. Moreover, the motivations that justify the research and the scope of the thesis have been explained in this chapter. **Chapter 2** is devoted to explaining the mutual coupling (MC) problem in microstrip antenna arrays, including the different antenna coupling mechanisms. That is, in this chapter, a definition of mutual coupling phenomenon is given, and the effects of MC on radiation pattern, correlation, and capacity is also explained.

Moreover, the various coupling reduction approaches are categorised into three subsections based on the coupling mechanism that they target for efficient suppression of antenna coupling. Furthermore, a new comparative study involving four different microstrip antenna array types (PIFA, patch, monopole, and slot), based on diversity performance (mutual coupling effects and correction), is explained in detail.

Chapter 3 reviews the development of multiple microstrip antennas in past decades and the state-of-the-art of these antennas for MC reduction is also presented. Previous works and methodologies for different wireless applications (narrowband, multiband and UWB) are also compared and summarised.

Chapter 4 starts with a brief overview of fractal geometries, i.e. the definition of the fractals and several of the typical linear fractal types, are provided. In this chapter, the development of a new high isolation MIMO antenna for narrowband applications is presented. High isolation is achieved through inserting a novel arrangement of Fractal based Electromagnetic Band Gap (FEBG) structure between dual antenna elements sharing a common substrate\ground. Additionally, in this chapter, the performances of the diversity antennas are investigated and verified, both numerically and experimentally.

Chapter 5 gives a background to UWB technology in terms of its advantages, applications and standards of the UWB. This chapter is primarily focused on the development of a novel planar MIMO antenna for UWB applications. The proposed antennas operate over the frequency band from 3.1 to 10.6 GHz and wide isolation is achieved through a novel planar decoupling structure inserted between the MIMO antennas. The proposed UWB-MIMO antenna is investigated and verified both numerically and experimentally. There is also a summarised comparison of the proposed UWB-MIMO antennas with other array works previously reported and recently published.

Chapter 6 contains a brief overview of multi-band technology, and the vital issues that need to be addressed to achieve high isolation, with the main focus being on the development of a new applicable multi-band MIMO design. The isolation is achieved through a combination of hybrid isolation enhancement mechanisms. Additionally, within this chapter, the performances of the MIMO antennas are investigated and also verified, both numerically and experimentally. Finally, the last chapter (**Chapter 7**) is split into three sections. A summary of the research work undertaken is provided in the first, whilst the second, lists the findings and main conclusions (including contributions) drawn from this study. Moreover, several suggestions for future work are identified in the last section to be carried out in connection with the current research work presented in this thesis.

Chapter 2: Overview of Mutual Coupling in Microstrip Array Antennas

2.1 Introduction

Mutual coupling is a well-known effect in multi element array antennas. Generally, mutual coupling is an unwanted phenomenon that distorts the behaviour of the radiating elements in an antenna array. The main goal of the undertaken research work is the development of multiple microstrip antennas for high isolation in different wireless applications. Before the development of these multiple antennas, it is necessary to familiarise with fundamentals antennas theory. Furthermore, it also essential to define and understand the main parameters which characterise the performance of these multiple antennas and have to be considered during their design.

This introductory section discusses the essential background theory to the mutual coupling (MC) problem in microstrip array antennas. In MIMO systems, more than one antenna is implemented on a small terminal, as mentioned earlier. It is feasible to implement multiple antennas at a base station, because there is no strict limitation on its size. However, having multiple antennas on small terminals (such as mobile handsets or PDAs), while maintaining their performance, remains a significant challenge task for each antenna designer in terms of reducing the MC and correlation effects between these MIMO antennas. In general, antenna implementation in handsets can limit the theoretical MIMO performance (i.e. capacity) in wireless systems. Hence, multiple antenna array elements need to be as small as possible when embedded in a small terminal. They also should meet some specific essential factors, such as minimum occupied volume, good isolation and effective diversity performance for multiple antennas. This in addition to the usual requirements of a single conventional antenna, including light weight, low profile, adequate bandwidth, isotropic radiation characteristics, low fabrication cost and robustness [26]. Moreover, major factor is that the antenna array should have low MC between the individual elements.

Following the introductory material presented in this chapter, the rest of the chapter is devoted to the study of the nature of mutual coupling in multiple antenna systems and to finding systematic ways for design, modelling, implementation and characterisation of highly-isolated multiple antenna systems tailored for various wireless applications. Even though mutual coupling has been investigated by antenna engineers for many decades in the context of antenna arrays, the coupling mechanisms are not properly classified as indicated earlier.

Therefore, this chapter presents classification of different mechanisms that contribute to mutual coupling in multiple antenna systems. The coupling reduction techniques available in open literature are then categorised based on the coupling mechanisms they effectively mitigate. For evaluations of multiple antenna systems various professional communities use different parameters such as transmission coefficient and envelope correlation coefficient.

In this thesis, various multiple antenna geometries pertaining to modern wireless applications are investigated and the different mechanisms that contribute to inter-element coupling are identified. This insight is used to classify coupling reduction approaches and devise innovative isolation enhancement techniques that are tailored for the specific application's operational requirements and form-factor constraints.

Furthermore, in this chapter, the most important requirements/challenges when designing multiple antennas in small terminals are identified in terms of the antenna coupling mechanisms and isolation enhancement approaches. Finally, a new comparative study involving four different microstrip antenna array types (PIFA, patch, monopole, and slot), based on diversity performance (mutual coupling effects and correction), is explained in detail.

2.2 Antennas Mutual Coupling

Mutual coupling is a physically complex phenomenon that refers to the electromagnetic interaction or the reaction that occurs between different coupled antenna array elements in an array system. It is intrinsic to the nature of antennas that when two antennas are in proximity, and one is transmitting, the second will receive some of the transmitted energy, the amount of which being dependent on their level of separation and relative orientation. Even if both antennas are transmitting, they will simultaneously receive part of each other's transmitted energy.

Furthermore, antennas re-scatter a portion of an incident wave and thus, act like small transmitters even when they are nominally only receiving. In other words, some of the energy transmitted by an antenna element is partially transferred to the other elements.

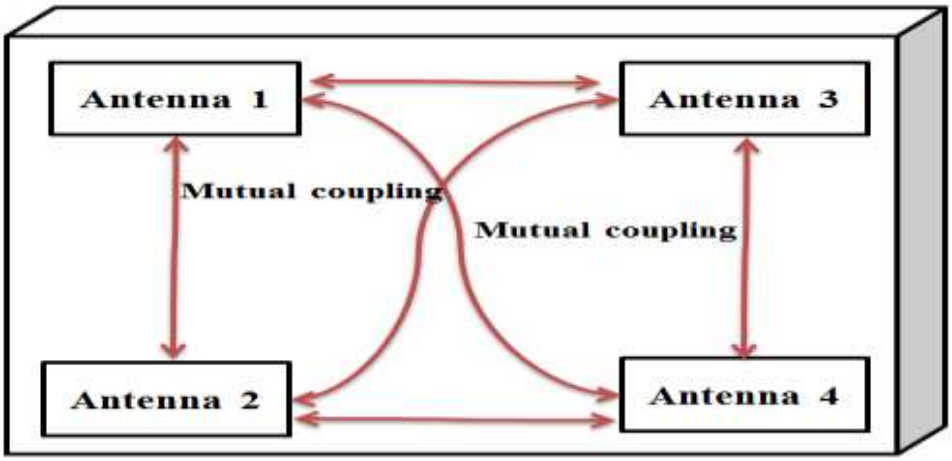

Figure 2.1: A schematic diagram illustrating the mutual coupling phenomena between elements in a compact array

Correspondingly, a portion of the energy in an incident field of a receiving element is transferred to a nearby antenna element (as presented in Figure 2.1). As a result, the feed current for each transmitting antenna in an array does not just consist of the current when transmitting alone, for it also includes that induced by the other antenna elements in close proximity and the same applies to the receiving elements of the array. This means that the various energy interchanges between a particular element of an array and a remote point occurs not only by the direct path, but also indirectly via scattering from the other antennas of the array.

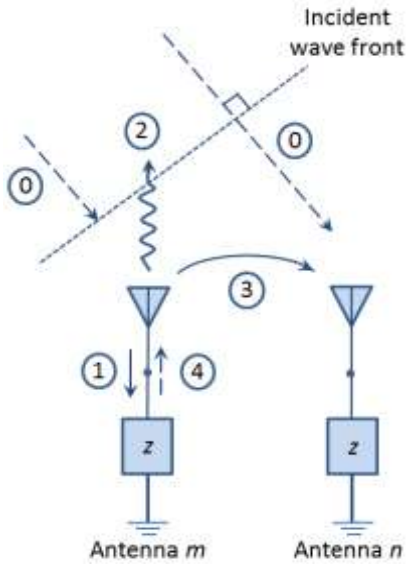

Figure 2.2: A schematic diagram illustrating the effect of MC between two antennas

This unwanted effect is the manifestation of mutual coupling (MC) that exists between array antennas. This often represents a more than negligible effect, thereby complicating the design of such antennas. Figure 2.2 illustrates the effect of MC between dual antennas. Suppose the

first antenna (Ant *m*) is connected to an active source, while the other antenna (Ant *n*) is terminated (passive) at the characteristic impedance $Z_0 = 50$ ohms.

This implies that the first antenna can produce electromagnetic waves that propagate into free space and a fraction of the radiated energy is received by the second antenna, thereby inducing a current on the element itself. A part of the induced energy travels towards the passive generator on the second element (Ant *n*), whilst another part is reflected and re-radiated. Some of the re-scattered energy will be received by the first antenna (Ant *m*) again, thus repeating the cycle. From an observation point in space, the total energy would therefore not just come from the first element (Ant *m*), which is the exciting element, for it also comes from second element (Ant *n*) as well. This mutual interaction between coupled antenna elements in an array will decrease the performance of the system when the antennas are in close proximity to each other. In sum, MC is a common problem in array antennas design, which significantly affects most types of the antenna radiating systems.

2.3 Measurement of Antennas Mutual Coupling

Numerous researchers consider the transmission coefficient as a measure for assessing different multiple-antenna systems regarding the level of MC. Specifically, the S_{ij} or S_{ji} parameters are numerical values used to describe and estimate the MC between elements i and j. They indicate what fraction of the energy applied to one element of an array is received by another element in the array.

A dual-ports circuit transmission coefficient S_{21} was previously defined as the power transferred to second port when only the first port is excited and all other ports are terminated to suitable characteristic impedance of the system. As we know; S-parameters are here dependent on the characteristic impedance of the transmission lines, peripherals or loads connected to the ports, etc.

This definition is a valid measure of the power amount that is coupled from one port towards another and it takes into account the following [1].

A) The efficiency of the source or input power delivered to the active (fed) antenna (i.e. how good and efficient the active antenna's input matching network is). The actual power delivered to the antenna is equal, where S_{11} is the reflection coefficient at first port and a_1 is the power incident at this port.

B) How efficient the active antenna couples the received power to the surrounding environment, whether this is in the form of radiating EM waves in space (i.e. how good the far field gain of the array antenna is) or coupling it to the antenna's surrounding environment (e.g. near-field coupling to an adjacent element or coupling to substrate-bound modes).

C) The wave propagation between the antennas, whether it is far-field radiation in free space, near-field radiation, or guided waves in substrate-bound modes.

2.4 Antennas Coupling Mechanisms

In order to find a correct method for suppressing antenna coupling in multi-antenna elements, first the ‘’coupling paths or ’coupling routes " should be carefully identified. Basically, the transmitter determines the amount of interfering electromagnetic fields/waves generated, whilst the coupling path ascertains how much of the fields reach the receiver and the receiver determines the quantity of the waves received.

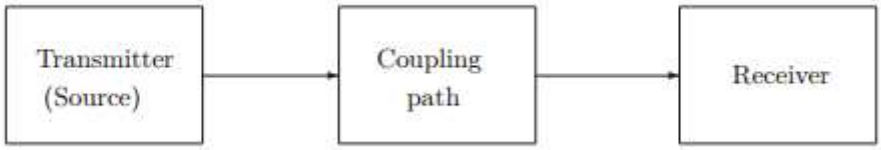

Figure 2.3: A schematic diagram of a coupling path between a transmitter and receiver

The coupling between the microstrip antenna elements in a MIMO array system occurs through three different paths or channels.

2.4.1 The common substrate \ ground (via surface waves propagation or substrate-bound modes)

In antenna arrays, it is desired that the microstrip antennas emit all of their supplied power into free space. Basically, part of the radiated power gets concentrated inside the substrate, depending on the antenna type, orientation, substrate thickness, number of metal layers, etc.

The common ground or sharing substrate can act as a good transmission medium to guide these surface waves from one antenna towards another. For instance, microstrip patch antennas on thick substrates couple strongly to surface-wave modes supported by a grounded dielectric slab [27]. In which case, antenna coupling to a substrate-bound mode leads not only to a drop in antenna radiation efficiency [28], but also to strong MC between antennas that sharing the same substrate. In general, the surface waves (as presented in Figure 2.4) are simply propagating electromagnetic waves, which are bound to the boundary between two dissimilar media, such as a metal (PEC) and free space (air).

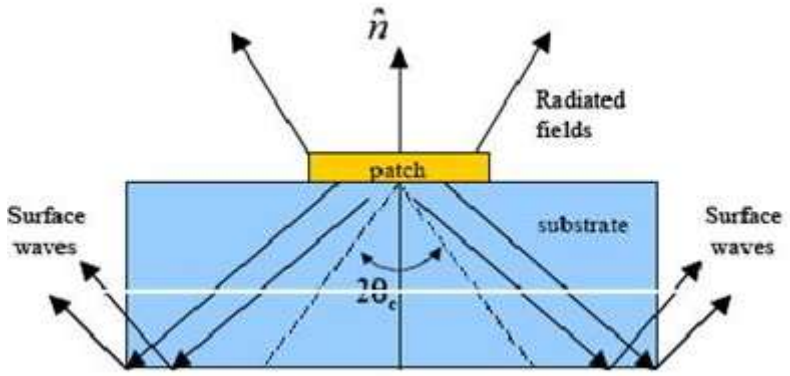

Figure 2.4: A schematic diagram illustrating the formation of surface waves: field lines radiating from an antenna

In a microwave field, surface waves refer to surface currents that occur on a metal surface and their associated field can extend to the surrounding space [29-30]. These currents flow over the metal surface and do not couple with external waves, if it is smooth and flat. Like conducting currents, surface currents are scattering and radiate whenever a metal surface has a discontinuity, curve or truncation. Consider Figure 2.5, where the region $y < 0$ is filled by a dielectric with permittivity $\varepsilon_r > 1$ and the region $y > 0$ is filled with vacuum and surface waves propagated on the X-Z plane [29].

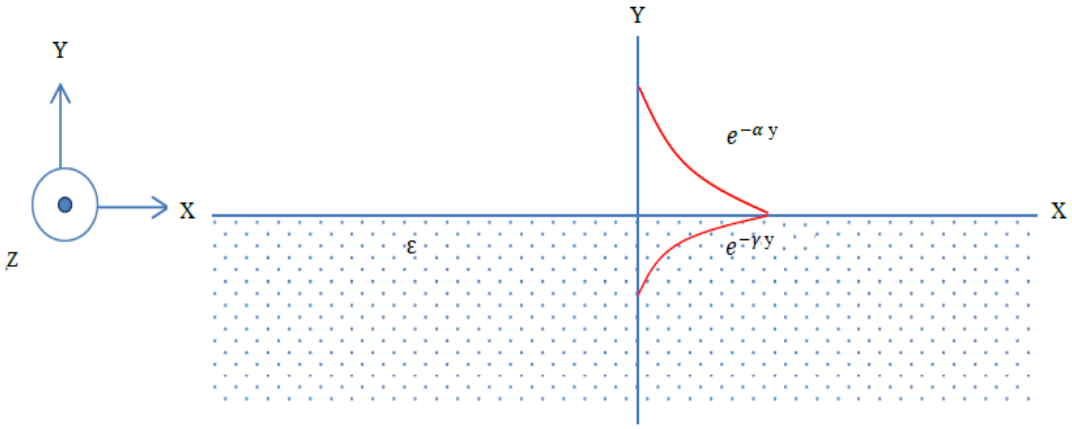

Figure 2.5: A schematic diagram of the surface wave on a dielectric vacuum interface

The decay constants for the dielectric and vacuum regions are defined as γ and α; respectively. In a single antenna, surface wave effects can be effectively eliminated by using some simple techniques, such as cavities or stacked substrates, whilst with multiple antennas these effects can be eliminated by using other common techniques, such as EBG, DGS, etc. However, this has the fundamental drawback of increasing the complexity of the antennas. In this thesis, different surface wave suppression techniques are presented in detail in the next chapters for coupling reduction through the common ground or a shared substrate.

2.4.2 Radiation into free space (via air or direct space waves)

In general, antennas are expected to radiate their electromagnetic waves efficiently into free space. However, the waves radiated into free-space by one antenna (an active antenna) are received by other nearby antennas (passive antennas), and this will lead to some undesirable MC effects. This kind of coupling is especially strong in compact antennas since their small radiating aperture areas lead to a wider radiation pattern.

2.4.3 Near-field coupling (via reactive antenna fields)

This coupling applies to some cases where different elements of the antenna array are very closely spaced (defined previously as radius $\leq 0.62\sqrt{D^3/\lambda}$) and are subjected to near-field interactions that are simply represented by capacitive or inductive coupling characteristics.

2.5 Antennas Coupling Effects

In large wireless (e.g. laptops, tablets or access points), medium-sized (e.g. mobile and smartphones) and small-sized devices (e.g. USB dongles) where MIMO antennas are placed very closely to each other, high MC appears and affects the performance of the antenna array, such as radiation patterns characteristics, reflection coefficient, input impedance of antenna elements and system channel capacity. Specifically, placement of the adjacent microstrip antennas at a separation of less than $\lambda_0/4$ causes high MC levels. This influences some of essential antenna parameters, of antenna elements adjacent to each other due to small separation between them. In this chapter, a unique systematic comparative study between different 2×2 antenna array systems types is modelled by using a scattering matrix (S-parameters).

The S_{21} is evaluated as the MC of a dual-element antenna array. Some numerical simulations are carried out using HFSS version 17.0 software and presented later (in section 2.9) to verify the relation between the MC and the separation between the elements. The antennas are optimised to resonate at 1.9 GHz (suitable for wireless PCS applications) and mounted with variable inter-element separation (*d*) on the ground plane. In general, the degraded performance appears due to the lack of maintaining a good impedance match and hence, wasting of the incident power amount to the antenna system occurs. Moreover, the received radiation by one antenna in the array causes currents to be induced in the other antennas, which may be reradiated causing a disruption in the designed radiation pattern of the antenna array. At the same time, antenna coupling leads to mutual impedances and hence, coupled impedance matrices, which further complicates the design of an efficient matching network.

Such a network requires a sophisticated coupled matching system to compensate for these coupling effects so as to ensure maximum power transfer to and from the diversity antennas

(this will be discussed in more detail in next section). In general, with a no MC effects scenario, the input impedance of an antenna is equal to its self-impedance. However, with another antenna in close proximity, the input impedance of the antenna becomes more dependent on both the self-impedance and the mutual impedance. This relation is expressed by the following equation [31]:

$$Z_{in} = Z_{11} + Z_{12}\left(\frac{I_2}{I_1}\right) \qquad (2.1)$$

where, Z_{11} and Z_{12} refer to the self and the mutual impedances, respectively. While I_1 and I_2 refer to the currents flowing through the respective first and second antennas, respectively.

In the case of multiple-antenna applications, such as a diversity antenna array, the MC between multiple antennas should always be minimised as much as possible to maintain higher efficiency characteristics of the multiple antennas [32-33]. For, MC disturbs the far-field pattern of the antenna system due to the destructive interference process between the coupled antenna elements. The impact of MC between dual dipole antennas [1] for different separation is presented in Figure 2.6. The radiation patterns of the first antenna have a significant difference in the separation (d) decrease [1]. Hence, when multiple antenna elements are employed to form a MIMO system on a compact wireless terminal device, antenna geometry and the position of antenna elements in the array need to be optimised by reducing the MC level between the antenna elements. Otherwise, the antenna array will not achieve the designed radiation efficiency.

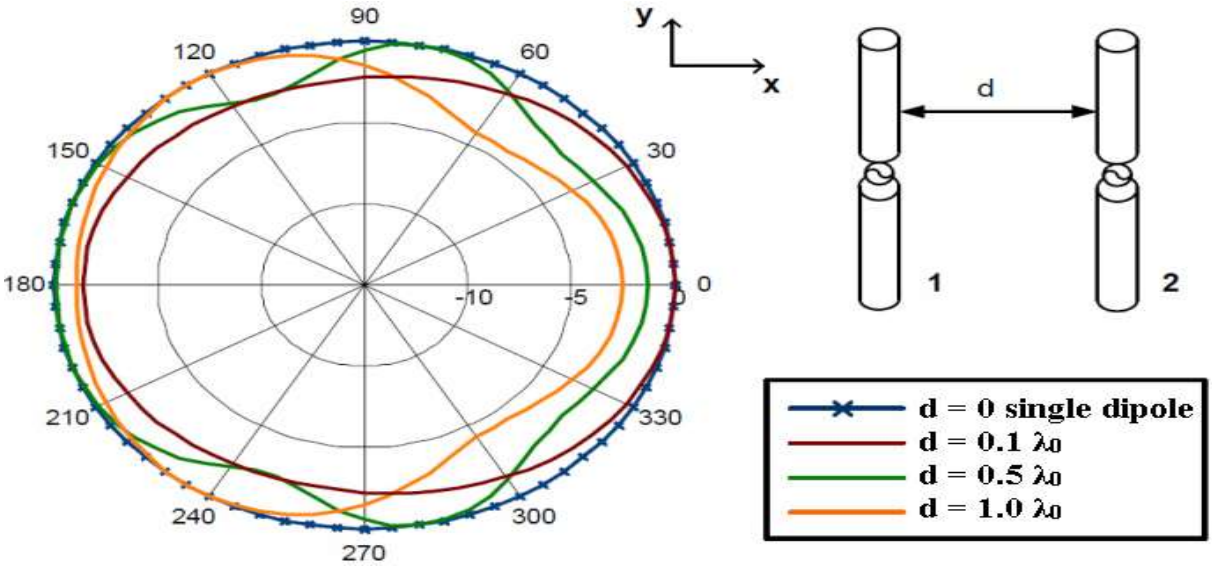

Figure 2.6: Radiation patterns of one dipole in a dual-element antenna array for different separations (d) [1]

MC depends on many factors, such as the system used, distance between antennas and/or the position of these antennas with respect to each other, antenna shielding, antenna orientation

and their polarisation states. That is, all these parameters play a significant role in determining the MC levels between the antenna in the array. Moreover, MC degrades not only their efficiencies, but also their correlation coefficients, thus diminishing the channel capacity that can be achieved. Meanwhile; in the open literature; there are many recent studies have provided important references for the design of MIMO antennas for systems capacity enhancement, but most of these references proposed only ideal dipoles or monopoles assuming those antenna elements radiating in an omnidirectional plane. In fact, when two or more dipoles/monopolies are placed closely to each other on a compact PCB terminal, the radiation patterns of each will no longer be as omni-directional due to the MC and correlation effects between them.

2.6 Coupling Reduction Techniques and Isolation Enhancement Approaches

The various isolation enhancement techniques and coupling reduction approaches reported in the open literature can easily confuse the antenna designer\researcher in terms of finding an apt solution that will fit with his/her specific application restrictions. In this section, various coupling reduction techniques commonly employed in this literature are categorised based on the coupling mechanism that they target for efficient suppression of antenna coupling. However; the coupling reduction approaches are often diverse based for a specific application and apply to a particular frequency bands (range), antenna type, and device form factor, etc. Most of the reported methodologies does not investigate the various mechanisms behind antenna coupling and there is a lack of such studies in generic modern multiple-antenna works. For a specific multiple-antenna configuration, it is essential to quantify the contribution of each of the underlying coupling mechanisms and to identify the dominant ones. Only through these types of investigations, is it possible to innovate a systematic method for improving antenna isolation, either by choosing one suitable coupling reduction approach or by a combination of a few. There are different possibilities for reducing MC between different microstrip antennas. In fact, several methods have been suggested in the extant literature for minimising or even eliminate such coupling effects based on the antenna structure and its radiation as well as feeding mechanisms, such as using EBG, DGS, resonators, or inserting slots/slits in the ground plane (as explained in detail in the next chapter) [35]. In general, each isolation technique has its advantages and disadvantages depending on the decoupling approach employed (a brief comparison of the isolation techniques is provided later in section 2.7).

2.6.1 Suppression techniques of antenna coupling through the common ground or substrate

As mentioned earlier, due to their radiating nature, antennas can vigorously alter or

change electromagnetic fields in their vicinity. Accordingly, their surrounding environment (e.g. ground, substrate, transmission lines and/or other components) is considered potentially a more supportive regarding any EM propagation. For instance, EM radiation from the antenna can easily couple inside the substrate and propagate as substrate-bound modes. The strength of the MC depends on factors such as the antenna and substrate geometries, operating frequency and orientation.

In fact, the majority of MC reduction techniques investigated in the recent literature addresses the suppression of this source of antenna coupling. Regarding this matter, different decoupling methods based on this coupling mechanism are introduced, including many common methods: Defected Ground Structure (DGS); Electric Band Gap (EBG), inserting slot and slit structures as well as applying ground stub and Current Localisation Structures (CLS),etc.

2.6.1.1 Defected Ground Structure (DGS) approach

The MC between adjacent MIMO antenna elements can be reduced by introducing some defects within the common ground plane. These act band rejection (stop-band) filters and can effectively suppress the coupled fields between adjacent elements when properly designed. This mechanism of reducing MC is denoted by the term Defected Ground Structure (DGS). There are various types of defects that can be introduced within the sharing ground plane to reduce the MC problem, e.g. introducing changes in the ground plane to vary or alert the surface current distribution and the propagation of the undesirable surface waves on it. Some of these are based on introducing a group of slits or slots, or other types of defects. DGS structures have been studied extensively over the past decade and in the next chapter, a detailed survey of such geometries for different wireless applications (Narrowband, UWB and Multiband) is provided. DGS circuits are widely used and have been successfully applied in the design of filters, amplifiers, resonators, dividers and couplers [36]. Their versatility has also been found effective in the antenna array field for coupling reduction due to their excellent pass and rejection frequency band characteristics. Consequentially, this gives a DGS the ability to suppress a surface wave over a limited frequency band [37].

In general, the properties of a DGS are equivalent to those of a resonance *LC* network and can be used to generate a limited stopband. This stopband can decrease the propagation of the surface waves and hence, reduce the MC levels between the MIMO antennas. The following formulas provide a DGS resonator:

$$Q = \frac{\omega L}{R} = \frac{2\pi f_0 L}{R} = \frac{1}{\omega CR} = \frac{1}{2\pi f_0 CR} \qquad (2.2)$$

$$FBW_{3dB} = \frac{\Delta f}{f_0} = \frac{1}{Q} \qquad (2.3)$$

where, f_0 is the resonance frequency, Q is the quality factor, FBW_{3dB} is the 3dB fractional bandwidth of the stop-band characteristics, whilst R, L and C denote the total distributed resistance, inductance, and capacitance at resonance, respectively.

The DGS method is an effective decoupling method that can be applied in various kinds of microstrip antennas. The structure does not need much modification when it is applied to different diversity antennas, since its operation depends on the resonance frequency, rather than the microstrip antenna type. Usually, it is very easy to implement as a structure on the ground plane. Moreover, the isolation mainly depends on the dimensions of the defects and number of these in the array itself. However, in practice there are some limitations regarding using this method. One serious drawback is that etchings in common ground plane destroy its integrity, sometimes not allowed in many cases due to the need of circuit integration.

2.6.1.2 Electromagnetic Band Gap (EBG) approach

A large group of researchers have taken a further step not only in ground texture but also the common substrate by embedding periodic EBG structures with forbidden frequency bands to mitigate electromagnetic waves propagation and increases the isolation levels between different microstrip antennas. When the periodicity of an EBG structure is small compared with the operating wavelength, such a structure can be described as being a high electromagnetic impedance surface (parallel resonant LC circuit model) [1]. It also acts as an electric filter, with the ability of suppressing the strong surface wave propagation in a specific frequency band, which helps to enhance the ports isolation in the printed microstrip antennas.

The operation mechanism of the EBG structure can be explained by an LC filter array [38]: the inductor L results from the current flowing along neighbouring patches through narrow lines or currents flowing through the vias, and the capacitor C due to the gap effect between these adjacent patches. For an EBG structure with patch width W, gap width g, substrate thickness h and dielectric constant ε_r, the values of the inductor L and capacitor C are determined by the following formulas [39]:

$$L = \mu_0 h \qquad (2.4)$$

$$C = \frac{W\varepsilon_0(1+\varepsilon_0)}{\pi}\cosh\frac{(2W+g)}{g} \qquad (2.5)$$

where, μ_0 is the permeability of free space and ε_0 is the permittivity of free space.

The surface impedance is equal to the impedance of a parallel resonant circuit and the central frequency of the band gap is calculated as below [40]:

$$Z = \frac{j\omega L}{1-\omega^2 LC} \qquad (2.6)$$

Reference [39] also predicts the frequency band gap as:

$$\omega = \frac{1}{\sqrt{LC}} \qquad (2.7)$$

$$BW = \frac{\triangle \omega}{\omega} = \frac{1}{\eta}\sqrt{\frac{L}{C}} \qquad (2.8)$$

where, η is the free space impedance, which is 120π. Usually, this method is not available or not applicable for wideband systems, such as the UWB, range because in this case a large number of EBG structures will be required to cover the entire range of a wide frequency. As a result, antennas will require a large area to embed these structures for broadband interest or UWB Diversity applications. Further, an intricate process is necessary to fabricate such non-planner structures, which involves cells being shorted to the ground through vias (shorting pins).Whilst proven to be effective in suppressing antenna coupling and improving efficiency characteristics, this depends on the number of EBG unit cells that are embedded between the microstrip antennas. In general, the ability of EBG structures to enhance antenna isolation depends on many factors, such as the device form, and its placement and layout constraints. However, as it is restricted by the reflection condition, an EBG structure requires a large circuit area, especially for low-frequency applications [31]. Due to its design complexity and because it has a comparatively large size, it is not commonly used for handset applications (In this thesis, a new and an applicable fractal based EBG is proposed for low-frequency application, as presented in chapter 4).

2.6.1.3 Slots / slits - etching approach

The principle of this approach is to stop the surface current flow due to the introduction of slots/slits, whereby the radiation of the antenna can be suppressed at a specific notched frequency. Surface current distribution on the common ground plane is a critical coupling source in multiple antenna systems. These slots/slits, which are similar in principle to the DGS method (as discussed in the previous subsection), form band-stop filter characteristics and create band notched functions to trap these surface currents, thus preventing them from flowing towards any passive antennas. Generally speaking, the isolation here is determined by the total length of these slots or cuts, which is commonly approximately half or quarter of the wavelength of the operating frequency (at the lowest operation frequency in multiband \ broadband applications).

2.6.1.4 Current Localisation Structures (CLS) approach

A current localisation structure is aimed at reducing the surface currents distributed on the ground plane from the perspective of the antenna itself, i.e. designing antennas with the capability of current localisation.

Usually; an extra small ground plane was located between the antennas (e.g. PIFAs) and the PCB so that the PCB was no longer acting as a ground plane for the antennas (e.g. PIFAs). The modified antennas (e.g. PIFAs) have little coupling to the PCB, and therefore this method suitable for multiple antenna implementation on non-small terminals.

The decoupling method of the current localisation can maintain the integrity of the ground plane, thereby making it convenient to integrate other components into it. However, this method has the drawback that the localisation structure designed for one antenna cannot be directly applied to others since its effectiveness largely depends on the geometries and the type of microstrip antenna. In general, the method described above is often considered to be too bulky to use in mobile devices. Several examples illustrate the utilisation of this approach in chapter three.

2.6.2 Suppression techniques of antenna coupling through space-wave radiation

As above mentioned, in a multiple-antenna system the issue is that the wave radiated by one antenna is partially received by the other(s), but this can be avoided by reconfiguring antenna radiation patterns to exhibit some nulls in its/their direction. However, strict size limitations on most state-of-art in multiple-antenna application translates into small radiating aperture areas making it difficult to realise deep nulls in the radiation pattern. In this subsection, different decoupling methods based on this coupling through space-wave radiation are introduced, including: antenna separation, Decoupling Wall Structures (DWS), the antenna placement and orientation technique, the Neutralisation Line (NL) technique, Decoupling and Matching Networks (DMN), parasitic structures and utilisation of the Meta-Material structures (MTMs) approach, etc.

2.6.2.1 Antenna separation approach

With small to medium size device dimensions, such as in handheld mobile phones, PDAs or USB dongles, MIMO antennas are very closely placed and hence, high coupling levels are inevitable. The amount of coupling depends on the separation between multiple antenna elements. In fact, this is the most critical parameter affecting MC levels. Many theoretical, analytical studies have shown that for minimum or no MC [9], the distance between antenna elements needs to be at least half wavelength to be considered as sufficient for minimising the effect of mutual coupling [9]. However, it is a major challenge to bring the two antennas closer than half the wavelength, while keeping the MC levels very low.

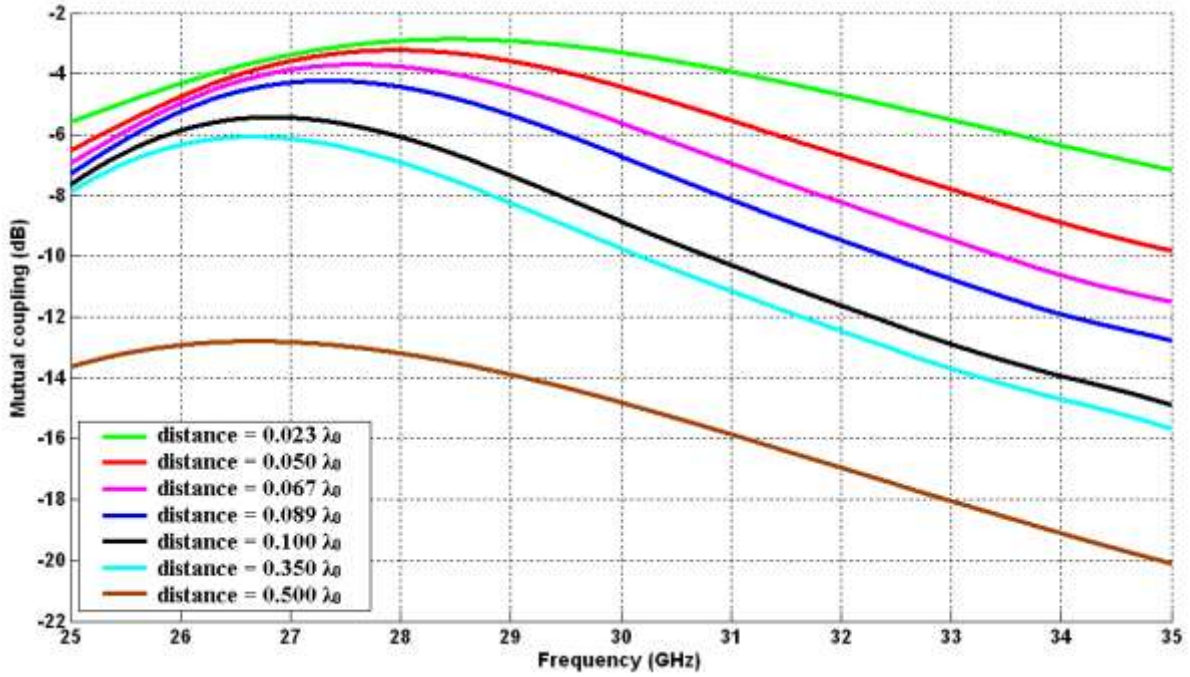

Figure 2.7: The effect of mutual coupling between two antennas with a variation of distance at 30 GHz frequency [1]

2.6.2.2 Decoupling Wall Structures (DWS) approach

To suppress antenna coupling through space-wave radiation, some researchers have adopted a conventional method of employing defects/shielding walls between different microstrip antennas [44]. In this case, the isolation level depends on the height of these defects walls and the geometries (shapes) of the embedded defects. The drawback of this solution is the needed high profiles (height of the walls) and the loading can affect antenna performance, thus making it not suitable for many practical applications.

2.6.2.3 Antenna placement and orientation approach

As is clear, closely positioned antennas within handheld mobile phones will have high coupling levels between them through the current in the ground plane as well as the radiated direct fields. This high MC will degrade both the efficiency and capacity of a MIMO system. Miniaturised multiple antenna elements are always desired, to shrink the size of the diversity system further, with there being no physical separation between each of them. A simple way to reduce these coupling effects is by placing the antennas far apart within the handset terminal, e.g. top corners, or another at bottom edges. Accordingly, a detailed position study should be conducted to access the diversity antenna parameters at various locations. The orientation of the antennas can also affect the phase of the coupling currents as well as the polarisation of the radiated fields. Adjacent antennas can be orthogonally oriented in quadrature with each other (i.e. 90^{o}) to minimise the ground as well as the field (space) coupling.

Some works relating this area will be discussed in the next chapter for different wireless applications (Narrow-band, UWB and Multi-band). In many cases, it is impossible to add any decoupling structures in a diversity system and thus, orthogonal polarisation becomes the most efficient decoupling method. In general, this solution is of great interest in MIMO systems as it not only suppresses MC, for it also adds some polarisation and pattern diversity with maximum use of the space available. In fact, this method has been used more than all other methods discussed in the literature for different wireless applications. Here, the isolation mainly depends on the spatial and angular variation of the radiating antenna elements. However, space restriction can be limit the feasibility of this isolation enhancement technique as many antenna geometries (e.g. wire antennas) occupy considerably larger areas in certain directions and impose antenna positioning limitations in compact devices. Further, most co-located antenna systems are 3D and not ideal for handset terminals. Moreover, some applications require an identical polarisation for all working antennas (such as point to point transmission).

2.6.2.4 Neutralisation Line (NL) approach

NL is a recent unconventional approach to the suppression of space-wave coupling between antennas elements. Here, an EM signal of the active antenna feeds it to the passive antenna with the proper phase to cancel out EM signal that is directly induced from the active to the passive antenna; use a suspended microstrip line to delay the signal and feed it to the active antenna A low impedance area (with minimum voltage but maximum current) of the antenna is a favourable location to connect the NL [39]. The current induced on the second antenna via the parasitic element is out of phase with that directly coupled from the first and thus, improves isolation levels. The NL prevents the surface currents flowing from one antenna towards others and traps the currents on the line (similar to the parasitic element method). The principal advantage of this technique is its simplicity and compactness; however, its design approach needs to be studied further. The isolation depends on the connection length and positioning. That is, the selection of the connection point is critical in this method, with the radiating antenna needing to have minimum impedance and maximum current. The effective bandwidth of the NL technique depends on the variation of the impedance at the selected point and thus, a low impedance point on the structure of the radiating antenna with stable impedance throughout the band of the operation is selected as the starting point. The use of this method to reduce MC between adjacent antenna array elements is covered in more detail in the next chapter for different wireless applications.

2.6.2.5 Decoupling and Matching Networks (DMN) approach

The MC between adjacent antenna elements can be reduced using decoupling

networks. Such networks will decouple the input ports of adjacent antennas, thus increasing their radiation efficiency and lowering their correlation level. Using a decoupling network usually requires the use of a matching network to provide proper input port matching. This technique has been applied to several designs, as presented in the next chapter for different wireless applications. A decoupling network method can be simple, with aim being to reduce the mutual impedance or transmission coefficients between the antennas to zero, whilst at the same time keeping good impedance matching of each antenna element. This technique does not contribute to the decoupling of EM signals received by the antennas. In other words, if ideal lumped matching networks, as well as distributed ones, are assumed, this method can be effectively used to enhance the isolation between adjacent antennas. In fact; this technique decouple electrical signals rather than electromagnetic signals and are often referred to as MC compensation techniques rather than MC reduction techniques. As a result, they do not prevent antenna coupling from degrading antenna efficiency, radiation pattern, etc. Finally, if desired, they can be combined with techniques that focus on the suppression of EM coupling between the antennas for further isolation.

2.6.2.6 Parasitic elements / structures approach

In the single antenna systems, parasitic scatterers are often used to create multi-resonance to enhance the bandwidth or design pattern reconfigurable antennas. Whilst with multiple antennas, they are added in between two radiating antenna elements as a reflector or as a resonator to reduce the MC between these antenna arrays. This is considered an applicable method for reducing MC between adjacent MIMO antenna elements, thereby enhancing efficiency, isolation and the correlation coefficient. It works as a simple principle to use parasitic elements to cancel part of the coupling fields between antennas. These parasitic elements create an opposite coupling field that reduces the original one, thus reducing the overall coupling on the passive antennas. Usually, parasitic elements are not physically connected to the antennas, such as those in or connected to the ground structure to form a sort of resonator [45]. These elements are designed to control the frequency band of isolation, the bandwidth as well as the maximum amount of coupling reduction. To summarise, the idea of using parasitic elements is to reduce MC by creating opposite fields to the original ones created by the excited antenna. Similar to the NL, a parasitic scatterer artificially creates an additional coupling path between the antenna elements and employs a parasitic radiator to provide a secondary signal to counteract the original inter-element coupling. The current induced on the second antenna via the parasitic element is out of phase with that directly coupled from the first antenna and therefore, improves isolation. In order to suppress or cancel the existing coupling, the amplitude and the phase of the coupling

coefficient can be varied by changing the structure of the scatterer.

2.6.2.7 Meta-Material Structures (MTMs) approach

Meta-materials are basically resonators structures that have negative permittivity or permeability or both. They are artificial materials, which exhibit new electromagnetic properties that cannot be found in nature. These structures have very interesting features; and can be used for isolation enhancement between adjacent elements of printed MIMO antenna systems due to the presence of a band gap in their frequency response. That is, if designed properly, the band gaps can act as a band reject filters and suppress MC between adjacent antenna elements. In this case, the isolation mainly depends on the unit cells geometries and their numbers in the array. Several examples have appeared in the literature that utilise MTM based structures for isolation enhancement in the form of, for instance, Split Ring Resonators (SRRs), Close Loop Lines (CLLs) or meander lines. (as presented in detail in the next chapter)

2.6.3 Suppression techniques of antenna coupling through near-field coupling (via reactive fields)

In cases where space restrictions impose small antenna spacing, antennas might also become subject to near-field coupling. For a fixed number of antennas in an array, the beam becomes wider as the antenna separation decreases. Diversity gain is also reduced, if antenna separation is smaller than half the operation wavelength. A wider pattern and/or a lower diversity gain implies a greater possibility of intercepting the radiation from one antenna to another.

2.7 Comparison of the Different Suppression Techniques and Isolation Approaches

A summarised comparison of the numerous coupling reduction techniques and isolation approaches that have been introduced in this section is provided in Table 2.1

Table 2.1: presents a comparative review of the different coupling methods across the many aspects drawn from the literature

issue / approach	Applications			Design complexity	Problems
	Narrow-band	UWB	Multi-band		
EBG	highly applicable	not applicable	rarely applicable	complex	EBG structure requires a large circuit area, especially for low frequency range
DGS	highly applicable	rarely applicable	rarely applicable	complex	Etching DGS in the ground plane destroys its circuit integrity.

Slots \ slits	highly applicable	moderately applicable	moderately applicable	moderate	Narrow BW characteristics and is determined by the total length of these slots or cuts
CLS	rarely applicable	not applicable	rarely applicable	moderate	This method considered too bulky to use in portable devices
Separation	highly applicable	rarely applicable	highly applicable	simple	Large size constraint for mobile handheld devices
DWS	rarely applicable	not applicable	not applicable	complex	High profiles needed and thus not suitable for many practical applications
Placement & orientation	highly applicable	highly applicable	highly applicable	simple	Space and polarisation restriction and thus, considered not ideal for handset terminals
Metallic stubs	rarely applicable	highly applicable	highly applicable	moderate	Increases weight, Placement dependent
NL	highly applicable	rarely applicable	rarely applicable	moderate	Modelling is difficult and selection of the connection point is critical in this method
Parasitic elements	highly applicable	rarely applicable	rarely applicable	simple	Causes a drop in efficiency and the radiation characteristics are changed
MTMs	highly applicable	rarely applicable	moderately applicable	complex	Narrowband operation

2.8 The Correlation / Diversity Performance Analysis

The correlation coefficient is the measure of the effectiveness of any MIMO system. It directly affects the diversity performance and it defines the independence between signals in the transmitter/receiver of the diversity system. The correlation between dual antennas is highly influenced by how the antennas are positioned on a handheld terminal, how they interact with each other, their field patterns significantly change and this difference in the antenna patterns affect on correlation also their polarisation in some cases will change the correlation characteristics. In general, a low correlation can be achieved when the received signals from multiple antennas have high diversity gain. Moreover, the power levels of the received signals should not be too different in the diversity system, especially when located in a multipath environment. The correlation coefficient measures this independence, varying from one and zero [46], with the ideal value being equal to zero (in practice, this is impossible).

If the envelope correlation coefficient is close to zero ($\rho_e \approx 0$) over the bandwidth, this means that the patterns of the multiple antennas are de-correlated and demonstrates an excellent diversity condition.

However, when correlation coefficient is greater than zero ($\rho_e > 0$), this means there is dependency between the signals such that the diversity gain will be reduced. Analysis has shown that where the correlation is not too close to unity or ($\rho_e \leq 0.7$), the degradation of the diversity gain due to envelope correlation is given by the degradation factor (DF) of the following equation [41].

$$DF = \sqrt{1-\rho_e} \qquad (2.9)$$

The correlation and the MC have a direct relationship, i.e. the lower the former, then the lower the latter. When designing an antenna array low MC characteristics are required to obtain an optimum diversity gain [47]. In other words, the correlation coefficient should be kept low enough so that diversity is still effective. In sum, low correlation between signals in the receiver / transmitter is essential for the capacity enhancement of wireless MIMO systems.

2.8.1 Envelope Correlation Coefficient (ECC) calculations

In diversity systems, there are two empirical methods had been used for envelope correlation coefficient calculations between diversity antennas. The first is based on the far-field radiation patterns characteristics; however, it is considered a very time-consuming process. That is. it requires corresponding numerical or experimental analysis and thus, is a cumbersome process. Alternatively, the correlation coefficient can be evaluated based on the radiation patterns obtained from the MIMO design. Then, their performance can be assessed through measurements in a reverberation chamber that can provide relative values for the measured correlation coefficient in a specific environment.

The independency can be measured using the general expression of the complex cross-correlation coefficient (ρ_c) between any multiple antennas, for the angular domain [48] in which the full spherical antenna pattern characteristics, including the phase and polarisation information in all the directions, are required. Also, this is under the assumption that the received signals have a Rayleigh distributed envelope and randomly distributed relative phases. The complex cross-correlation ρ_c is evaluated using the radiation pattern characteristics given in [49]:

$$\rho_c = \frac{\left(\oint \left(XPR\, E_{\theta 1}(\Omega) E^*_{\theta 2}(\Omega) P_\theta(\Omega) + E_{\phi 2}(\Omega) E^*_{\phi 2}(\Omega) P_\varphi(\Omega) d\Omega\right)^2}{\oint \left(XPR\, G_{\theta 1}(\Omega) P_\theta(\Omega) + G_{\phi 1}(\Omega) P_\phi(\Omega)\right) d\Omega \cdot \oint \left(XPR\, G_{\theta 2}(\Omega) P_\theta(\Omega) + G_{\phi 2}(\Omega) P_\phi(\Omega)\right) d\Omega} \qquad (2.10)$$

where, $\Omega = (\theta, \phi)$, $G_\theta = E_\theta(\Omega) E^*_\theta(\Omega)$, $E_{\theta 1}(\Omega)$ and $E_{\theta 2}(\Omega)$ are the θ polarised complex radiation patterns of antenna-1- and antenna-2- in the diversity system and $d\Omega = \sin\theta \, d\theta \, d\phi$. $P_\theta(\Omega)$ and $P_\phi(\Omega)$ represent the incident power spectrum for both polarisations,

whilst XPR (cross polar discrimination of the incident field) is the ratio of time average

vertical (θ) power to time average horizontal (ϕ) power [50]:

$$XPR = \frac{p_v}{P_H} \qquad (2.11)$$

where, P_V is the average vertical power and P_H is the average horizontal power. XPR is also referred to as the cross-polarisation power ratio or cross-polar discrimination (XPD). $P_\theta(\Omega)$ and $P_\phi(\Omega)$ are the angular density functions of the vertical and horizontal plane respectively. For reference purposes, θ is the angle relative to the vertical axis z and ϕ is the angle in the horizontal plane, as shown in Figure 2.8.

Correlation can also be expressed using the envelope correlation coefficient ρ_e relating to complex cross- correlation coefficient by the following relationship [43]:

$$\rho_e \approx |\rho_c|^2 \qquad (2.12)$$

As mentioned earlier, this is a complicated expression requires three-dimensional radiation pattern measurements and numerical integration to get the envelope correlation coefficient. Thus, a second method has been derived, which is suitable for experimental measurements and requires a knowledge of the scattering parameters obtained on the antennas elements. This applicable method is that which has been adopted throughout the thesis.

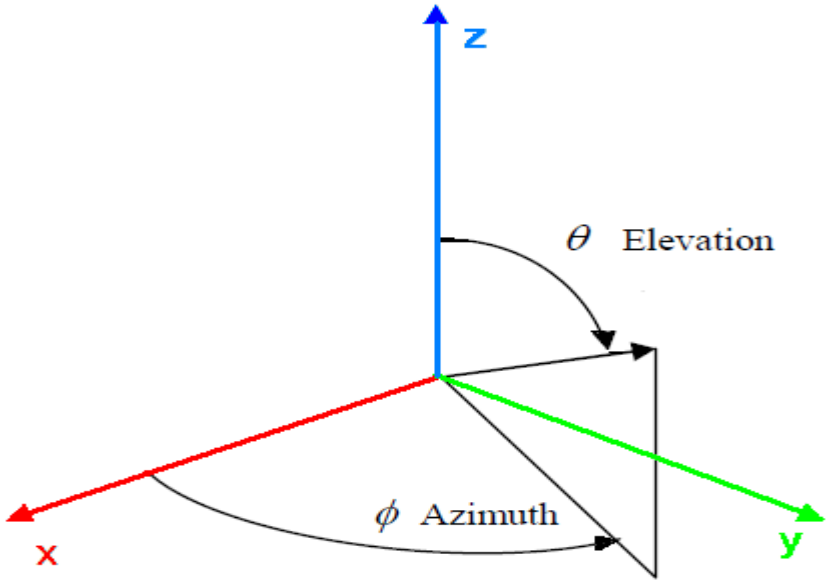

Figure 2.8: Diagram showing the relation of angular coordinates to cartesian coordinates

As above mentioned, it is a much more convenient approach to calculate the envelope correlation coefficient using the scattering parameters, rather than the 3-dimensional radiation pattern characteristics of the antennas array system, as follows [51,58]

$$\rho_{12} = \frac{|S^*_{11}S_{21} - S^*_{12}S_{22}|^2}{(1-|S_{11}|^2-|S_{21}|^2)(1-|S_{22}|^2-|S_{12}|^2)} \qquad (2.13)$$

In this formula, only the S-parameters need to be known and the radiation efficiencies can be evaluated easily, as compared to 3D radiation patterns required by the previous equation (2.10). At the same time, with the S-parameters approach, the ECC is directly evaluated using S-parameters of the array system, under the following assumptions: i) the antenna system is a lossless structure; ii) one antenna is excited, while the other(s) is/are terminated with a reference impedance (such as 50 ohms); and iii) the antenna system is in a uniform scattering environment (such as indoor propagation).

It is important to mention that the isolation and correlation coefficient are two different things. High isolation does not guarantee a low correlation coefficient and vice versa; however, both are required for good performance out of a diversity antenna system. In this thesis, the correlation coefficients in different multiple antennas are calculated from scattering matrices, which are easy obtained from simulated results. Whilst several methods have been proposed to improve the isolation between adjacent antenna array elements, this does not guarantee good correlation performance, because Eq. (2.13) does not consider field interactions, as mentioned before.

2.9 Different Antennas Arrays for Coupling and Diversity Comparison

As described earlier, In MIMO systems, multiple antenna elements are required at both receiver and transmitter side [52]. However; installing multiple antenna elements in the small space available in portable devices will inevitably cause severe mutual coupling and significantly degrades the diversity performance [53].

Thus one of the main challenges to employing MIMO systems in mobile devices is the design of small MIMO antennas with lowest mutual coupling [53]. A separation between multiple antenna elements is the most critical parameter affecting mutual coupling [4].

When a multiple-element antenna embeds into the small mobile terminal, it should be compact as much as possible. Additional requirements should be met, e.g., low mutual coupling and robustness while maintaining on the compactness with acceptable diversity performance for multiple antennas [5]. Therefore, in designing the antenna for the mobile terminal, it is important to balance the trade-off between compactness and performance [5],[52]. In the open literature; very few investigations have been done as a comparative study based on the diversity performance (such as mutual coupling and envelope correction coefficient) between more than two microstrip antennas types.

However; this study presents a new comparative study between four different microstrip

antenna array types (PIFA, patch, monopole, and slot) with regular shapes such as rectangular and square. One of the important considerations in designing these antennas is maintaining on the compactness (total antennas dimensions: 110 mm × 60 mm); to be working in a single narrow frequency band. However; all these antennas are proposed and designed to operate at frequency 1.9 GHz band which is suitable for PCS applications.

Diversity performances such as mutual coupling and envelope correlation coefficient for different antennas array types have been carried out to investigate the effect of the antenna separation. It provides a complete view compared with other works in the literature that most of them are focused only on just one or two common microstrip antenna types such as the patch or monopoles antennas only [56-57].

2.9.1 Antenna design and configuration

The four different microstrip antennas are etched on a thin FR_4 substrate ($\varepsilon_r = 4.4$ and h = 1.6 mm) with total dimensions: 110 mm × 60 mm to be suitable for most mobile PCB circuit boards. A good impedance matching ($S_{11} < -10$ dB, VSWR < 2) is achievable across the operating frequency (1.9 GHz) for all the antenna designs. These antennas are separated by a distance *d*, which is made to vary from 0.3 λ_0 to 1.0 λ_0 to investigate an antenna diversity performance such as the mutual coupling and envelope correlation coefficient.

2.9.1.1 Dual PIFA antenna array

The dual PIFAs antenna array are shown in Figure 2.9. The minimum space distance of these antennas is *d* = 50 mm (corresponds 0.3 λ_0 approximately) measured from element centre to centre. Each PIFA element has a square patch outline of 35 mm as equal width and length (corresponds $\lambda_0/4$ approximately).

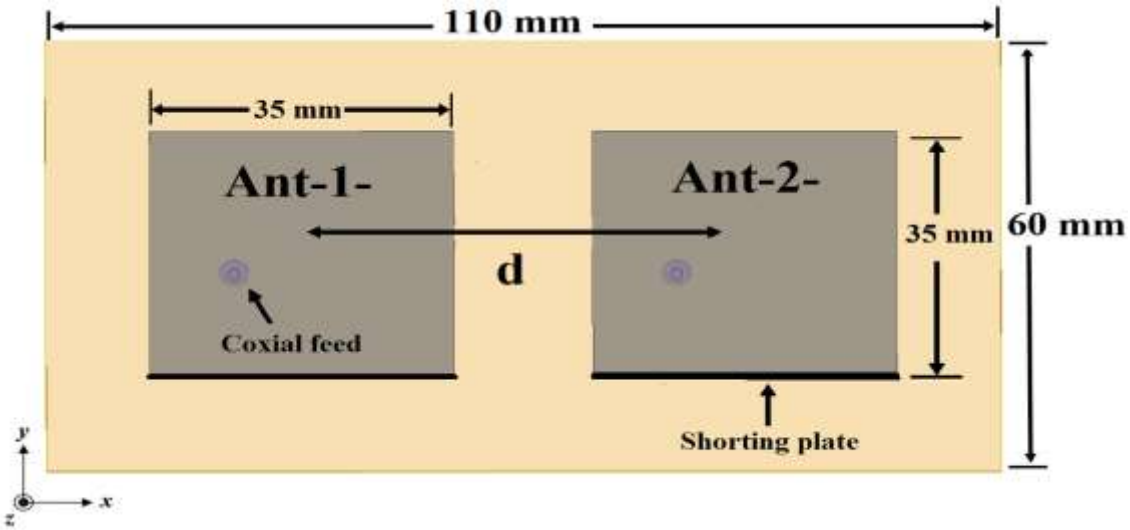

Figure 2.9: Configuration of the dual PIFA antenna array (Top view)

The return loss (S_{11}) and mutual coupling (S_{21}) of the dual PIFA antennas are illustrated in Figs. 2.10(a) and (b); respectively. The result of the return loss, as presented in Figure 2.10(a), indicates that the PIFA antenna at −10 dB has fixed low BW of 0.036 GHz approximately. The Figure 2.10(b) clearly shows that the strongest mutual coupling is found at the resonant frequency of the dual antenna elements, while the mutual coupling is decaying away from the PIFA resonance as the space between antennas linearly increases. An average of 22 dB reduction in the mutual coupling level is obtained as the distance is increased from 0.3 λ_0 to 1.0 λ_0.

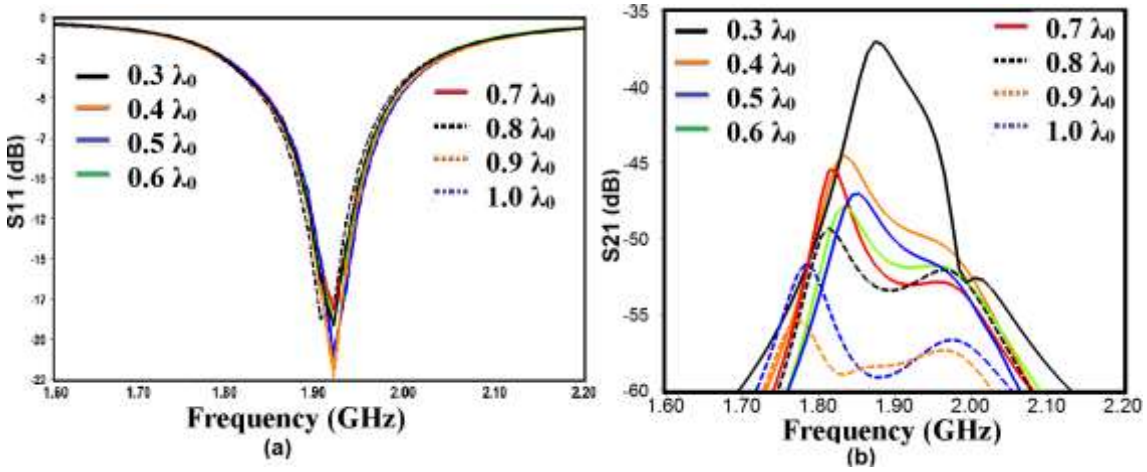

Figure 2.10: The simulated S-parameters of the PIFA antenna array when *d* varying in terms of λ_0 **(a)** S_{11}, **(b)** S_{21}

2.9.1.2 Dual patch antenna array

The dual patch antenna array are shown in Figure 2.11. The minimum space of the antennas is *d* = 48 mm (corresponds 0.3 λ_0 approximately at the resonant frequency) measured from element centre to centre. Each patch element has a rectangular outline with 35 mm width and 45 mm length (corresponds 0.28 λ_0 approximately).

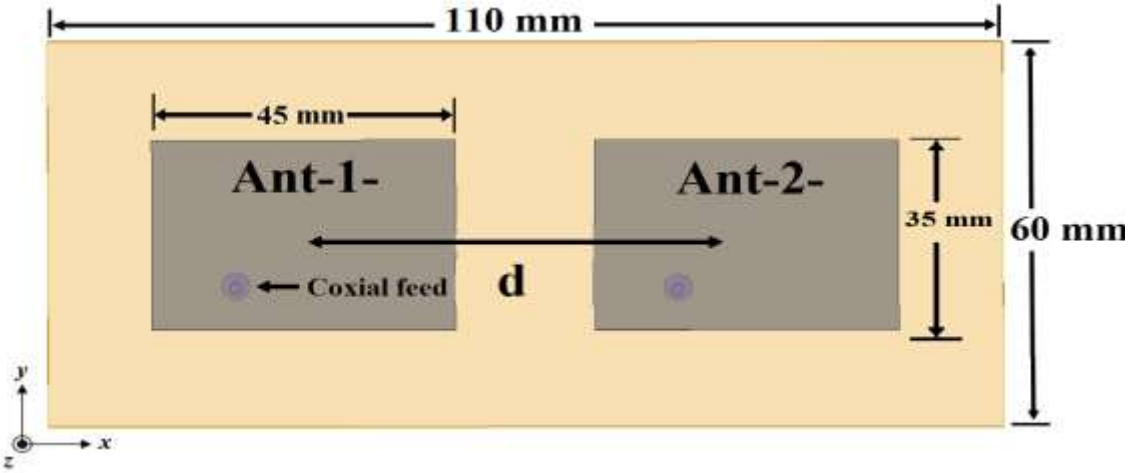

Figure 2.11: Configuration of the dual patch antenna array (Top view)

The return loss (S_{11}) and mutual coupling (S_{21}) of the dual patch antennas are illustrated In Figures 2.12(a) and (b); respectively. The result of return loss, as presented in Figure 2.12(a), shows that the patch antenna at −10 dB has reasonable BW of 0.05 GHz approximately. The Figure 2.12(b) clearly shows that mutual coupling is decreasing linearly as the space between antennas increase. An average of 6 dB reduction in the mutual coupling level is obtained as the distance is increased from 0.3 λ_0 to 1.0 λ_0.

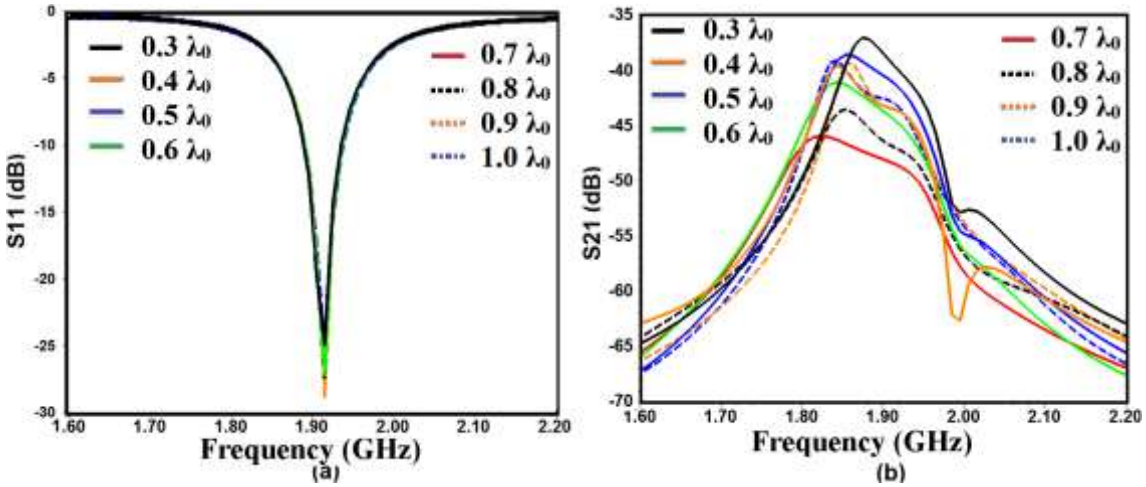

Figure 2.12: The simulated S-parameters of the patch antenna array when *d* varying in terms of λ_0 **(a)** S_{11}, **(b)** S_{21}

2.9.1.3 Dual monopole antenna array

The dual monopole antenna array are shown in Figure 2.13. The minimum space of these antennas is *d* = 50 mm (corresponds 0.3 λ_0 approximately) and measured from element centre to centre. Each monopole element has a rectangular outline with 33 mm width and 47 mm length (corresponds 0.28 λ_0 approximately).

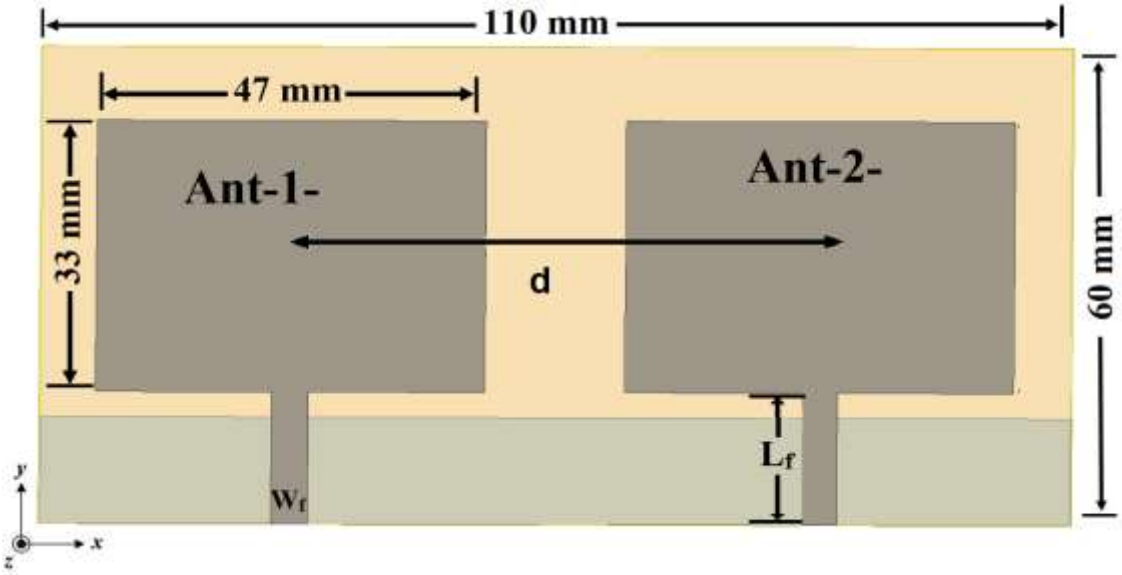

Figure 2.13: Configuration of the dual monopole antenna array (Top view)

The return loss (S_{11}) and mutual coupling (S_{21}) of the dual monopole antennas are illustrated in Figures 2.14(a) and (b); respectively. The result of return loss, as presented in Figure 2.14(a), indicates that the monopole antenna at −10 dB has wide BW of 0.6 GHz approximately. The Figure 2.14(b) clearly shows that the mutual coupling is decreasing linearly as the space between antennas increase. An average of 17 dB reduction in the mutual coupling level is obtained as the distance is increased from 0.3 λ_0 to 1.0 λ_0.

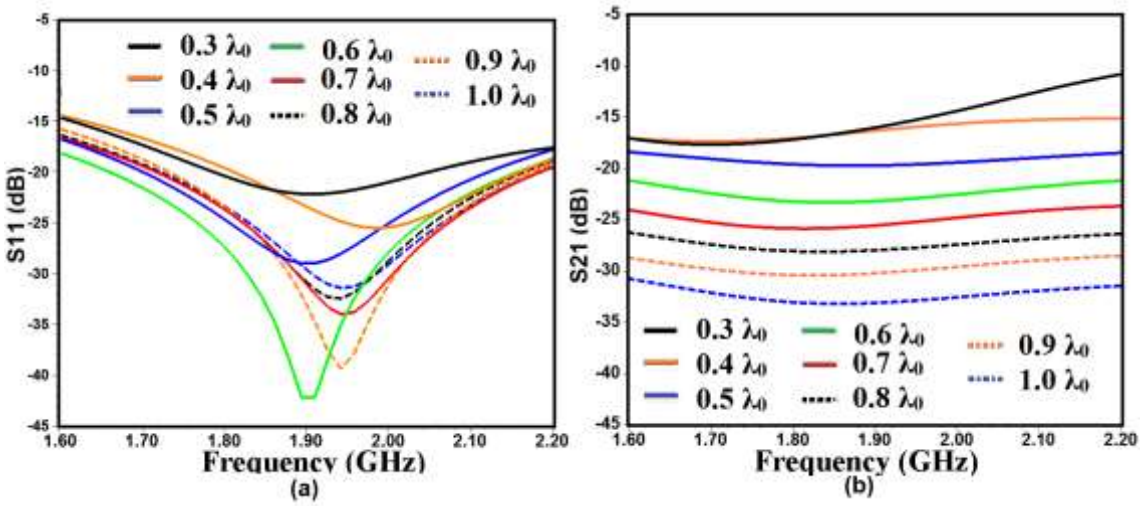

Figure 2.14: The simulated S-parameters of the monopole antenna array when *d* varying in terms of λ_0 **(a)** S_{11}, **(b)** S_{21}

2.9.1.4 Dual slot antenna array

The dual slot antenna array are shown in Figure 2.15. The minimum space of these antennas is *d* = 52 mm (corresponds 0.3 λ_0 approximately) measured from element centre to centre. Each slot element has a rectangular outline plate with 60 mm width and 48 mm length (corresponds 0.29 λ_0 approximately).

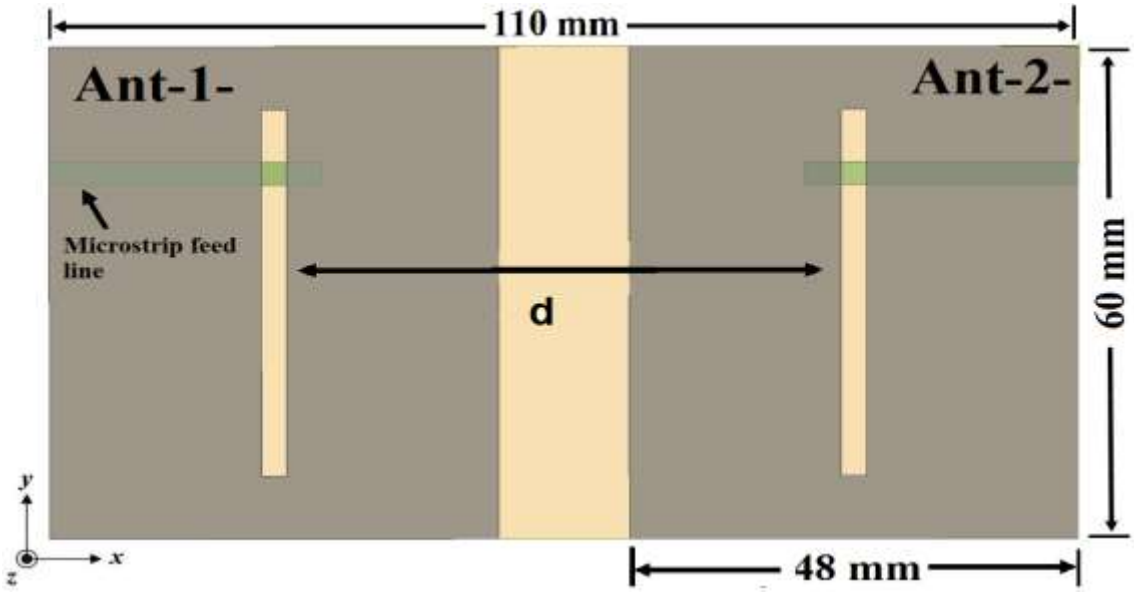

Figure 2.15: Configuration of the dual slot antenna array (Top view)

The return loss (S_{11}) and mutual coupling (S_{21}) of the dual slot antennas are illustrated in Figures 2.16(a) and (b); respectively. The result of return loss, as presented in Figure 2.16(a), indicates that the monopole antenna at −10 dB has moderate BW of 0.23 GHz approximately. The Figure 2.16 (b) clearly shows that the mutual coupling is decreasing linearly as the space between antennas increase. An average of 16 dB reduction in the mutual coupling level is obtained as the distance is increased from 0.3 λ_0 to 1.0 λ_0.

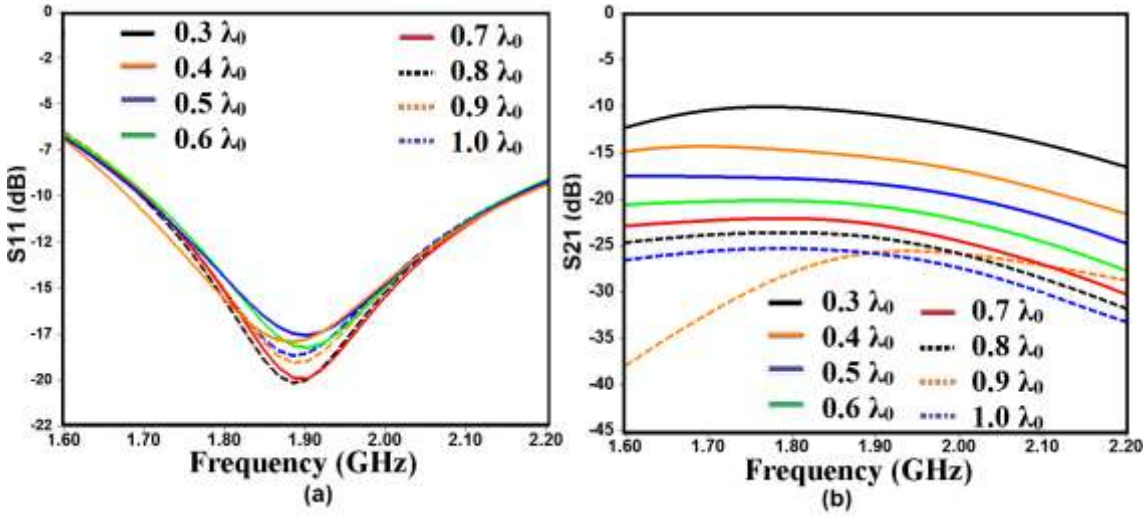

Figure 2.16: The simulated S-parameters of the slot antenna array when *d* varying in terms of λ_0 **(a)** S_{11}, **(b)** S_{21}

2.9.2 Performance summary and comparison

2.9.2.1 Coupling of different antennas types at varying separation

First; the mutual coupling of various antenna array types is investigated when the separation between these antennas are varying from 0.3 λ_0 to 1.0 λ_0 as presented in Table 2.2.

Table 2.2: Comparison of MC (S_{21}) in dB at 1.9 GHz between four different antenna types at varying separation (in terms of λ_0)

Separation	PIFA	Patch	Monopole	Slot
0.3 λ_0	-37.2	-38.8	-16.3	-10
0.4 λ_0	-45.74	-43.1	-16.4	-11
0.5 λ_0	-49.13	-40.17	-19.4	-15.5
0.6 λ_0	-50.6	-43.9	-23	-18
0.7 λ_0	-51.5	-48.15	-25.5	-20.7
0.8 λ_0	-52.3	-46	-27.7	-22.5

0.9 λ_0	-58.4	-43.3	-30	-24
1.0 λ_0	-59.12	-44	-33	-26

In Figure 2.17, the mutual coupling for the various antenna types is investigated when the separation between these antennas are varying from 0.3 λ_0 to 1.0 λ_0. From the simulated results, it clear that highest isolation (better case) can be obtained between two PIFA antennas of ≤ -58 dB (linearly decreases at separation > 0.4 λ_0), and smaller than the mutual coupling of the patch antennas, followed by monopole antennas and finally slot antennas suffering highest mutual coupling (worst case) compared with other antenna types.

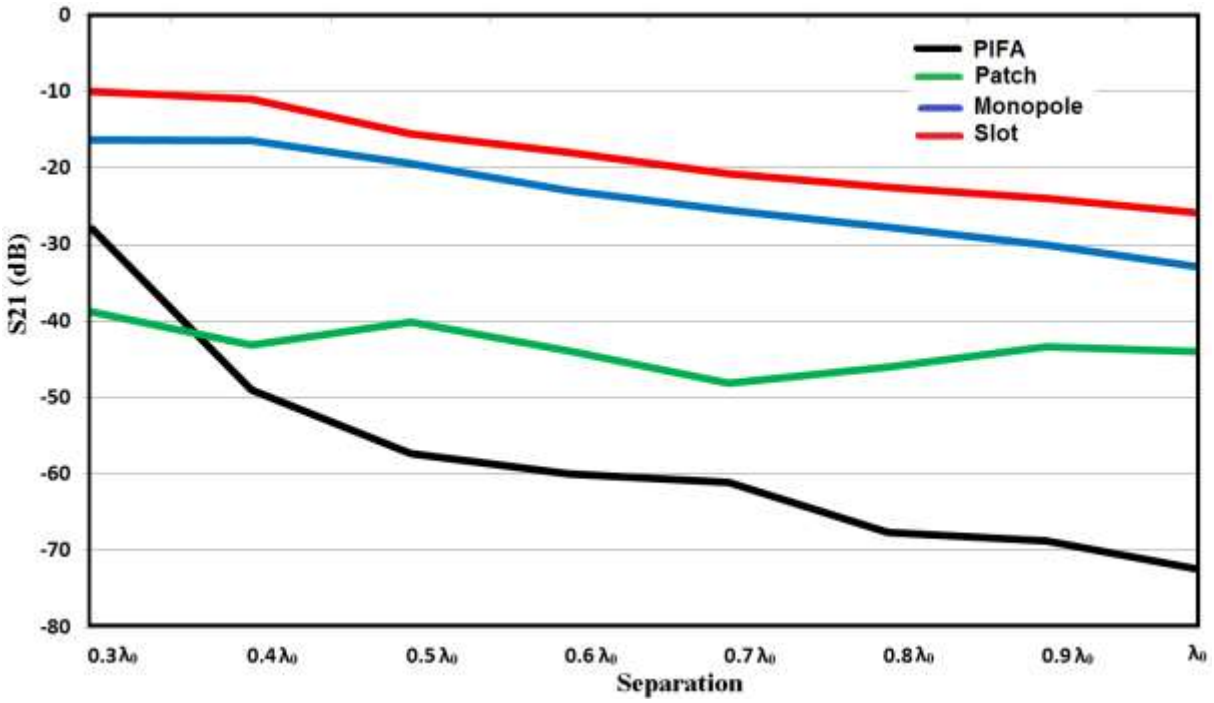

Figure 2.17: Comparison of MC with different antennas types at varying separation (in terms of λ_0)

2.9.2.2 Correlation of different antennas types at varying separation

Secondly; Envelope Correlation Coefficient (ECC) between antenna array elements is investigated according to antennas separation variation, in this work, ECC of different microstrip antenna array types was evaluated using S-parameters of the MIMO system as defined before in Eq. (2.13), which assumed that antennas system are lossless, and the antennas are excited separately, keeping the other antennas matched terminated. Although the calculation of ECC using S-parameters approach in is a very simple and fast, it is only accurate for the case of loss free antennas. In general; the antennas tend to be more correlated (coupled). A strong mutual coupling means a high correlation between the received signals by antenna elements; the high level of correlation affects and degrades all the performance

parameters of the MIMO and diversity system, as an example, the antenna efficiency becomes worse and both system channel capacity and diversity gain will decrease.

Table 2.3: Comparison of the ECC in dB at 1.9 GHz between four different antenna types at varying separation (in terms of λ_0)

Separation	PIFA	Patch	Monopole	Slot
0.3 λ_0	-38	-30	-14.83	-10.6
0.4 λ_0	-31	-33.8	-21.87	-19.2
0.5 λ_0	-42	-56	-22	-27.8
0.6 λ_0	-40.5	-34	-16	-29.7
0.7 λ_0	-48.9	-33.16	-22	-31.5
0.8 λ_0	-51.8	-36	-24.4	-38.8
0.9 λ_0	-50	-41	-23.1	-40.2
1.0 λ_0	-50	-45	-17.35	-40.1

In Figure 2.18, the envelope correlation coefficient for the different antenna types is investigated when the separation between these antennas are varying from 0.3 λ_0 to 1.0 λ_0.

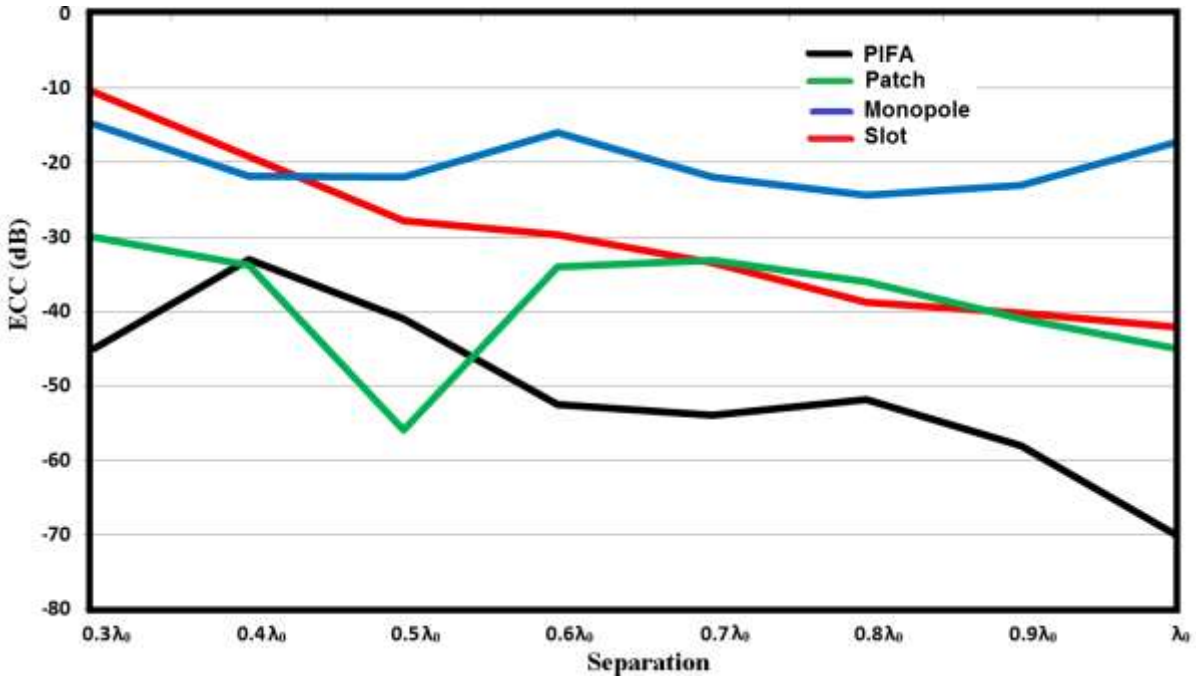

Figure 2.18: Comparison of envelope correlation coefficient (ECC) with different antennas types at varying separation (in terms of λ_0)

From the simulated results, the envelope correlation coefficient in the working band of the Patch antenna and PIFA antenna are respectively; lower than -30 dB (at separation ≤ 0.58 λ_0) and -40 dB (at separation ≥ 0.58 λ_0), which are smaller than that other antenna types (slot and monopole). This observation indicates better behaviour and diversity performance of MIMO antenna system will be achieved by using these antenna types (PIFA and patch).

2.9.2.3 Performance of different antennas types at a fixed separation

Finally, a comparison of various antenna performance parameters at resonant frequency including return loss, BW, gain, directivity and radiation efficiency for different microstrip antenna array types is shown in Table 2.4 at fixed minimum separation between these antennas ($d = 0.3\ \lambda_0$).

Table 2.4: Comparison table of the antennas performance between four different antenna types at fixed separation ($d = 0.3\ \lambda_0$)

Antenna type	f_r, GHz	S_{11}, dB	BW, %	Gain, dBi	Dir, dBi	Rad eff, %
PIFA	1.93	-23.2	1.90	2.7	3.8	75
Patch	1.92	-21	2.63	3.1	5.45	55
Monopole	1.93	-22	30	1.4	1.5	90
Slot	1.94	-24.8	12.2	2.3	2.48	86

It is apparent from Table 2.4 that both PIFA and patch arrays achieve a narrower (lower) performance in terms of BW, with a close values of 1.90 % and 2.63 %, respectively, followed by the slot antenna array with a moderate BW value of 12.2 % and finally the monopole antenna array achieves a wider BW performances with a value of 30 %. It should be noted that the considered BW corresponds to the frequency range over which VSWR is < 1.92. Means a return loss of 10 dB or about 11% reflected power. As regards the radiation characteristics, the patch antenna array offers a higher directivity and gain with an average efficiency factor (55 %) as seen in the same table. In the second position comes the PIFA array that achieves a reasonable directivity of 3.8 dB with moderate radiation efficiency of 75%, immediately followed by slot and monopole antenna arrays with highest radiation efficiency (≥ 90 %), with a reasonable directivity of 2.48 dB and 1.5 dB; respectively.

2.10 Chapter Summary

In MIMO systems, more than one antenna is implemented on a small terminal. However, having multiple antennas on small terminals (such as mobile handsets or PDAs), while maintaining their performance, remains a significant challenge task for each antenna designer in terms of reducing the MC and correlation effects between these MIMO antennas. In this chapter, the essential background theory to the mutual coupling (MC) problem in microstrip array antennas has been discussed.

The essential requirements/challenges when designing multiple antennas in small terminals regarding the antenna coupling mechanisms and isolation enhancement approaches have been identified.

For a multiple-antenna configuration, it is essential to quantify the contribution of each of the underlying coupling mechanisms and to identify the dominant ones. Only through these types of investigations, is it possible to devise a systematic method for improving antenna isolation, either by choosing one suitable coupling reduction approach or through a combination of more than one.

There are different possibilities for reducing MC between different microstrip antennas. In fact, several methods have been suggested in the extant literature for minimising or even eliminating such coupling effects based on the antenna structure and its radiation as well as feeding mechanisms, such as using EBG, DGS, resonators, or inserting slots/slits in the ground plane (as explained in detail in section 2.6).

In general, each isolation technique has its advantages and disadvantages depending on the decoupling approach employed; a brief comparison of the isolation techniques has been provided in section 2.7.

Furthermore, a new comparative study involving four different microstrip antenna array types (PIFA, patch, monopole, and slot), based on diversity performance (mutual coupling effects and correction), has been explained in detail (in section 2.9).

The major content of this chapter is a manuscript published and presented at the Loughborough Antennas and Propagation Conference (LAPC 2017) [R5]. The introduction and other sections of this chapter have been rewritten to create a better flow and to prevent a repetition of the materials already to be found in other chapters.

Chapter 3: Survey of coupling suppression techniques for different wireless applications

3.1 Survey of Techniques for Mutual Coupling Reduction and Isolation Enhancement

In this thesis, various mutual coupling reduction methods or techniques that commonly employed in the open literature are mainly categorised based on the coupling mechanisms that they target for more efficient suppression of antenna coupling, and then in this chapter; we provided a summarised overview of previous methodologies as sub-sections under these main classifications.

Therefore, in these subsections; we define and discuss three major wireless applications that are central to this research work. These main three wireless applications concentrated on narrowband, Ultra-wide-band (UWB) and multiband.

3.1.1 Suppression techniques of antenna coupling through common ground \ substrate

In this category, different decoupling methods or approaches based on the coupling mechanism (surface waves) are introduced, including: Defected Ground Structure (DGS) structures, Electromagnetic Band Gap (EBG) structures, Inserting slots\slits structures, inserting GND stubs, Current Localization Structures (CLS), shorting pins\vias approach, etc.

3.1.1.1 Defected Ground Structures (DGS) approach

Narrow-band-MIMO Antennas – Most of the works explored so far include different DGS shapes based on introducing a group of slits such as use of the dumb-bells like DGS as presented in [59-67], rectangles defects [68-73], spirals periodic DGS [74-75], S-shaped periodic DGS [76], other defective strips as proposed in ref [36, 78].

Moreover; a few types of fractals defects also exist, and an excellent survey of such geometries can be found in the recent literature [79-82]. Most of these existing works have been investigated for *E*-plan coupling only and DGS structures in these arrays not proposed for *H*-plan coupling except the works introduced in [66, 75-76, 81-82]. However; in these works, there are some weaknesses such as a lack of impedance matching and not mentioned other valuable information (e.g. how much droopiness in radiation efficiency).

Briefly; one of these designs is now described in more detail as below: In ref [81], A new Fractal based DGS (FDGS) was investigated. The structure is proposed with bandgap filter characteristic are used to reduce mutual coupling between diversity antenna elements, as shown in Figure 3.1.

More than 30 dB mutual coupling reduction between dual coplanar antenna elements is obtain ed by using third iterative FDGS.

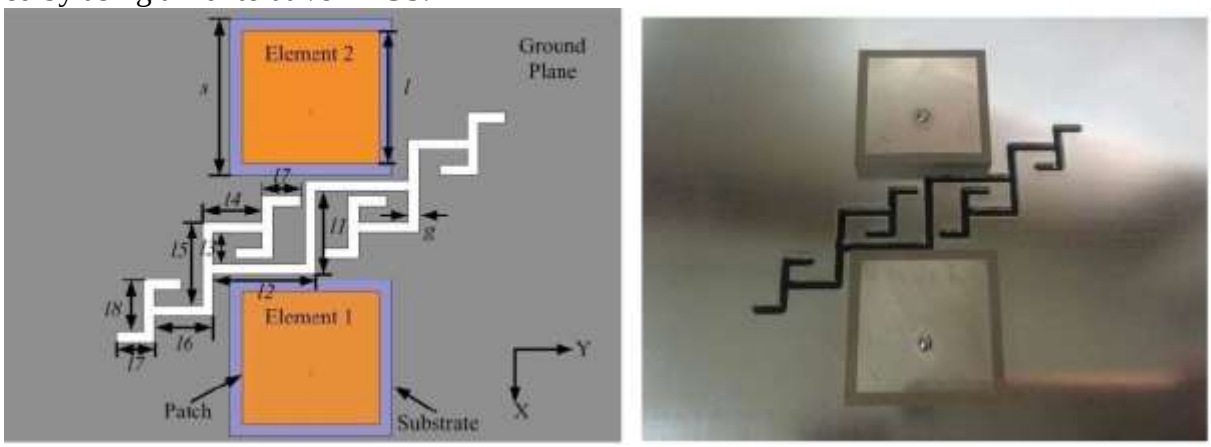

(a) **(b)**

Figure 3.1: Configuration of closely-packed antenna with FDGS structure used as an isolation method for narrowband applications. **(a)** Schematic and **(b)** Fabricated MIMO [81]

UWB-MIMO Antennas – Many previous works are presented in literature such as single DGS embedded in the ground plane to reduce the coupling between diversity UWB antennas as introduced in [83-87]. Other works introduced some multiple DGS etched on the common ground to enhance the isolation between UWB-MIMO antennas as presented in ref [88-91]. Most of these works; DGSs were embedded with cooperation with other approaches except ref [89]. Almost all DGS based techniques are combined with other methods (i.e. placement and orientation approach) because of DGS structures are applicable in narrowband\multiband only rather than UWB operation.

However; the diversity antenna in this [89] has good isolation (<-20 dB) over a band spanning from 7 GHz to 10.6 GHz (after DGS insertion), and the drop in radiation efficiency (also peak gain) is not measured (before and after DGS insertion).

Briefly; one of these designs is now described in more detail as below:

In [88], a compact wide-band (from 2.4 GHz to 6.5 GHz) MIMO antenna is presented. Here; new bent slits are etched into the common ground plane (as shown in Figure 3.2). The bent slits can reduce the mutual coupling effectively and have a slight effect on the reflection coefficient. It has found that the isolation is more than – 18 dB over the wide bandwidth with edge-to-edge separation of nearly 0.08 λ_0 at frequency of 2.5 GHz.

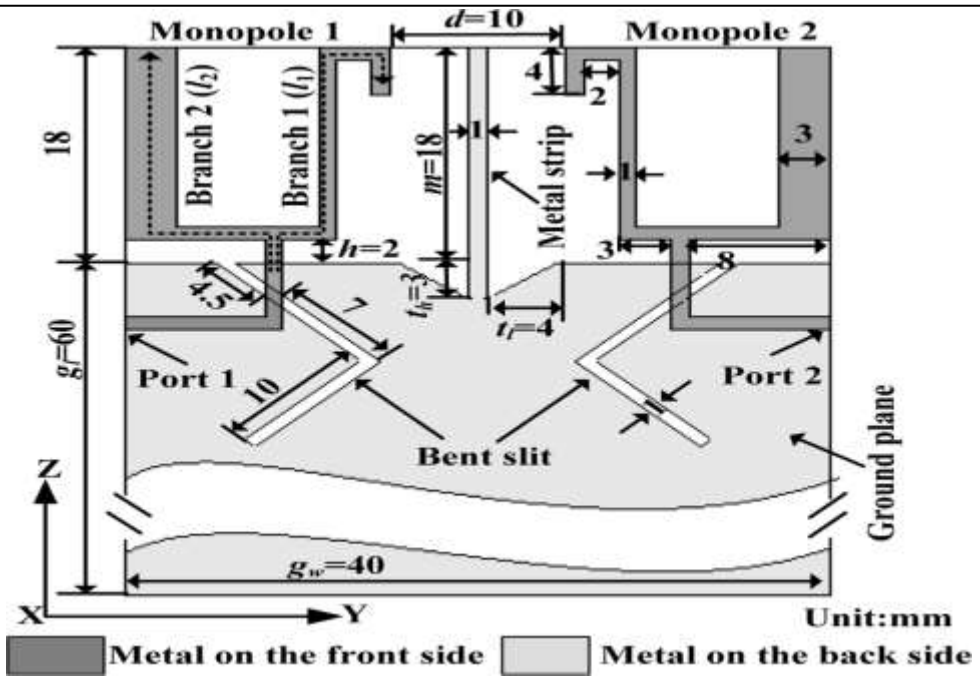

Figure 3.2: Structure of the UWB antenna with bent DGS used as an isolation method for UWB applications [88]

Multi-band-MIMO Antennas – A previous works related to dual-band applications were presented in ref [92-100], tri-bands [101-102], and quad-bands [103-104]. Briefly; one of these designs is now described in more detail as below: In [104], proposed a novel quad-band antennas with two radiating elements suitable for LTE and Wi-Fi applications in handheld devices, To achieve high isolation between the dual radiating elements, a defected ground plane (a combination of rectangular slot ring and inverted T-shaped slot stub) is employed (as shown in Figure 3.3). However; MIMO design provides good isolation (more than 24 dB achieved) also, the author showed that the dual antenna elements have excellent ECC and relative MEG for all the operating bands.

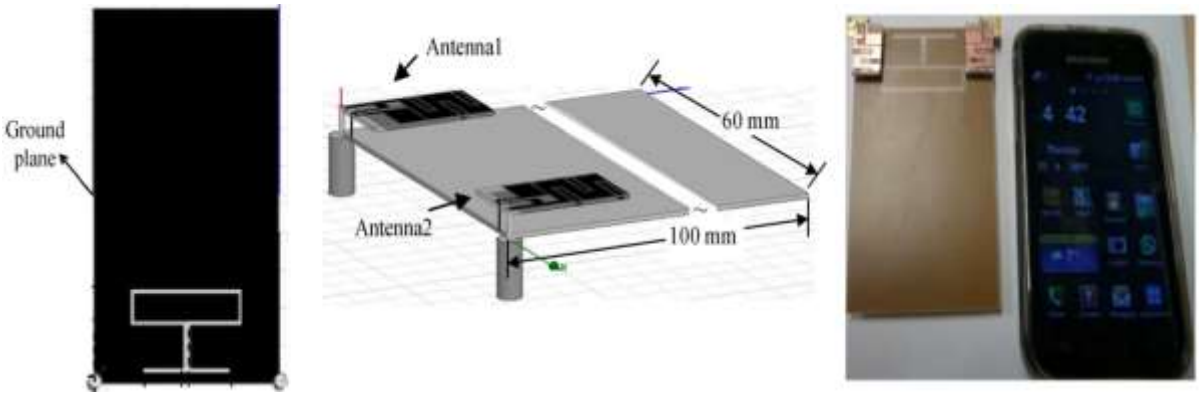

(a) **(b)** **(c)**

Figure 3.3: Configuration of the MIMO antenna with DGS used as an isolation method for multiband applications. **(a)** Top view of DGS **(b)** 3D view, and **(c)** Fabricated antenna [104]

3.1.1.2 Electromagnetic Band Gap (EBG) approach

Narrow-band-MIMO Antennas – In recent year, several of the narrow-band MIMO antennas have been designed using these applicable structures to reduce the mutual coupling effects [105]. Basically; EBG structure behaves as a band-stop filter in antenna decoupling. It is constructed by arranging multiple cells periodically.

Meanwhile; many works are reporting the use of EBGs as via-based structures or utilising the concept of shorting pins as presented in ref [27, 105, 107-114], multi-layers EBG implementation [115-121], soft-surfaces [122-123] and fractals like EBG [124].

Most of these existing works EBG structures are either non-planar [27, 105, 107-114], have multilayers [115-121] or occupy a comparatively large area [122-123]; so increasing the antennas size, fabrication cost and complexity of the array circuits.

Recently, Due to its advantages; other publications are focused on planer EBG structures as presented in [125-134]. However; it is noticed that these antennas either are complex in term of unit cell configuration (i.e. shape challenging to optimise) as introduced in [125-126, 128, 130, 133] or have a considerable antenna separation distance ≥ 0.4 λ_0 as presented in ref [129] or antennas working in higher frequency range slightly lower one as presented in ref [127, 131-132, 134]. Briefly; one of these designs is now described in more detail as below:

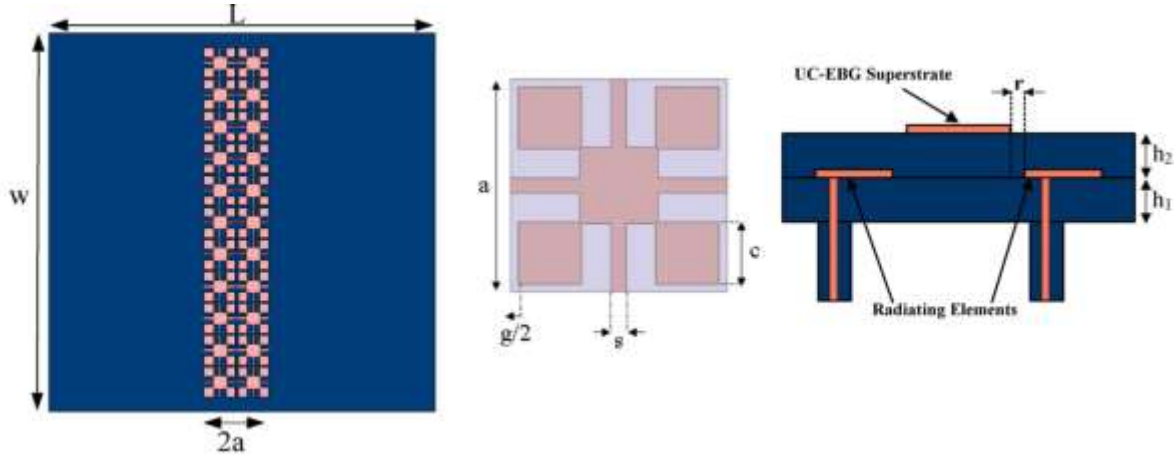

Figure 3.4: The antenna array with EBG used as an isolation method for narrowband applications. **(a)** Top view, **(b)** UC-EBG unite cell, and **(c)** Side view [117]

In ref [117], a configuration of uni-planar compact UC-EBG structures was used for both mutual coupling reduction and miniaturisation purposes, as shown in Figure 3.4. The antenna array with the UC-EBG super substrate has a relatively larger directivity, which was capable of suppressing the surface waves within a particular frequency band. The results showed about 10 dB reductions in coupling at working frequency f_c = 5.75 GHz.

UWB-MIMO Antennas – In general; this technique is widely used for narrow-band MIMO systems, yet it has some limitation and constraints. Recently, there are few limited works proposed for UWB applications using this method [135-138]. In these existing works; there are some drawbacks such as EBG structure had been implemented in multilayers, and its stop-band frequency only cover a lower UWB range (e.g. 3.3 to 4.5 GHz). Briefly; one of these designs is now described in more detail as below: In ref [137], miniaturised two-layer EBG structures are presented for reducing the electromagnetic coupling between closely spaced UWB planar monopole antennas on the common ground. The proposed slit–patch EBG structures have a small footprint (as shown in Figure 3.5) and produce an excellent mutual coupling reduction (S_{21} values < −20 dB) across lower frequency range (3–6 GHz) of the UWB diversity monopole antennas.

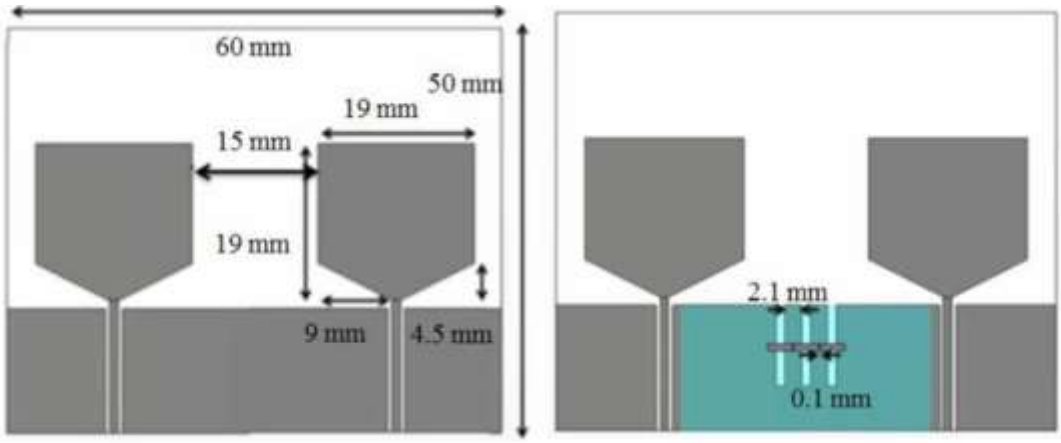

Figure 3.5: Dual-element UWB planar monopole array. **(a)** Conventional design and **(b)** Array with EBG used as an isolation method for UWB applications [137]

Multi-band-MIMO Antennas – Several publications have discussed the use of EBG in multi-band applications such as uniplanar compact EBG (UC-EBG) concept [139], using spiral-shaped with vias [140] or fractals [141-142].

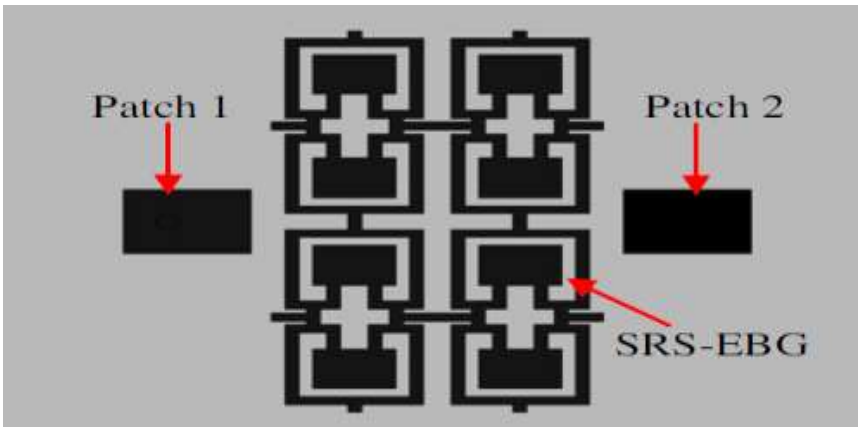

Figure 3.6: Schematic of a dual microstrip patch antenna separated by SRS-EBG to be used as an isolation method for multiband applications [139]

Briefly; one of these designs is now described in more detail as below:

In ref [139], a split-ring slotted electromagnetic bandgap (SRS-EBG) based on a uniplanar compact EBG (UC-EBG) concept is applied to achieve multi-frequency bandgap feature.

The EBG structure is inserted between dual microstrip patch antennas to reduce the mutual coupling effects (as shown in Figure 3.6), The isolation was as -21dB and -20 dB at the first bandgap (5.11-9.40 GHz) and the second bandgap (10.69-15.85 GHz); receptively.

3.1.1.3 Slots / slits - etching approach

Narrow-band-MIMO Antennas - Some works incorporating various slots or cuts were demonstrated to create filtering effects, e.g., a series or multiple slits are etched in the ground as presented in ref [143-146], and it is noticeable using of the several pairs of slots makes the structure complicated. Recently, a single slit proposed in ref [43, 148], miniaturised convoluted slits in [149], dual quarter-wavelength slots in [150] and dual half-wavelength slots in [151]. Briefly; one of these designs is now described in more detail as below:

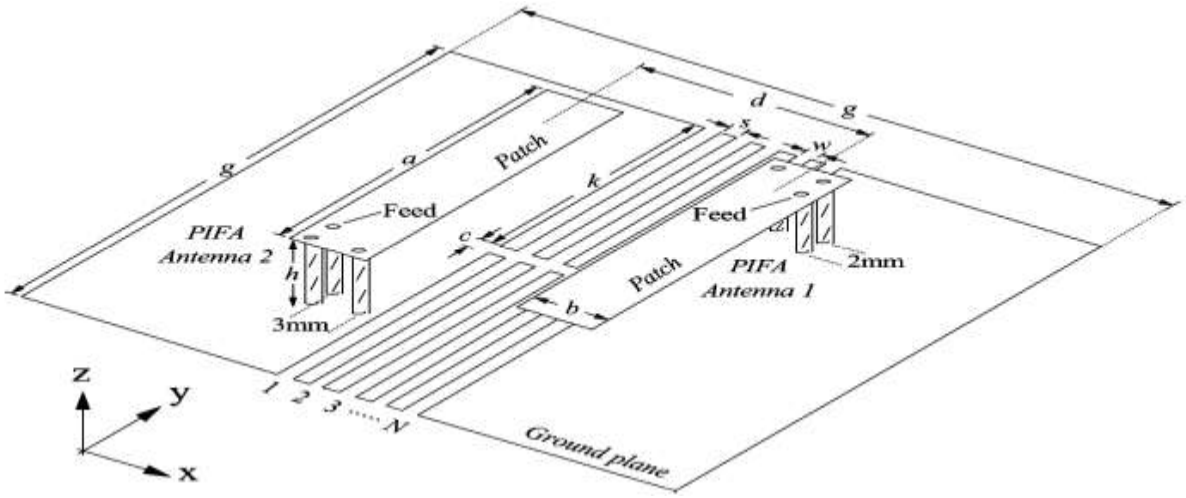

Figure 3.7: Configuration of closely-packed PIFAs with the slotted ground plane used as an isolation method for narrow applications [145]

In ref [145], the ground plane structure consisting of five pairs of slits etched into the middle of a ground plane of two closely packed PIFAs was investigated, as shown in Figure 3.7. The structure behaves here as a band-stop filter based on a parallel resonator (a combination of capacitance and inductance) which effectively suppresses the propagation of the surface waves, and thus it provides a lower mutual coupling between the diversity microstrip antennas. The isolation was improved by 12 dB at the working frequency (2.5GHz). In general; this approach also limited in term of narrow BW characteristics and almost it is determined by the total length of these slots / slits.

UWB-MIMO Antennas – In this application; some researchers adopt the trivial solution of disconnecting the ground planes [152-153] for isolation enhancement in UWB antennas. Recently, other works having various slots or cuts, e.g. introducing a single narrow rectangular slot that cut on the common ground plane as presented in [154-157], other multiple narrow slots/slits with different shapes are inserted into the common ground plane as introduced in ref [88, 90, 158-161]. Most of these works; slots/slits were embedded with cooperation with other approaches. Almost it is combined with other approaches (e.g. placement and orientation) because these structures are mainly applicable in narrowband\multiband only rather than UWB operation. Briefly; one of these designs is now described in more detail as below:

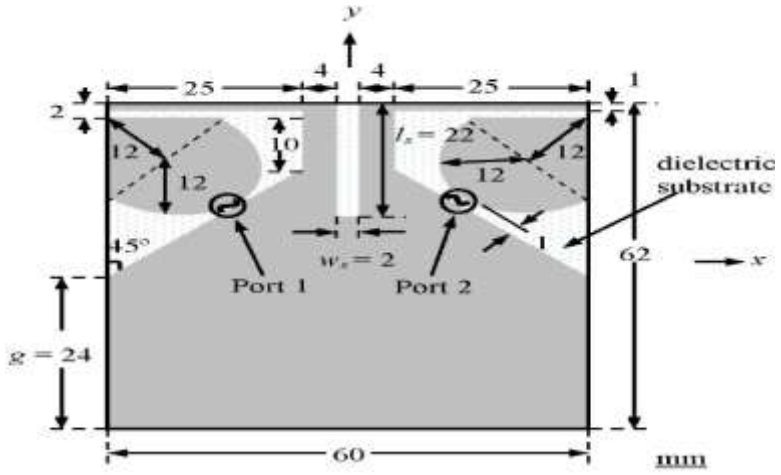

Figure 3.8: Configuration of the cone-shaped radiating MIMO antenna with a slot in between to be used as an isolation method for UWB applications [154]

In ref [154], a cone-shaped diversity antenna with a compact size of 60 × 62 mm^2 was designed (as shown in Figure 3.8). A slot was introduced at the upper centre portion of a protruded T-shaped ground plane for improving the isolation and the impedance matching. The results showed that the antenna can operate frequency bandwidth from 3.1 to 5.8 GHz for $S_{21} <$ - 20 dB; the gain variation is about 2 dB.

Multi-band-MIMO Antennas – Recently, multi-band antennas having different slots or cuts, e.g., with slot to break ground or substrate [162], a single narrow slot on the centre of the ground plane [163-169], a multiple narrow rectangular slots/slits are inserted into the ground plane [170-177], Dual U-shaped slots [178], band-notched $\lambda_0/4$ slots on the ground plane [179-182] and other works presented in ref [183-185]. Briefly; one of these designs is now described in more detail as below:

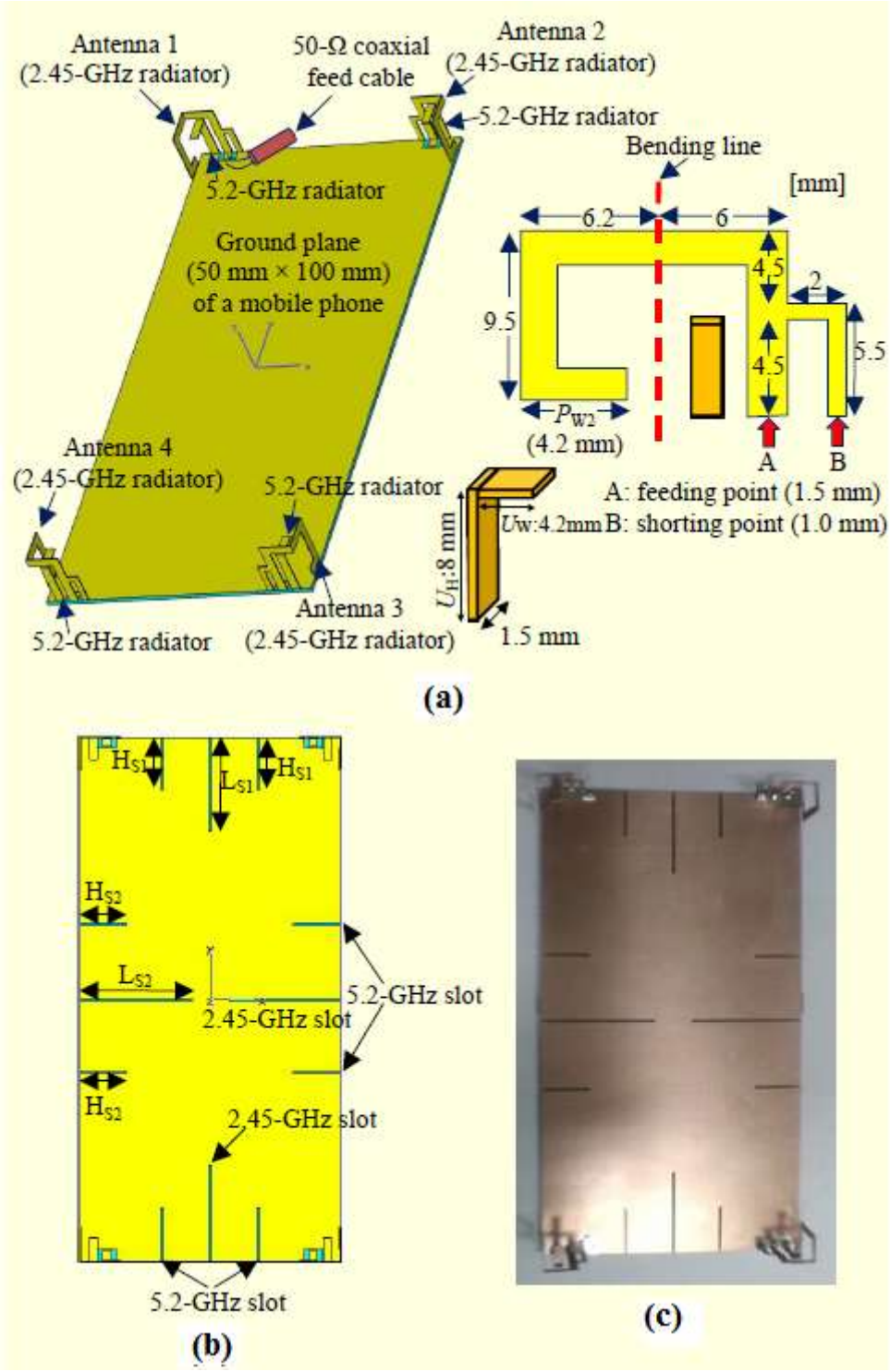

Figure 3.9: Dual-band antennas. **(a)** Detailed 3D view, **(b)** Slot on a ground plane used as an isolation method for multiband applications, and **(c)** Photograph of the MIMO antenna [173]

In ref [173], presents a compact antenna size (50 × 65 × 1.6 mm^3) and dual-band MIMO antennas for LTE mobile terminals (as shown in Figure 3.9). Here; to improve the isolation of the diversity antenna, several narrow (rectangular) slots are inserted into the ground plane. The isolation is more than 20 dB in the lower band and more than 16 dB in the upper band

with a small antenna distance which is less than half wavelength at the dual resonant frequencies.

3.1.1.4 Metallic stubs / GND plane branches approach

Narrow-band-MIMO Antennas – Different stub structures are presented in the open literature such as T-shape [186-190] or cross-shaped [472]. In general; this method increases weight and placement dependent thus rarely applied for narrowband handset applications. Briefly; one of these designs is now described in more detail as below:

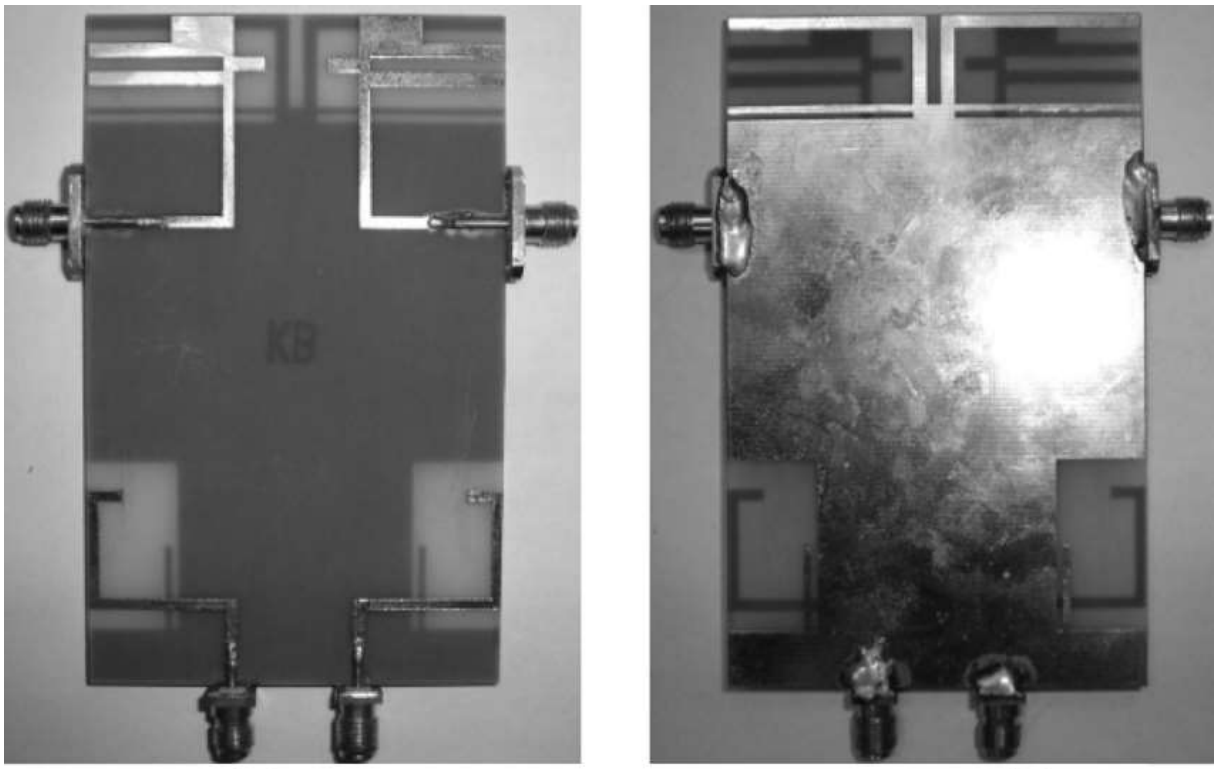

(a) **(b)**

Figure 3.10: Photograph of the four-element antenna system with stubs used as an isolation method for narrowband applications. **(a)** Front view **(b)** Back view [186]

In [186], a multi-antenna diversity system with four printed monopolies is presented. Two different forms of the monopolies that are positioned at the four corners of a printed circuit board have been given. The diversity antenna consists of two orthogonal C-shaped monopoles. A protruding T-shaped stub at the ground plane and dual inverted-L-shaped ground branches (as shown in Figure 3.10) are used to increase the isolation. Based on the simulation, a prototype for the UMTS operation has been constructed and tested.

The measured -10 dB impedance bandwidths of the four elements are larger than 320 MHz with higher than -11.5 dB isolation.

UWB-MIMO Antennas – The method of inserting ground stubs is mainly found in the literature for UWB-MIMO antennas and introduced either in multiple stubs as introduced in ref [155, 191-202] or other important works introduced as a single ground stub structure as

presented in ref [203-208].

Moreover; some of the common works presented in open literature including: a rectangular ground stub [88, 209-216], an extended T-shaped stub [156, 158, 217-224], a cross-shaped stub [225-227], a fork-shaped stub [228-230], a tree like stub structure [231-232],a F-shaped stub [233] an inverted Y-stub [234], an inverted L-stub [235], a meander shaped ground stubs [236-237], other stub structures acting as a band-stop filter [238], etc.

Yet; most of these existing work; these stubs were embedded with cooperation with other approaches (e.g. almost placement and orientation or other methods) except the works introduced in ref [191, 204, 218, 219, 223, 225, 228, 234]. However; these mentioned works either the isolation BW not adequately cover the entire UWB range (i.e. poor isolation at some frequencies) as presented in [191, 204, 219, 234] or isolation BW cover the whole UWB but maximum isolation <-18 dB as introduced in ref [218, 223, 225, 228]. Briefly; one of these designs is now described in more detail as below:

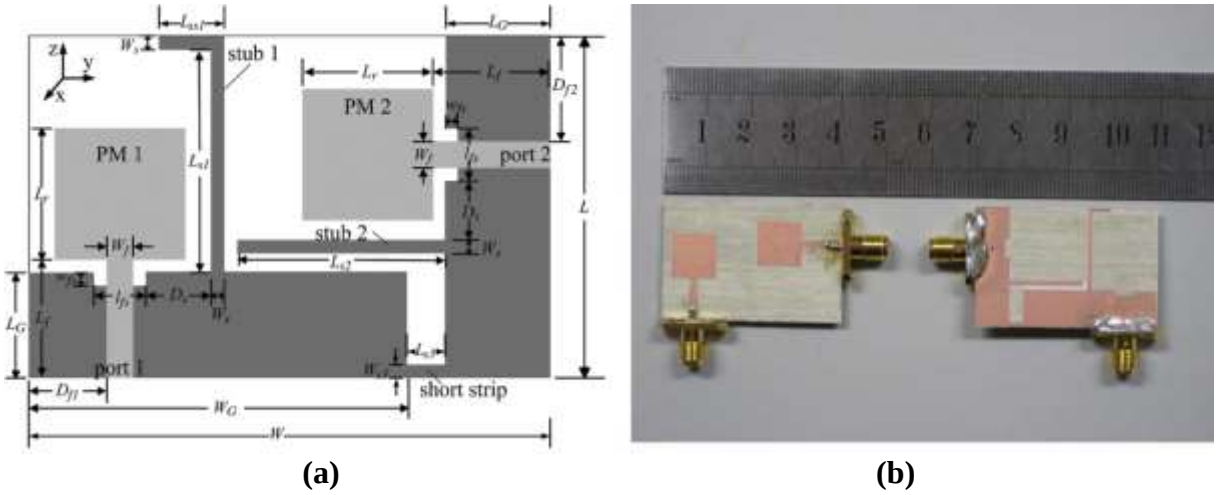

Figure 3.11: Configuration of a UWB-MIMO antenna with stubs used as an isolation method for UWB applications. **(a)** Schematic and **(b)** Fabricated MIMO antenna [194]

In ref [194]; a dual planar patch elements antennas placed perpendicularly to each other to achieve good isolation between the input ports, with two long ground stubs placed adjacent to the radiating elements and a short ground strip connecting the two ground planes are employed to enhance the isolation, as shown in Figure 3.11. The return loss bandwidth was achieved from 3.1 to 10.6 GHz with mutual coupling of less than -15 dB between the two feeding ports.

Multi-band-MIMO Antennas – Recently, different metallic ground stub structures are presented in the literature such as T-shaped [96, 101, 181, 239-245], L-shaped [248-249], narrow rectangular stubs [167,176,250-252], etc. Yet; most of these existing work; introduced stubs were embedded with cooperation with other approaches (almost placement and

orientation) and complicated to adjust.

Briefly; one of these designs is now described in more detail as below:

In ref [241], proposed a novel compact wideband planar diversity antenna for mobile terminals. It has a -10 dB impedance bandwidth from 1.904–2.504 GHz covering UMTS band and 2.4 GHz WLAN band. To obtain the wide bandwidth and low mutual coupling, T-shaped and dual inverted-L-shaped ground technique had been used in the design (as shown in Figure 3.12). In the whole band, the mutual coupling between the two antennas is below -15 dB (about – 20 dB in most of the operation band).

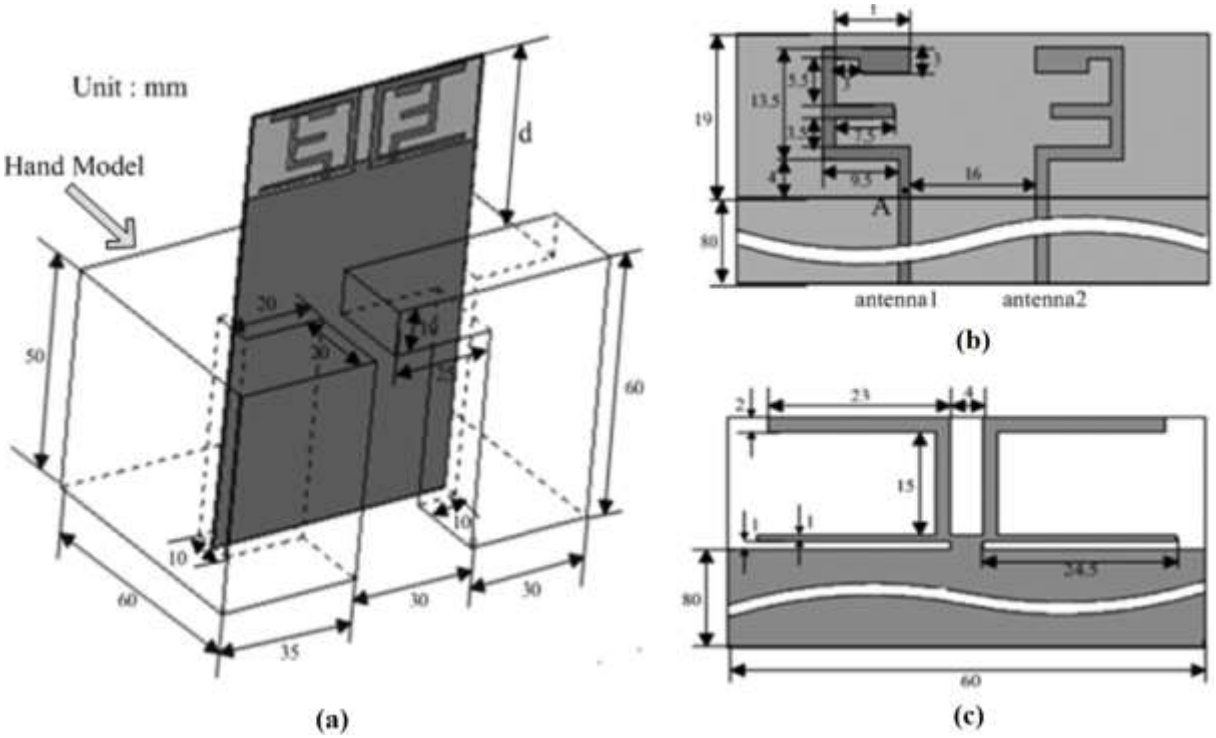

Figure 3.12: Configuration of the antennas with stubs used as an isolation method for multiband applications: **(a)** General view, **(b)** Front side, **(c)** Back side [241]

3.1.1.5 Currents Localisation Structures (CLS) approach

Narrow-band MIMO Antennas – A few publications have discussed the use of additional ground concept [41, 214, 253-255]. In general; this method considered too bulky to use in portable devices (i.e. mobile handsets). Briefly; one of these designs is now described in more detail as below:

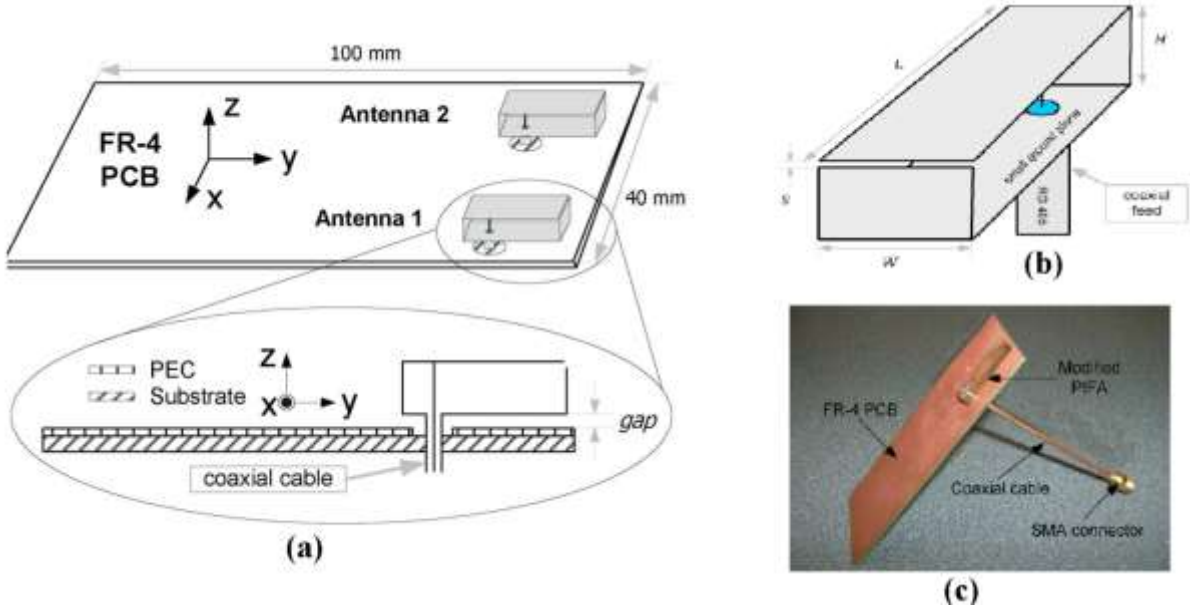

Figure 3.13: Configurations of the antennas. **(a)** Dual PIFAs with small ground used as an isolation method for narrow applications **(b)** Single PIFA, and **(c)** Fabricated antenna [41]

In [41], a compact dual-element PIFA array on a PCB operating in 2.5 GHz band for MIMO application is presented. The PIFA elements used were modified by introducing a small ground plane between the PIFA and the PCB. Here; a small local ground plane is separated from the main ground is an efficient method to localise the currents induced by the antenna to the confined local ground. The antenna configuration is presented in Figure 3.13 [41]. The PIFA element is modified by introducing a small local ground plane between the PIFA and the main ground plane. The surface currents are localised underneath the antenna, rather than distributed along the whole ground plane, and here; isolation between the antennas exceeds 20 dB.

UWB-MIMO Antennas – Yet, this technique is not significantly employed yet for planner UWB-MIMO systems in the open literature to the best of author's knowledge.

Multi-Band-MIMO Antennas – A few recent works have been proposed in the literature [256-257].

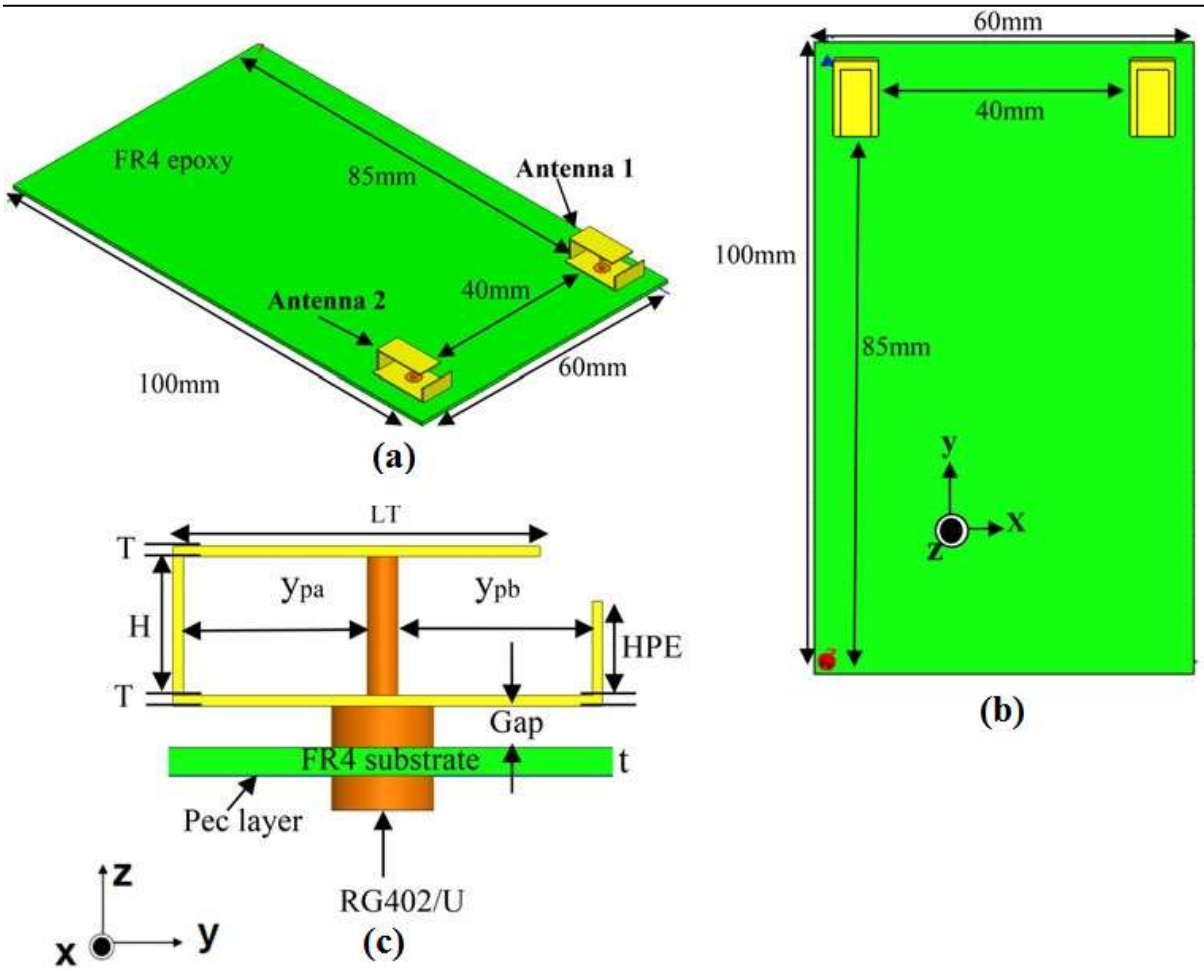

Figure 3.14: Configuration of the MIMO antenna with small ground used as an isolation method for multiband applications: **(a)** 3D view and **(b)** Top view **(c)** Side view [257]

For instance, in ref [257], a MIMO dual-element PIFA array (as presented in Figure 3.14) for broadband operation covering WLAN, and WiMAX for high-performance wireless devices was presented. In this design; PIFA array provides a broad bandwidth (0.67 GHz), and high isolation between ports are obtained (< -26 dB). It is excellent performances are achieved due to inserting a small ground plane technique between the original PIFA and the PCB allowed achieving the real diversity characteristics of the MIMO antenna.

3.1.1.6 Metallic shorting pins / vias approach

Narrow-band MIMO Antennas – A few publications have discussed the use of shorting pin or via concept for isolation enhancement as proposed in ref [215], [247], [327]. In these works, obviously insertion of an extra small ground will increase the complexity of printed circuit board (PCB) fabrication. Thus this approach considered very limitedly in different wireless applications.

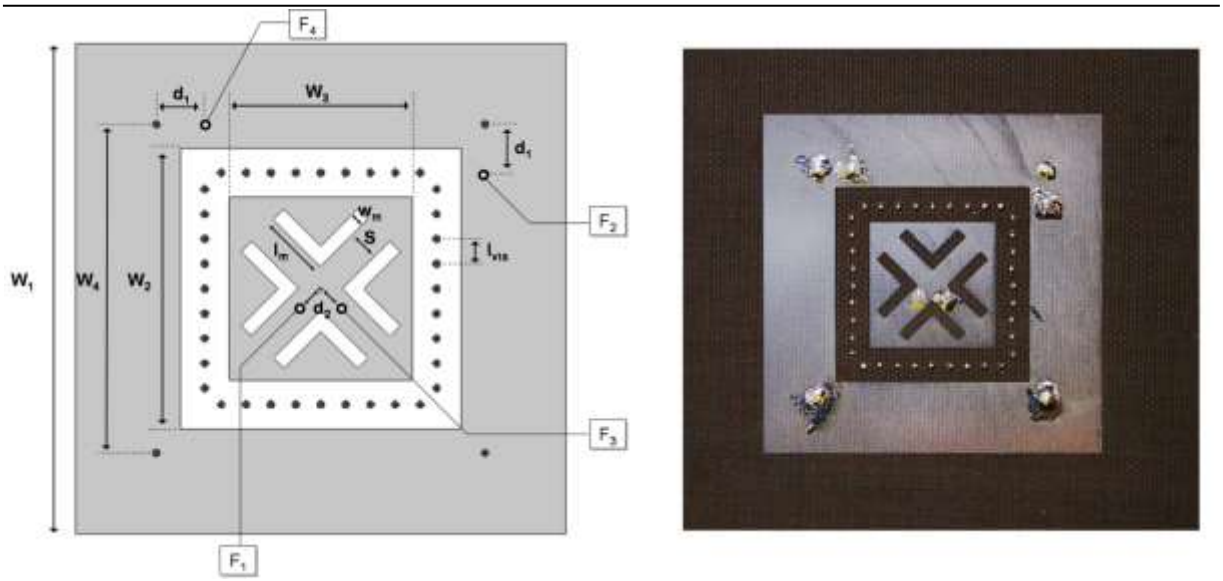

(a) **(b)**

Figure 3.15: Configuration of the MIMO antenna with shorting pins used as an isolation method for narrowband applications: **(a)** Schematic **(b)** Fabricated [327]

For instance; in ref [327], the antenna system, as shown in Figure 3.15, composed of a dual-polarised microstrip patch and a dual-polarised microstrip square-ring.
In addition; L-slots have been etched on the patch to reduce its dimensions, and metallic vias have been introduced to reduce the strong coupling between patch and square-ring modes. The measured results show without via, the maximum coupling is about -16.5 dB whereas with vias, the coupling is better than -21 dB (4.5 dB as improvement has been obtained).

UWB-MIMO Antennas – Yet, this technique is not significantly employed yet for planner UWB-MIMO systems in the open literature to the best of author's knowledge.

Multi-Band-MIMO Antennas – A few recent works have been proposed in the literature [184, 333]. However, utilisation of this method in these works will increase a thickness of the substrate.
For instance, in ref [333], a new dual-band (2.45GHz and 5.8GHz) diversity antenna array for portable wireless terminals is proposed. High-isolation performance (< -27 dB at a 2.45 GHz and < -21 dB at the 5.8 GHz) is achieved by introducing a connecting line and a shorted pin, as shown in Figure 3.16.

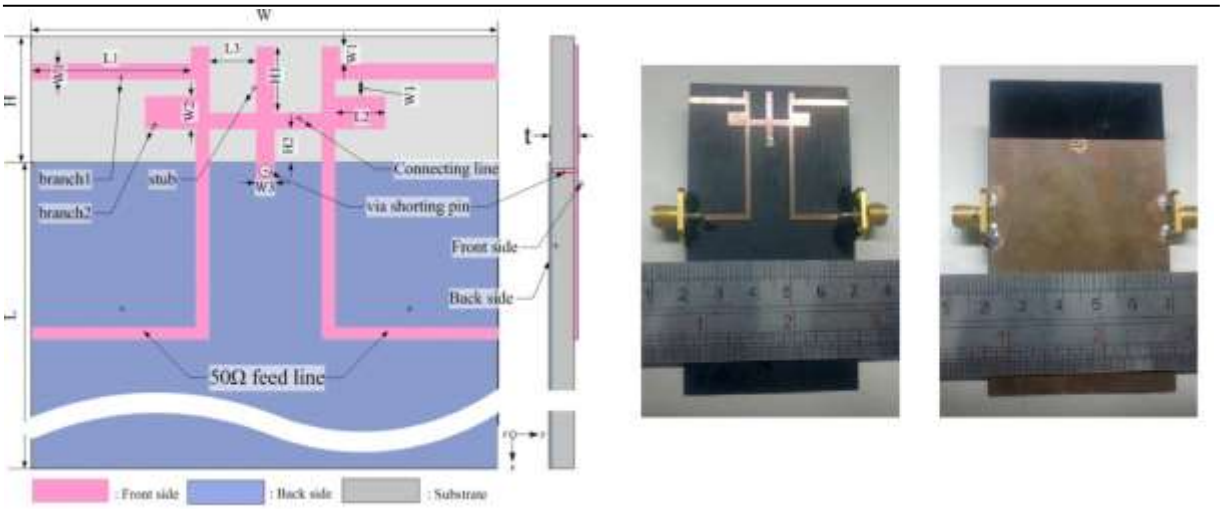

(a) **(b)** **(c)**

Figure 3.16: Configuration of the array with a shorting pin used as an isolation method for multiband applications: **(a)** Top view **(b)** Side view, and **(c)** Fabricated antennas [333]

3.1.2 Suppression Techniques of Antenna Coupling Through Space-Wave Radiation

In this category, different decoupling methods based on this coupling mechanism (direct or space coupling) are introduced, including: Antennas separation, Decoupling wall structures (DWS), Antenna placement and orientation technique, Neutralization Line (NL), Decoupling and Matching Networks (DMN), parasitic structures, heterogeneous elements and utilisation of Meta-Material Structures (MTMs) approach, etc.

3.1.2.1 Antennas separation approach

Narrow-band-MIMO Antennas – This approach considered as a traditional method of maintaining a good separation between multiple antennas is mainly found in the open literature [258-264].

In these works; antennas relatively have a significant distance from each other. However; this method is limited for mobile handheld devices due to massive size constraint.

For instance, in ref [262], miniaturised MIMO antennas have been proposed in this work. Here; the achieved mutual coupling was around -15 dB without using any external elements or change in PCB design, as shown in Figure 3.17, only with the help of design optimisation and maintaining on good separation between the proposed antennas.

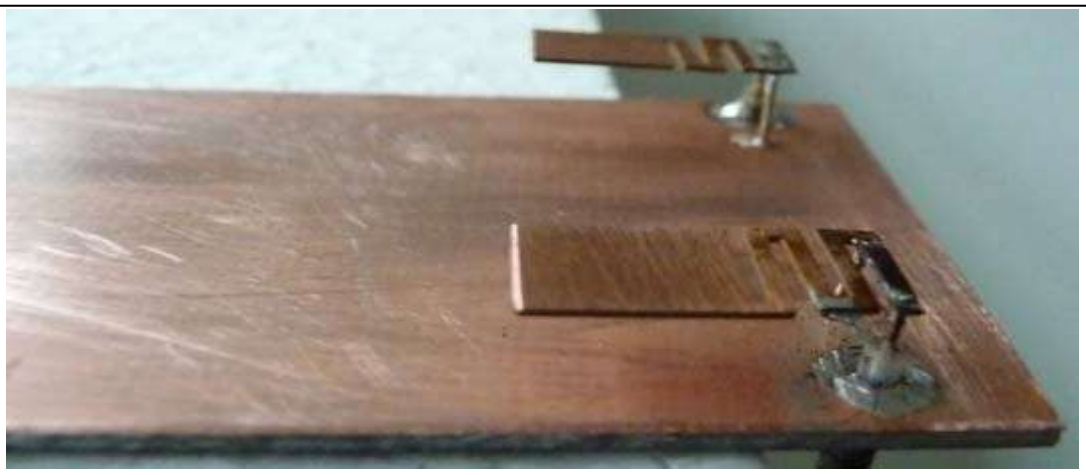

Figure 3.17: Prototype of the dual meander PIFA elements with good separation for narrowband applications [262]

UWB-MIMO Antennas – Several other previous works for MIMO-UWB applications have been proposed in [267-270]. Obviously; this approach is not suitable for small portable devices because of the limited space. Meanwhile; it has required to be embedded with other decoupling methods to obtain high isolation characteristics.

Briefly; one of these designs is now described in more detail as below:

In ref [267], the coupling effects between array elements of dual and four-antenna element UWB linear arrays have been enhanced (is around -15 dB in the whole band) when the element spacing is greater than one wavelength at the upper frequency for UWB arrays.

Figure 3.18: Fabricated dual- elements **(left)** and quad-elements **(right)** array with good separation for UWB applications [267]

Multi-band-MIMO Antennas – Many other works for MIMO Multi-band applications have been recently presented in [271-277]. Although; this method not required any extra decoupling networks, quite low isolation is obtained.

For instance, in ref [272], a new antenna structure comprising four elements; each includes a rectangular patch along-side a small rectangular shape ground proximity fed by a microstrip line, as shown in Figure 3.19. The array designed for operating in quad-bands. Half-

wavelength separates the elements of the array at lowest frequency (1.8 GHz), the achieved mutual coupling is quite low (S_{ij} < -15 dB).

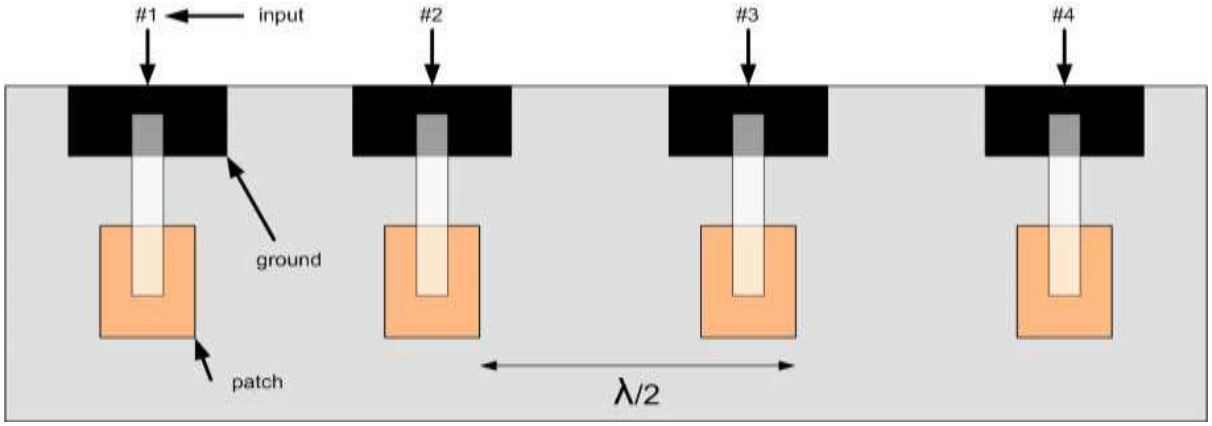

Figure 3.19: Geometry of the 4×1 patch array antenna with good separation used as an isolation method for multiband applications [272]

3.1.2.2 Decoupling wall structures (DWS) approach

Narrow-band-MIMO Antennas - Different lattice pattern loadings as defected wall structures were applied to reduce mutual coupling between closely space antennas such as a single layer of mushroom walls as introduced in ref [144-145, 278-279], a wall with a double layer of mushroom wall structure is positioned in between the four antenna elements in ref [280-281], metallic wall combined with two open-ended slots [282, 289], Asymmetrical coplanar strip wall [290], and utilisation of meta-materials walls [291-292], etc.

Although most of these designs were novel, they have several drawbacks such as the height of these decoupling structures (walls) is relatively large and the bandwidth is relatively narrow; thus it is difficult to use them in real practical applications (e.g. handsets). Briefly; one of these designs is now described in more detail as below:

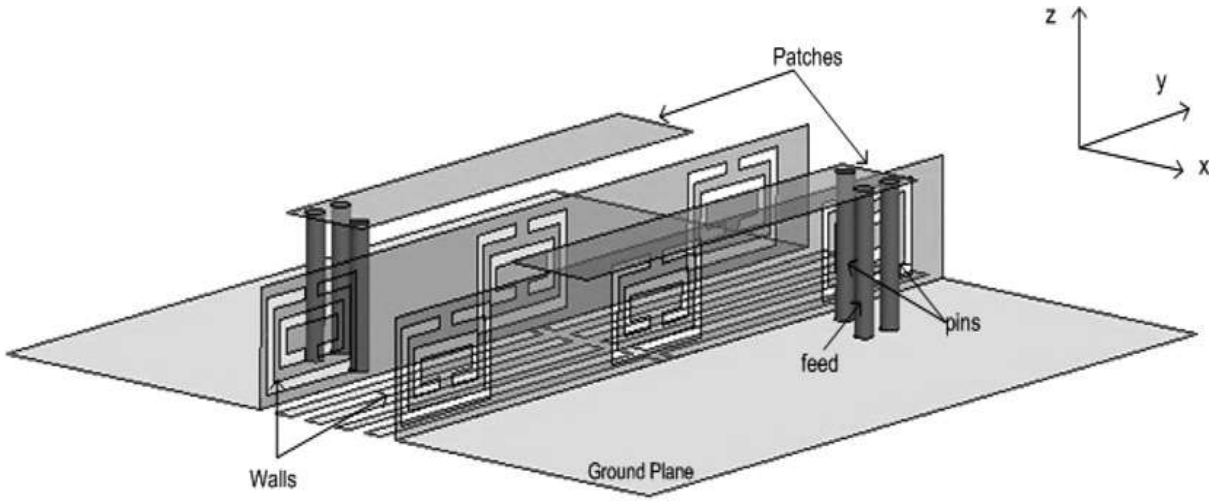

Figure 3.20: Geometry of PIFA antennas with the DWS used as an isolation method for narrowband applications [278]

In ref [278], here; new DWS with slot loadings investigated between PIFAs, as shown in Figure 3.20. However; the isolation of (-56 dB) can be achieved.

Here; the structure used in this work has a relatively low dielectric constant resulting in a higher air coupling than surface waves; this wall structure can be thought of as a band-stop filter and provides an effective EM shield to reduce air coupling between the adjacent PIFA's antennas effectively.

UWB-MIMO Antennas –Yet; this technique is not significantly employed yet for planner UWB-MIMO systems in the literature to the best of author's knowledge.

Multi-band-MIMO Antennas – Yet; this technique is not significantly employed yet for planner UWB-MIMO systems in the literature to the best of author's knowledge.

3.1.2.3 Antenna placement and orientation approach

Narrow-band-MIMO Antennas - In recent years, many collocated works for MIMO narrowband applications have been proposed [62, 255, 279-280, 293-315]. Re-orienting microstrip antennas, which allows for benefiting from radiation pattern nulls and most importantly from polarisation mismatch between the antennas, is an effective way of suppressing the direct or space-wave coupling. In general; this approach considered not ideal for handset terminals due to space and polarisation restriction. Briefly; one of these designs is now described in more detail as below:

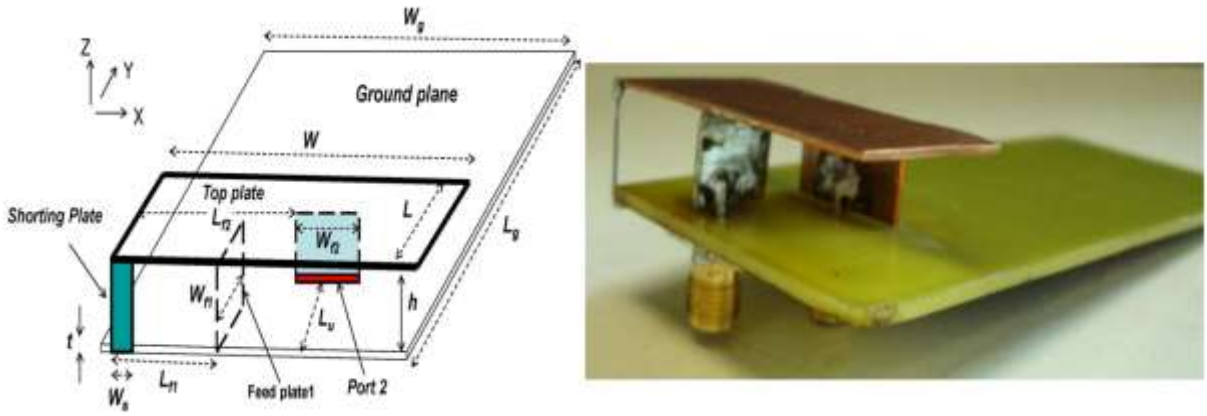

Figure 3.21: Configuration of the dual-feed PIFA antenna with perpendicular feed used as an isolation method for narrow applications: **(a)** Schematic **(b)** Fabricated [307]

Recently, a dual-feed planar PIFA using two isolated feeding port on a common radiating plate was proposed in [307], as shown above in Figure 3.21.

To reduce the mutual coupling an approach of removing the most of the conductor to reduce the current flow on the ground plane between the two ports was implemented. The results showed that the antenna has an operating bandwidth from 2.4 to 2.7 GHz with more than 12 dB improvement in isolation.

UWB-MIMO Antennas – Commonly; UWB antennas utilising spatial and angular variations drawn considerable attention from researchers for high isolation applications. Moreover; many developments have already been reported in ref [154-156, 193-197, 200, 202-203, 205, 208, 210, 212, 226, 235, 238, 316-338, 429]. However, many of them not contains measurements results as introduced in ref [154, 195, 200, 202-203, 210, 227, 316-319, 321, 324, 326, 328, 334, 337] or other designs equipped with band-notch functionality as introduced in ref [156, 196-197, 205, 208, 212, 226, 235, 237-238, 322-323, 329, 336, 338, 429]. Although; some works as in ref [193-194, 325, 330-331, 332, 335, 455] have a measured good isolation (<-21 dB) but either has complex feeding network (e.g. four ports network) or a large ground plane. Briefly; one of these designs is now described in more detail as below:

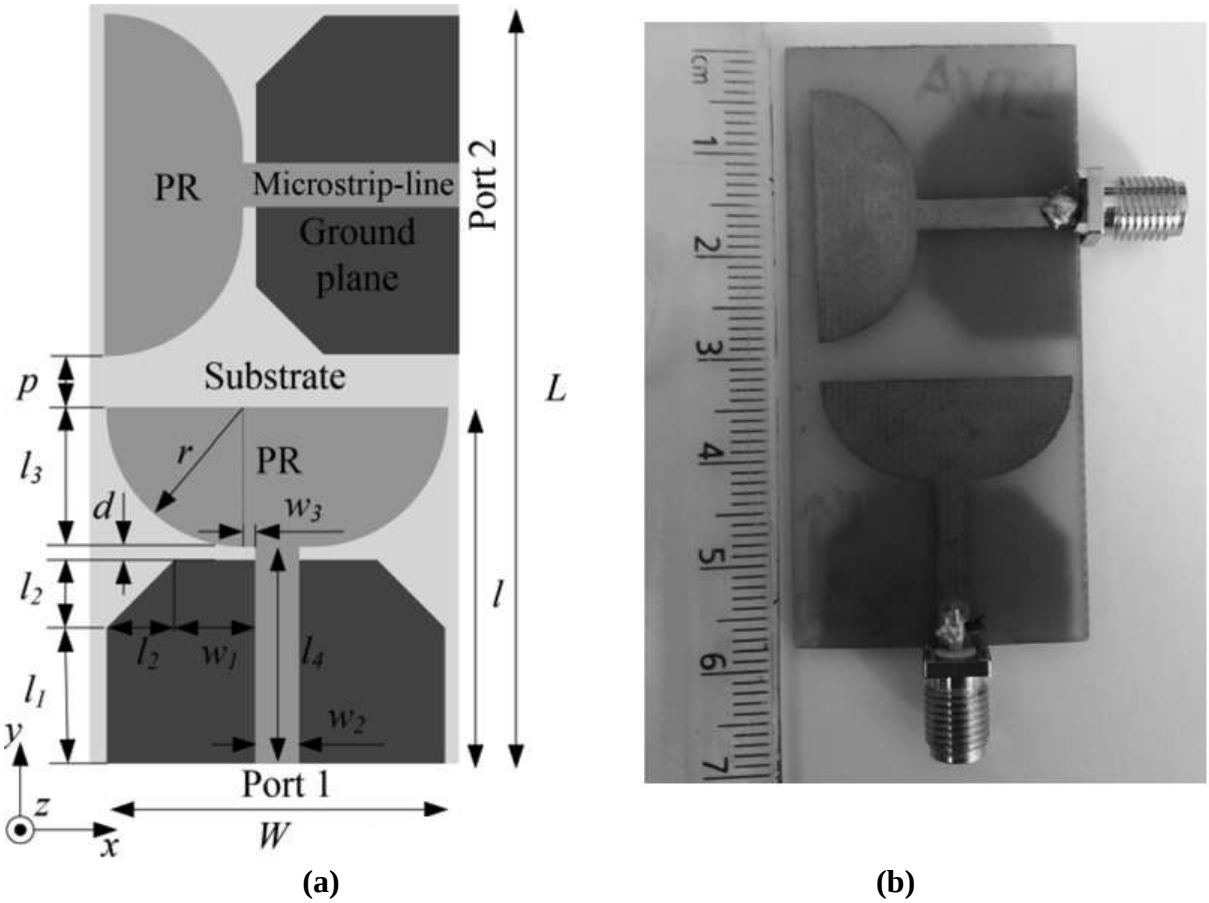

Figure 3.22: Configuration of UWB dual radiator elements with perpendicular feed used as an isolation method for UWB applications: **(a)** Schematic **(b)** Fabricated [325]

In ref [325], compact (26 ×55 mm^2) array antennas consist of dual identical antenna radiators elements, as shown in Figure 3.22. The antenna elements were fed orthogonally to achieve good isolation between the two input ports. The array designed for the ultra-wide-band (UWB) applications operation, i.e. 3.1- 10.5 GHz, and the achieved isolation between two antenna elements is greater than 20 dB across the band.

Multi-band-MIMO Antennas – Many works for Multi-band MIMO applications have been presented in ref [178, 169, 185, 249, 271, 344, 339-375, 456]. In most of these works, dual feeding structures were used to excite dual-polarization, thus making the feed structure quite complex. Briefly; one of these designs is now described in more detail as below:

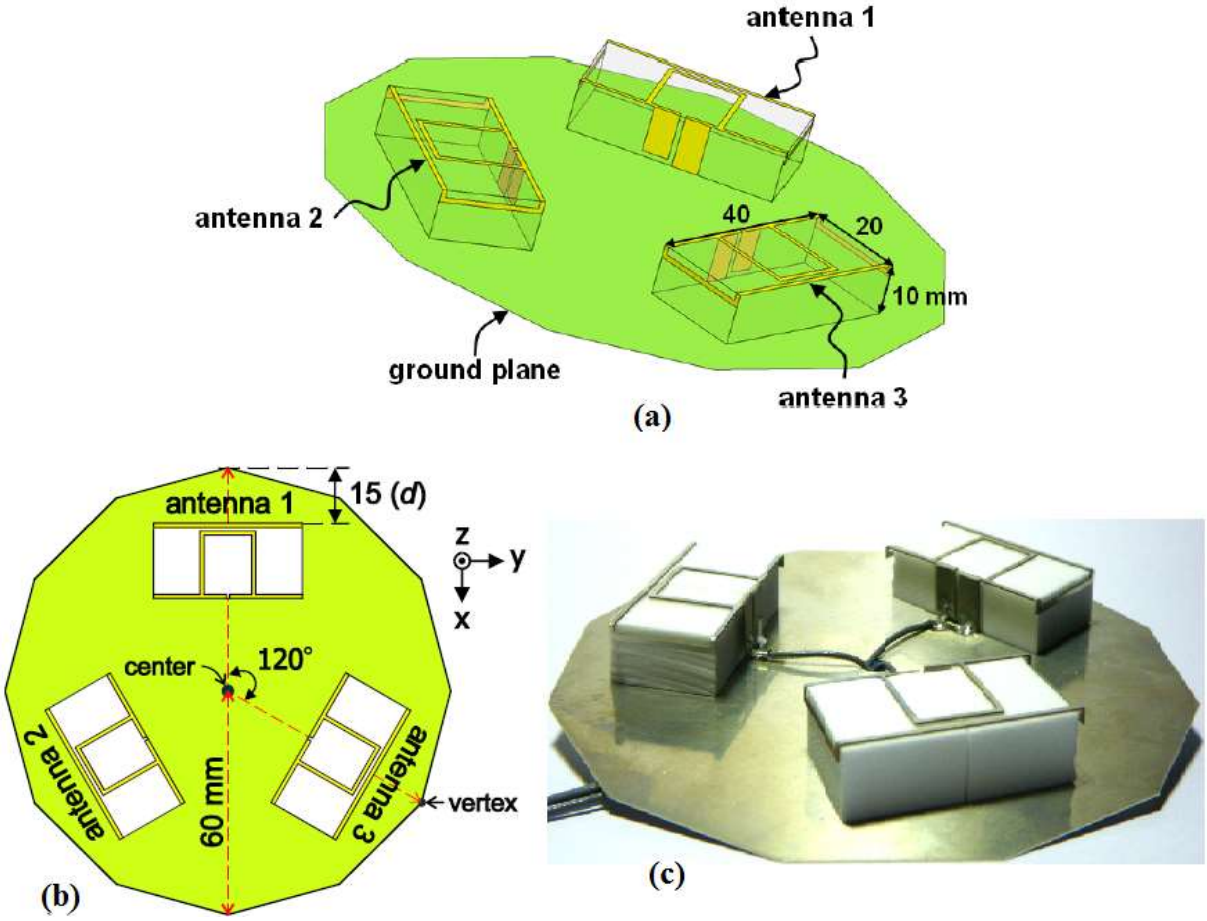

Figure 3.23: (a) Configuration of the dual-loop antenna array with 120^0 orientation used as an isolation method for multiband applications **(b)** Top view **(c)** Fabricated array [344]

In ref [344], demonstrated a novel three antennas system aimed to operate in the 2.4 and 5.2/5.8 GHz bands as internal MIMO access point (AP) antennas. Besides, the proposed antennas were placed in a sequential, rotating arrangement on a ground plane with an equal inclination angle of 120° to form a symmetrical multiple antenna structure (as shown in Figure 3.23). Low mutual coupling with a port isolation of less than -15 dB and -20 dB between any two antennas has been obtained over the 2.4 and 5.2/5.8 GHz bands respectively.

The measured results show that well ports isolation can be obtained together with high gain, directional radiation characteristics. Calculated ECC is less than 0.007 within the bands of interest. The proposed multiple antennas are well suited for internal MIMO antennas embedded in a wireless AP for WLAN operation as a promising alternative to conventional, high-gain patch or microstrip antennas.

3.1.2.4 Neutralisation Line (NL) approach

Narrow-band-MIMO Antennas – It can be noticed that much work has been presented to get better isolation using NLs for narrowband applications. The technique of using a neutralised or suspended line for mutual coupling reduction between different microstrip antennas operating in the same frequency band can be found in [299, 376-379] for mobile handset applications. This technique is frequently used to decouple the PIFAs antenna as presented in [380-382]. Here; it is a connecting line between the feedings or the shorting strips of the PIFAs.

Moreover; it can be efficiently used for decoupling MIMO antennas for USB dongles applications as presented in [300, 305, and 383]. In general; Modelling is complicated, and selection of the connection point is critical in this method. Briefly; one of these designs is now described in more detail as below:

In ref [381], a suspended NL physically connected to the dual PIFAs element (operating in 1.92-2.17 GHz within UMTS band), as shown in Figure 3.24. The MIMO antenna achieved a good mutual coupling reduction (< -18 dB) at a frequency of 1.96 GHz.

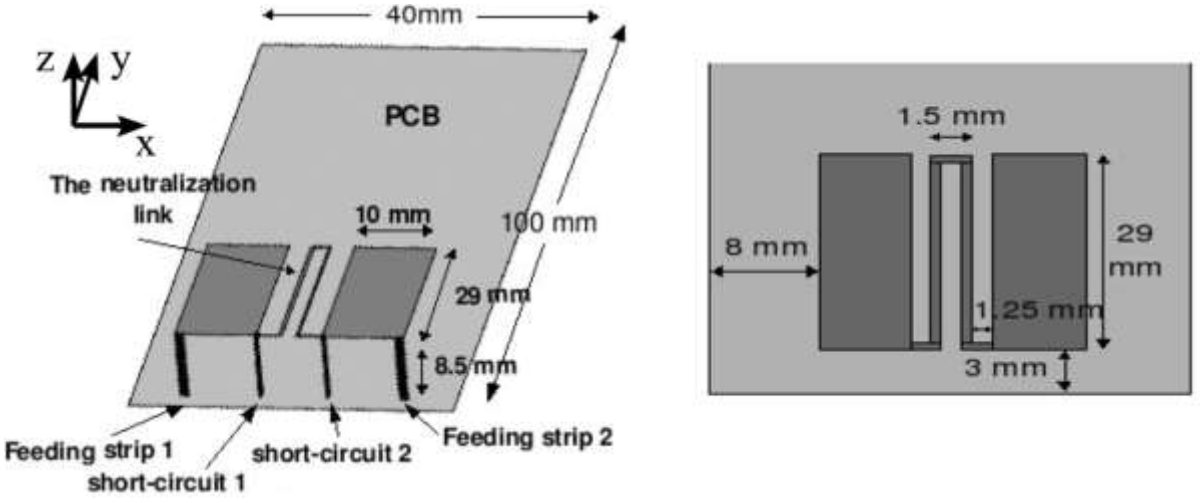

(a) **(b)**

Figure 3.24: The optimised PIFAs with the NL used as an isolation method for narrow applications. **(a)** 3D view, **(b)** Top view [381]

The introduction of the NL was used to cancel out the existing mutual coupling since the line stores a certain amount of the current/signal delivers from one antenna element to the other antenna element. In other words, an additional coupling path was created to compensate for the electrical currents on the PCB from one antenna to another.

UWB-MIMO Antennas – A few works presented in the recent literature [323], [384-386]. However, this technique is not commonly tractable for UWB-MIMO systems. These works are not capable of providing enough isolation bandwidth for the whole UWB band range except the work introduced in ref [384-385] offering good UWB isolation. Although; the design in ref [384-385] shows some isolation improvement on wide BW, it is still a considerably complex design and bulky for a mobile handset.

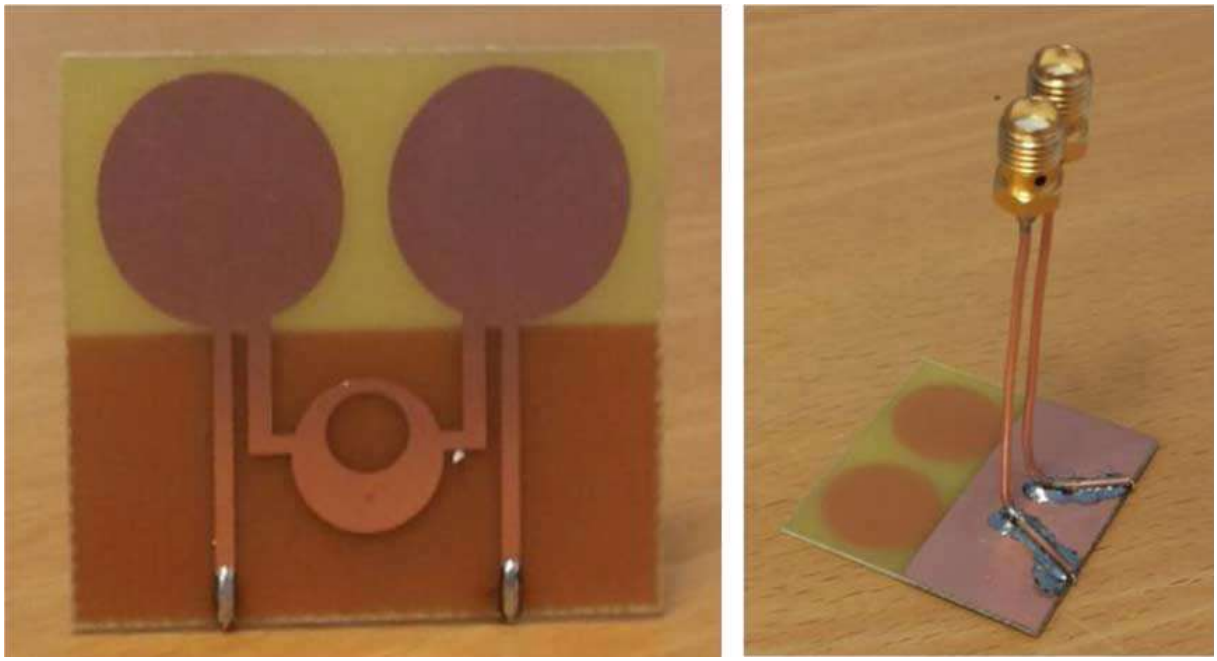

(a) **(b)**

Figure 3.25: Fabricated UWB antenna with NL used as an isolation method for lower band UWB applications [386]

Recently, in ref [386], a new wideband neutralisation line is connected to and inserted between two monopoles. The neutralization line consists of two metal strips and a metal circular disc, as shown in Figure 3.25. The results showed by implementing the proposed neutralization structure, low mutual coupling (S_{21} < -22 dB) between the antenna elements and good impedance matching (< -10 dB) can be realised over very wide bandwidth covering the lower band of UWB frequency band from 3.1 to 5 GHz.

Multi-band-MIMO Antennas – Other works related technique of using a neutralised or suspended line for mutual coupling reduction between different microstrip antennas operating in the multi-frequency band can be found in ref [175, 183, 358, 387-393, 406, 457].

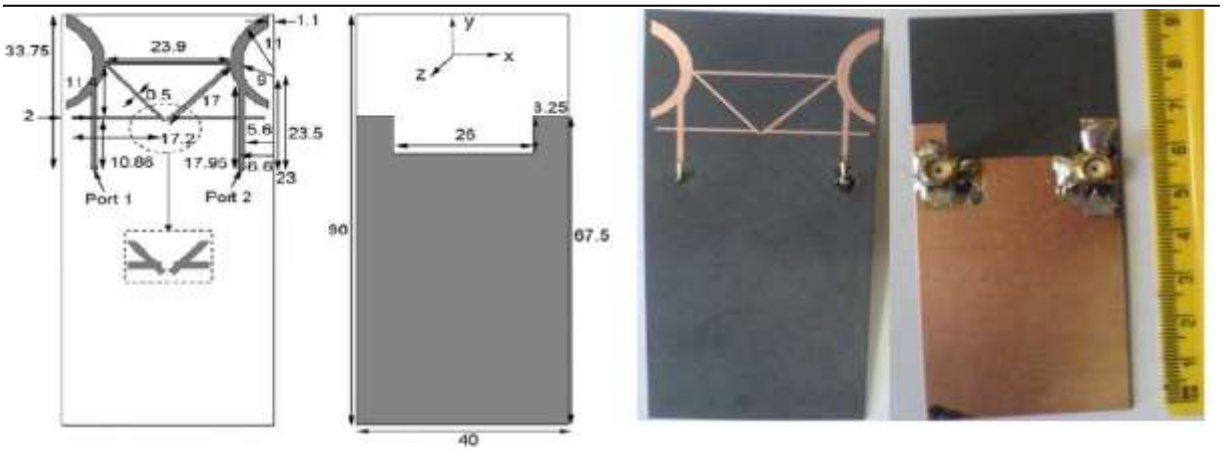

(a) **(b)**

Figure 3.26: The structure of printed antennas with the NL used as an isolation method for multiband applications: **(a)** Schematic **(b)** Fabricated [389]

Recently, a new printed monopole MIMO antenna was presented for Wi-Fi/WiMAX applications in [389], based on the same concept, but with much more complex neutralisation line integration. The configuration of the array antenna is shown in Figure 3.26.

The antenna comprises two crescent-shaped radiators placed symmetrically with respect to a defected ground plane, and neutralisation lines were connected between them with an achieved mutual coupling of less than -17 dB for an impedance bandwidth of 2.4-4.2 GHz.

3.1.2.5 Decoupling and Matching Network (DMN) approach

Narrow-band-MIMO Antennas –Some design approaches for the decoupling matching networks are described in ref [394-400].

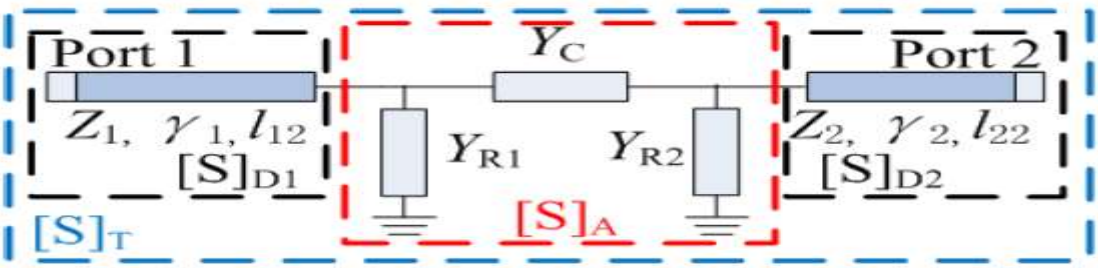

Figure 3.27: The π-shaped equivalent circuit of a closely packed antenna system

Different realisations of the decoupling network are proposed, such as a combination of lumped elements (including capacitors and inductors) [394], the hybrid 180° coupler [395-398], and employing an embedded decoupling line as presented in ref [399-400].

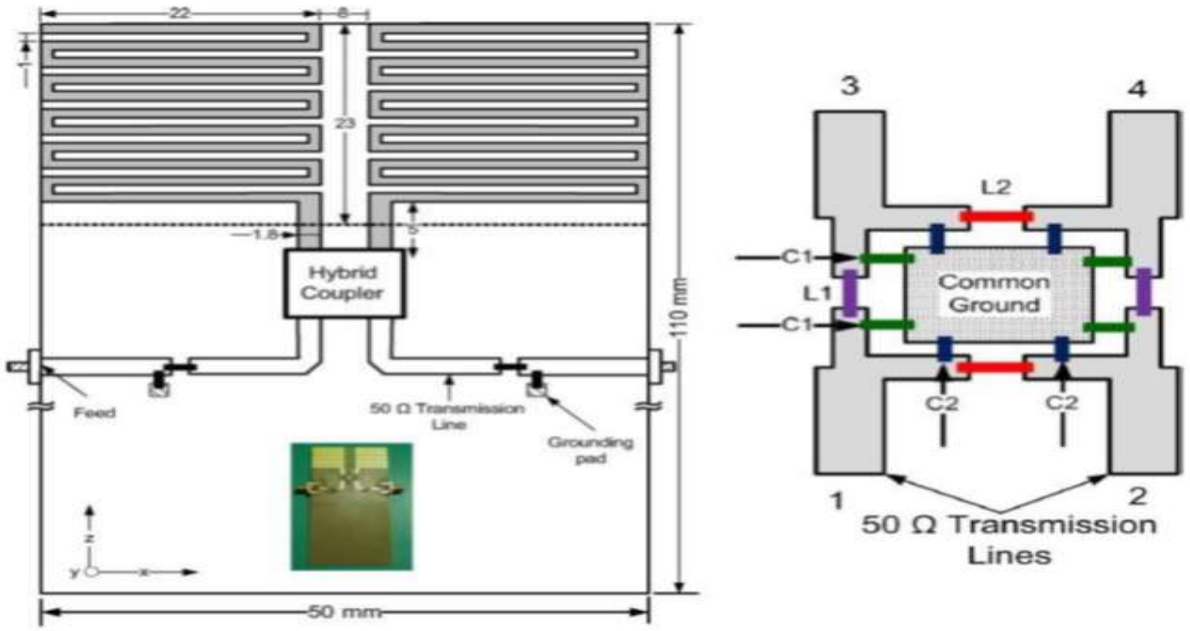

Figure 3.28: The layout of the meander-line monopole antennas **(left)**, and LC-based branch-line coupler **(right)** used as an isolation method for narrow applications [396]

In these works, some reactive components between the transmission lines are added. Although; the design shows some improvement on narrow BW isolation, it is still a considerably complex design, and additional ohmic losses are expected from these decoupling networks. Briefly; one of these designs is now described in more detail as above:

A decoupling network technique approach was investigated in [396] to improve an isolation of dual-element antenna, as shown in Figure 3.28. Here; an LC components based branch line hybrid coupler (using the passive inductors and capacitors) was used and designed at 0.71 GHz to decouple the antenna elements. A series inductance and two parallel capacitances were placed instead of each $\lambda_0/4$ section of the branch line coupler. The achieved isolation between the ports is better than 35 dB with matching ports at 0.71 GHz.

UWB-MIMO Antennas – The matching networks are usually applicable to design and to realise for narrow-band\multi-band antennas. However; wideband and ultra-wide-band MIMO systems are difficult enough to implement this method. Thus, this technique is not significantly employed yet for planner UWB-MIMO systems in the literature to the best of author's knowledge.

Multi-band-MIMO Antennas – A few works are presented in this application [401-405]; in these previous studies, most of them used many circuit components on multiple frequencies. However, the decoupling network can increase the overall footprint of the multiple antenna systems. Moreover; the complexity involved in the implementation of the modal feed network may limit the application of this method to smaller arrays.

Briefly; one of these designs is now described in more detail as below:

In ref [405], a dual-frequency (2.46-2.7 GHz and 5.04-5.5 GHz) MIMO antenna had been proposed for WLAN applications.

High isolation (over 30 dB) in dual bands is achieved by using a decoupling network is inserted between the two antennas without increasing the footprint, as shown in Figure 3.29.

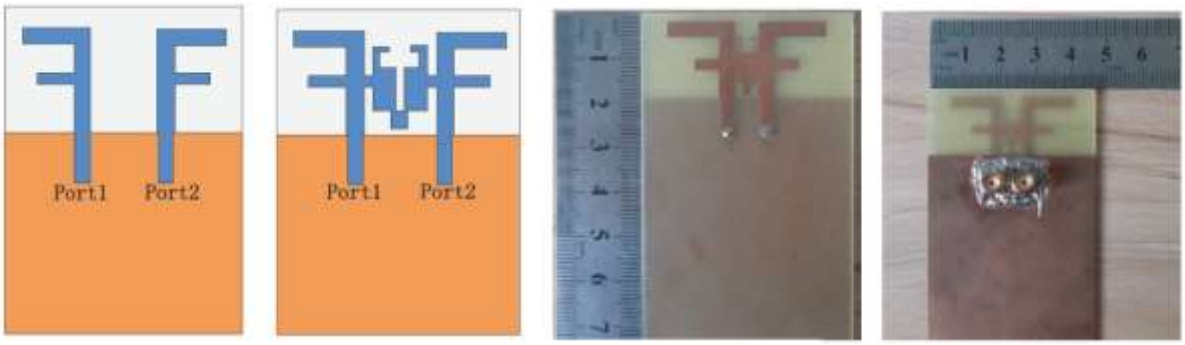

(a) **(b)**

Figure 3.29: Implementation of the DMN used as an isolation method for multiband applications. **(a)** Schematic, and **(b)** Fabricated array [405]

3.1.2.6 Parasitic elements / structures approach

Narrow-band-MIMO Antennas – These parasitic scatterer elements can be of simple and efficient decoupling structures, such as rectangular strips [407-411], squares strips [412], a simple U-shaped microstrip strip [413], other structures are used as parasitic elements to give good isolation improvement levels [414-417]. In these existing works, this technique is not attractive at low frequencies for handset applications except ref [413, 415-416] because the implementation of additional parasitic elements requires significant space. Although; antennas coupling are reduced by introducing simple parasitic structures in ref [413, 415-416], less impedance matching noticed after inserting these structures.

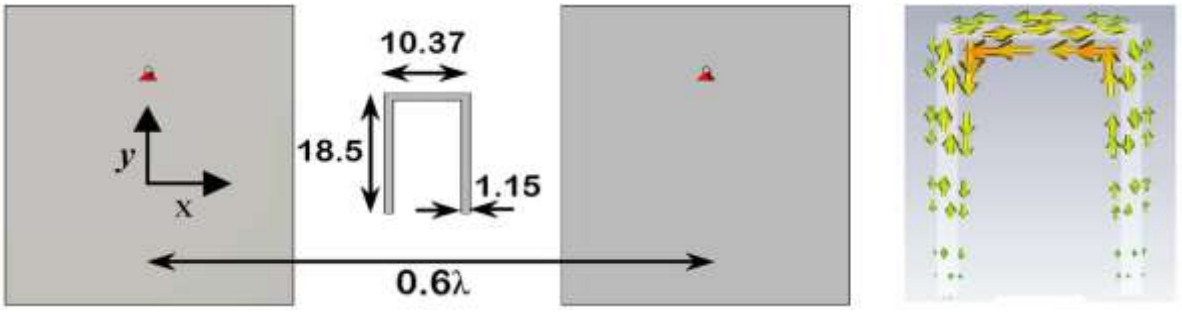

(a) **(b)**

Figure 3.30: **(a)** Antennas structure with a parasitic U-section used as an isolation method for narrow applications, **(b)** Simulated current density vectors [413]

Briefly; one of these designs is now described in more detail as below:

In ref [413], presents a novel coupling structure suppressing the mutual coupling between nearby patches. It is composed of only a simple U-shaped microstrip (as shown in Figure 3.30), which reduces the mutual coupling considerably. By adding a U-shaped microstrip section, an additional coupling path can be created and as we know direct MC between two elements can be cancelled out by adequately adding an extra indirect coupling path. The technique has been experimentally evaluated, and the measured results prove the advantage of the method over other works, in the sense that it effectively combines simplicity, mutual coupling reduction, wide bandwidth, and radiation pattern conservation altogether.

However; the proposed design can achieve more than 15 dB isolation between closely packed antennas operating at 2.4 GHz frequency share a solid ground plane with 0.6 λ_0 inter-antenna spacing (Centre to Centre).

UWB-MIMO Antennas –Several parasitic strips have also been used to achieve mutual coupling reduction between UWB antennas [156, 334-335, 329, 418-423, 429]. To the best of author's knowledge, most of the proposed MIMO antennas in the literature use different designs for decoupling structure to achieve good isolation between elements, but the designs are often difficult to fabricate, and isolation BW do not fully cover entire UWB frequency band.

Briefly; one of these designs is now described in more detail as below: In ref [420], a UWB antenna with high isolation was investigated by placing a floating digitated parasitic decoupling structure that provides wideband isolation characteristics.

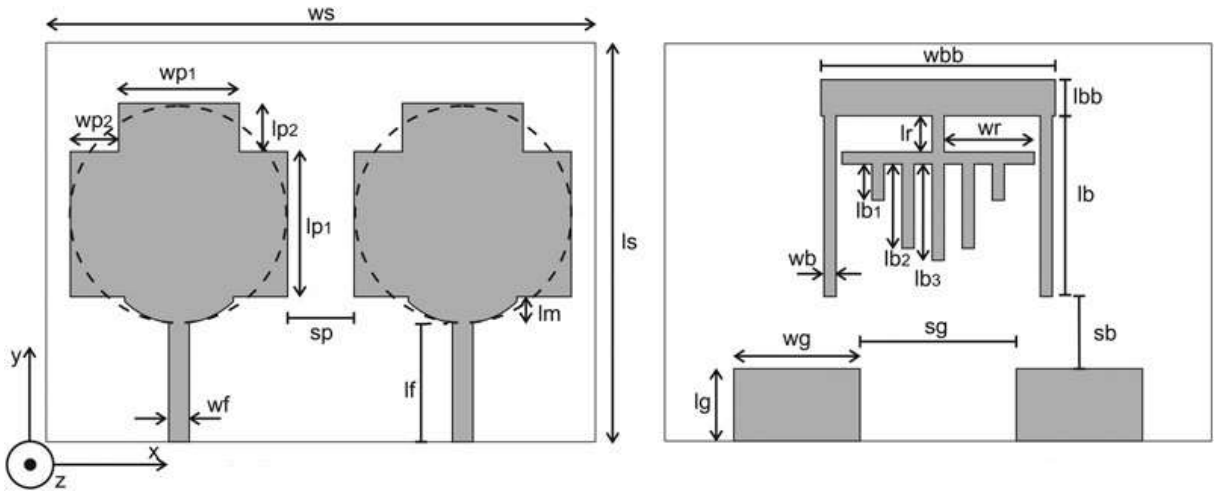

Figure 3.31: Geometry of the optimised antenna elements with decoupling structure used as an isolation method for UWB applications. **(a)** Top view, **(b)** Bottom view [420]

The decoupling structure is introduced on the backside of the diversity antenna, as shown in Figure 3.31 and it provides coupling suppression of better than 20 dB in most of the UWB spectrum along with a compact footprint.

Multi-band-MIMO Antennas – Recently, increasing the isolation between multiband array elements are mainly obtained using new strips such as inverse T and Pi strips [99, 424-428].

Briefly; one of these designs is now described in more detail as below:

In ref [424] a new compact two element dual-band MIMO array operating in WLAN frequency bands of 2.4GHz and 5.2GHz; respectively has been presented. The array has good isolation (for dual-band better than -20dB and -24dB; respectively) by adding a simple structure of the inverted-T shape isolator between the array elements, as shown in Figure 3.32.

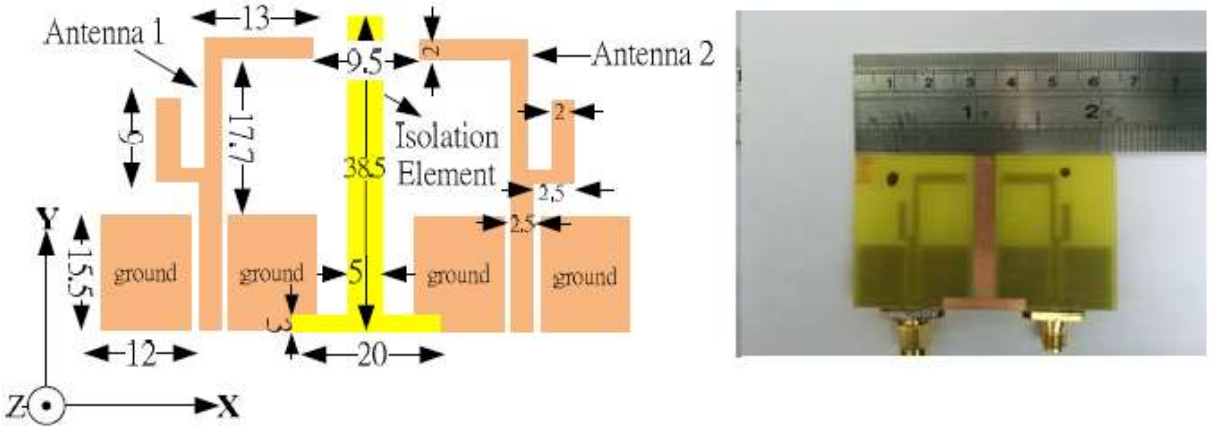

(a) **(b)**

Figure 3.32: (a) The schematic of a dual-element array with isolator, **(b)** Fabricated MIMO with inverted-T isolator used as an isolation method for multiband applications [424]

3.1.2.7 Heterogeneous radiating elements approach

Narrow-band-MIMO Antennas – The term "heterogeneous" is used to indicate that the constituent elements are not identical. A few works presented here; for instance, in ref [143], proposed a compact planar MIMO antenna system of four elements with similar radiation characteristics for the whole 2.4 GHz WLAN band. It consists of two proximity-coupled fed square ring microstrip patch antennas and two $\lambda_0/4$ microstrip slot antennas of the same linear polarisation, as shown in Figure 3.33. These two types of antennas have been printed on different sides of the substrate to reduce mutual coupling.

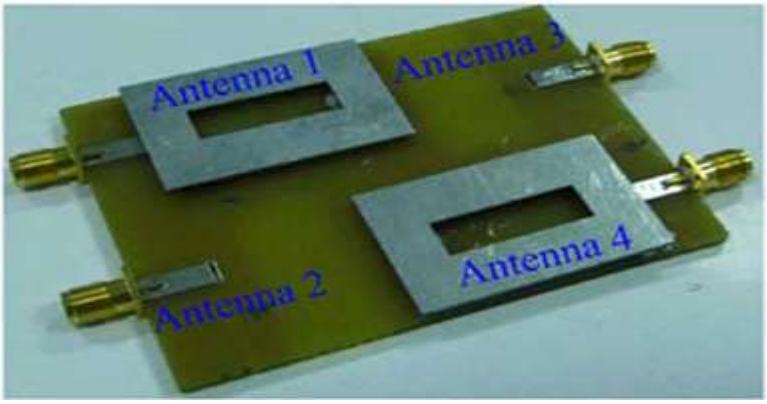

Figure 3.33: MIMO antenna with heterogeneous antenna (different elements types) used as an isolation method for narrow applications [143]

Here; good impedance matching (S_{11} < -10 dB) is achieved across the operating band for all the antenna elements, and high port isolation (better than -25 dB) and good MIMO performance are achieved. Besides, a similar approach was also demonstrated in ref [295].

UWB-MIMO Antennas – For instance, in ref [430], the planar MIMO antenna system consists of two heterogeneous antenna elements printed on the same substrate. The presented antenna system works efficiently in the UWB frequency range of 3.1-10.6 GHz with good isolation (< -14 dB), a very lower correlation coefficient and high diversity gain are obtained. In addition, a similar approach was also demonstrated in ref [431, 496].

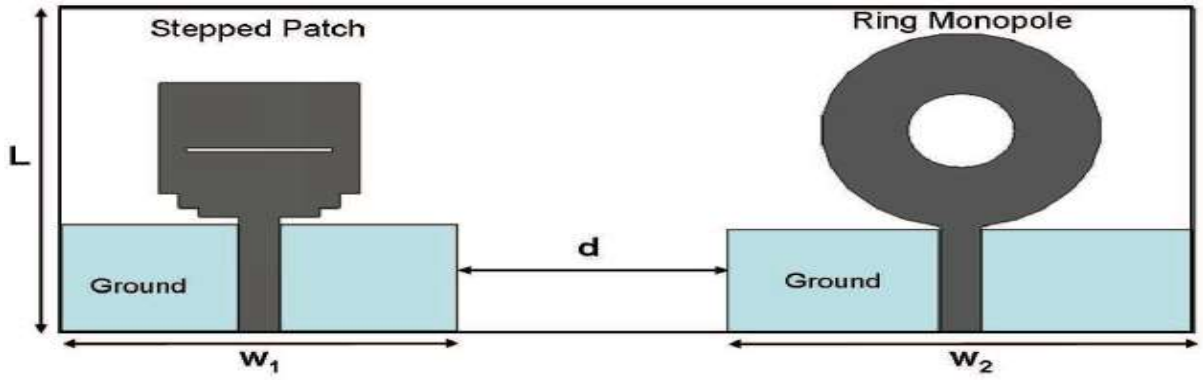

Figure 3.34: A heterogeneous UWB antenna elements used as an isolation method for UWB applications [430]

Multi-band-MIMO Antennas – In ref [432], a dual-band antenna system is designed for lower coupling (< 12 dB) using heterogeneous antennas where the separation is merely less than quarter wavelength (0.24 λ_0); In this array; the left antenna (port 1) is a PIFA-based antenna while right one is monopole-based antenna (port 2) as shown in Figure 3.35.

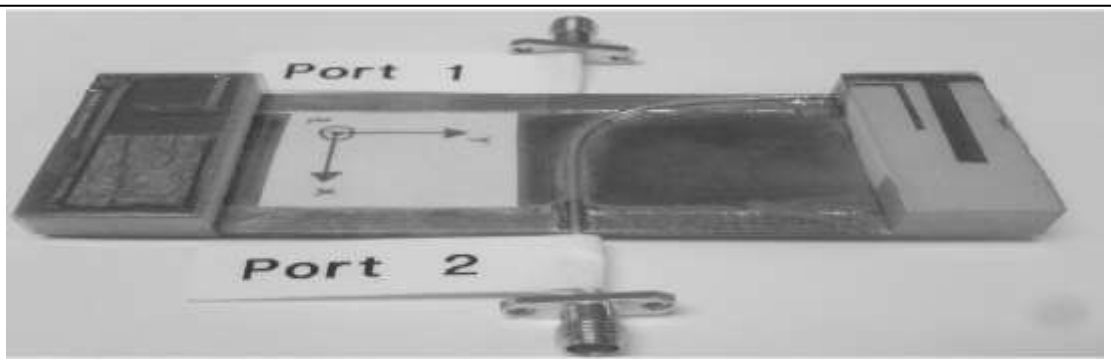

Figure 3.35: A multi-band heterogeneous antenna used as an isolation method for multi-band applications [432]

3.1.2.8 Meta-Material resonators (MTMs) approach

Narrow-band-MIMO Antennas –A lot of works have been appeared in open literature that utilized Metamaterials based structures for isolation enhancement such as: inserting broadside split-ring resonators (BC-SRR) as introduced in ref [133, 292, 436-438], interdigital SRRs [306], Slotted-Complementary SRRs [442-444], capacitively-loaded-loops (CLL) [439-441], spiral resonators [189, 433-435], etc. It has to be noted, though, that in many works under this approach either complex (hard to fabricate) or they are inherently narrowband, and limited by the antenna bandwidth. Briefly; one of these designs is now described in more detail as below:

In ref [292], provide a high isolation performance by properly inclusions of broadside split ring resonators (SRRs) between closely-spaced high-profile monopole antennas.

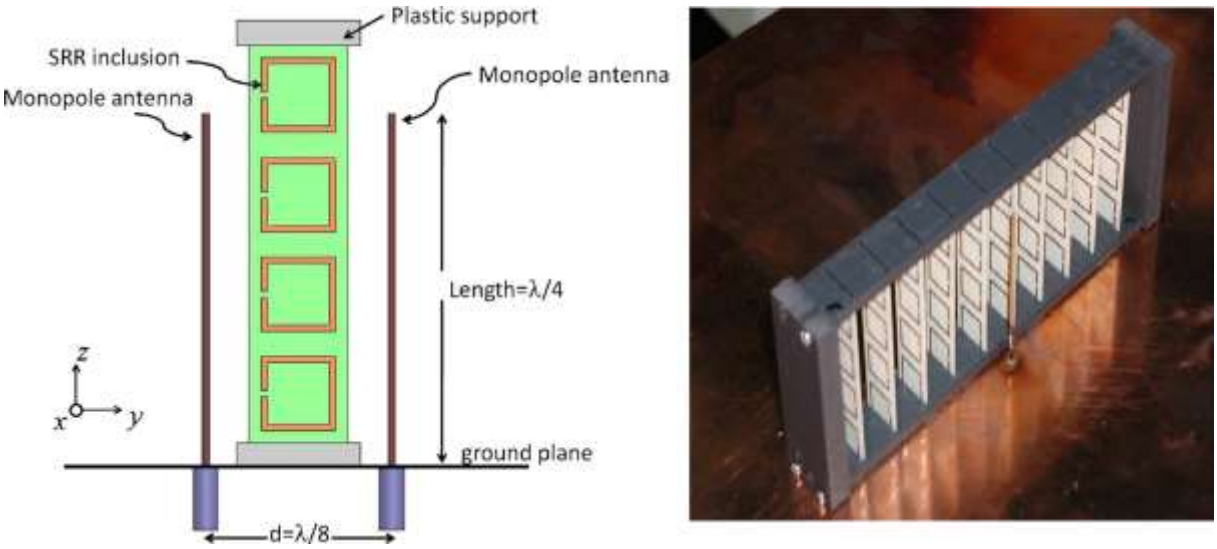

(a) **(b)**

Figure 3.36: (a) A schematic of dual-monopole antennas with SRR inclusions, **(b)** Fabricated MIMO with MTMs used as an isolation method for narrow applications [292]

However, the inter-element distance has been remaining around $\lambda_0/8$, a minimum of 44 dB suppression was achieved using ten strips case is as illustrated in Figure 3.36(b).

Meanwhile, the use of metamaterials to reduce mutual coupling usually involves larger, bulky formations that are not particularly appealing when ease of implementation and miniaturisation become critical issues.

UWB-MIMO Antennas – Relatively; very few designs are available in the open literature for achieving high isolation using MTM structures. For instance, in ref [445], a novel compact UWB-MIMO antenna dual element has been proposed (as illustrated in Figure 3.37). The isolation had been enhanced by inserting the CSRR structure in the ground plane. The effectiveness of the CSRR structure has been demonstrated. The antenna system has a wide impedance bandwidth from 3.1 to 10.6 GHz and good isolation (better than -20 dB) across the whole band.

However; in this design, moderate isolation (10 dB) obtained in a lower UWB range (3.5 to 6.35 GHz). Besides, a similar approach was also demonstrated in ref [201, 446].

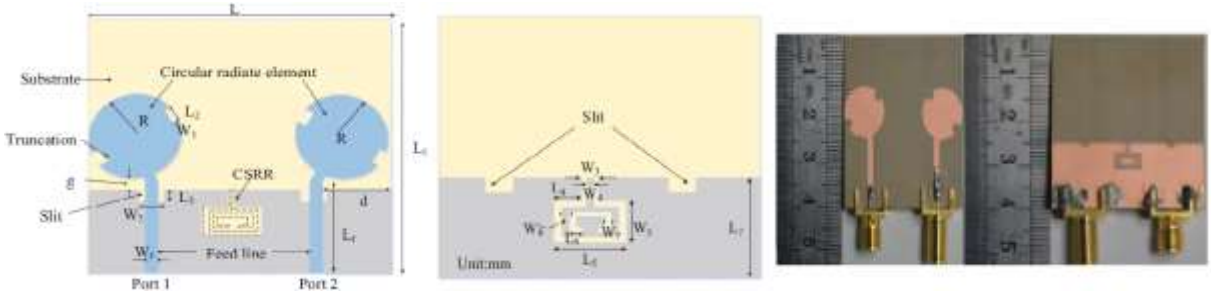

(a) **(b)**

Figure 3.37: (a) A schematic of UWB array antennas with MTMs used as an isolation method for UWB applications, **(b)** Fabricated MIMO [445]

Multi-band-MIMO Antennas – Plenty of previous works utilising MTMs were proposed in [123, 172, 364, 447-452]. In these exciting works (except ref [452]) are either built-in multi-layer or large size [447-450] or only applicable to the decoupling of arrays over a small bandwidth at only a dual-band frequencies [123, 172, 364, 451].

However; in ref [452] a compact four-port MIMO antenna designed for quad-band applications but unfortunately it resonating at uncommon frequencies (1.75 and 1.82 GHz; respectively). Moreover; poor isolation (-17 dB) between antenna ports in the higher bands was noticed. Briefly; one of these designs is now described in more detail as below:

In ref [447], a dual-element dual-band MIMO antenna system based on 4-shaped printed antenna structures was presented (as shown in Figure 3.38):

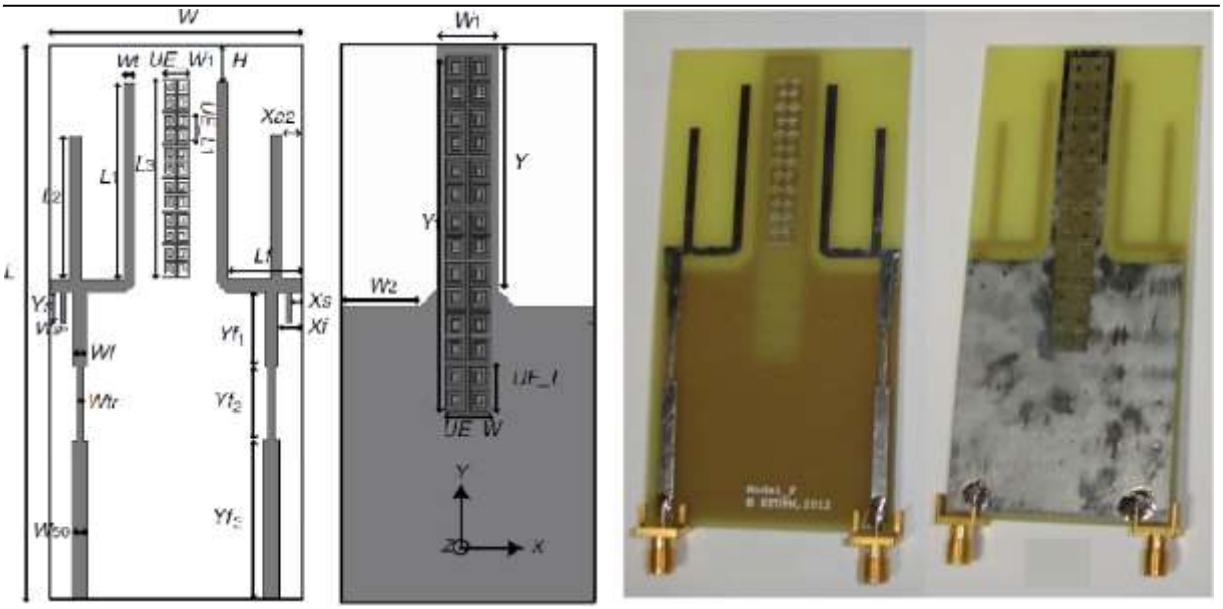

(a) **(b)**

Figure 3.38: (a) Geometry of the 4-shaped MIMO antenna system with MTMs used as an isolation method for multi-band applications **(b)** Fabricated MIMO [447]

The isolation method was based on using arrays of compact capacitively loaded loops (CLL) on the top layer of the PCB while complementary CLLs were used on the bottom layer of the board. The fabricated model of the printed MIMO antenna is shown in Figure 3.38. The printed antenna was fabricated on a 100 × 50 × 1.56 mm^3 FR_4 substrate. The MIMO antennas system covers dual-band (0.82 - 0.85 GHz and 2.32 - 2.98 GHz). The isolation improvement was more than 10 dB in the lower band and 3 dB in the higher band.

3.1.2.9 Combination / Hybrid approaches

Another more attractive and vital approach is used widely for high isolation applications; it can be treated as a hybrid approach that combines the former two methods or more. Easily; by using this approach, compact size and low mutual coupling usually can be achieved.

Narrow-band-MIMO Antennas – Many works related to the utilisation of hybrid approaches have been introduced in the open literature. Commonly; spatial and angular variation technique was combined with the other methods for isolation enhancement applications such as: It could combine with MTM [306], with CLS [255], with NL [299-300, 305, 453], with slots insertion [143, 145, 147], with stub insertion [188, 472], with DWS [279-280]. Other hybrid works include EBG and MTM Structures [133], MTM and stub [189], or using the wall structure combined with slot insertion [144,146]. Briefly; one of these designs is now described in more detail as above: In ref [472], A hybrid approaches (including both stub and antenna orientation methods) have been utilised to obtain good isolation (14 dB) in MIMO antenna working for satellite navigation (1.1 to 1.7 GHz), as shown in Figure 3.39.

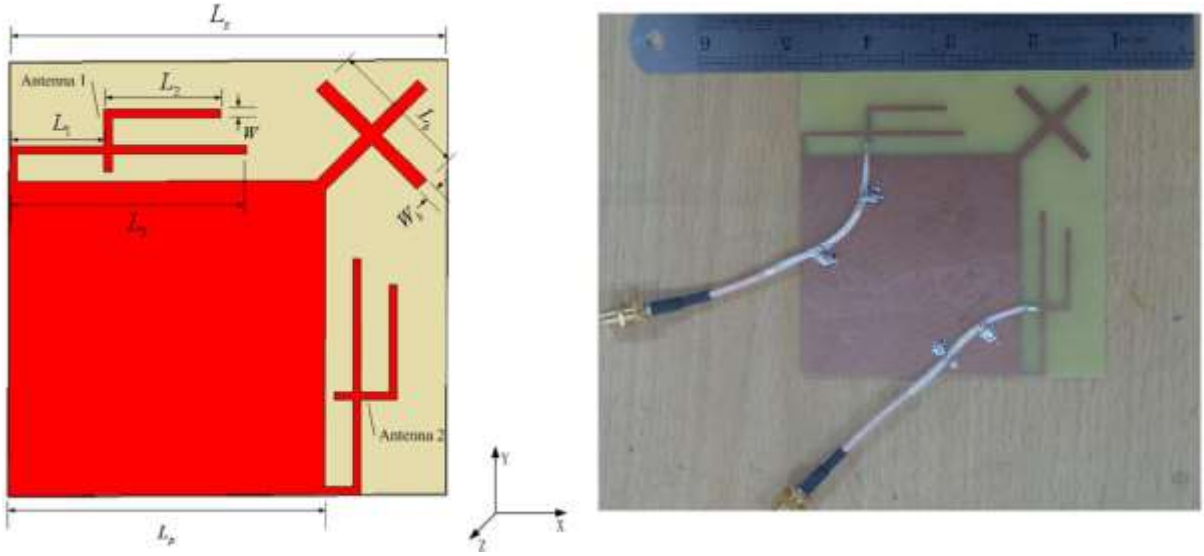

(a) **(b)**

Figure 3.39: (a) A schematic of a dual-element array with a cross-shaped stub, **(b)** Fabricated MIMO [472]

UWB-MIMO Antennas – In this UWB application also hybrid approaches have been introduced for isolation enhancement. Commonly a spatial and angular variation combined with the following methods such as: with different stub structures [154, 193-197, 202, 205, 208, 210, 212, 226-227, 235, 237-238, 317, 321, 328, 455], with NL [323], with slots [154-156], with parasitic structures [156, 226, 329, 334, and 429]. In addition; other important works introduced a combination of slot and stub structures to isolate both ports from each other as in presented in ref [88, 155, 157-158, 161, 201, 210]. Briefly; one of these designs is now described in more detail as below:

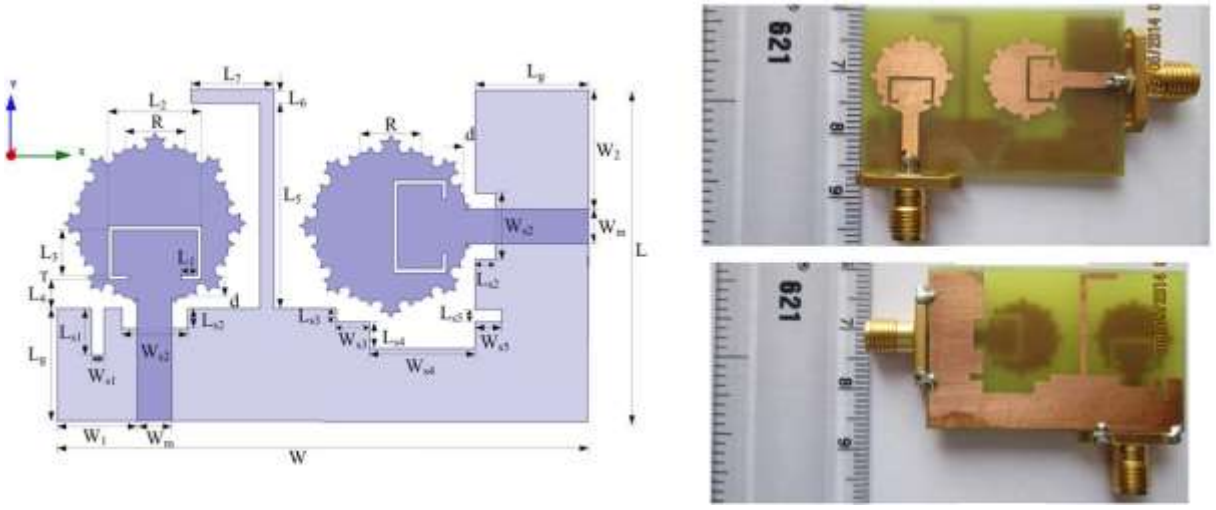

(a) **(b)**

Figure 3.40: (a) A schematic of a dual-element array with an inverted L-shaped stub, **(b)** Fabricated MIMO (Top and back view) [235]

In ref [235], a hybrid approaches as shown in Figure 3.40 (including both the stub and antenna orientation methods) have been utilised to obtain acceptable isolation (< -15 dB) in compact fractal UWB-MIMO antennas with WLAN band-notched characteristics.

Multi-band-MIMO Antennas –In the open literature; many hybrid approaches have been exploiting for isolation enhancement. Commonly; Spatial and angular variation technique combined with other methods such as:

It could combine with different stub structures [249, 252, 459-460], with NL [457-458] , with slots [166, 178], with MTMs [364], etc. Meanwhile; other hybrid works are used to isolate antenna ports from each other such as: a combination of DGS and parasitic structures presented in ref [181, 425], A combination of DGS and stub structures are introduced in ref [96,101], A combination of NL and DGS are introduced in ref [175, 183], A combination of stubs and slots are introduced in ref [165, 167, 461], A combination of MTM and slots are introduced in ref [172], etc. Briefly; one of these designs is now described in more detail as below:

In ref [183], A compact printed MIMO antenna (as shown in Figure 3.41) for USB dongle application covers the WLAN (2.4–2.48 GHz), WiMAX (3.4–3.8 GHz), and HiperLAN (4.7–5.83 GHz) bands. Here; combination methods (NL and DGS) have been utilised to obtain good isolation (better than -14 dB) at both operating frequency bands.

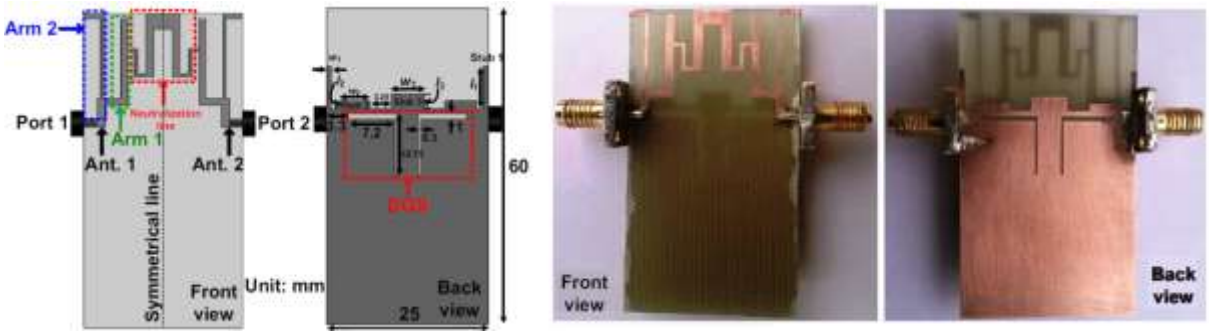

Figure 3.41: (a) A schematic of the dual-element array (Top and back view), **(b)** Fabricated MIMO (Top and back view) [183]

3.1.3 Suppression Techniques of Antenna Coupling Through Near-Field Coupling

Narrow-band-MIMO Antennas – Most of coupling reduction techniques that have proven to be useful in suppression of this type of coupling employ either resonant-type parasitic slots intercept the near fields from the active antenna and re-emit the EM field into free space as presented in ref [71, 147, 295, 469-475].

Other works introduced parasitic scatterers (resonator) in between [78, 412, 416, 462-468, 480], spatial and angular variation [301, 310, 473], or utilisation of MTMs [437, 476-478] or utilisation of NL [300, 305, 383, 379, 381, 479], or utilisation of defected wall structures [144, 278, 282], etc.

However; decoupling structures in these works need to be used with great caution to make sure that radiation from the parasitic elements does not degrade the radiating performance of the multi-antenna system. Briefly; one of these designs is now described in more detail as below:

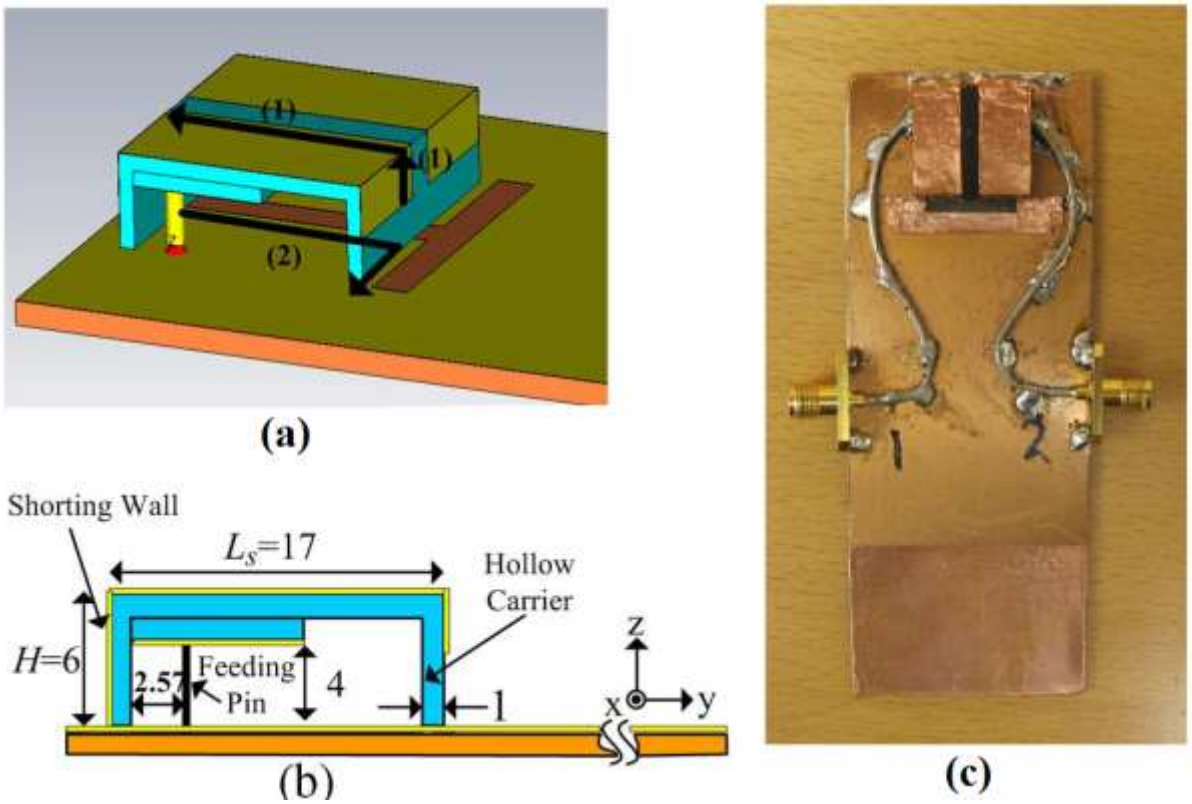

Figure 3.42: (a) 3D view of the dual-element array, **(b)** Side view, **(c)** Prototype of the proposed MIMO [471]

In ref [471], demonstrates an efficient decoupling technique for dual PIFAs that is enabled by a T-shape slot impedance transformer; neighbouring edges of the PIFAs form a quarter-wavelength slot (as shown in Figure 3.42) used as isolation method for suppression near-field between antennas. Here; the array covers the 2.4 GHz WLAN band (2.4–2.48 GHz), and within the WLAN band isolation of over 20 dB is achieved

UWB-MIMO Antennas – Several works available in the open literature that introduced resonant-type parasitic slots/strips for near-field coupling suppression between antennas as presented in ref [88, 159, 420, 481-482]. Briefly; one of these designs is now described in more detail as below:

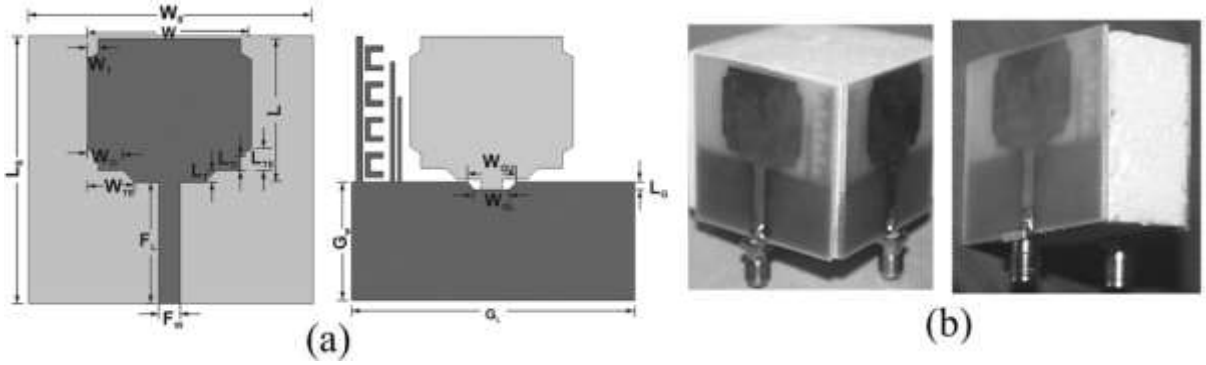

Figure 3.43: (a) Antenna with decoupling structure (Top and back view), **(b)** Prototype of the proposed MIMO (3D view) [481]

In ref [481], MIMO elements are decoupled using four C-shaped strips placed between three vertical stubs, as shown in Figure 3.43. The proposed arrangement results in good isolation (better than 20 dB) and improved impedance matching.

Multi-band-MIMO Antennas – Several works available in the literature that proposed different resonant-type parasitic slots/strips between MIMO antennas for near-field coupling suppression as presented in ref [168, 240, 471, and 483]. Briefly; one of these designs is now described in more detail as below: In ref [471], demonstrates an efficient decoupling technique for dual PIFAs through a dual-isolation property that is enabled by a T-shape slot impedance transformer. Simply; neighbouring edges of the PIFAs form a quarter-wavelength slot (as shown in Figure 3.44) used as an isolation method for suppression near-field between antennas. Here; the array covers the 2.4 GHz WLAN band (2.4–2.48 GHz) and the WiMAX band of 3.4–3.6 GHz, with isolations of over 19.2 dB and 22.8 dB, respectively.

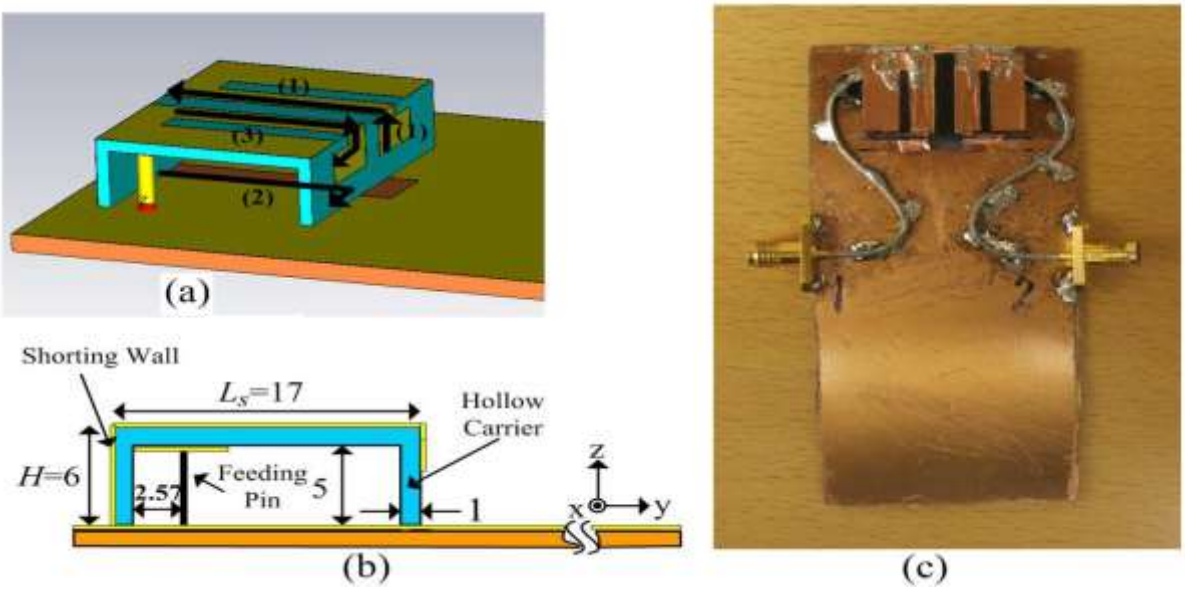

Figure 3.44: (a) 3D view of dual-element array, **(b)** Side view, **(c)** Prototype of the proposed MIMO [471]

3.2 Summary of the important mutual coupling suppression techniques

3.2.1 Narrow-band-MIMO Antennas –A summarised state of art of Narrowband-MIMO antennas contain important previous works are listed in Table 3.1, which detailing in the operation frequency, volume, and the isolation level obtained by different mutual coupling suppression approaches.

Table 3.1 Summarised states of the art on Narrow-band -MIMO antennas

Ref.	Centre Frequency (GHz)	MIMO Antenna Structure	Separation (λ_0)	Volume (mm^3)	Isolation (dB)	Suppression Approach
[81]	2.53	Dual-patch array	0.24	N/A	-46	DGS
[117]	5.75	Dual-patch array	0.5	398	-32	EBG
[145]	2.5	Dual-PIFA array.	0.265	516	-20	Slots/slits
[186]	2.05	Four-monopole array	N/A	4560	-22	Stub
[41]	2.5	Dual-PIFA array.	0.17	20000	-20	CLS
[327]	5.22	Dual-patch array	0.1	125	-23.5	Shorting pins
[262]	2.6	Dual-PIFA array.	N/A	20000	-22	Separation
[278]	2.5	Dual-PIFA array.	0.4	116100	-53	DWS
[307]	2.45	Dual-PIFA array.	0.14	40000	-31	Placement and orientation
[381]	2.14	Dual-PIFA array.	0.127	34000	-15	NL
[396]	0.71	Dual-patch array	0.025	5500	-28	DMN
[413]	2.4	Dual-patch array	0.6	38620	-30	Parasitic elements
[143]	2.45	Dual-patch-slot array	N/A	4210	-25	Heterogeneous
[292]	1.24	Dual-monopole array	0.125	5400000	-40	MTMs
[472]	1.5	Dual-PIFA array.	N/A	300.6	-14	Combination

3.2.2 UWB-band-MIMO Antennas –A summarised state of art of UWB-MIMO antennas contains important previous works are listed in Table 3.2, which detailing in the operation frequency range, volume, and the isolation level obtained by different mutual coupling suppression approaches.

Table 3.2 Summarised states of the art on UWB-MIMO antennas

Ref.	Frequency Range (GHz)	MIMO Antenna Structure	Separation (λ_0)	Volume (mm^3)	Isolation (dB)	Suppression Approach
[88]	2.4-6.5	Dual-monopole array	0.1	4992	-18	DGS
[137]	3-6	Dual-monopole array	0.1	4800	-20	EBG
[154]	3.1-5.8	Dual-monopole array	0.25	5654.4	-20	Slots/slits
[194]	3.1-10.6	Dual-monopole array	N/A	1040	-15	Stub
[267]	3.1-10.5	Four-monopole array	0.5	5040	-16	Separation

[325]	3.1-12.3	Dual-monopole array	0.1	2240	-20	Placement and orientation
[386]	3.1-5	Dual-monopole array	0.12	448	-22	NL
[420]	3.1-10.6	Dual-monopole array	0.2	2372	-20	Parasitic elements
[430]	3.1-10.6	patch-monopole array	0.2	4080	-14	Heterogeneous
[445]	3.1-10.6	Dual-monopole array	0.2	1400	-20	MTMs
[235]	3.1-10.6	Dual-monopole array	N/A	1600	-15	Combination

3.2.3 Multi-band-MIMO Antennas –A summarised state of art of Multi-band-MIMO antennas contains important previous works are listed in Table 3.3, which detailing in the operation frequency bands, volume, and the isolation level obtained by different mutual coupling suppression approaches.

Table 3.3 Summarised states of the art on Multi-band-MIMO antennas

Ref.	Frequency bands (GHz)	MIMO Antenna Structure	Separation (λ_0)	Volume (mm^3)	Isolation (dB)	Suppression Approach
[104]	0.74-0.78, 1.85-1.99, 1.92-2.17, and 3.60–3.70	Dual-PIFA array	0.1	4800	-24.6	DGS
[139]	5.11-9.40, and 10.69-15.85	Dual-patch array	0.8	5200	-20 -21	EBG
[173]	2.35-2.6, and 5.1-5.3	Dual-PIFA array	0.3	4000	-16 -20	Slots/slits
[241]	1.904–2.504, and 2.400–2.484	Dual-monopole array	0.1	4752	-15 -20	Stub
[257]	5.1-5.56	Dual-PIFA array	0.74	37800	-16.5	CLS
[333]	2.45 and 5.8	Dual- monopole array	0.1	2600	-27 -21	Shorting pins
[272]	1.71–1.88, 1.88-1.99, 1.90-2.20, and 5.15-5.35	Four-patch array	0.5	5600	-15	Separation
[344]	2.4 and 5.2/5.8	Three-loop array	0.65	8000	-15 -20	Placement and orientation
[389]	2.4-4.2	Dual-monopole array	0.19	2844	-17	NL
[405]	2.46-2.7, and 5.04-5.5	Dual-monopole array	0.1	5600	-30	DMN
[424]	2.3-2.6, and 5-5.5	Dual-monopole array	0.08	1600	-20 -24	Parasitic elements
[432]	0.85, 1.8 and 2.1	PIFA and monopole array	0.24	32000	-15	Heterogeneous
[447]	0.82-0.85, and 2.32-2.98	Dual-monopole array	0.06	7800	-10 -18.9	MTMs
[183]	2.4–2.48, 3.4-3.8, and 4.7–5.83	Dual-PIFA array	N/A	2400	-14	Combination

3.3 Chapter Summary

In this chapter, a comprehensive literature review on different microstrip array antennas has been provided. It has become apparent that despite a lot of research activities in the past decade regarding the field of antenna coupling reduction, there is still the lack of a systematic and coherent approach in the identification of different mechanisms that contribute to antenna coupling problems. To address this gap, in this chapter, there has been comprehensive analysis of the sources of the antenna coupling that occur between multiple-antennas in different wireless applications, including: narrow-band, ultra-wideband and multiband applications. Moreover, the various mechanisms that contribute to the mutual coupling problem between multiple antenna systems have been identified. In this chapter, various mutual coupling reduction techniques that are commonly employed in the literature are categorised based on the coupling mechanisms that they target for efficient coupling suppression. Moreover, an overview of the previous methodologies as subsections under these main classifications has been provided. In addition, there has been a thorough review of some approaches proposed for controlling the issue of mutual coupling between the multiple antenna elements. The impact of many coupling suppression techniques owing to surface waves has been assessed in terms of their merits, including: Defected Ground Structure (DGS); Electromagnetic Band Gap (EBG) structures, inserting slots\slits structures, inserting GND stubs, Current Localisation Structures (CLS) and the shorting pins\vias approach. Similarly, the impact of other coupling suppression approaches due to direct or space waves has been presented in depth in terms of their capability of controlling mutual coupling, including: antenna separation; Decoupling Wall Structures (DWS), the antenna placement and orientation technique; Neutralisation Line (NL); Decoupling and Matching Networks (DMN); parasitic structures, heterogeneous elements; and utilisation of the Meta-Material Structures (MTMs) approach. It has been observed from the reported research in the literature review that, many decoupling approaches are either complex in terms of implementation or still need to be enhanced without degrading the other antenna performance to meet the demand for portable devices (i.e. mobile handsets). Hence, more research is essential to develop new multiple antennas with applicable decoupling methods that offer attractive characteristics for different wireless applications, such as high isolation, geometric simplicity and compactness in terms of total antenna size. Some of these attractive features are provided through the work in the following chapters (chapter 4, chapter 5 and chapter 6).

Chapter 4: Development of Multiple Antennas with High Isolation for Narrowband Applications

4.1 Introduction

The concept of designing multiple antennas on small mobile terminals has been introduced in chapter two. The essential requirements of multiple antennas on a size-limited mobile terminal for MIMO systems are that the multiple antennas should have a good isolation characteristic (low mutual coupling) between microstrip antenna elements even though they are closely spaced. In the literature many researchers have proposed several techniques to reduce mutual coupling over a narrow operating frequency band for MIMO antennas. However, no significant contribution has been made for mutual coupling reduction in MIMO antennas based on fractal geometry combined with EBG theory. In this chapter, a new high isolation MIMO antenna for narrowband applications is presented. The high isolation is achieved through inserting a novel arrangement of Fractal based Electromagnetic Band Gap (FEBG) structure between dual antenna elements sharing a common substrate \ ground. The proposed MIMO antennas can operate at approximately 2.65 GHz for Long Term Evolution (LTE) application with compact design dimensions. The FEBG band-gap characteristic is verified using a more computationally efficient analysis. The performances of the multiple antennas are investigated and verified both numerically and experimentally.

4.2 Fractals Classification

The term fractal means broken, or irregular fragments initially introduced to describe complex shapes that possess an inherent self-similarity or self-affinity in their geometrical structures. A fractal is a self-similarity structure, which means that a small part of the structure is a scaled-down copy of the original structure. The main idea of utilising fractal geometries in the design of microstrip antennas is to increase the effective electrical length through which current travels. Fractals classified into two main categorises (linear and nonlinear), the use of fractals to design compact structures between different microstrip antennas for isolation enhancement is a recent and an applicable technique.

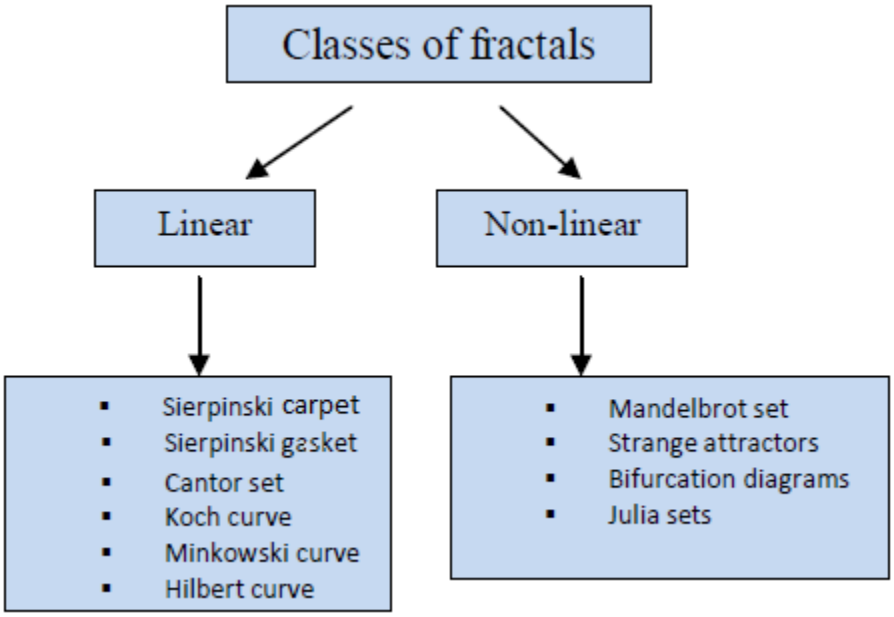

Figure 4.1: Classification diagram of fractals

Here; some essential examples of ordinary linear fractal geometry as the following:-

4.2.1 Sierpinski carpet fractals

The Sierpinski carpet is a linear fractal. It is arguably the simplest of fractals and a good place to begin the discussion on linear fractals, as shown in Figure 4.2.

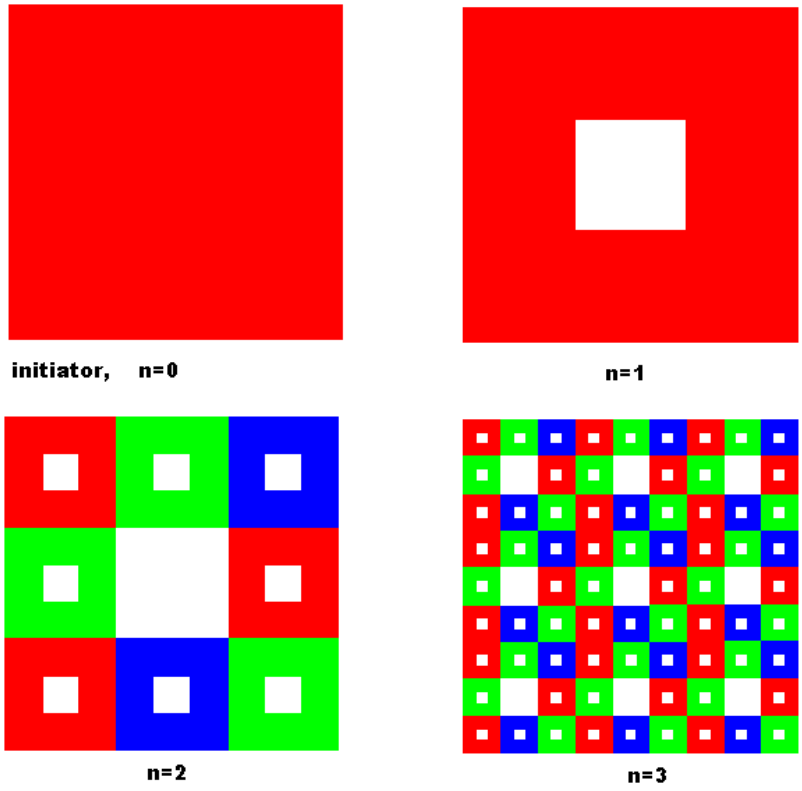

Figure 4.2: Steps of construction of the Sierpinski carpet

In order to start this type of fractal curve, it begins with a square in the plane, and then it is divided into nine smaller congruent squares where the open central square is dropped (n = 1). The remaining squares are divided into nine smaller congruent squares which each central square is dropped (n = 2) [482]. This process is continued to infinity. Many Sierpinski carpet fractal based structures have been proposed to produce printed microstrip monopole antennas with compact size and multiband performance for different applications. However; in this chapter, Sierpinski carpet fractals had been utilised between multiple antennas as a new isolation method based on EBG theory as illustrated in section 4.3.

4.2.2 Sierpinski gasket fractals

The construction of the Sierpinski gasket is illustrated in Figure 4.3. It is another well-documented fractal. The Sierpinski gasket is constructed analogously to the Sierpinski carpet, but it uses triangles instead of squares. The initiator, in this case, is a filled triangle in the plane. The inverted central triangular section is subtracted from the original triangle. Then, the middle triangular sections are removed from the remaining triangular elements and so on. After endless iterations, the Sierpinski gasket is formed. Each pre-fractal stage in the construction is composed of three smaller copies of the preceding stage, each copy scaled by a factor of one half [483].

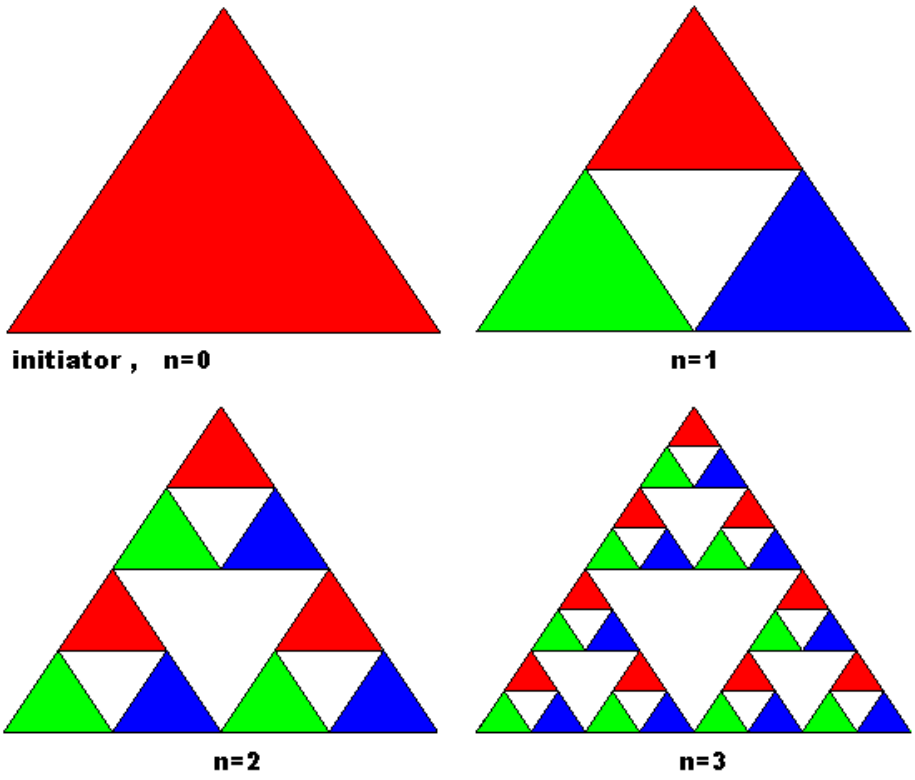

Figure 4.3: Steps of construction of the Sierpinski gasket

4.2.3 Koch curve fractals

The method of construction of the Koch curve is illustrated in Figure 4.4. The Koch curve s constructed merely using an iterative procedure beginning with the initiator of the set as the unit line segment (step $n = 0$ in the figure). The unit line segment is divided into thirds, and the middle third is removed. The middle third is then replaced with two equal segments, both one-third in length, which form an equilateral triangle (step $n = 1$): This step is the generator of the curve. At the next step (n = 2), the middle third is removed from each of the four segments, and each is replaced with two equal segments as before. This process is repeated to an infinite number of times to produce the Koch curve [106]. A remarkable property of the Koch curve is that it is seemingly infinite in length. This may be seen in the construction process. At each step n, in its generation, the length of the pre-fractal curve increases to 4/3 L_{n-1}, where L_{n-1} is the length of the curve in the preceding step [485]. The Koch curve is one of the most familiar fractal curves which can be used as wire antennas to reduce the size and for multiband operation.

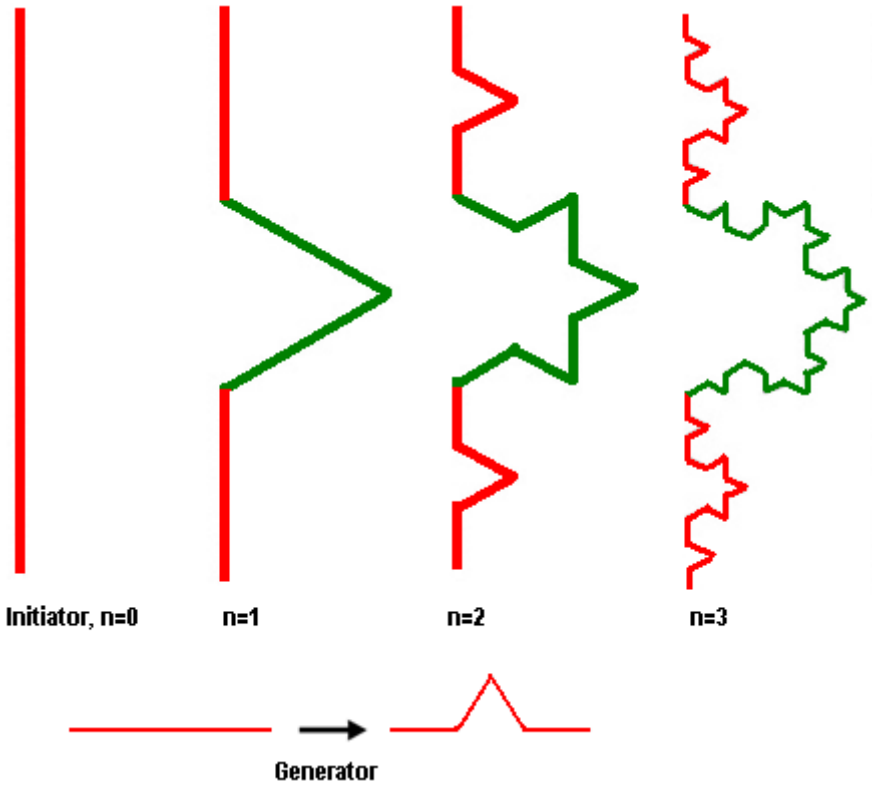

Figure 4.4: Four stages in the construction of the Koch curve

4.2.4 Cantor set fractals

Cantor fractal or Cantor set, shown in Figure 4.5 is also a simple example of fractals. Typical construction is a middle third Cantor set constructed by an iterative process.

The Cantor set consists of an infinite set of disappearing line segments in the unit interval. The best aid to the comprehension of the Cantor set fractal is an illustration of its method of construction, and this is given in Figure 4.5 for the purest form of Cantor set.

The set is generated by removing the middle third of the unit line segment (step n = 1 in the figure). From the two remaining line segments, each one-third in length, the middle thirds are again removed (step n = 2 in the figure). The middle thirds of the remaining four line segments, each one-ninth in length, are then removed (step n =3) and so on to infinity [486].

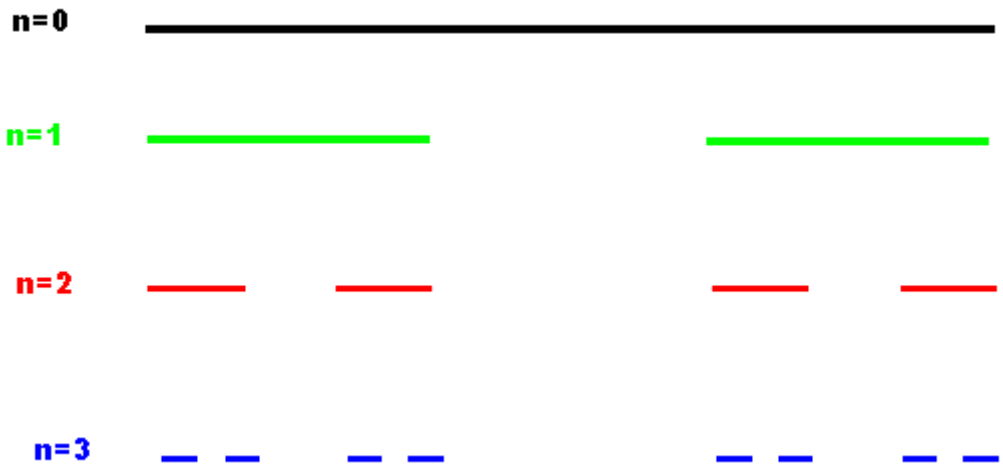

Figure 4.5: Four stages in the construction of the Cantor set

4.3 Electromagnetic Band-Gap (EBG) Theory

As mentioned before in chapter two, Electromagnetic Bandgap (EBG) materials are periodic structures capable of prohibiting electromagnetic (EM) wave propagation within a particular frequency band for certain arrival angles and polarisations.

Surface waves are undesirable in any antenna array design. The surface waves degrade the essential parameters such as peak gain, radiation pattern and efficiency of the antenna as these waves travel along a surface plane. The implementation of Electromagnetic Bandgap structures can resolve this issue. EBG structures have periodic metal patches settled on a dielectric substrate.

Basically; the frequency region where the incident waves cannot propagate through the structure is termed the ‘band-gap’ or ‘stopband’. In other words; when the frequency is in the stopband region, there is no transmission through the material (the incident wave does not travel through the media). While, if the frequency is in the passband (i.e. outside stopband) region, the energy will propagate through the material, as shown in Figure 4.6.

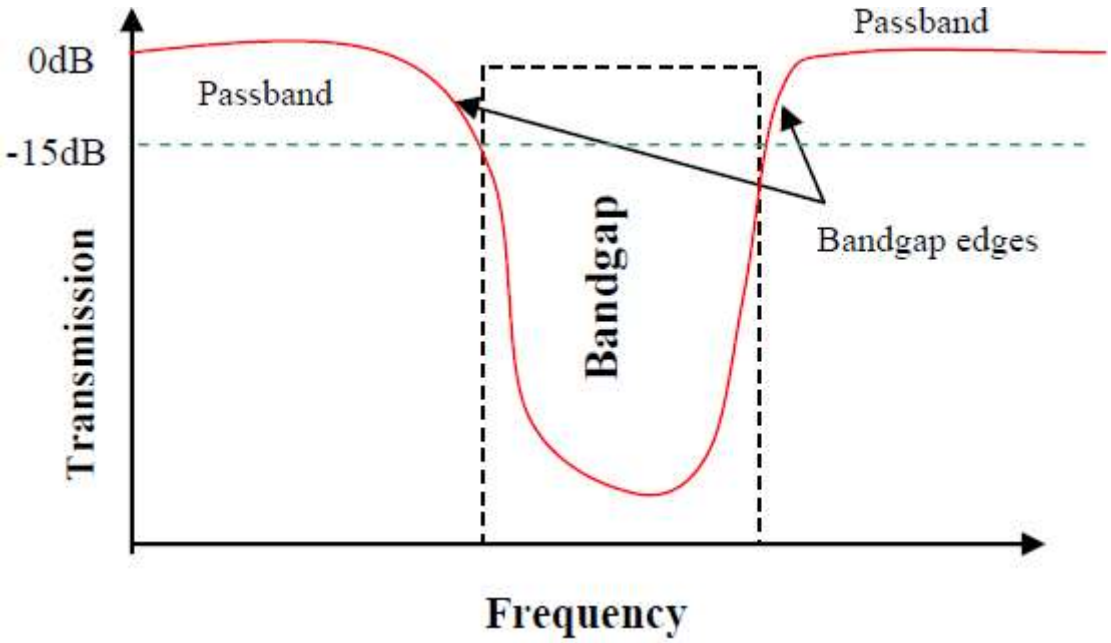

Figure 4.6: A diagram showing passband and bandgap behaviour of an EBG

The EBG reflector allows propagation for waves at passband frequencies, and the metal inhibits waves at all frequencies. This idea has attracted microstrip antennas engineers to use it in some narrow-band applications to prevent the propagation of the electromagnetic waves in a specified frequencies band. EBG structures have a property of obstructing the surface waves at a specific frequency and also reflect any incoming wave without any phase shift, This concept is illustrated in Figure 4.7.

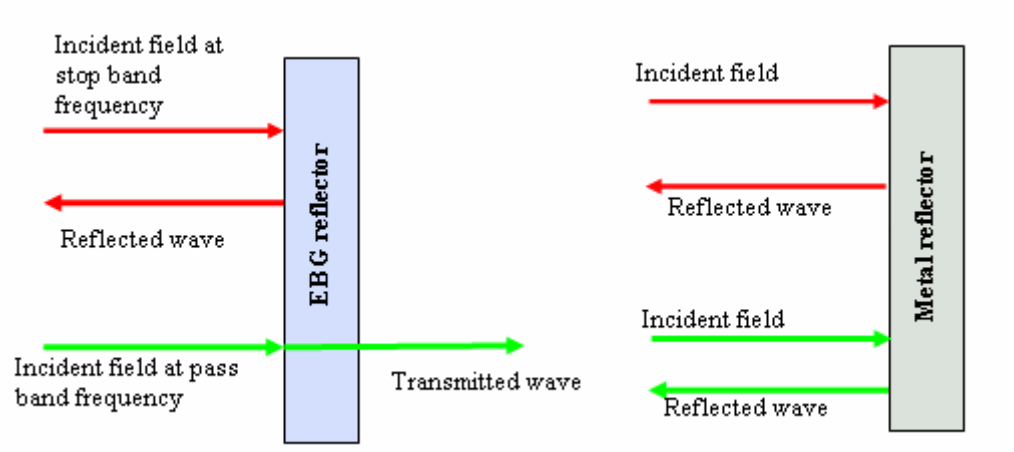

Figure 4.7: Diagram illustrating the application of EBG as a mirror and its comparison with a metal reflector [470]

The EBG structures also have the ability to suppress the surface wave propagation on the ground plane of the microstrip antennas and thus minimise the mutual coupling, also an improvement of the radiation pattern of the antennas on finite ground plane as the currents do not reach the outer edges with high density and thus limits the interfering radiation produced by the spurious waves radiated at the boundaries of the microstrip antennas.

As mentioned before; surface waves can occur on the interface between two dissimilar materials, such as metal and free space. They are bound to the interface, and decay exponentially into the surrounding material. Figure 4.8 shows the comparison operation phenomenon of the antenna with and without EBG structures.

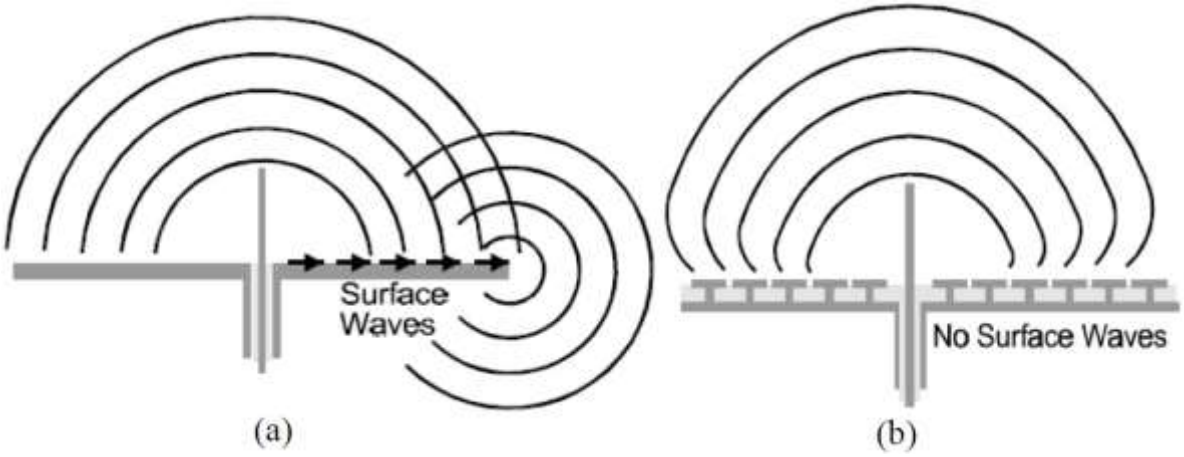

Figure 4.8: Surface wave. **(a)** without EBG, and **(b)** with EBG [470]

EBGs can be practically implemented as 1D, 2D or 3D structures. For instance; they are arranged in a two-dimensional lattice and can be visualised as mushrooms from the surface.

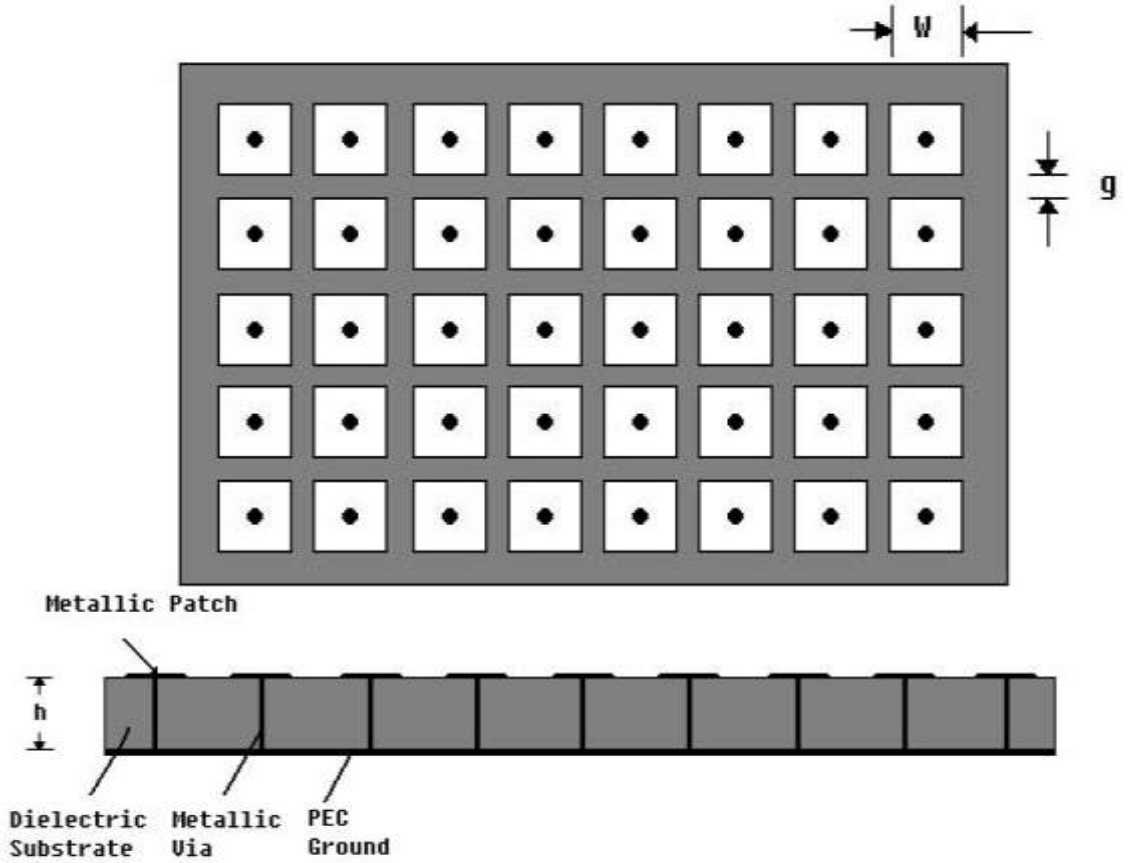

Figure 4.9: Geometry of the mushroom-like structure on a dielectric slab (Top and side view) [39]

These structures are formed as metal patches on the top surface of the board, connected to the solid lower conducting surface by metal plated vias (as shown in Figure 4.9). Here; *w*, *g* and *h* are the width of the patch, a gap between patches and height of substrate; respectively

The electromagnetic properties of this basic structure can be described by using lumped-circuit elements including capacitors, *C*, and inductors, *L*, when they are small compared to the operating wavelength. They behave as a network of parallel resonant *LC* circuits, which act as a two-dimensional electric filter to block the flow of surface currents along the sheet [487]. When the structure interacts with electromagnetic waves, currents are induced in the top metal plates, as shown below in Figure 4.10.

A voltage applied parallel to the top surface causes charges to build upon the ends of the plates, which can be described as a capacitance [29]. As the charges flow around a long path through the vias and bottom plate. A magnetic field associated with these currents results and hence can be described as an inductance.

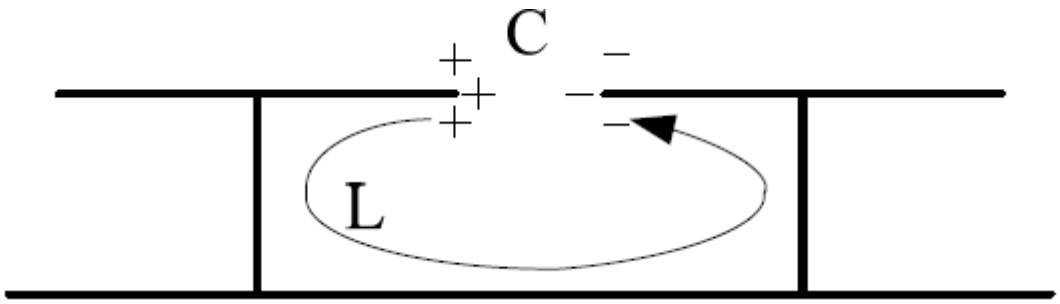

Figure 4.10: Capacitance and inductance in the high-impedance surface [29]

The following formulas can be used to calculate the bandgap frequency of EBG structures [488]:-

$$C = \frac{\varepsilon_0 (1+\varepsilon_r) W}{\pi} \cosh^{-1}\left(\frac{W+g}{g}\right) \qquad (4.1)$$

$$L = \mu_0 h \qquad (4.2)$$

Where ε_0 and μ_0 are permittivity and permeability of the free space, ε_r is the relative permittivity of the dielectric substrate.

The surface impedance is high close to the resonant frequency ω_0 which can be determined from the *L* and *C* as follow [5]:

$$\omega_0 = \frac{1}{\sqrt{LC}} \qquad (4.3)$$

Where ω_0 is the bandgap centre frequency, C is the capacitance due to the gap between the EBG patches. *L* is the inductance resulting from the current flowing along the vias to the ground plane (as shown in Figure 4.10). These characteristics of EBG structures enhance the performance of the microstrip antenna [484].

Recently; EBG structures are used for the isolation enhancement in MIMO systems.
However, this has not been of interest to the mobile phone manufacturers because these structures are complicated and are too costly to produce.
Hence, another more straightforward method based on EBG theory is proposed and discussed in the next section 4.4.
Meanwhile; there are a few kinds of research on the combination of the fractal geometry to EBG theory for mutual coupling reduction applications.
Thus; a miniaturised FEBG has been proposed for narrow-band applications between MIMO antennas. In the same context, our proposed antennas also exploit the similar ideas available in the open literature to reduce the mutual coupling effects.

4.4 Multiple Microstrip Antennas with High Isolation for Narrowband Applications

4.4.1 Fractal electromagnetic bandgap structure (FEBG)

As mentioned earlier; fractal structures are comprised of multiple smaller elements patterned after self-similar (with scaled-down designs) to increase the physical length of current paths or redistribute the surface current density; these properties made these structures more applicable at low-frequency ranges in wireless applications.
The use of fractal geometry is mainly considered an appropriate technique to design multi-band and meets the miniaturisation requirements of the mobile equipment [141, 491].
In the literature, extensive research was done using fractal-based EBG for mutual coupling reduction between the various microstrip antennas.
Recently; fractals have been employed to numerous applications in the modern MIMO antenna designs, such as compact antennas, mutual coupling reduction, filter applications, leakage suppression, and harmonic tuning for power amplifiers..etc.
The present study focuses on mutual coupling reduction using these compact fractal structures. Fractal-based EBG structure has a unique property of compactness with longer current paths that it could work efficiently in low-frequency range due to space filling features. Additionally, these fractal structures, due to self-similarity features, are also found to be able to provide a band-stop effect for a particular frequency band owing to the impedance (These filtering effects due to the combination of inductances and capacitances).
In this work; a popular fractal type, Sierpinski carpet, applied as a planar EBG structure between dual antennas (PIFAs) elements to have a high isolation characteristics.
In comparison with other common structures (e.g. mushroom-like EBG) that occupy a large

space between elements, FEBG structures have a more compact size and less complicated configuration (applicable without the use of vias and does not require any shorting pins or other types of vertical connection) [29, 128].

Meanwhile, these properties are integrated easily with other radio frequency and microwave components, and relatively, they have a broader stopband bandwidth that provides an adequate surface wave suppression effect.

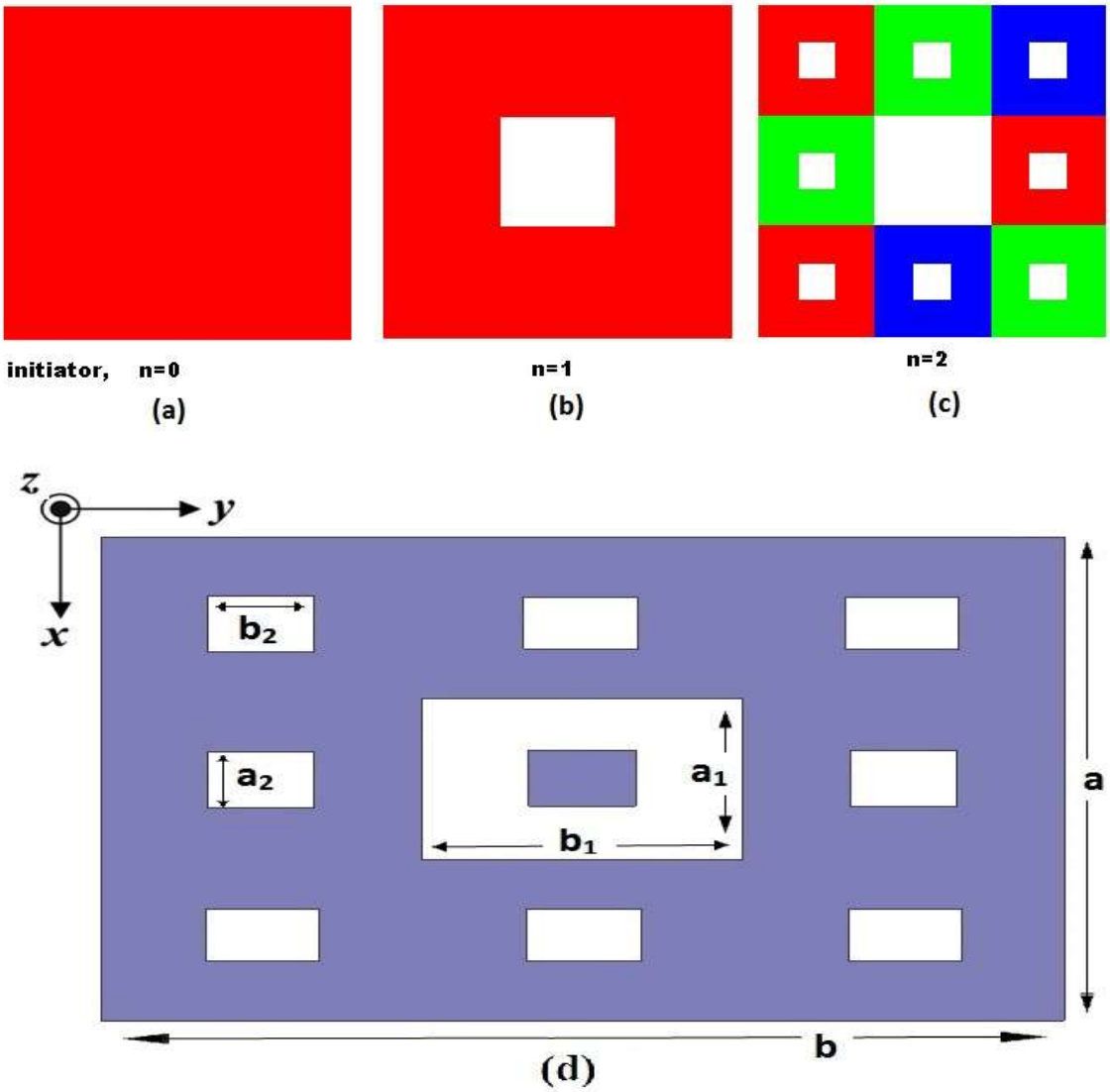

Figure 4.11: Illustration of the fractal geometry: **(a)** Zero-iteration order, **(b)** First-iteration order, **(c)** Second-iteration order, **(d)** Layout of the proposed second iterative order FEBG unit cell

The designed fractal geometries are zero, first, and second-order iterative structures based on a well-known fractal structure called Sierpinski carpet (as mentioned before in section 4.2.1). The zero-order iterative fractal structure is a single metallic (copper) square, as shown in Figure 4.11(*a*). The first-order iterative fractal structure is divided into nine small congruent squares, where the open central square is dropped (n = 1), as shown in Figure 4.11(*b*). The second-order iterative fractal structure evolves from a first-order iterative fractal structure, as

shown in Figure 4.11(*c*). The remaining squares are divided into nine small congruent squares, in which each central square is dropped (n = 2). In this study, a well-known fractal type, Sierpinski carpet, is utilized and applied as a planar EBG structure between two antenna (PIFA) elements to obtain a high isolation characteristic. Figure 4.11(d) illustrates the proposed design of the second iterative order FEBG unit cell. The parameters optimisation based on scaling down with many iterations by a particular factor (1/3) and the optimised parameters of the proposed second iterative order FEBG used in this work are:

$$\mathrm{a} = 9\ \mathrm{mm}, \mathrm{b} = 13\ \mathrm{mm}, \qquad \mathrm{a}_1 = \frac{1}{3} \times \mathrm{a},\ \mathrm{b}_1 = \frac{1}{3} \times \mathrm{b}, \qquad \mathrm{a}_2 = \frac{1}{3} \times \mathrm{a}_1,\ \mathrm{b}_2 = \frac{1}{3} \times \mathrm{b}_1$$

The unit cells are etched on an FR_4 dielectric substrate with ε_r = 4.4 and thickness h =1.6 mm.

4.4.2 FEBG unit cell design and bandgap characterisation

The EBG with a periodic shape provides a rejection band in some frequency ranges. This bandgap filtering characteristic of EBG enables the mutual coupling reduction between antenna array elements. In the present work, the eigenmode analysis is performed using a full-wave simulation tool (HFSS software ver. 17.0) to demonstrate the filtering characteristics of the proposed second-order iterative FEBG structure.

The frequency band gap over which surface waves cannot propagate, and this can be verified from the dispersion diagram.

Dispersion diagram different from driven modal (transmission line) method or reflection phase diagram, which response to a standard wave incidence case.

Although these approaches can be calculated quicker, it can only show quasi-TEM modes which are excited by ports.

Mode-coupling and the isotropic nature of an EBG unit cell are not considered in these approaches. Full characterisation of the unit cell structure can be done by using the eigenmode solver.

The 2-D dispersion diagram generation requires an eigenmode solution.

The eigenmode approach solves the problem for natural resonances of the structure and gives information about mode-coupling and structure isotropy.

The eigen-mode solution needs significantly more resources and time compared to the driven modal method. It calculates the propagation constant (β) for different angles of an incident wave [494].

Dispersion diagram includes an EBG response for every possible incidence angle, thereby providing a complete picture of EBG frequency bandgaps [495, 496] considering that surface waves are mainly concentrated in the substrate and at the substrate/air interface [493].

However, the FEBG structure prevents surface wave propagation in a specific frequency band of interest for all incident wave angles and polarisation states.

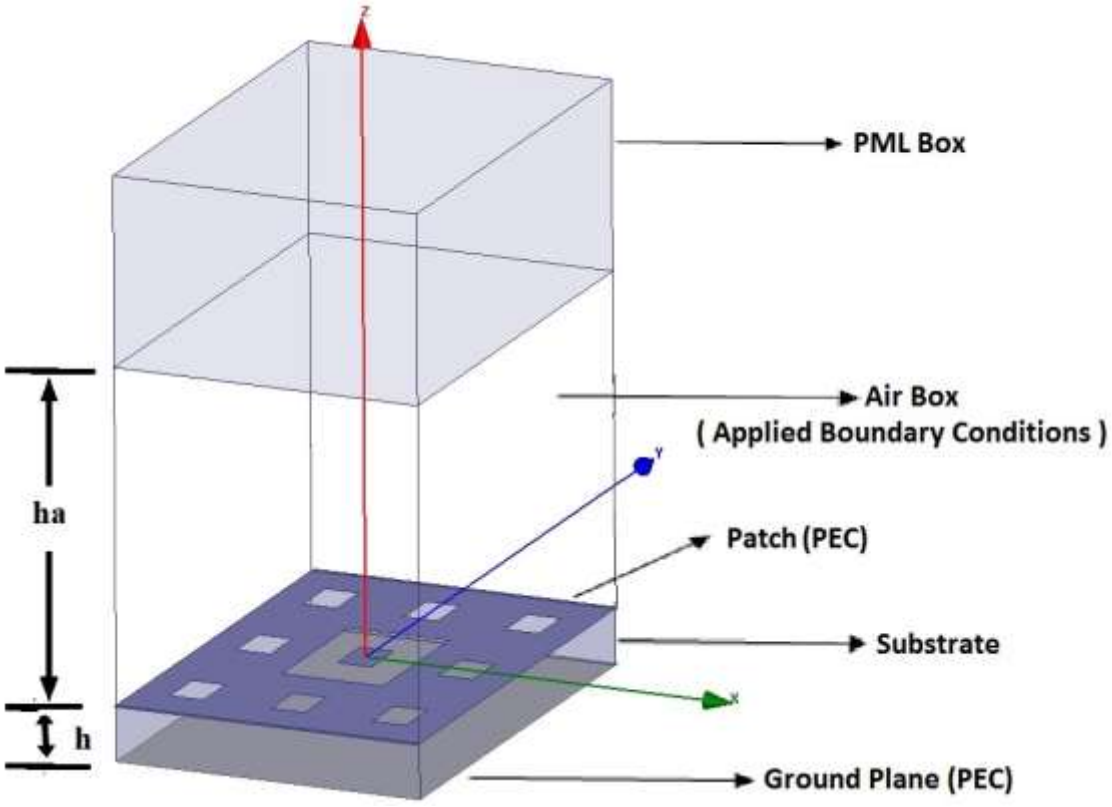

(a)

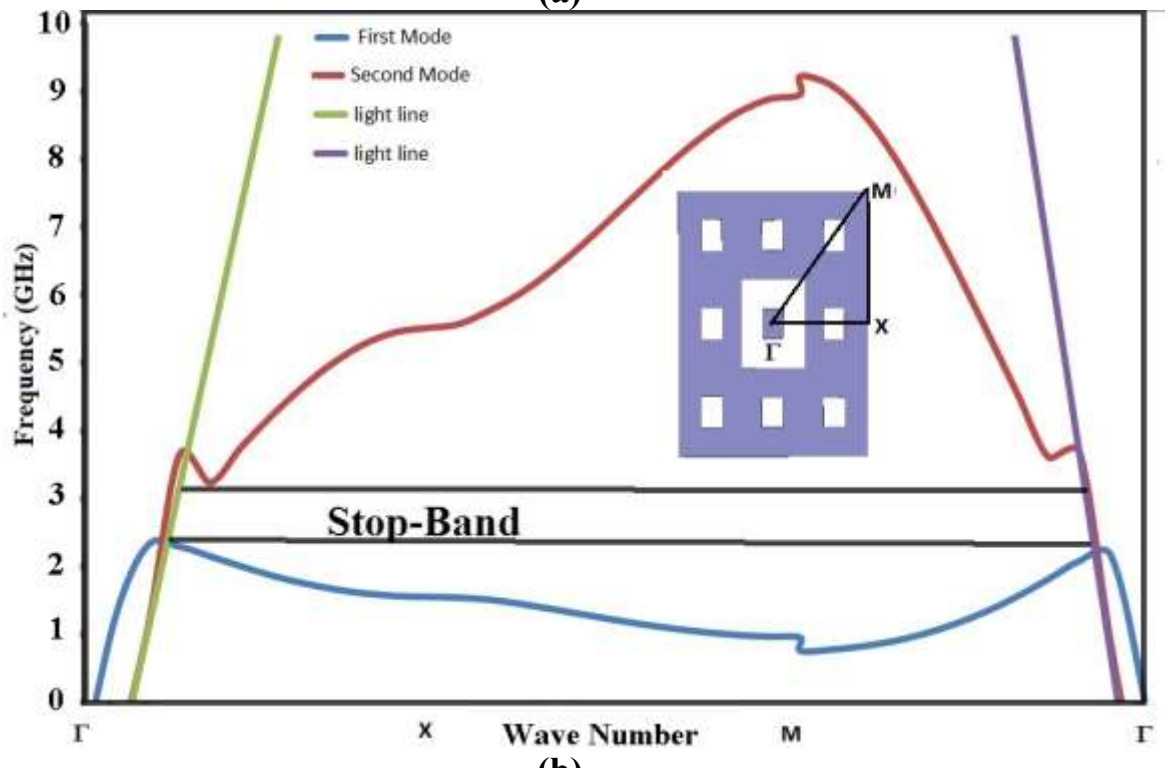

(b)

Figure 4.12: FEBG characterization. **(a)** FEBG unit cell with PML and PBC and **(b)** Dispersion diagram

In this work, the airbox height (*ha*) was placed above the dielectric substrate, it is defined to be ten times larger than the substrate thickness ($ha = 10 \times h$) to emulate the free space over the structure, and this will guarantee that higher angle of incidence waves are also considered. The modal setup and its relative boundary conditions as presented in Figure 4.12(a).

To generate the 2-D dispersion diagram for the FEBG unit cell, a phase sweep with fixed step size is run along the path Γ to X, X to M and M to Γ of the irreducible Brillouin zone [492], as illustrated in Figure 4.12(b).

An irreducible Brillouin zone is a useful tool for analysing EBGs since it identifies the fundamental part of the reciprocal lattice. Mainly; It offers a visual representation of the reciprocal lattice and enables the accurate mapping of the wave-modes within EBG unit cell with respect to various frequencies.

The two-dimensional dispersion diagram is generated for the first two resonance modes. It verifies the existence of a band-gap for the proposed structure where the surface waves cannot propagate on the patch surface. Theoretically; resonant frequency of the proposed structure is given by the relationship:

$$f_r = \frac{1}{2\pi\sqrt{LC}} \qquad (4.4)$$

Where L and C are the effective inductance and capacitance; respectively. In this work; the dimensions of the proposed FEBG unit cell are optimised to obtain an excellent rejection band between 2.5 GHz and 2.9 GHz. Figure 4.12(*b*) illustrates the simulated dispersion diagram with a band gap between the first and second modes. The centre bandgap frequency of the proposed FEBG is f_c = 2.65 GHz approximately.

4.4.3 Antennas configuration for mutual coupling reduction

The designed antennas are illustrated in Figure 4.13 including without and with the proposed second iterative order FEBG structure. Here; PIFA antenna elements working at f_c = 2.65 GHz are placed collinearly along the y-axis, and the separation of these antennas is 40 mm from element centre to centre (corresponds 0.35 λ_0 at 2.65 GHz).

The substrate of the proposed antenna is FR_4 with loss tangent ($tan\ \delta$) = 0.02 and dielectric constant ε_r = 4.4 with appropriate 50 Ω coaxial connectors are used as the feed ports of the proposed PIFAs.

Each PIFA element has a rectangular outline with a width W = 19 mm and patch length L=30 mm. The dimensions of the ground plane are 68 × 40 mm^2 (corresponds 0.6 λ_0 × 0.35 λ_0); other detailed dimensions are presented in Table 4.1.

Table 4.1: Detailed dimensions of the proposed antennas

Parameters	Values
Frequency (f_c)	2.65 GHz
Height of substrate (h)	1.6 mm
Ground length (L_g)	68 mm
Ground width (W_g)	40 mm
Patch length (L)	30 mm
Patch width (W)	19 mm
FEBG structure length (L_s)	39 mm
FEBG structure width (W_s)	18 mm
Distance (D)	5 mm
Separation (S)	40 mm (0.35 λ_0)
Shorting pin radius	0.3mm
Coaxial pin radius (Outer)	1.6 mm
Coaxial pin radius (Inner)	0.7 mm

The designed PIFA antenna is working in the higher-order mode. The optimisation was performed for the proposed multiple antennas to operate at a higher order mode to cover 2.64–2.68 GHz LTE band with best return loss characteristics as possible and at the same time have an appropriate load impedance matching without using an additional circuit of the proposed antennas.

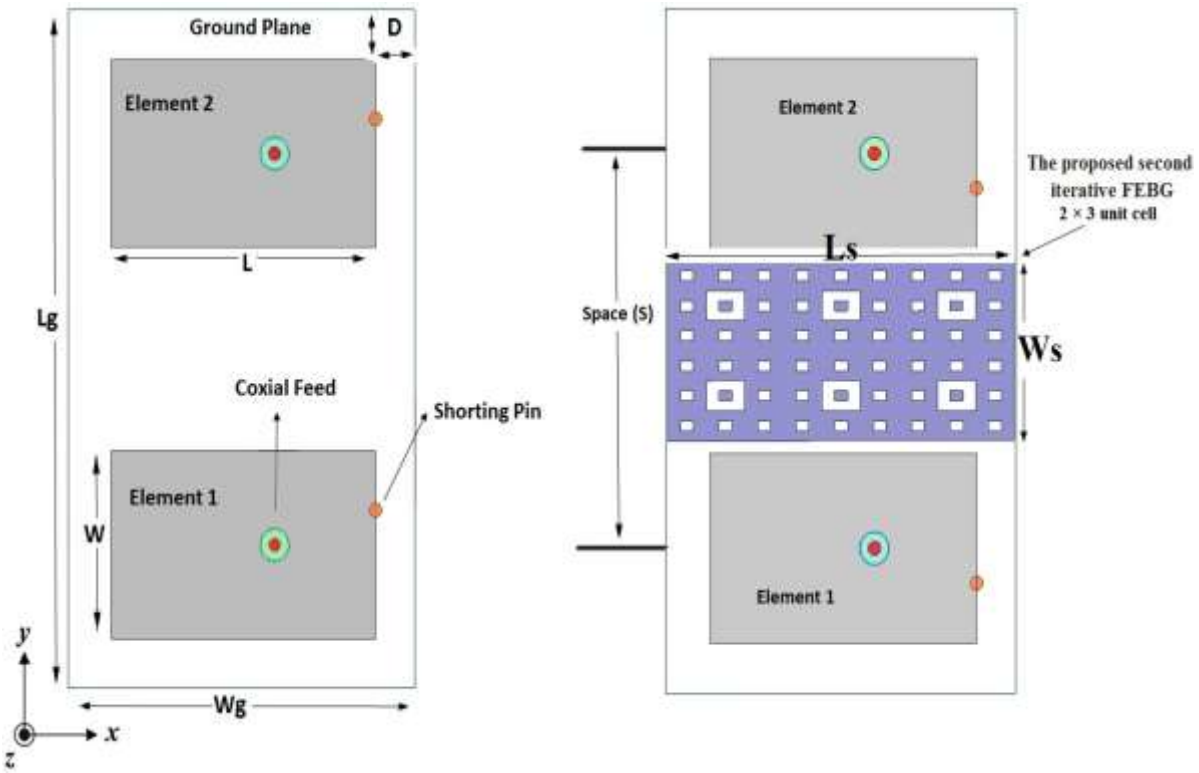

Figure 4.13: Schematic PIFAs antenna layout without **(left)** and with **(right)** FEBG structure

The dimensions of the PIFAs, as well as other parameters such as feeding and shorting pins positions, were carefully fine-tuned with the help of the HFSS ver 17.0 electromagnetic software to obtain a required operational mode (higher-order mode) working at the frequency of interest. Through parameters sweep and optimisation, best antenna parameters have been achieved for maximising the isolation values.

The proposed second iterative order FEBG is etched as planar PEC layer between the PIFAs elements and located above the ground plane, as shown in Figure 4.13.

The basic structure of the second iterative order FEBG etched between dual antenna elements is the same as the fractal geometry illustrated before in Figure 4.11(*c*). Here; it consists of 2 × 3 periodic unit cells forming a compact lattice ($L_s \times W_s$). The mutual coupling reduction characteristic of the proposed second iterative order FEBG can be analysed by calculating S_{12} or S_{21} of the antennas array as presented in next section.

4.4.4 Theoretical Analysis

4.4.4.1 Scattering parameters performances

The return loss (reflection coefficient) and transmission loss (coupling) for the dual antenna array elements are presented in Figure 4.14(*a*) and Figure 4.14(*b*); respectively, in both without and with the proposed second iterative order FEBG structure, the spacing between these antennas is S = 40 mm from element centres (corresponding to 0.35 λ_0 at 2.65 GHz). Figure 4.14(a) illustrates the return loss by adding the second iterative order FEBG between antenna elements.

The simulated mutual coupling is significantly reduced as shown in Figure 4.14(b), more than 27 dB (Z-X-plane) and 40 dB (Z-Y-plane) coupling reduction have been achieved by inserting second iterative order FEBG structure between the dual antenna elements.

All these analyses were conducted with one antenna element transmitting and the other terminated with 50 Ω load.

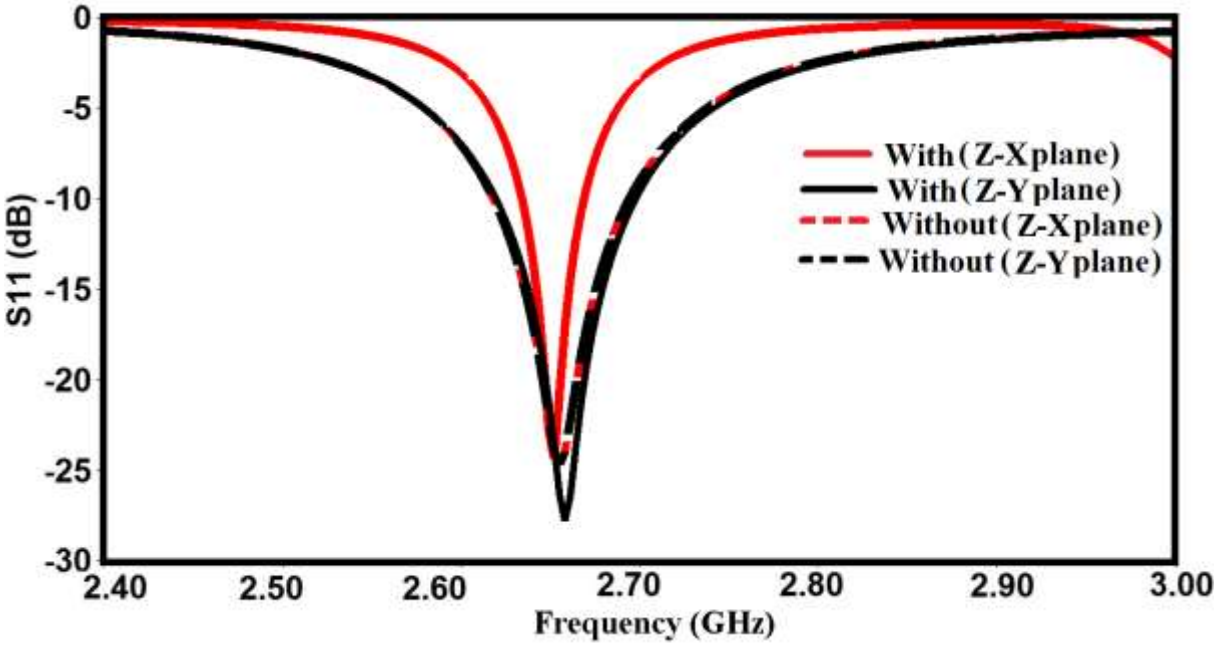

(a)

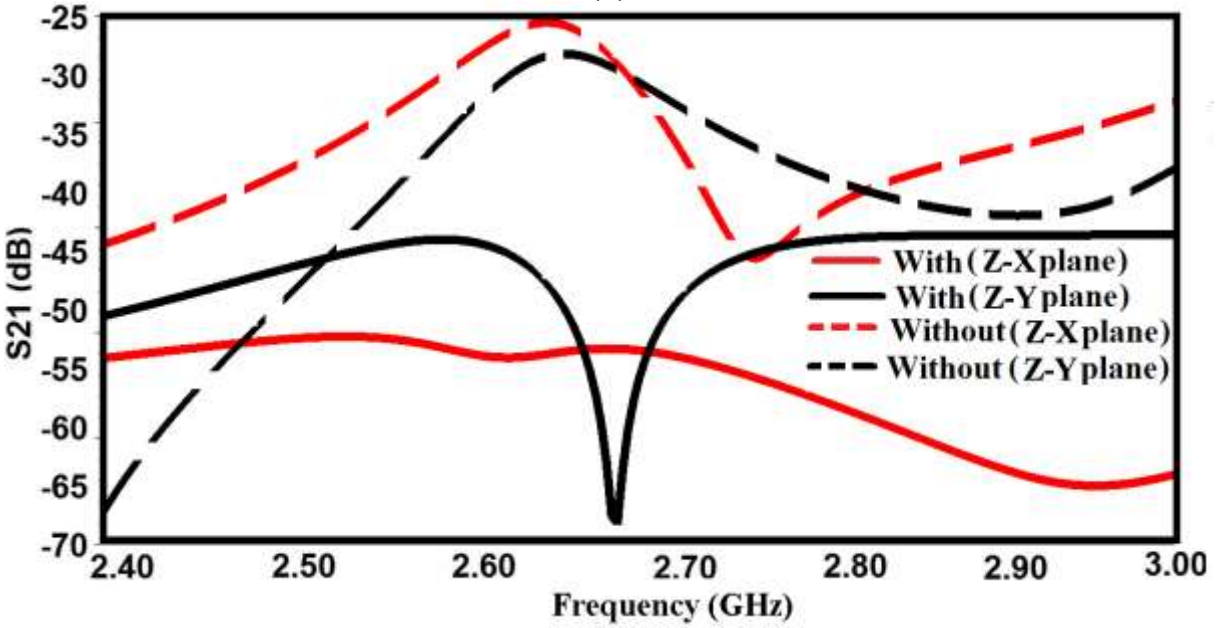

(b)

Figure 4.14: Simulated scattering parameters of the antennas without and with FEBG structure. **(a)** Reflection coefficient (S_{11}) and **(b)** Transmission coefficient (S_{21})

Analyses were also performed with a lossless substrate with a permittivity of 4.4 to investigate the effects of the lossy substrate. A comparison of the antennas coupling level on lossless and lossy substrates is shown in Figure 4.15:-

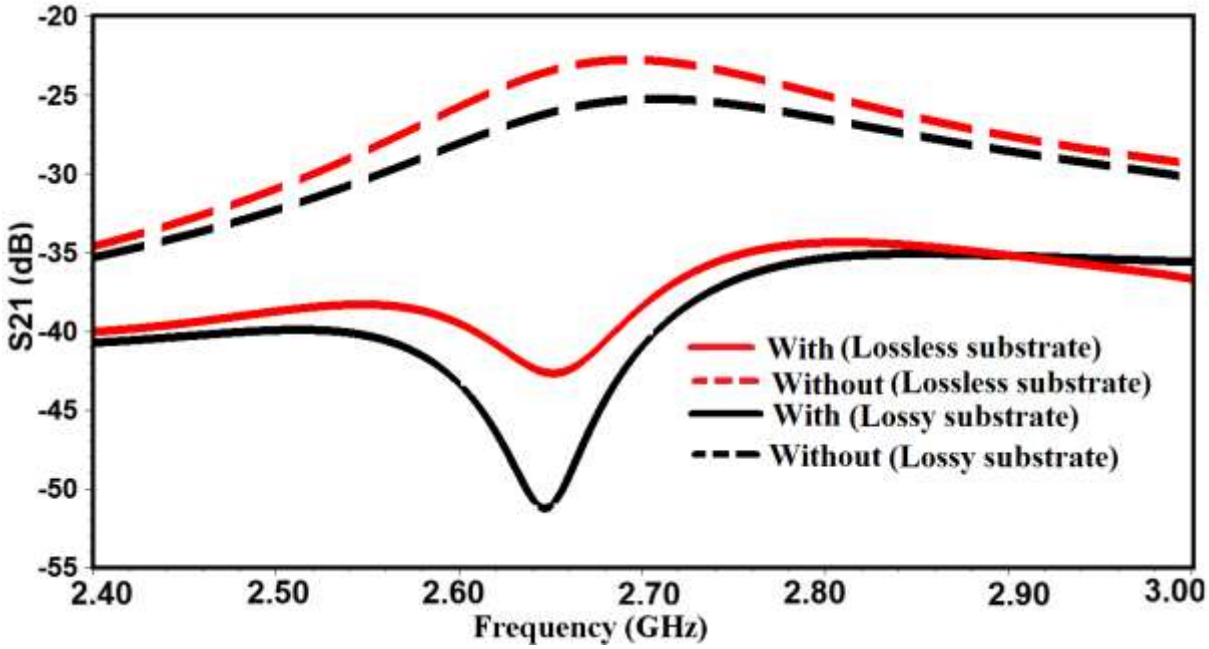

Figure 4.15: Coupling level comparison on lossless and lossy substrates

Another S_{21} comparison results of the designed zero, first, and second iterative fractal structures (as illustrated in Figure 4.16) shows the effect of these structures on the resonant frequency.

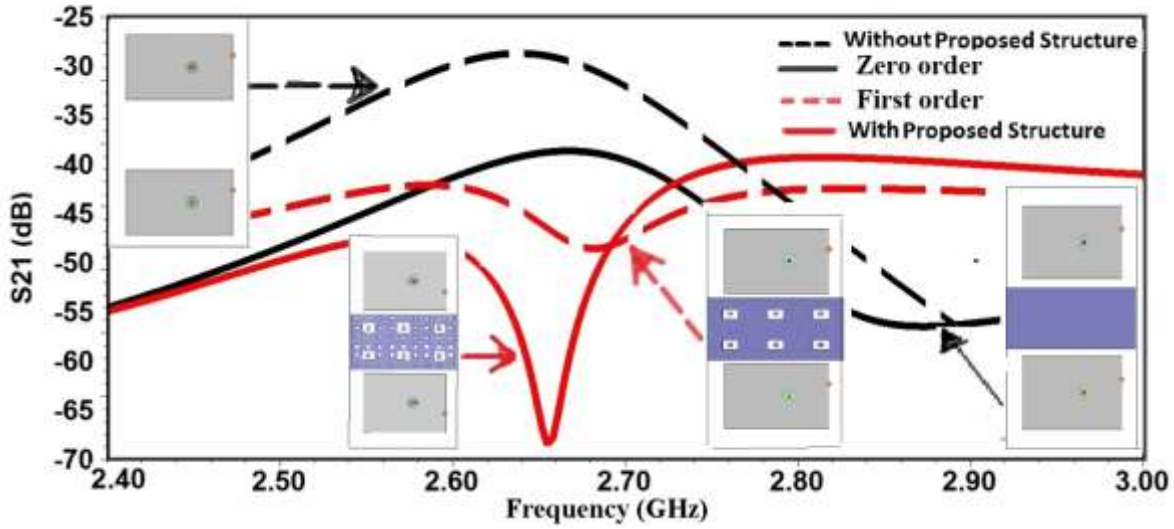

Figure 4.16: S_{21} comparison between different iterative orders FEBG structures (zero, first and second)

Meanwhile, the high-level iterative fractal structure has longer current lines compared with the lower-level iterative fractal structure with the same outline dimension (total size). These results show the significance of using the fractal geometry in a relatively shorter spacing. As the second-order iterative FEBG is inserted (Figure 4.16), the electrical length increases and the stopband frequencies decrease in compared with the zero and first-order iterative FEBG. Although the lower-order fractal EBG is not designed for a working frequency of 2.65 GHz, the first- and second-order iterative fractal structures have specific bandgap filter components

with distinctive characteristics. Therefore, the proposed first and second-order iterative fractal structures can be employed to reduce mutual coupling between the antenna elements. In the present work, the second-order iterative FEBG is taken as an example to illustrate the design procedure of the proposed FEBG for optimum MIMO performance.

4.4.4.2 Radiation patterns, gain and efficiency

The orientation of the MIMO antenna with respect to the coordinate system is shown in Figure 4.13. The normalised far-field radiation patterns on the ZX plane, ZY plane and XY plane, are shown in Figure 4.17 (a-c), respectively. No significant degradation of the radiation patterns is noticed between the designs (with and without the second-order iterative FEBG) of the two orthogonal planes.

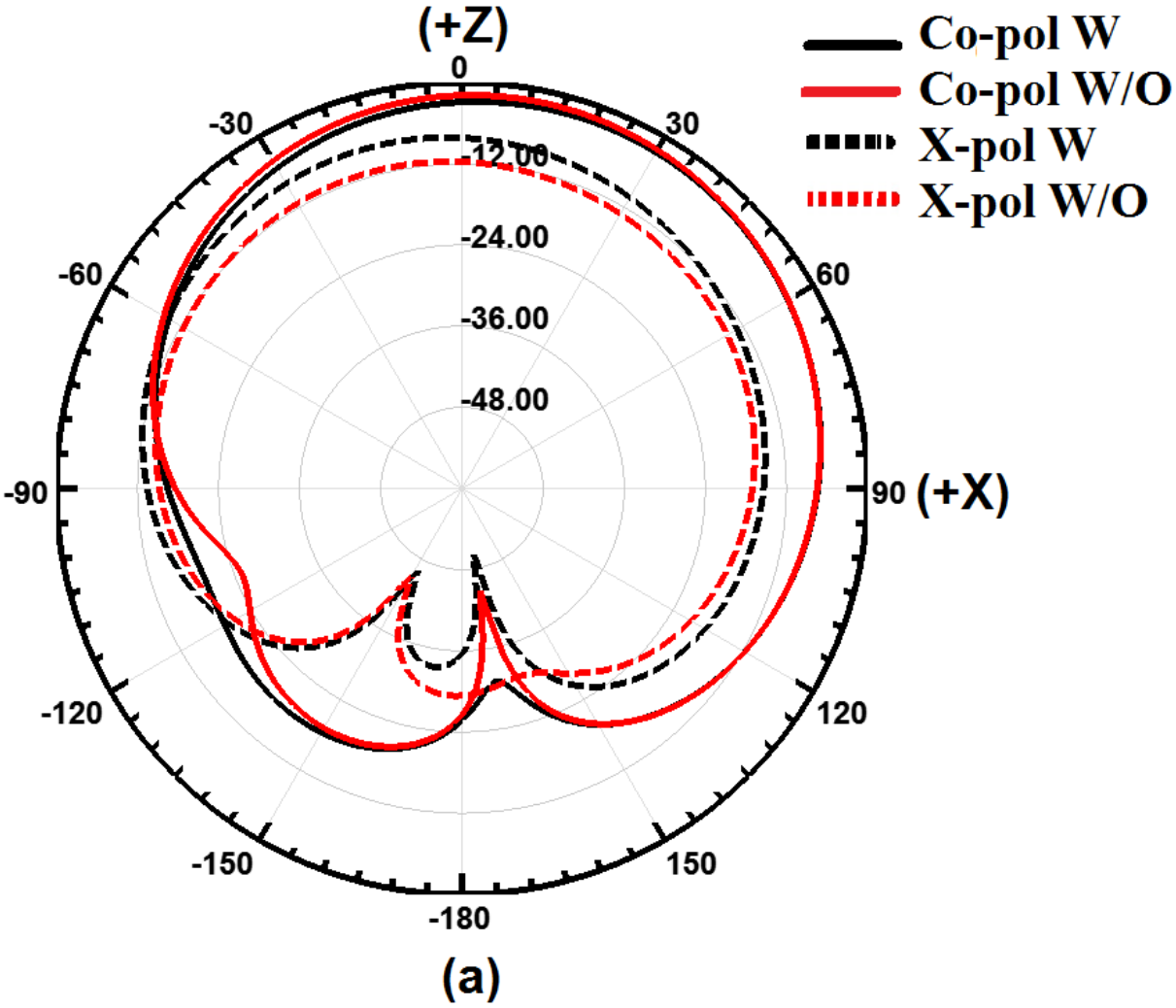

(a)

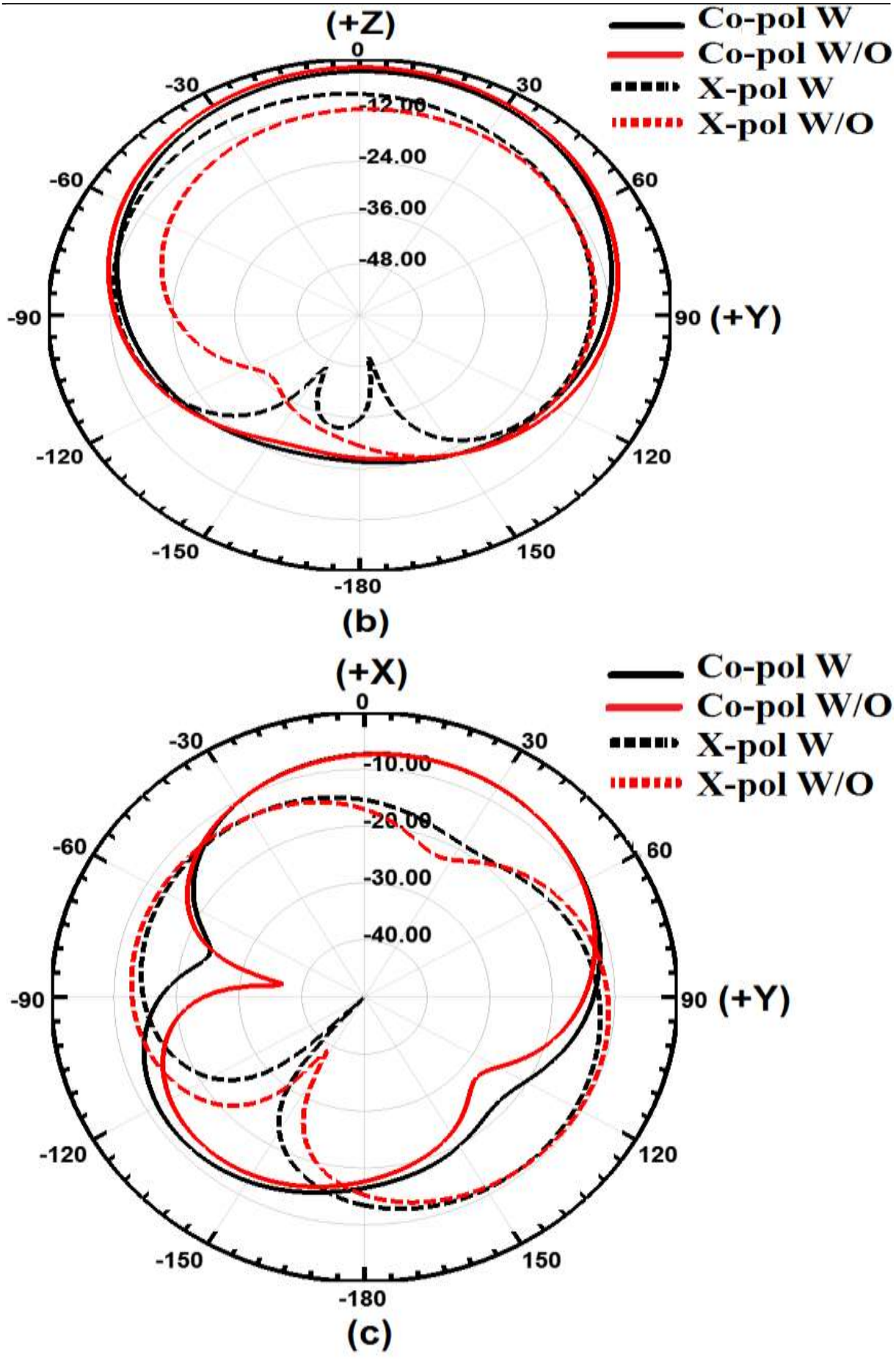

Figure 4.17: Simulated far-field patterns (normalised) with and without second iterative order FEBG at 2.65 GHz **(a)** ZX plane, **(b)** ZY plane, and **(c)** XY plane

As shown in Figure 4.17, the radiation patterns exhibit a good omnidirectional characteristic in the upper semi-plane, at both of the XZ and YZ planes, which means that the proposed MIMO antennas can transmit and receive signals in a half-spherical perpendicular to the patch; also a nearly omnidirectional pattern is obtained in the XY plane, this a non-directional pattern required to receive information signals from all directions.

During the measurements, one of the input ports was excited, and the other was terminated with a load of 50 Ω.

Meanwhile; the antenna radiation efficiency is simulated with and without FEBG structure to analyse the effect of the structure on radiation characteristics. Table 4.2 provides the summarised comparison.

Table 4.2 Simulated peak gain and radiation efficiency of the proposed antennas

Parameters	Without FEBG	With FEBG
Frequency (GHz)	2.63	2.65
Peak Gain (dB)	1.75	2.57
Radiation Efficiency (%)	64%	68%

Stronger currents on the patches lead to higher energy losses due to lossy substrates. As expected, the inclusion of the FEBG structure has resulted in less mutual coupling and currents on the 2nd antenna. Since the antennas are fabricated on a lossy substrate, the losses induced on the 2nd antenna will be less with low coupling currents leading to higher radiation efficiency with the FEBG structure.

4.4.4.3 MIMO Characteristics

As mentioned before, Envelope Correlation Coefficient (ECC) between antenna elements is one of the most important parameters to evaluate diversity performance because it is directly related to the antenna scattering parameters and may significantly degrade MIMO system performance.

In this work, ECC is evaluated using S-parameters of the MIMO system as defined before in Eq. (2.13), which assumed antenna system is lossless, and the antennas are excited separately, keeping the other antennas matched terminated.

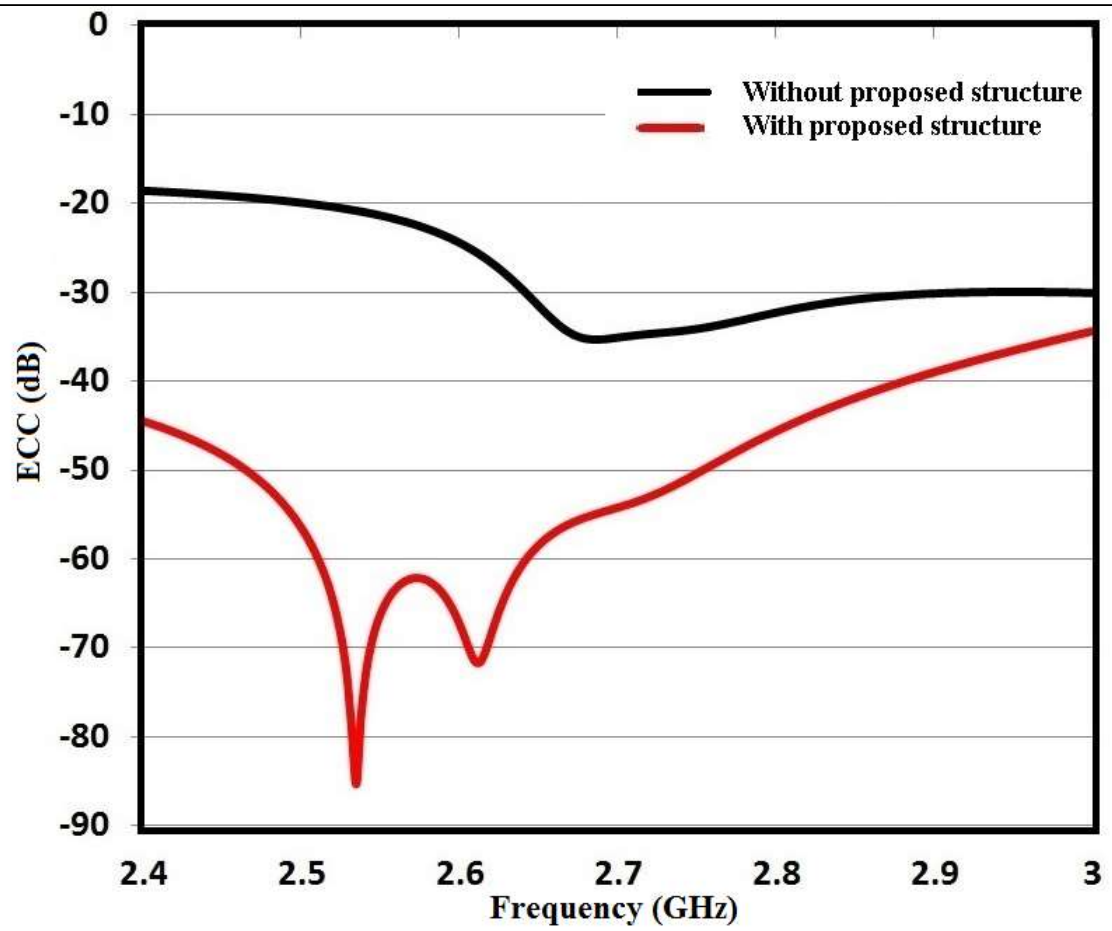

Figure 4.18: Envelope correlation coefficient of MIMO antenna with and without FEBG

In Figure 4.18; the envelope correlation coefficient for the antenna elements with and without the second iterative FEBG is shown against frequency.

It can be noticed from these simulated results, the envelope correlation coefficient in the working band of antenna elements with FEBG is -70 dB smaller than that of the antenna elements without FEBG. This observation indicates better behaviour and diversity performance of the MIMO antenna system will be achieved by using the proposed second iterative FEBG.

4.4.5 Fabrication and Experimental Demonstration

In this section, the performances of the MIMO antennas are verified through the measurement procedures. A prototype of the proposed multiple antennas without and with proposed structure in both Z-X plan and Z-Y plan coupling are fabricated as presented in Figure 4.19(a) and Figure 4.19(b); respectively.

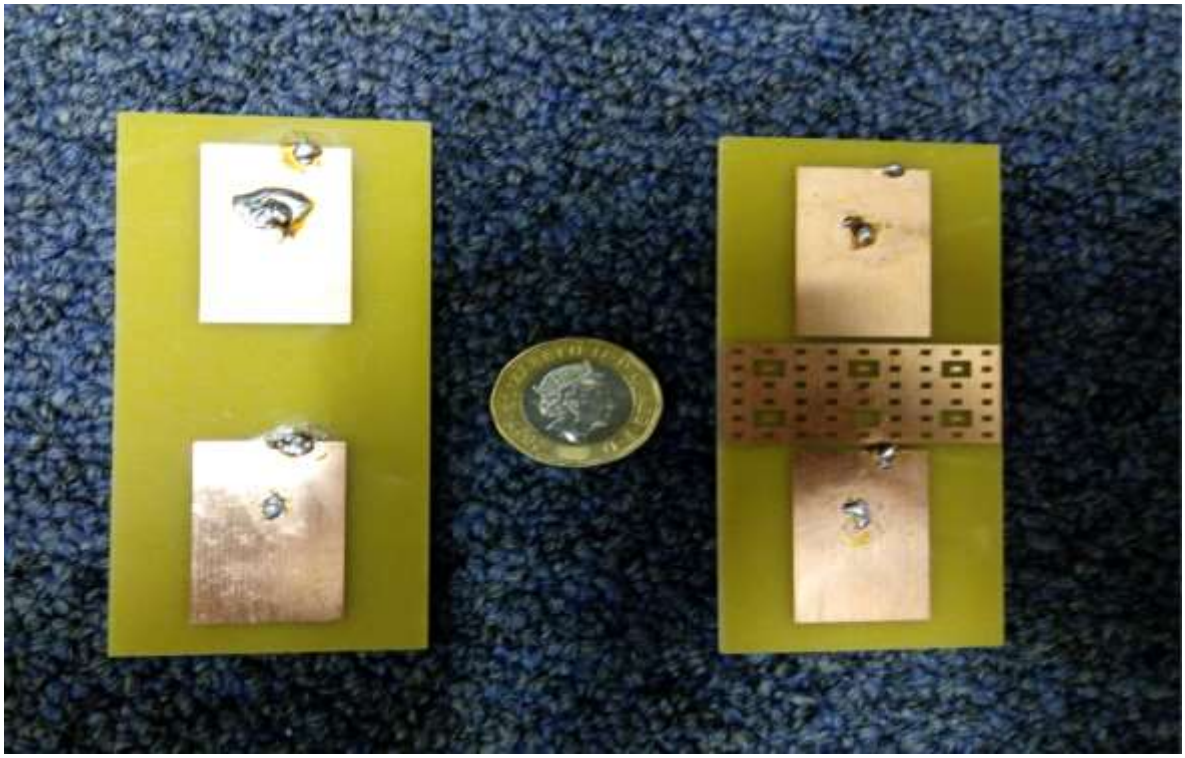

(a)

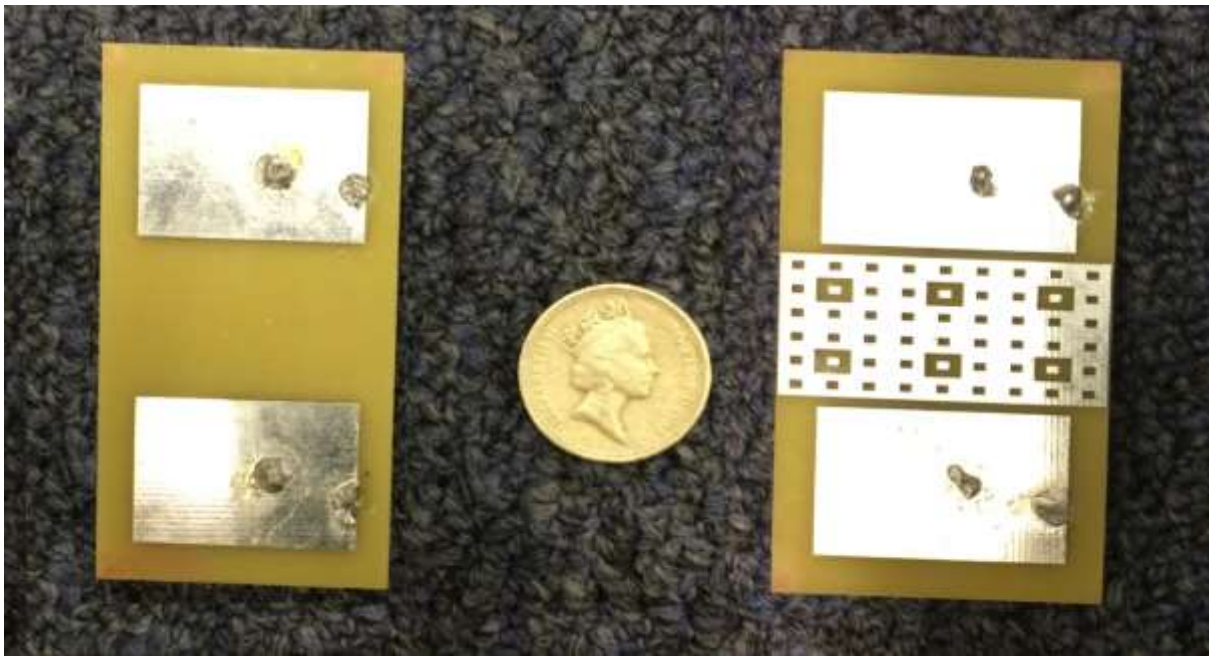

(b)

Figure 4.19: Prototype of the fabricated PIFAs antenna without (left) and with (right) proposed FEBG structure. **(a)** Z-X plane coupling **(b)** Z-Y plane coupling

4.4.5.1 Measured scattering parameters

The proposed MIMO antennas were measured using Agilent N5230 a vector network analyser (as shown in Figure 4.20) inside Brunel University London allowing measurements of microwaves in 300 KHz − 20 GHz range. After calibration with the network analyser, both a return loss and transmission losses have been measured.

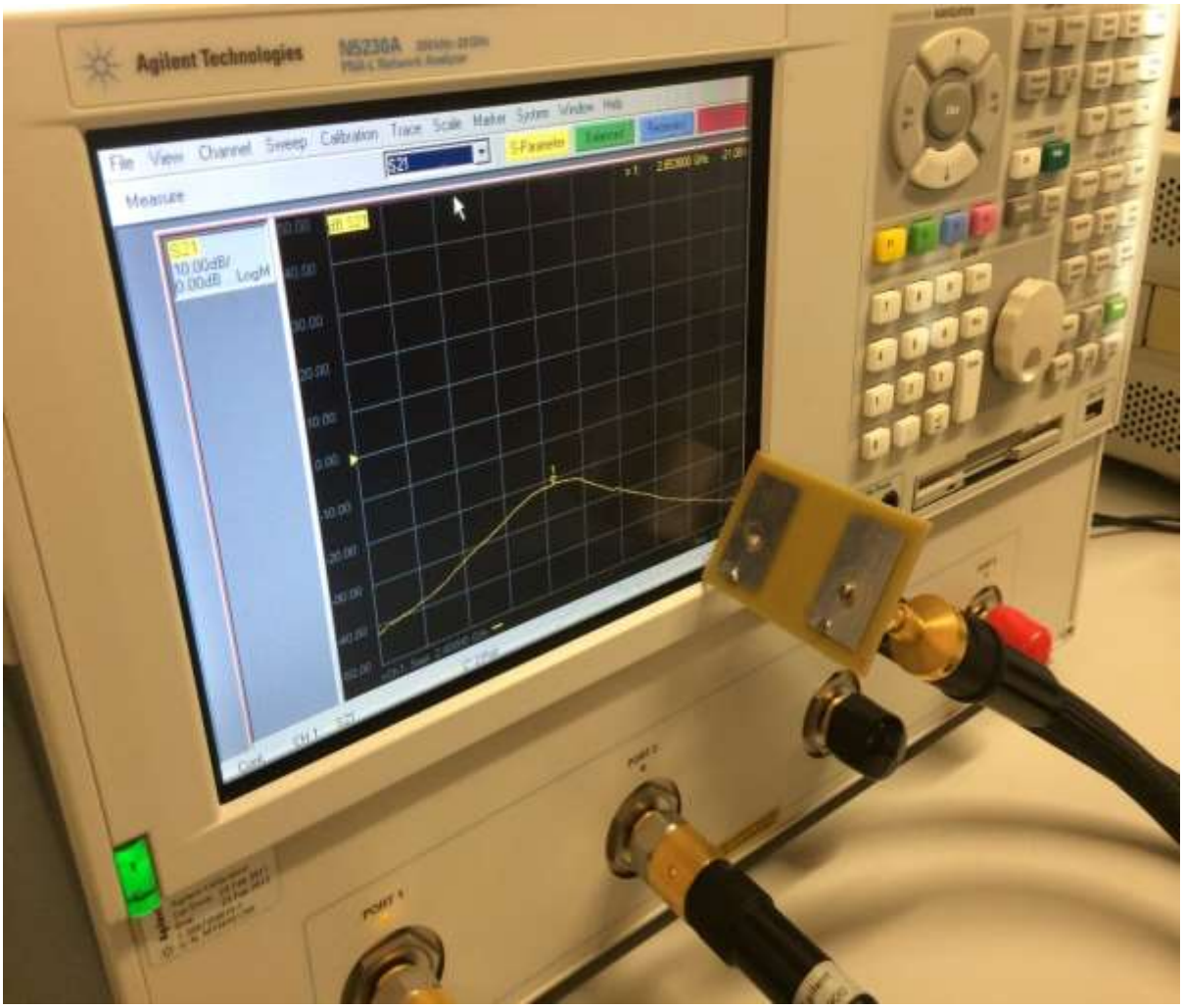

Figure 4.20: Photograph of the proposed antennas measured using a network analyser

Figure 4.21(a) shows the measured return loss of the impedance bandwidth ($S_{11} < -10$ dB). The proposed antennas resonate at 2.65 GHz with a return loss higher than 10 dB, which corresponds to an impedance bandwidth of 3.16% for both cases.

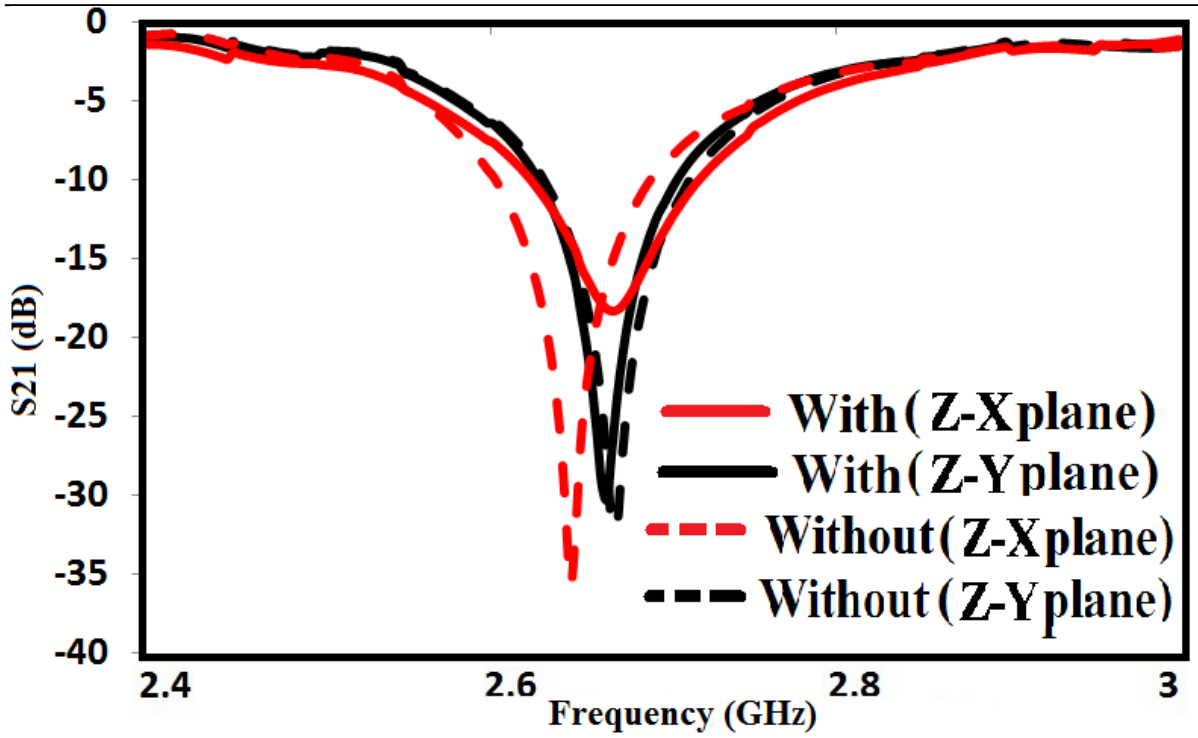

(a)

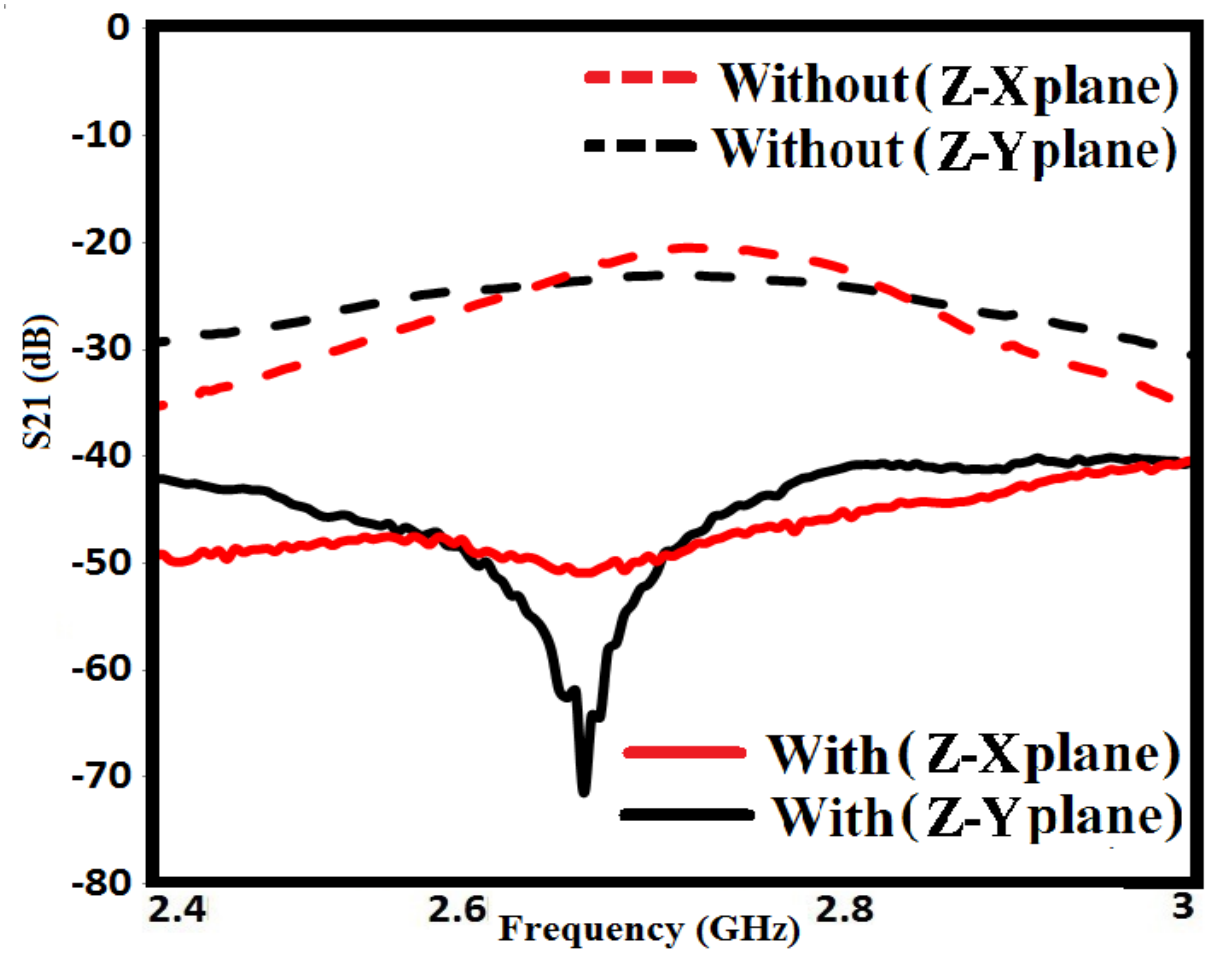

(b)

Figure 4.21: Measured scattering parameters of the antenna without and with second iterative order FEBG structure. **(a)** Reflection coefficient (S_{11}) and **(b)** Transmission coefficient (S_{21})

Figure 4.21(b) shows the measured mutual coupling between antennas without the FEBG structure which is only -20 dB (*Z-X* plane) and -25 dB (*Z-Y* plane).

While; after inserting the proposed structure to be significantly reduced to levels: -51 dB (*Z-X* plane) and -70 dB (Z-Y plane). These measured results agree well with the simulated results (as previously introduced in Figure 4.14). However; a significant agreement exists between the measured and simulated S-parameters results. A slight difference between these results may be attributed to the common factors, such as inaccuracy in the fabrication process, inappropriate quality of the substrate, and the effect of the SMA connector (solder roughness). From this experimental verification, it can be concluded that the second iterative order FEBG structure can be utilised to reduce the mutual coupling between antenna array elements.

4.4.5.2 Radiation patterns characteristics

The measurement of radiation patterns is carried out in an anechoic chamber (inside University of Greenwich campus). The measured radiation pattern data obtained from the anechoic chamber were relatively small. Hence, relative radiation patterns were employed for comparison. These values were normalised to the maximum co-pol for comparison with the simulation results.

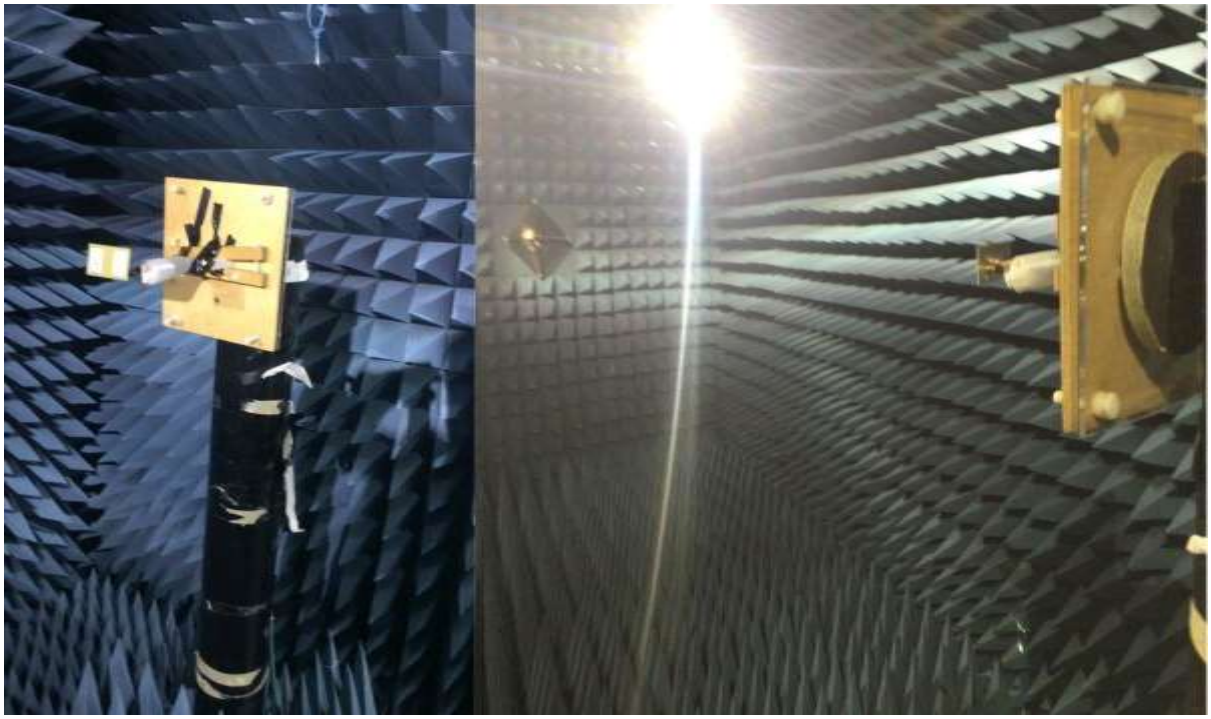

Figure 4.22: Photograph of the AUT mounted inside the anechoic chamber.

The measured and simulated far-field radiation patterns are normalised in the three principal planes (XZ, YZ, and XY plane) in both prototypes, without and with the second-order iterative FEBG at a designed frequency of 2.65 GHz, as shown in Figures 4.23(a-c) and 4.24(a-c), respectively.

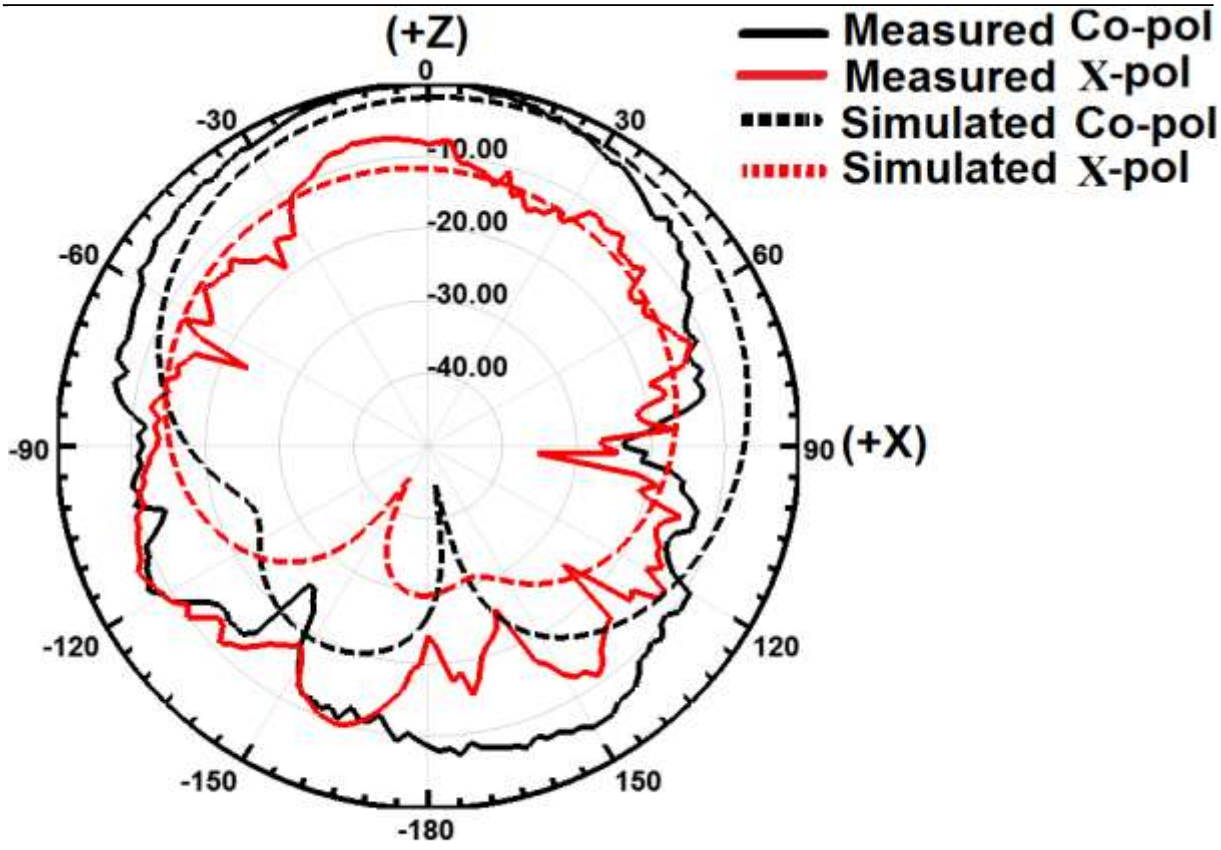
(+Z)
0
30
60
90
120
150
-180
-150
-120
-90
-60
-30
-10.00
-20.00
-30.00
-40.00
(+X)
Measured Co-pol
Measured X-pol
Simulated Co-pol
Simulated X-pol

(a)

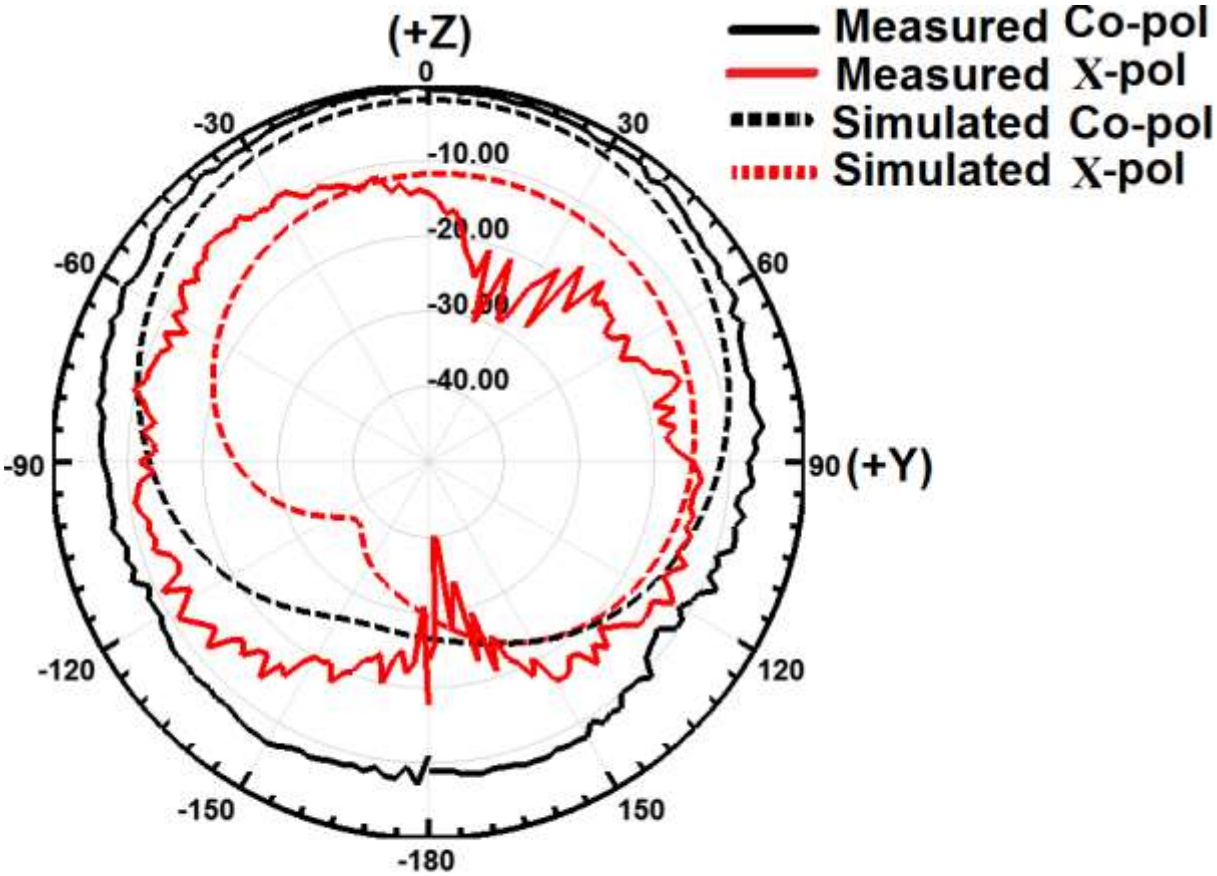
(+Z)
0
30
60
90
120
150
-180
-150
-120
-90
-60
-30
-10.00
-20.00
-30.00
-40.00
(+Y)
Measured Co-pol
Measured X-pol
Simulated Co-pol
Simulated X-pol

(b)

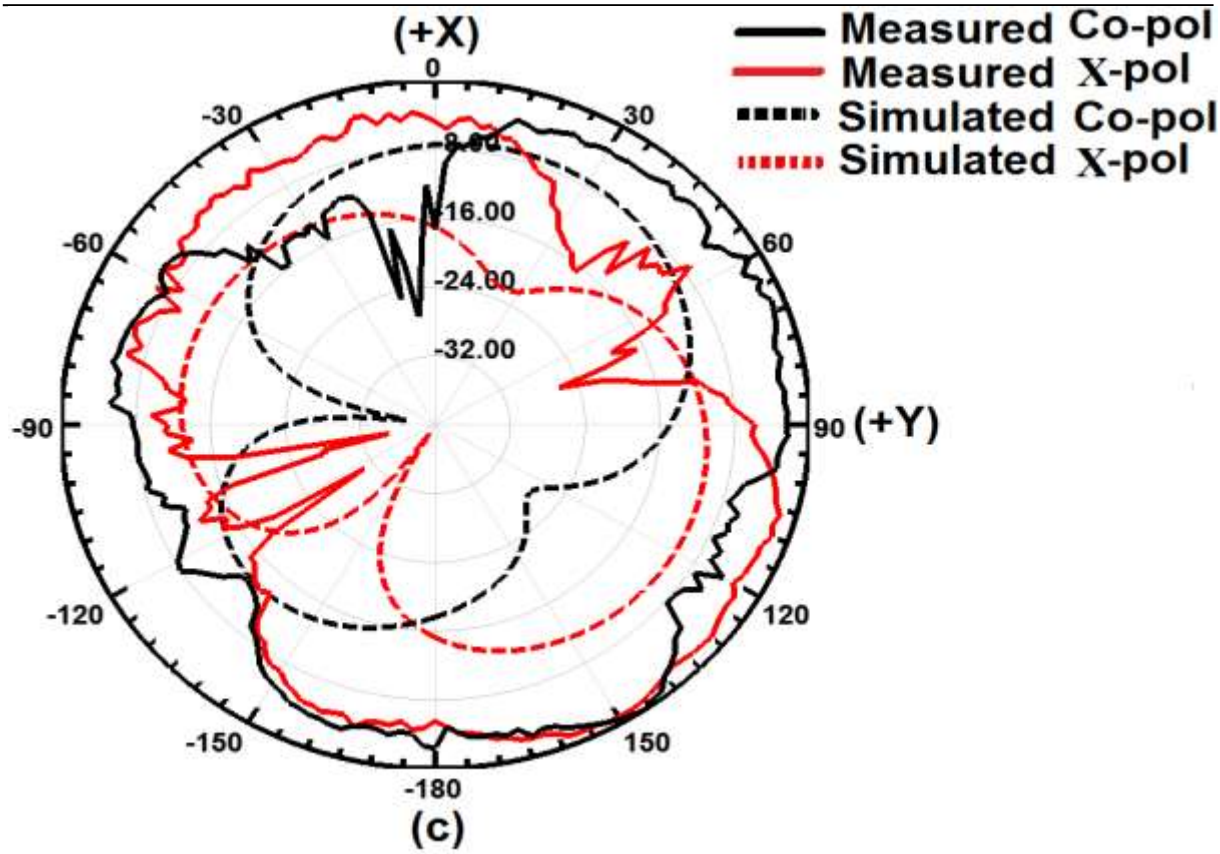

Figure 4.23: Measured versus simulated Co-Pol and X-Pol far-field relative radiation patterns (normalised) without FEBG at frequency of 2.65 GHz for **(a)** ZX plane, **(b)** ZY plane, and **(c)** XY plane

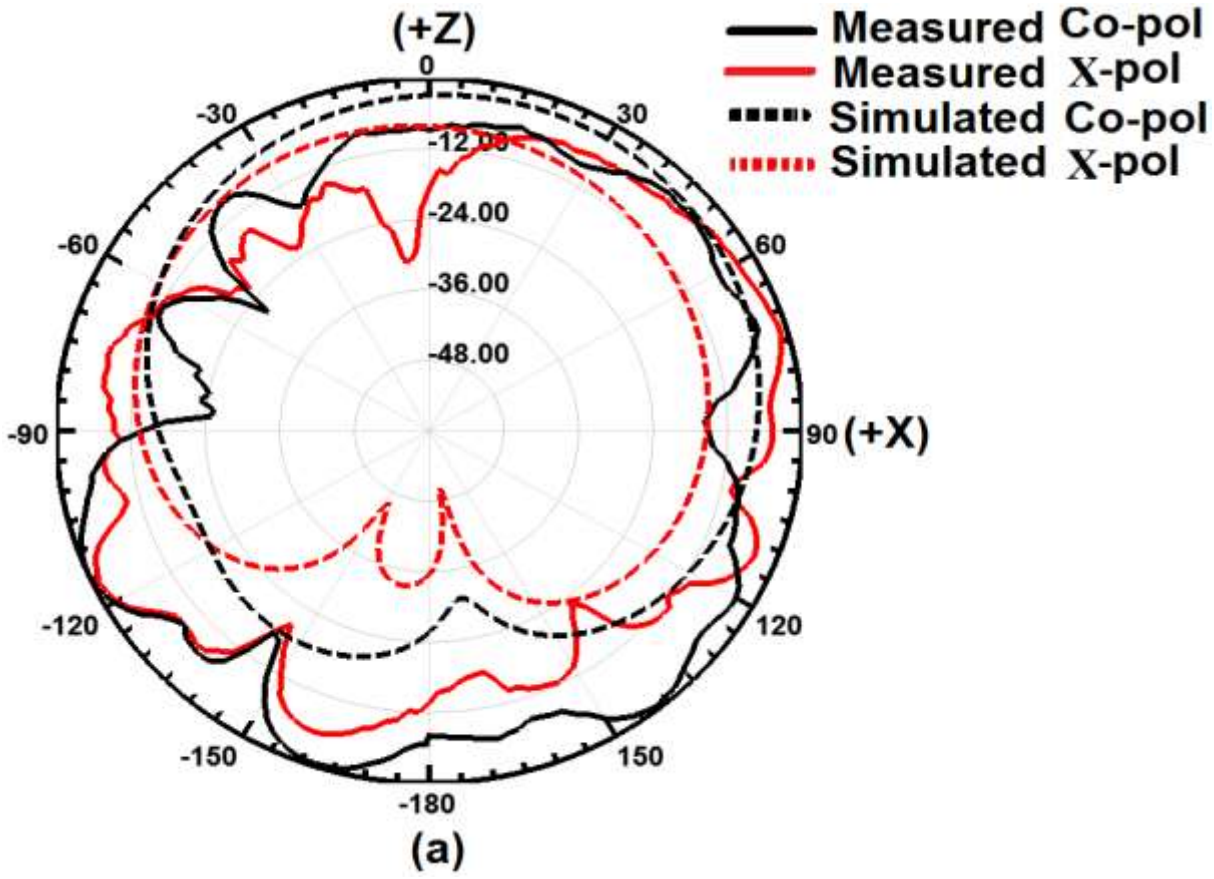

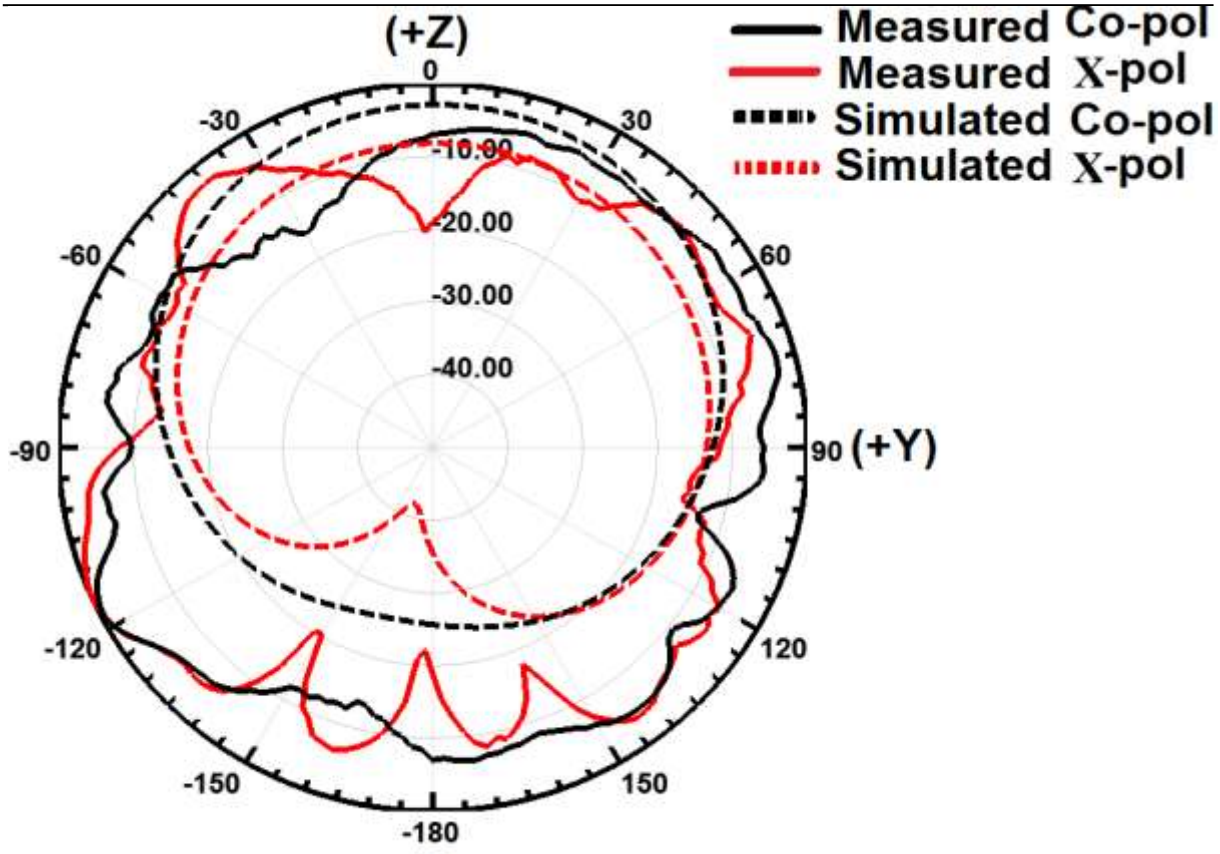

(b)

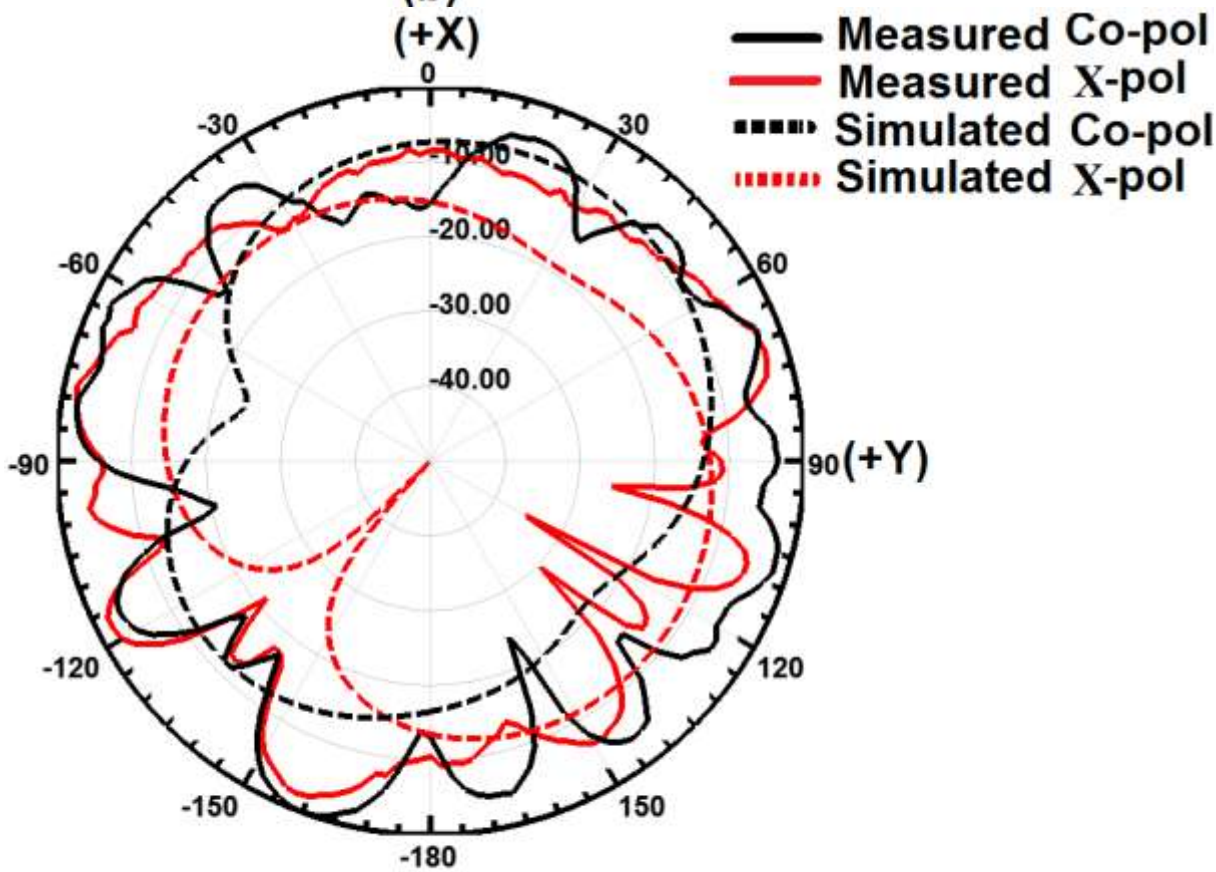

(c)

Figure 4.24: Measured versus simulated Co-Pol and X-Pol far-field relative radiation patterns (normalised) with FEBG at a frequency of 2.65 GHz for **(a)** ZX plane, **(b)** ZY plane and **(c)** XY plane

The whole figures of the obtained radiation patterns are acceptable and suitable for modern communication systems. The radiation patterns possess a good omnidirectional characteristic in the upper semi-plane, at both X-Z and Y-Z planes.

In azimuthal (X-Y) plane, also a nearly omnidirectional pattern can be noticed in both cases. However, some nulls appear in comparison with other planes after inserting FEBG, especially in measured cross-polarised.

A large cross-polarisation is observed from the patterns. This characteristic can be an advantage for the wireless communication application in a rich multipath environment. However, probes are used in the present work due to its vertical portion. A large amount of leak and spurious radiation from the probes are produced inside the FR_4 substrate.

Therefore, a low XPD level or a high cross-polarisation level is observed. Moreover, discrepancies between the calculated and measured results in the band of interest exist due to the SMA connectors, cable losses, and inaccurate implementation.

In addition; an imperfect placement/connection of shorting pins or via during the fabrication and measurements process must have contributed towards the discrepancies between measured and simulated patterns.

The ground surface waves can produce more spurious radiations or couple some energy at imperfectly placed shorting pins, feed connections for PIFA probes or any other discontinuities, which in turn will lead to some distortions in the main patterns or unwanted loss of power.

The author believe that this is one of the reasons that had been lead to this discrepancy, especially in the measured results. Finally; during the measurements, one of the input ports was excited, and the other was terminated with a load of 50 Ω.

4.4.6 Comparison with other Approaches and Published Works

It is instructive to compare the proposed FEBG structure with other methods used to reduce the mutual coupling. To reduce the mutual coupling between antenna elements, besides FEBG, different approaches such as the removal of both substrate and common ground have also been reported [60]. Figure 4.25 plots the coupled antenna structures to be compared:

a) Normal antennas (reference).

b) Substrate between antennas removed.

c) The ground between antennas removed,

d) FEBG structure between antennas.

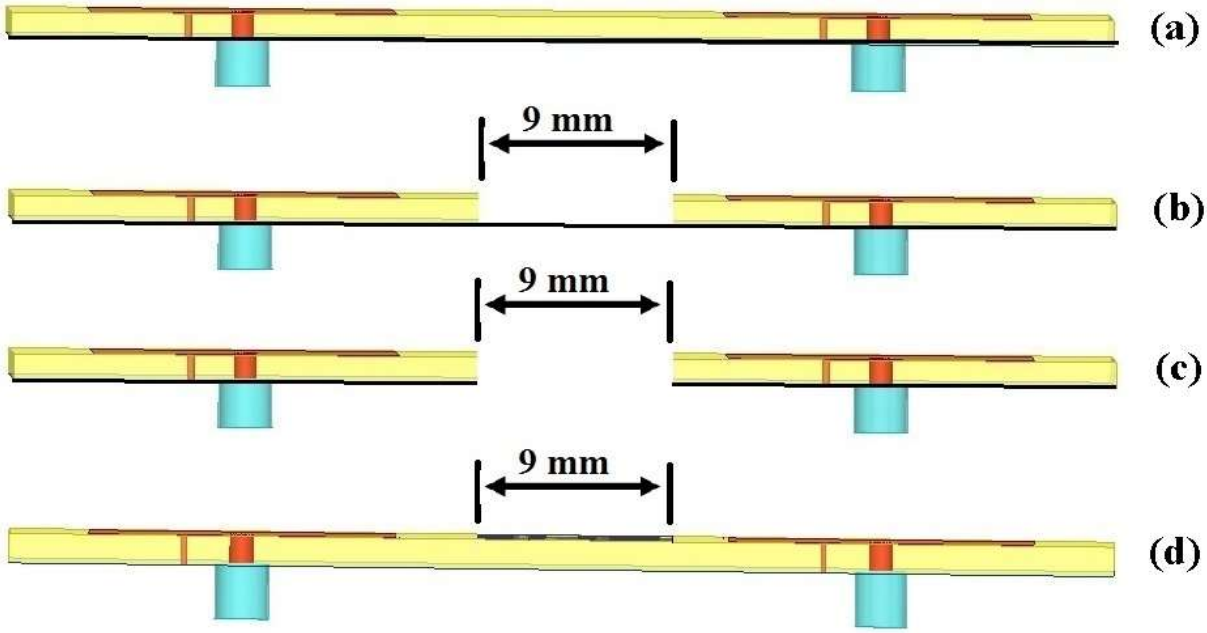

Figure 4.25: Other techniques to reduce the mutual coupling between PIFAs (side view): **(a)** Normal antennas, **(b)** Substrate between antennas removed, **(c)** Ground between antennas removed, and **(d)** FEBG structure in between

All physical parameters such as antenna size, substrate properties, and antenna distance in all the structures were kept identical to the second iterative order FEBG case.

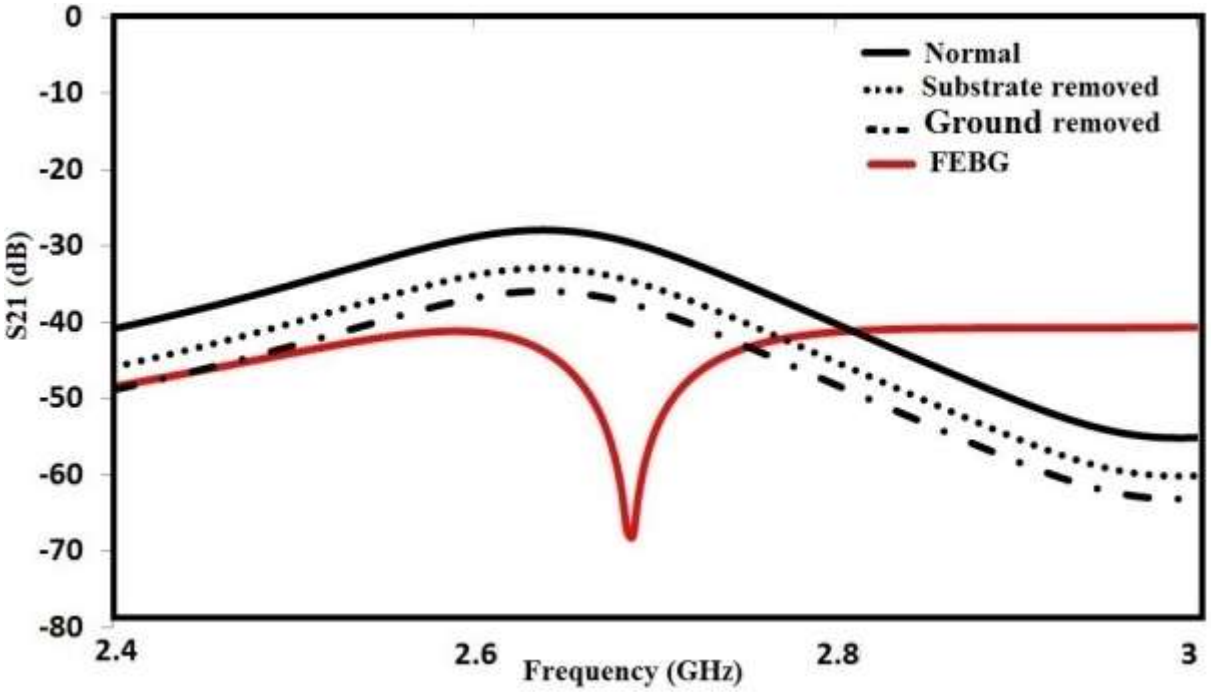

Figure 4.26: Mutual coupling comparison of the four different techniques. PIFA antennas resonate at 2.65 GHz

A 9 mm substrate width was removed between the antennas (as illustrated in Figure 4.25(b)); this width is chosen to be the same as the total width of rows of the FEBG patches.

When the ground was removed between the antennas, the separation between adjacent patch antennas was also selected to be 9 mm (as illustrated in Figure 4.25 (c)). Figure 4.26 displays the mutual coupling reduction results of four different approaches.

The conventional antennas show the highest coupling. The substrate and ground removal cases have some effects on the mutual coupling reducing. A 5 dB coupling reduction is noticed for the former case, and an 8 dB reduction is observed for the latter case. The highest mutual coupling reduction is seen with the second iterative order FEBG case compared to other approaches (as presented in Figure 4.26).

This comparison demonstrates the unique capability of the FEBG structure to reduce the mutual coupling. Moreover, as mentioned before in chapter three, some other published works have employed different methods such as DGS structures, slotted and slits ground plane, resonators and neutralisation techniques to reduce the mutual coupling between antenna elements. A summarised comparison is provided in Table 4.3.

Table 4.3: Performance comparison of different planar multiple antennas

Ref	BW (GHz)	S_{21} With case (dB)		S_{21} Without case (dB)		Space (λ_0)	Volume (mm^3)	Isolation technique	Geometric complexity
		Z-X plane	Z-Y plane	Z-X plane	Z-Y plane				
[41]	2.42-2.59	-28	N/A	-10	N/A	0.17	100×40×5	Parasitic ground	Medium
[119]	2.5-2.58	-29	-32	-20	-18	0.50	100×40×3	Dual Layer EBG	Complex
[128]	2.38-2.47	-22	N/A	-13	N/A	0.12	100×50×6.5	Planner EBG	Complex
[149]	1.85-2.15	-27	N/A	-9.4	N/A	0.50	100×40×2	Slits on ground	Medium
[310]	2.40-2.65	-16	-20	-8	-9.5	0.42	105×55×5.7	Good separation	Simple
[387]	1.92-2.18	-27	N/A	-10	N/A	0.13	100×40×5	Neutralisa -tion line	Complex
[473]	2.32-2.68	-38	N/A	-18	N/A	0.15	100×40×5	Slot in between	Complex
[489]	2.55-2.75	-32	-40	-22	-24	0.40	75×65×5	Walls in between	Medium
This work	2.64-2.68	-52	-67	-25	-27	0.35	68×40×1.6	Compact FEBG	Simple

4.5 Chapter Summary

Many array designs presented in the literature have reported excellent designs with a narrowband operation. However, some of these multiple microstrip antennas suffer from large size, high profile, not enough isolation being obtained in the operation band, utilisation of complicated decoupling methods that can affect the fabrication cost and/or increase antenna complexity. In this chapter, the above issues have been tackled through the proposal of a new isolation approach that exploits fractals with EBG corporation for narrowband applications. All the multiple antennas presented in this chapter are small (total antenna dimensions of $68\times40\times1.6$ mm^3) and thin (fabricated on FR_4 substrate), which makes them attractive for compact wireless devices. In section 4.4, a new isolation method based on planar fractal-based EBG structure for mutual coupling reduction between dual microstrip antenna (PIFA) elements for LTE applications at a frequency of 2.65 GHz was proposed. First, the coupling mechanism was identified as being mainly through surface wave coupling and space wave radiation. Then, a coupling reduction technique by adding second iterative order FEBG with the bandgap filter characteristic to reduce mutual coupling between dual PIFAs elements due to its capability of suppressing surface waves propagation in a given frequency range was proposed and operationalised. All the simulations were carried out using Ansoft HFSS ver 17.0 (High-Frequency Simulator Structure). A designed MIMO antenna was fabricated and measured to verify the simulated results. The measured and simulated results of the scattering parameters and far-field radiation patterns showed excellent agreement. Moreover, the analysis results (theoretically and practically) demonstrated that the proposed MIMO antennas guarantee a high coupling reduction of more than 27 dB (Z-X plane) and 40 dB (Z-Y plane), this being obtained between the antennas for antenna spacing less than 0.35 λ_0, without much degradation of the radiation characteristics.

Finally, the proposed MIMO antennas have been compared in detail with other design work regarding bandwidth, mutual coupling level, geometric size and implementation complexity. Through this, it has been found that the proposed antenna with fractal-based EBG structure (FEBG) is effective for low-frequency narrow-band MIMO applications, thus being suitable for employment in some portable devices, such as mobile handsets or laptops. The main content of this chapter has been a manuscript published as a full-length journal paper in IET microwave Antenna and Propagation [R1] and also as a full-length conference paper in Loughborough Antennas & Propagation Conference (LAPC 2016) [R6]. The introduction and other sections of this chapter have been rewritten to create a better flow and to prevent a repetition of the materials already presented in other chapters.

Chapter 5: Development of Multiple Antennas with High Isolation for UWB Applications

5.1 Introduction

Multiple microstrip antennas are considered an important component in modern UWB systems; recently researchers have developed many different MIMO antennas designs for UWB applications with wide impedance bandwidth, reasonable gain, linear phase and stable radiation characteristics across the entire UWB frequency range. These developments in modern wireless communication systems have imposed additional challenges to produce new designs that are miniaturised and have a good broadband performance [1, 228].

In this chapter, a new planar MIMO antenna for UWB applications is presented. The proposed antennas operate over the frequency band from 3.1 to 10.6 GHz. The wide isolation is achieved through a novel planar decoupling structure that is being inserted between the dual antennas. The effectiveness of the decoupling structure is analysed, and performance study was performed to investigate the mutual coupling reduction. Good isolation of more than 31dB has been achieved through the entire UWB band (more than 12 dB improvement over the reference antenna). The proposed UWB-MIMO antenna is being investigated and verified both numerically and experimentally. Then proposed UWB antenna has been compared with previous works regarding antenna size, geometric complexity, bandwidth and isolation level.

5.2 UWB Technology

An ultra-wideband (UWB) signal is characterised by its very wide bandwidth compared to the conventional narrowband systems. UWB spectrum is between 3.1 GHz and 10.6 GHz so that the result is a ratio spectrum that is spread over a very wide bandwidth. Commonly, a UWB signal is defined as a signal with a fractional bandwidth of larger than 20% or an absolute bandwidth of at least 500 MHz [1, 526].

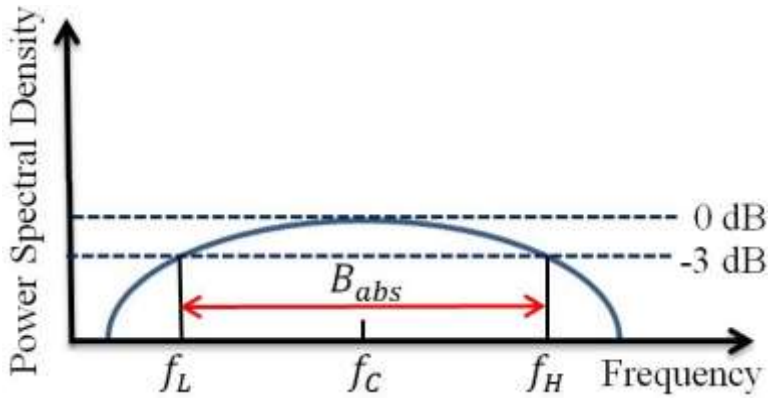

Figure 5.1: Illustration of a UWB bandwidth

The absolute bandwidth can be calculated as the difference between the upper cut-off frequency (f_H) and the lower cut-off frequency (f_L) of the -3 dB power level, as shown in Figure 5.1. However; the absolute bandwidth (B_{abs}), centre frequency (f_C) and fractional bandwidth (B_{frac}) are given in equations (5.1), (5.2) and (5.3); respectively.

$$Absolute\ bandwidth = B_{abs} = f_H - f_L \tag{5.1}$$

$$Centre\ frequency = f_C = \frac{f_H + f_L}{2} \tag{5.2}$$

$$Fractional\ bandwidth = B_{frac} = \frac{Absoulate\ Bandwidth}{Centre\ frequency} = \frac{2(f_H - f_L)}{(f_H + f_L)} = \frac{1}{Q} \tag{5.3}$$

Where Q is defined as a quality factor, which is inversely proportional to the half power fractional bandwidth of the antenna. Since the UWB systems use a wideband of the spectrum, which could easily be interfered by the existing nearby communication systems such as Wireless Local Area Networks (WLANs) operating at the bands of 2.45 GHz (2.4-2.48 GHz), 5.25 GHz (5.15-5.35 GHz) and 5.75-GHz (5.72-5.82 GHz), Worldwide Interoperability for Microwave Access (WiMAX) systems operating in the 2.35 GHz (2.3-2.4 GHz), 2.6 GHz (2.5-2.6 GHz), 3.35 GHz (3.3-3.4 GHz), 3.5 GHz (3.4-3.6 GHz), 3.7 GHz (3.6-3.8 GHz) and 5.8 GHz (5.72-5.85 GHz) bands, downlink of X-band satellite communication system operating at the band of 7.25-7.75 GHz and ITU band of 8.01-8.5 GHz; respectively [283].

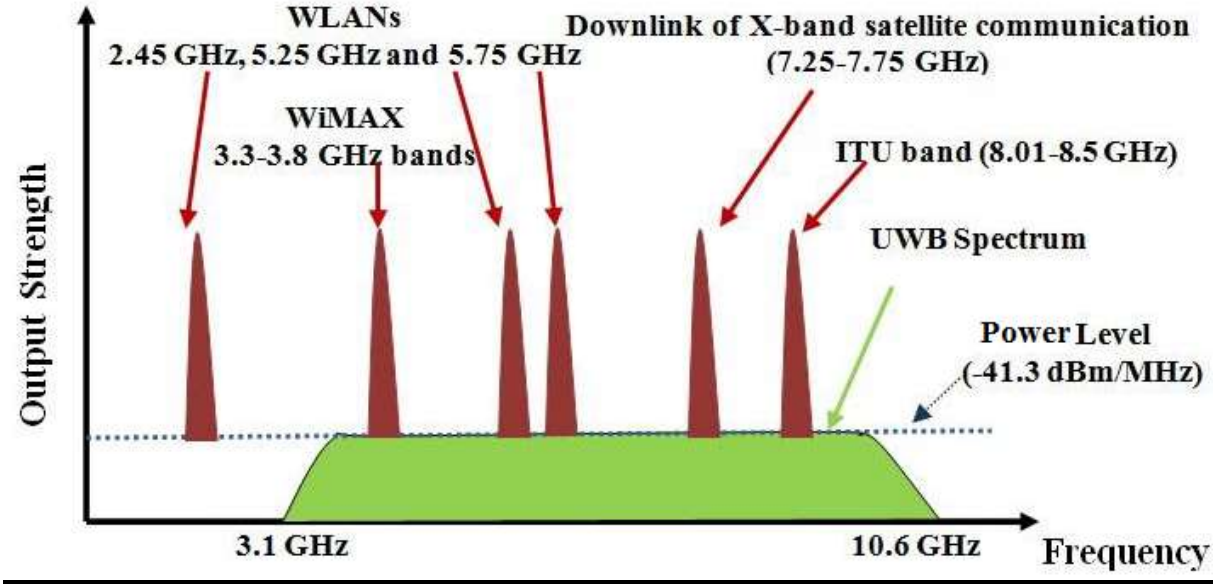

Figure 5.2: Comparison of UWB and other band communication systems in term of PSD [283]

The relative power-spectrum density (PSD) in the UWB and some existing narrow-band communication systems is illustrated in Figure 5.2. UWB transmissions are virtually undetectable by ordinary radio receivers and therefore can concurrently with existing wireless

communications without demanding additional spectrum or exclusive frequency bands; but this technology is limited to short-range communications due to the low allowable transmitted power of -41.3 dBm/MHz.

However; technical challenges also exist in the areas of modulation and coding techniques suited for UWB radio systems. Thus, adequate characterization and optimisation of transmission techniques (e.g., adaptive power control, duty cycle optimization) will be required. To cope with difficult signal propagation environments (e.g., industrial and manufacturing or commercial areas), advanced technologies such as UWB multiple-input multiple output (MIMO) systems may be able to provide the required high degree of link reliability and (rate) adaptation capability.

A particularly challenging area at the physical layer level today appears to be antenna design and implementation for UWB radio devices. Generally, portable communication devices require small and preferably unobtrusive antennas that can be integrated into miniature devices and are capable of operating effectively under varying environmental conditions, often in near-field propagation conditions (e.g., near objects, or carried on or close to the body). The design and implementation of effective antennas is more challenging for UWB radio systems than for conventional narrow-band systems given the large bandwidths, linearity requirements, and variable conditions of operation.

There are some of the advantages cited for ultra-wideband technology [320]:-

1- Very low energy spectral density (limited to -41.3 dBm/MHz bandwidth), as shown in Figure 5.2, besides a very low probability of interference with other radio signals over its wide bandwidth.
2- High immunity to interference from other radio systems and extremely difficult to intercept.
3- Low probability of interception or detection by other than the desired communication link terminals.
4- Higher multipath immunity.
5- Higher data rate ultra-wideband channels can operate concurrently so that transmits data at speeds between 50 to 1000 megabits per second.
6- Excellent range-resolution capability, impulse, carrier free, and baseband, non-sinusoidal, time domain signalling.
7- Relatively simple, Low power cost construction, based on nearly all digital architectures

On the other hand, MIMO technology takes advantage of using multiple antennas at wireless terminals, which can be used to enhance the communication performances in terms of

capability, improved signal quality, high data rate and better reliability (especially in rich scattering environments). Thus, the combination of MIMO and UWB technologies may enhance performance and offer higher system reliability. However, the requirement for the compactness of MIMO enabled terminals may introduce strong mutual coupling between the closely packed antenna elements, which can dramatically degrade the MIMO system performance.

Therefore, one of the research topics of the thesis is to design new planar UWB-MIMO antennas with applicable decoupling structure with high isolation that optimised to cover the entire UWB range.

However, the design of MIMO antennas in small handset devices for UWB operation is more challenging due to the following issues:

1) The closely spaced multiple antennas tend to be more coupled (correlated); the high correlation level destroys the performance parameters of the MIMO system.

2) To decrease the coupling level and correlation between MIMO antennas, a suitable and reliable isolation (decoupling) technique should be employed.

3) Antennas with small footprint and low profile are highly demanded to meet the recent handset design fashions in the mobile market. This adds another design difficulty in which MIMO antennas with a broadband operation (UWB) are needed.

Although; there is extensive research and development of UWB-MIMO antennas for mutual coupling reduction in the past decade (As presented before in the literature survey chapter), the following essential issues needed to be focused and addressed:

1- ultra-wideband operation including an extremely wide operating bandwidth, multiple antennas must be designed to cover either the entire UWB band of 3.1-10.6 GHz (110%) or the lower or upper UWB bands of 3.1-4.8 GHz (43%) or 6-10.6 GHz (55%), respectively, at least in terms of the good impedance matching. Besides; it is desirable high isolation characteristics to be obtained that cover this wide isolation BW.

2- The radiation performance of the MIMO antennas should be consistent with an acceptable gain and unchanged polarisation along the desired transmission or reception direction across the whole operating bandwidth in order to avoid the big change in received signals or energy.

3- The overall size of the multiple antennas should be small. This challenge is caused by the fact that recently the majority of UWB-enabled systems are usually embedded into portable / handset devices. Physically, these antennas must be more compact versions featuring (small-sized) and easy to integrate with other decoupling methods.

Therefore, it is desirable that decoupling methods been not implemented in multilayers to keep the compactness of the wireless devices as possible.

4- The multiple antennas geometric complexity including any embedded decoupling structure that used as an isolation method which in turn will reduce the cost of the fabrication. The cost is one of the killer factors for any commercial product. In fact, several factors may also affect the cost of manufacturing antenna arrays, such as the material used for fabricating or fabrication process itself, and even the installation of the multiple antennas. Therefore, applicable and straightforward multiple antenna designs with acceptable diversity performance are always desired.

5- Other essential factors such as the reliability of MIMO antennas performance and the compatibility of integration with other systems.

The contributing work in this chapter addressed all the above crucial issues using applicable multiple antennas with new decoupling structure used as an isolation method that was presented in section 5.3.The proposed antenna has some outstanding characteristics such as a geometric simplicity, compact size, broad BW and low correlation which give the antennas an excellent diversity performance to be a good candidate for UWB applications.

5.3 Multiple Microstrip Antennas with High Isolation for UWB Applications

5.3.1 UWB-MIMO Antennas Configuration

The multiple antennas are fabricated on an inexpensive FR_4 substrate with a thickness of 1.6 mm and relative permittivity of 4.4. The circularly shaped radiators are adopted due to its excellent performance. The designed UWB-MIMO antennas without the proposed wideband decoupling structure are illustrated in Figure 5.3.

It consists of two symmetrical circular-shaped monopole radiating elements [288] (referred as Ant-1- and Ant-2-), which are located on the same sides of the common FR_4 substrate with dielectric constant equals to $\varepsilon_r = 4.4$ (loss tangent = 0.018) and thickness h =1.6 mm [288].

The selection of the circular disc antenna can be justified by its good performance, compact size, and ease of integration [234]. Here; the monopolies antennas working at UWB frequency range (3.1-10.6 GHz) are placed collinearly along the x-axis, and the spacing between antenna array elements is approximately equal to 0.35 λ_0 of the lowest frequency band (measured from element centre to centre).

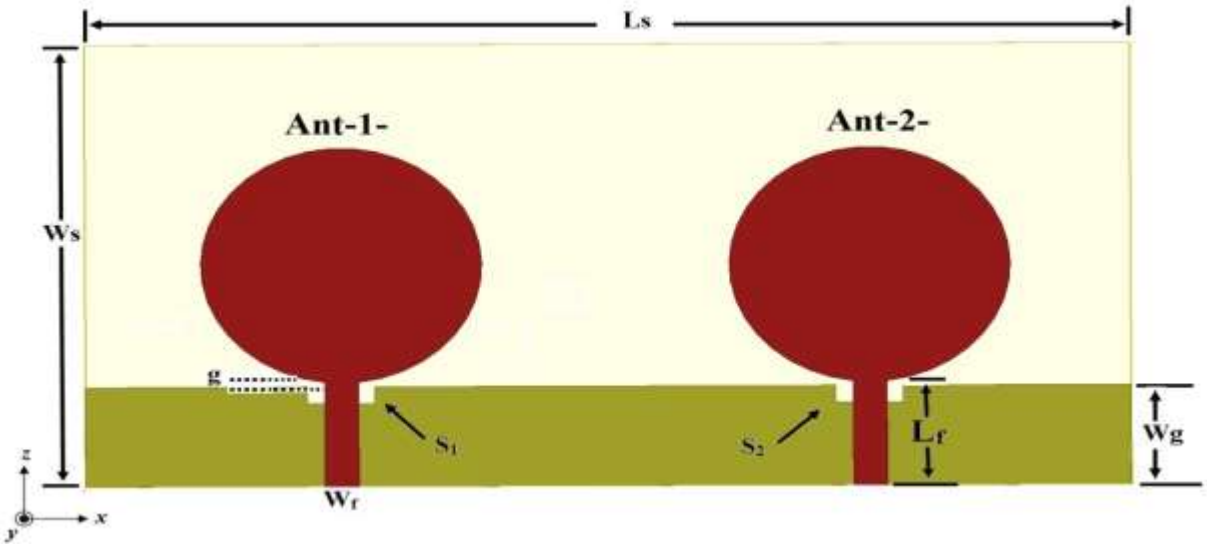

(a)

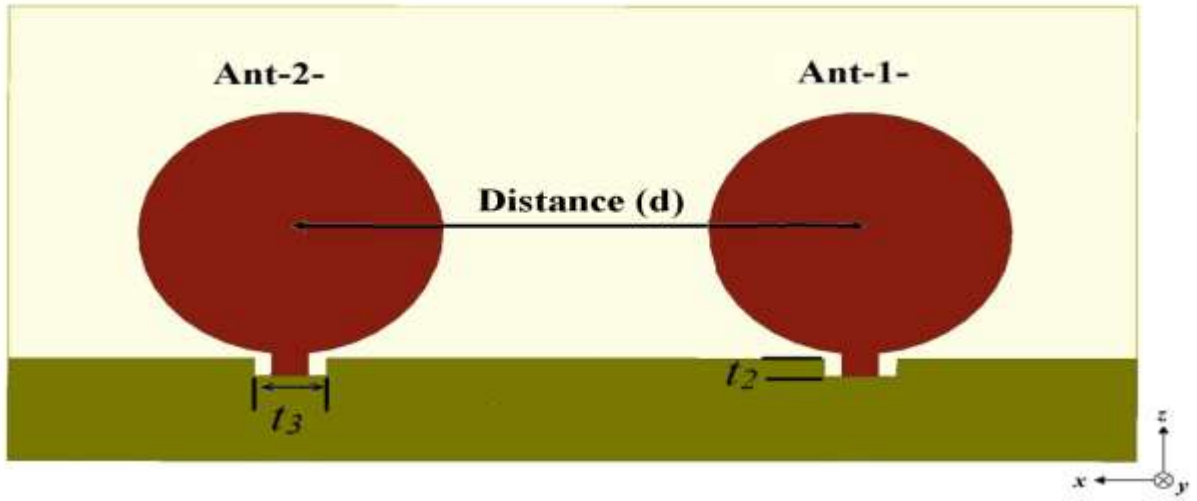

(b)

Figure 5.3: Geometry of a UWB-MIMO monopolies antennas. **(a)** Front view **(b)** Back view

As mobile terminals; such as handsets and PDAs have become smaller, the design of smaller antenna elements are required; thus, the dimensions of the monopolies should be further reduced. The antenna is formed by a metallic disc of radius R = 12 mm, a shared ground plane is implemented and placed on the back side of the substrate with a ground length L_g = 93 mm, and a ground width W_g = 10.6 mm, which ensures a good impedance matching over a broad frequency range. The radiators are fed by a microstrip line of the characteristic impedance of 50-ohm, the length of the feedline is denoted as length (L_f) and its width (W_f) are fixed at 12.5mm and 1.5 mm; respectively. The distance between the identical dual radiators (centre to centre) is denoted as S. The overall size of UWB-MIMO antennas are: 93 × 47 × 1.6 mm^3 (corresponds approximately 0.95 λ_0 × 0.49 λ_0 × 0.016 λ_0) to be suitable for most mobile PCB circuit boards, other antenna dimensions obtained after optimisation process are illustrated as follows:

Table 5.1: Detailed dimensions of the proposed UWB-MIMO antennas

Parameters	Values
frequency (f)	3.1-10.6 GHz
height of substrate (h)	1.6 mm
ground length (L_g)	93 mm
ground width (W_g)	10.6 mm
substrate length (L_{sub})	93 mm
substrate width (W_{sub})	47 mm
circular patch radius (R)	12 mm
distance (d)	0.35 λ_0
Feed-line length (L_f)	12.5 mm
Feed-line width (W_f)	1.5 mm
gap (g)	0.5 mm

The gap distance (g) between the ground plane and the antenna radiating element effects the impedance bandwidth and hence this distance had been optimised at g = 0.5 mm.

Moreover, for getting a better impedance matching (particularly in the higher frequencies), two small rectangular slots (denoted as $\boldsymbol{S_1}$ and $\boldsymbol{S_2}$) of compact dimensions 1.6 × 6 mm^2 were introduced on the common ground plane to enhance the impedance bandwidth. These slots are cut on the upper edge of the ground plane underneath each feed line. Finally; the radiating circular patch is made up of a very thin copper sheet with a thickness of 0.1 mm.

5.3.2 Multiple UWB antennas with decoupling structure for isolation enhancement

Figure 5.4 illustrates the geometry of the UWB-MIMO antennas with a new wideband decoupling structure. The proposed wideband planar decoupling structure has been inserted between the dual-monopole antennas elements to reduce mutual coupling; it will provide additional coupling paths and reduce directly induced coupling currents in the radiating elements (as presented in next section).

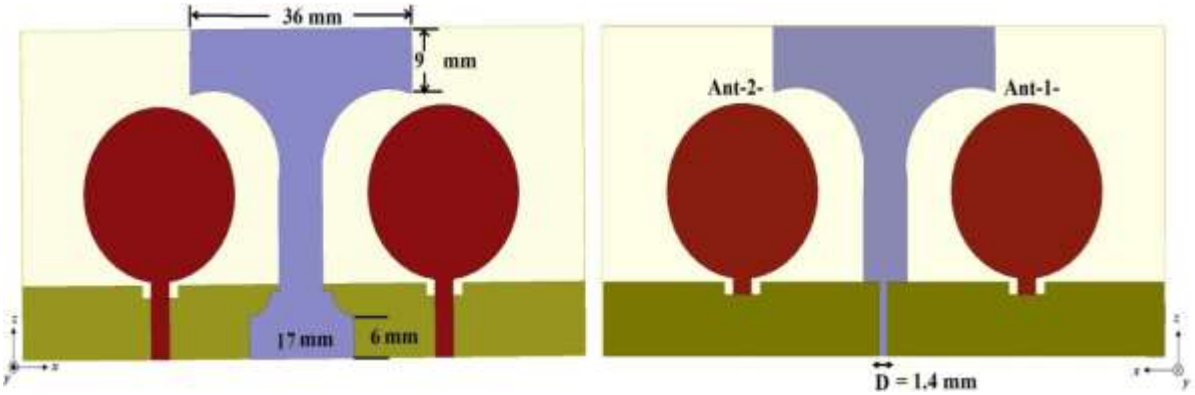

Figure 5.4: Schematic UWB-MIMO antenna with decoupling structure. **(a)** Front view and **(b)** Rear view

This decoupling structure composes of modified metallic patch like T on the upper side with optimised dimensions L_2 = 9 mm × W_1 = 36 mm, another smaller metallic patch like inverse T on the lower side (with optimised dimensions L_3 = 6 mm × W_2 = 17 mm) are joint and subtracted by four half-circular slots. Dual half-circular in the upper side and another twin smaller half-circular on the lower side to form a parasitic strip that has been applied as a compact wideband planar decoupling structure between UWB antennas. The structure is symmetrical along the Z-axis from the centre. The proposed wideband decoupling structure has longer current paths that it could work in the low-frequency range. Figure 5.5 illustrates the layout of the proposed wideband decoupling structure.

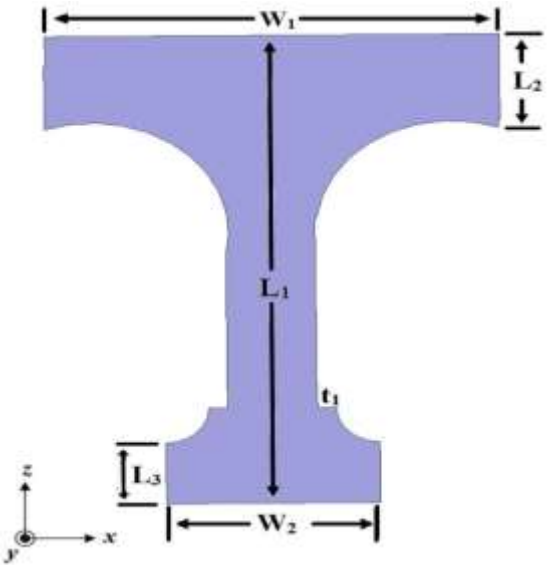

Figure 5.5: Detailed layout of the proposed decoupling structure

The parameters given in Figure 5.5 were optimised using the simulation software (HFSS ver 17.0), and the detailed optimum dimensions of the proposed decoupling structure used in this work are written in Table 5.2.

Table 5.2: Detailed dimensions (in mm) of the proposed decoupling structure

Optimised parameters	Values in mm
Length of the proposed structure, L_1	47
Upper width of the proposed structure, W_1	36
Height of the top portion of the T-shaped strip, L_2	9
lower width of the proposed structure, W_2	17
Height of bottom portion of the inverse T-shaped strip, L_3	6
Span on one side, t_1	1.5

5.3.3 Theoretical Analysis

5.3.3.1 Scattering parameters performances

The return loss (reflection coefficient) and the transmission loss (mutual coupling) for the dual antennas without and with the proposed decoupling structure are plotted in Figure 5.6(*a*) and Figure 5.6(*b*); respectively. Figure 5.6(*a*) illustrates the reflection coefficient performance; it was observed that the UWB-MIMO antennas in both cases (without and with structure) has a wide broadband bandwidth ranging from 3 to 11 GHz (S_{11} < - 10 dB). Thus; the antenna array satisfies the impedance matching requirement for the entire UWB range specified by the FCC. The mutual coupling between antenna elements can be determined by scattering parameters; S_{21} or S_{12}. The simulated mutual coupling is shown in Figure 5.6(*b*). Isolation of less than -31dB has been achieved through the entire UWB range (more than 12 dB improvement over the reference antennas).

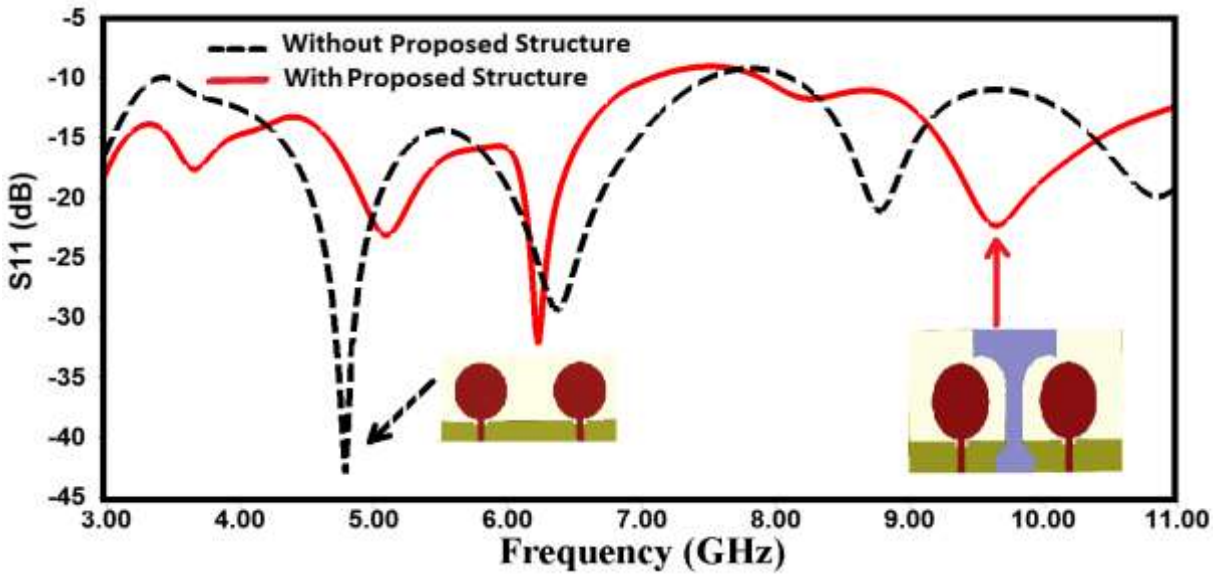

(a)

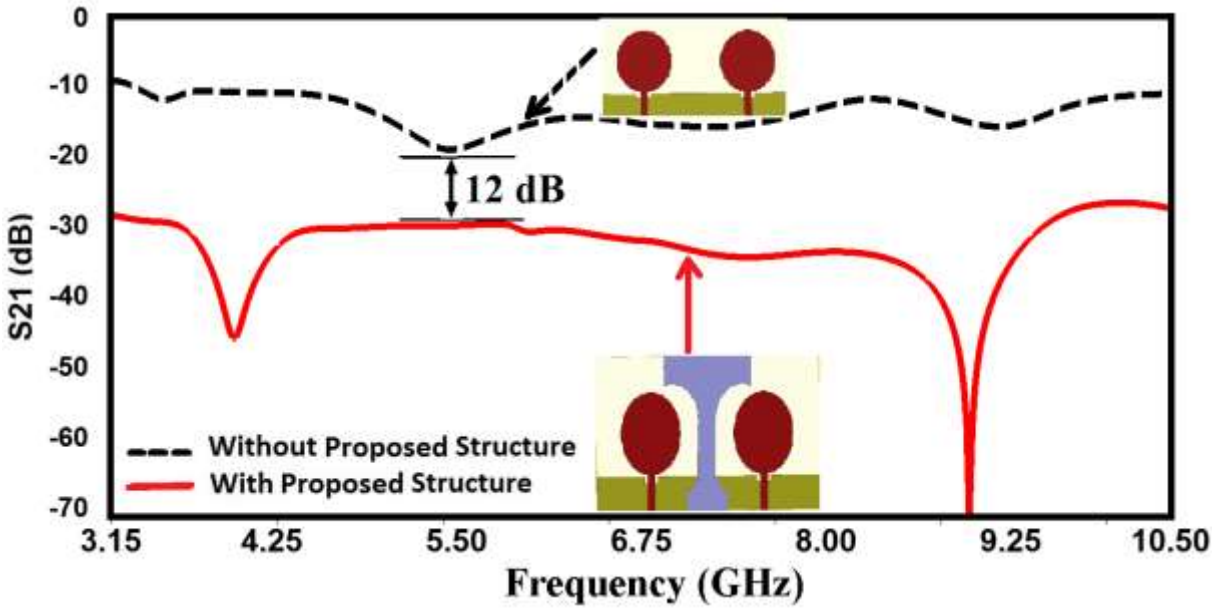

(b)

Figure 5.6: The simulated scattering parameters of the antennas without (dashed line-black colour) and with the proposed decoupling structure (solid line-red colour). **(a)** Reflection coefficient (S_{11}) and **(b)** Transmission coefficient (S_{21})

This result satisfies the required condition for mutual coupling reduction between the antennas for proper operation of the MIMO system in the UWB frequency range. All these analyses were conducted with one antenna element transmitting and other antenna terminated with 50 Ω load.

5.3.3.2 Isolation mechanism and working with the various decoupling structures

The direct mutual coupling between two antenna elements can be cancelled out by adequately adding an additional indirect coupling path. Here; a proper design aims at creating indirect signal coming via the extra coupling path that opposes the signal going directly from element to element. If the two amplitudes are comparable and out of phase, the two signals add up destructively, and the mutual interaction is considerably reduced. An extra requirement is that the inserted decoupling structure should not significantly degrade the radiation properties. In the approach followed here, by placing and adding a non-resonating and parasitic decoupling structure between antennas, other active coupling paths can be created. The coupled radiation introduces induced currents on the neighbouring antenna.

The proposed wideband decoupling structure can also capture the near coupling fields and converts them in surface currents to be shorted with a ground plane and such that multiple coupling paths reduce the strong direct coupling between ports and hence reducing the mutual coupling.

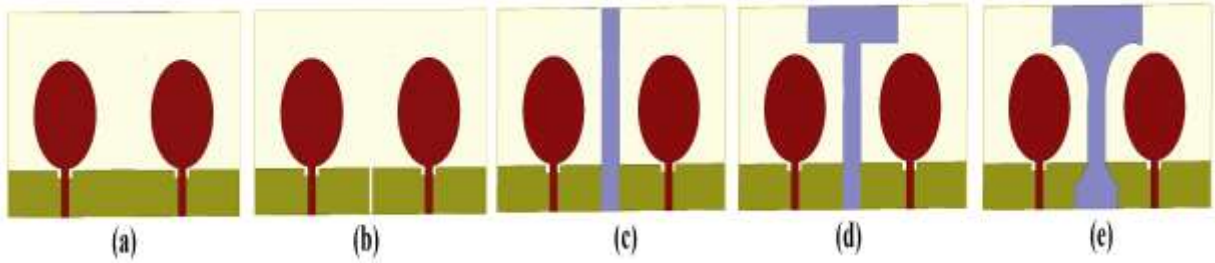

Figure 5.7: UWB-MIMO antennas with different geometrical models **(a)** Without any decoupling structure (Model I), **(b)** With a centre slot on the ground only (Model II), **(c)** With conventional rectangular shaped decoupling structure (Model III), **(d)** With T-shaped decoupling structure (Model IV), and **(e)** With proposed wideband planar decoupling structure (Model V)

In this work, the dimensions of the proposed decoupling structure were optimised to obtain a maximum surface currents pickup strategy. The surface currents analyses are presented in the next section.

To further inspect the performance of the proposed MIMO-UWB antenna and investigate the best decoupling structure arrangement to be utilised for isolation enhancement in UWB-MIMO antennas configuration, five different geometrical models are given in Figure 5.7, and individual simulated S_{21} parameter variations plot for these five models is presented in Figure 5.8.

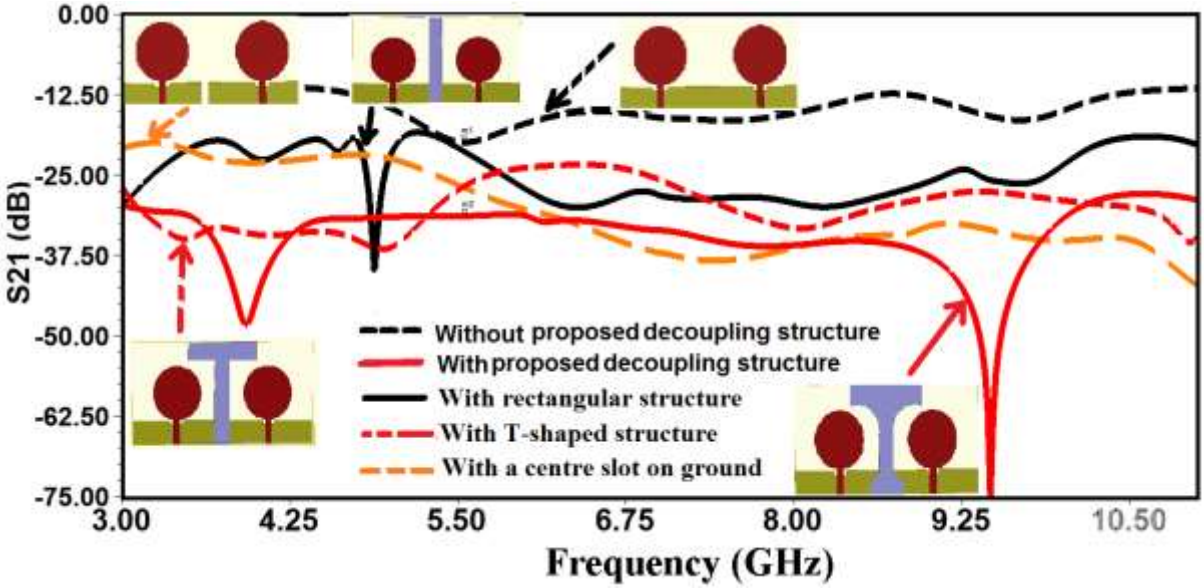

Figure 5.8: Simulated S_{21} parameters for different geometrical models of UWB-MIMO antennas

However, inserting both a centre slot in common ground (Model II) and a conventional rectangular structure (Model III), as given in Figure 5.7(b) and Figure 5.7(c); respectively, help to improve isolation between the antennas array but not for the entire UWB range, only a real enhancement, $S_{21} \leq -24$ dB can be seen in the higher frequencies range.

To further increase the isolation between antennas especially in lower frequencies range of the UWB operation; a T-shaped structure (Model IV) has been presented in the middle of the substrate as illustrated in Figure 5.7(d), thus; the S_{21} parameter here has some good values (< −28 dB) towards lower UWB frequencies but remains with high coupling as is to be expected in higher frequencies (> 5.5 GHz).

Finally; by introducing the proposed wideband decoupling structure (Model V) as seen in Figure 5.7(e), an excellent isolation of less than -31 dB (more than 12 dB improvement over the reference) has been achieved through the entire UWB band, and hence this case can satisfy the requirements of an applicable UWB operation with highest isolation.

5.3.3.3 Radiation patterns, gain and efficiency

The orientation of the proposed antenna with respect to the coordinate system as previously shown in Figure 5.3.

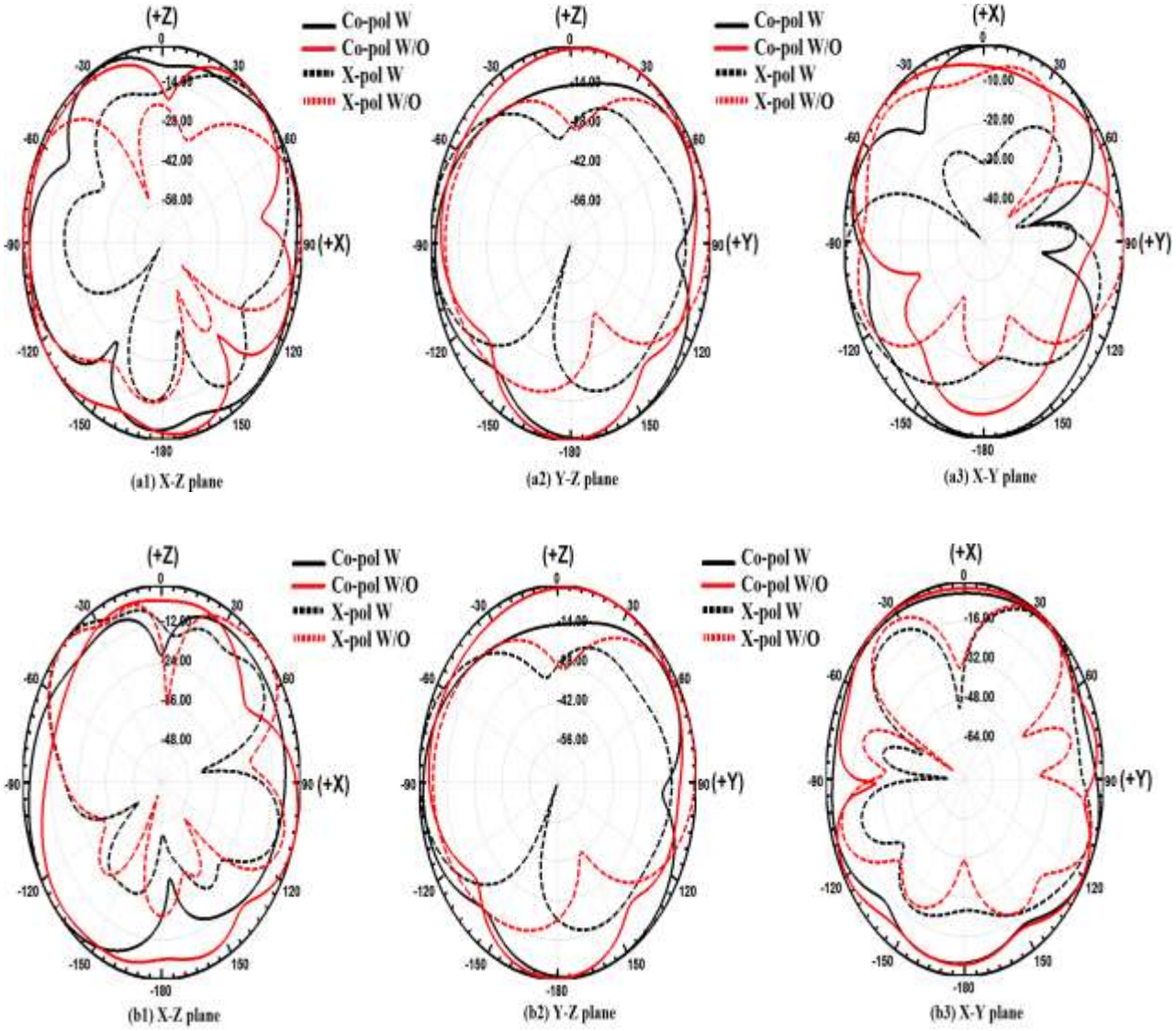

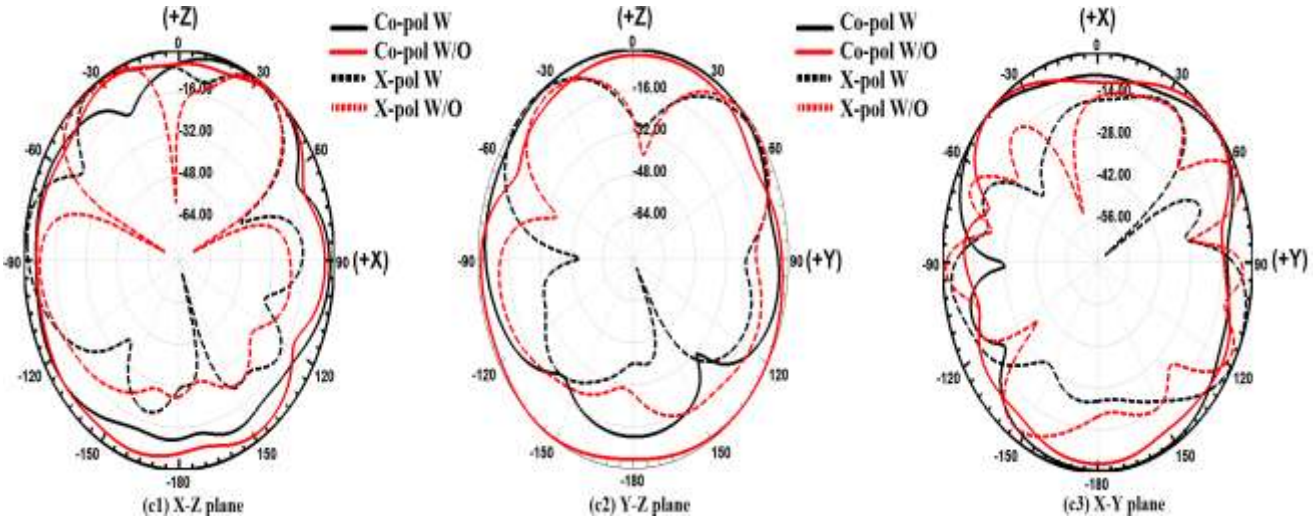

Figure 5.9: The simulated 2D radiation patterns (normalised) without and with the proposed decoupling structure: **(a1)** XZ plane, **(a2)** YZ plane, and **(a3)** XY plane at 4 GHz; **(b1)** XZ plane, **(b2)** YZ plane, and **(b3)** XY plane at 6 GHz; and **(c1)** XZ plane, **(c2)** YZ plane, and **(c3)** XY plane at 8 GHz; respectively, with port 1 excited. (solid line: co-pol, dashed line: cross-pol, black colour: with, and red colour: without)

This section presents the study performed on the effect of far-field radiation patterns as a comparison between both cases (with and without inserting the proposed decoupling structure). The simulated far-field radiation patterns are normalised with respect to the realised gain on the major principal planes (YZ, and XY planes) in both prototypes, without and with decoupling structure, are presented in Figure 5.9. In general, we can see that the overall radiation patterns are relatively stable across the different UWB frequencies. Still, nearly omnidirectional patterns are obtained at various frequencies (e.g. 4 GHz, 6 GHz and 8 GHz) before and after inserting the wideband decoupling structure, no significant degradation of radiation patterns are noticed between the two designs (with and without decoupling structure) especially in YZ and XY planes.

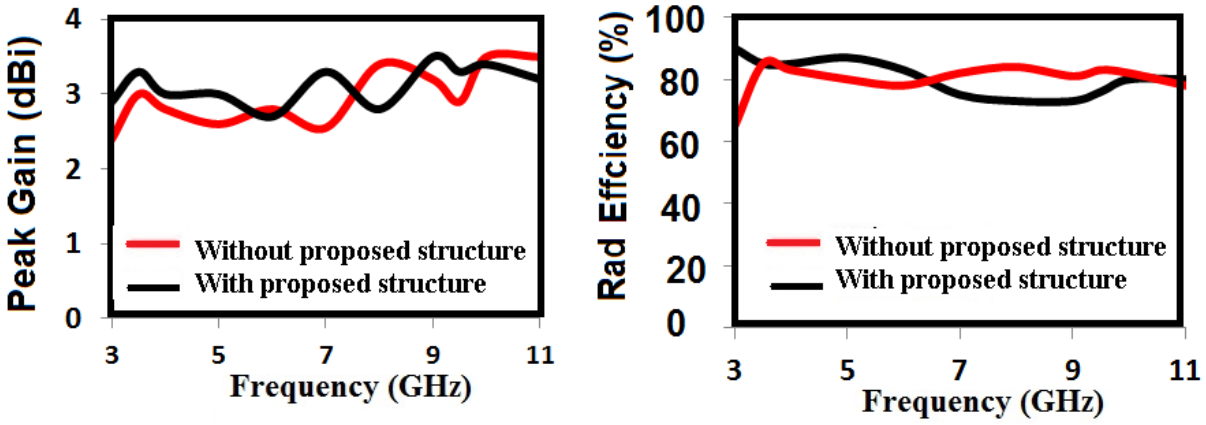

Figure 5.10: Simulated antenna gain variation (**left**) and radiation efficiencies (**right**) over the radiating band of the proposed UWB-MIMO antenna

Generally, an enhancement in radiation characteristics helps to improve peak gain of the antennas, it is noticed that gain variation without decoupling structure is 1.4 dBi, this difference reduces to < 0.5 dBi with a peak gain of 3.5 dBi at a frequency (9 GHz), when the proposed wideband decoupling structure is inserted, which makes it more consistent over the radiating bandwidth.

Since the isolation is achieved by using a wideband parasitic decoupling structure, there is the possibility of a reduction in radiation efficiency. The antenna radiation efficiency is simulated with and without wideband decoupling structure.

The comparison is provided in Figure 5.10.

The radiation efficiency of UWB antennas remains above 70 % in the complete frequency band. The radiation efficiency only varies by < 10% in the whole band which certifies that the parasitic wideband decoupling structure does not have any noticeable effect on radiation characteristics.

The radiation efficiency at the lower UWB frequencies is better with a decoupling structure which indicates that the decoupling structure reduces the return loss at lower frequencies. At the upper UWB frequencies, the radiation efficiency with decoupling structure is less than an antenna without a decoupling structure which indicates an increase in mismatch loss at higher frequencies.

5.3.3.4 Simulated surface currents distribution

To further understand the effectiveness of the insertion of the decoupling structure, the degree of isolation in the proposed UWB antenna can be observed by presenting surface currents distribution.

Figure 5.11(a-c) shows the currents distribution with and without the wideband decoupling structure at different three frequencies (e.g. 4 GHz, 6 GHz and 8 GHz) when Ant-1- is excited while Ant-2- is terminated with a load impedance of 50 Ω.

The effects of the proposed wideband decoupling structure on the currents distribution can clearly be noticed by comparing with those without structure.

The surface currents are absorbed by wideband decoupling structure, and thus it ameliorates the port isolation between two UWB monopoles.

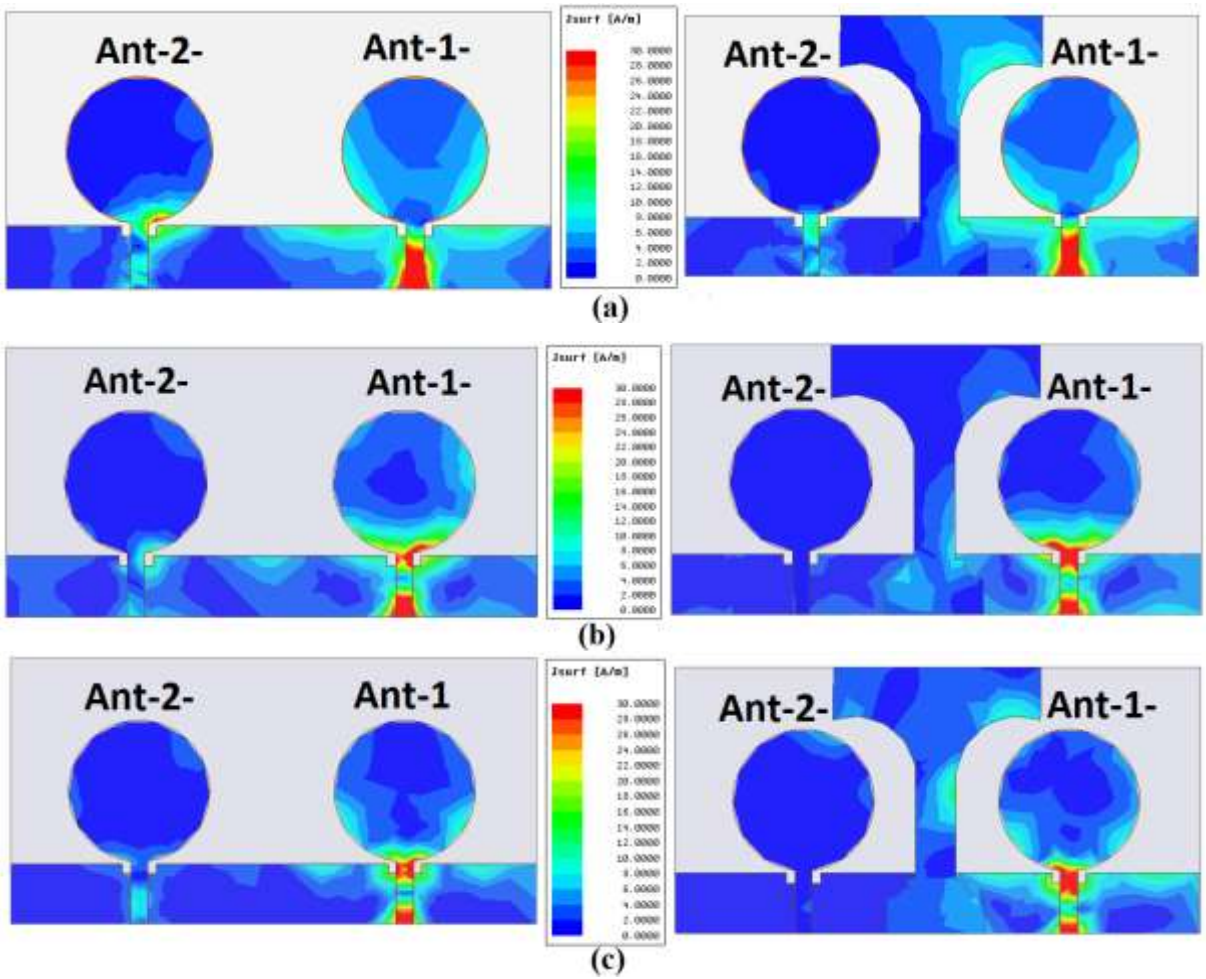

Figure 5.11: Simulation of surface currents distribution on the multiple antennas without structure (**left side**) and with decoupling structure (**right side**), when the first port is excited and the second port is terminated with a 50 load at a frequency: **(a)** 4 GHz, **(b)** 6 GHz, **(c)** 8 GHz

It is observed from Figure 5.11(a-c) that less amount of surface currents are induced in the second UWB antenna because most of the antenna's direct coupling field is concentrated in the planar wideband decoupling structure. This shows the creation of additional current paths between the dual radiating elements and prevents most of the induced currents to be transferred towards the second antenna. In this work; a simple and an effective approach is to work on a common ground plane to limit the current flow from one port to the other, ultimately to reduce mutual coupling between dual feeding ports. The effect is same when Ant-2- was excited while Ant-1- was terminated with 50 Ω load.

5.3.3.5 MIMO characteristics

In this work, ECC (ρ_{12}) was calculated using S-parameters of the MIMO system as defined before in Eq. (2.13), which assumed ideal and uniform propagation multipath environment, the antenna system is lossless and, one of the antenna elements is excited separately while keeping the other antennas matched terminated.

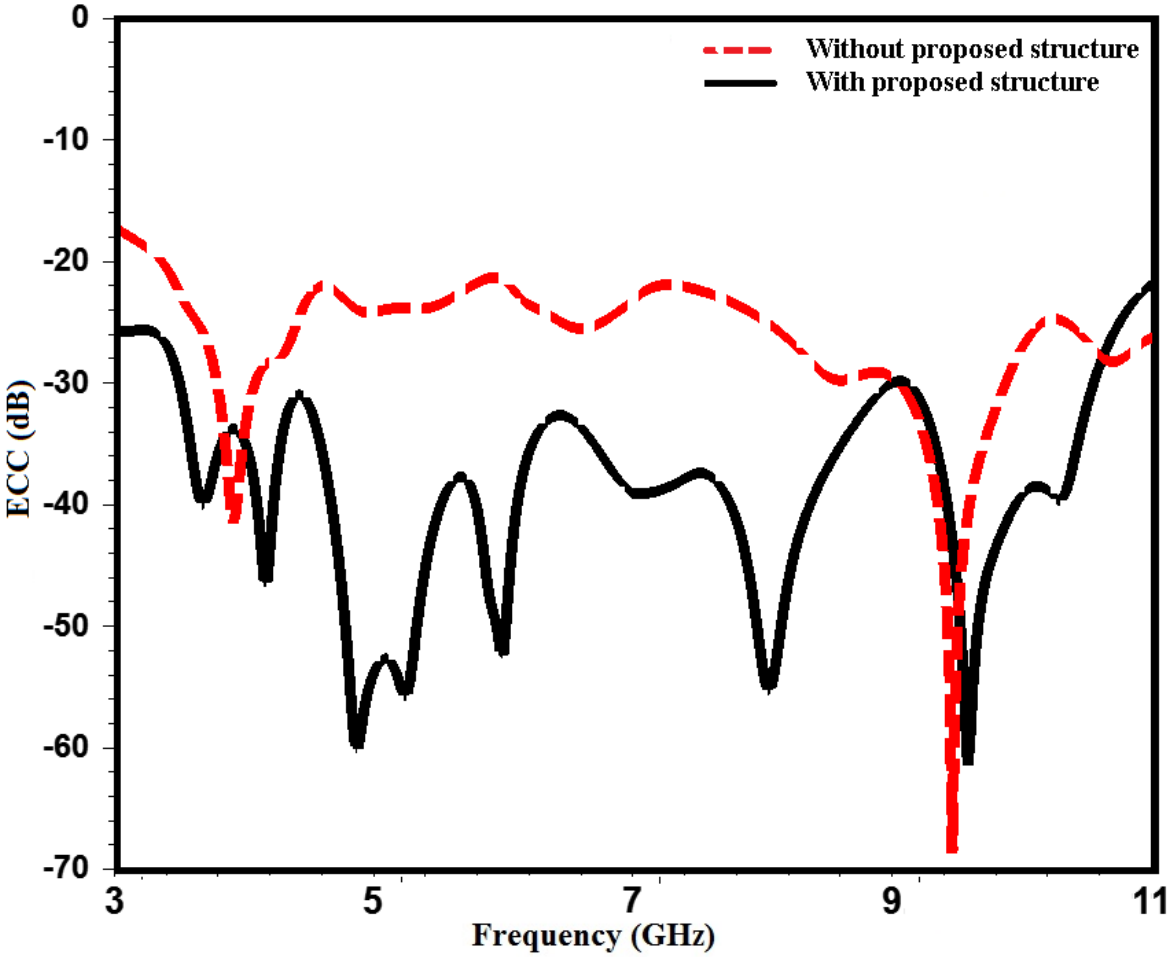

Figure 5.12: Simulated envelope correlation coefficient of the UWB-MIMO without (dashed line-red colour) and with proposed structure (solid line-black colour).

In Figure 5.12, the ECC for the UWB antennas with and without the proposed decoupling structure is shown against the operation frequency range. It is noticed from the simulated results, the maximum envelope correlation coefficient of -29 dB over the UWB range of the antenna elements with the proposed decoupling structure is smaller than that of the array without structure insertion. This observation indicates better behaviour and an excellent diversity performance of the UWB antennas system will be achieved by using the proposed decoupling structure.

5.3.4 Fabrication and Experimental Demonstration

In this section, the performances of the proposed UWB-MIMO antennas are verified through the antennas fabrication and measurements. A prototype of the proposed multiple antennas without and with decoupling structure is fabricated as presented in Figure 5.13(a) and Figure 5.13(b); respectively.

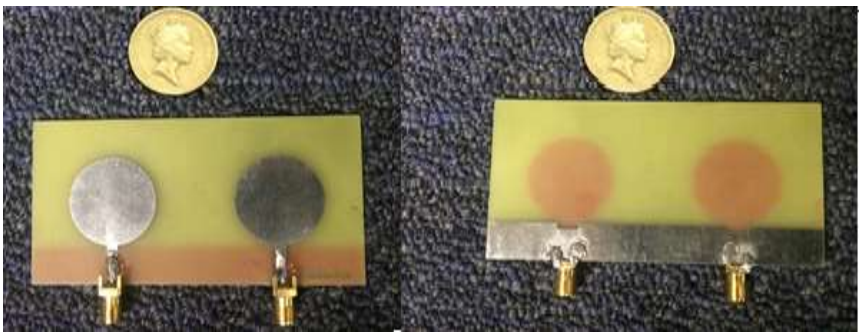

(a)

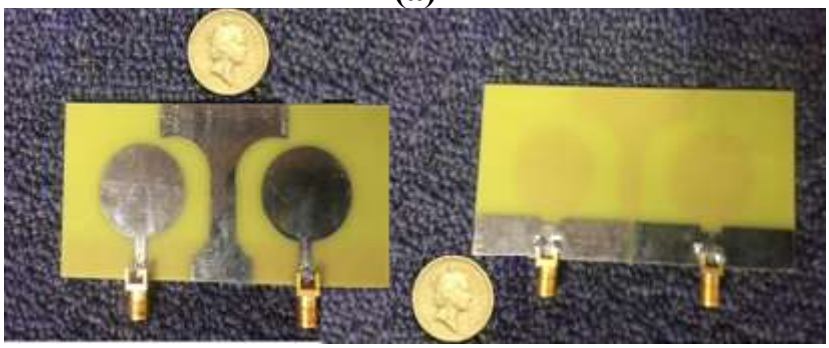

(b)

Figure 5.13: Prototype of the fabricated UWB-MIMO antenna (Top and back view) **(a)** Without **(b)** With decoupling structure

5.3.4.1 Measured scattering parameters

The performance of the UWB-MIMO antenna has been verified through accurate measurements performed by means of Agilent Technologies N5230A PNA–L a vector network vector analyser (as shown in Figure 5.14) inside Brunel University London allowing measurements of the reflection coefficients of microwaves in 300KHz −20 GHz range.

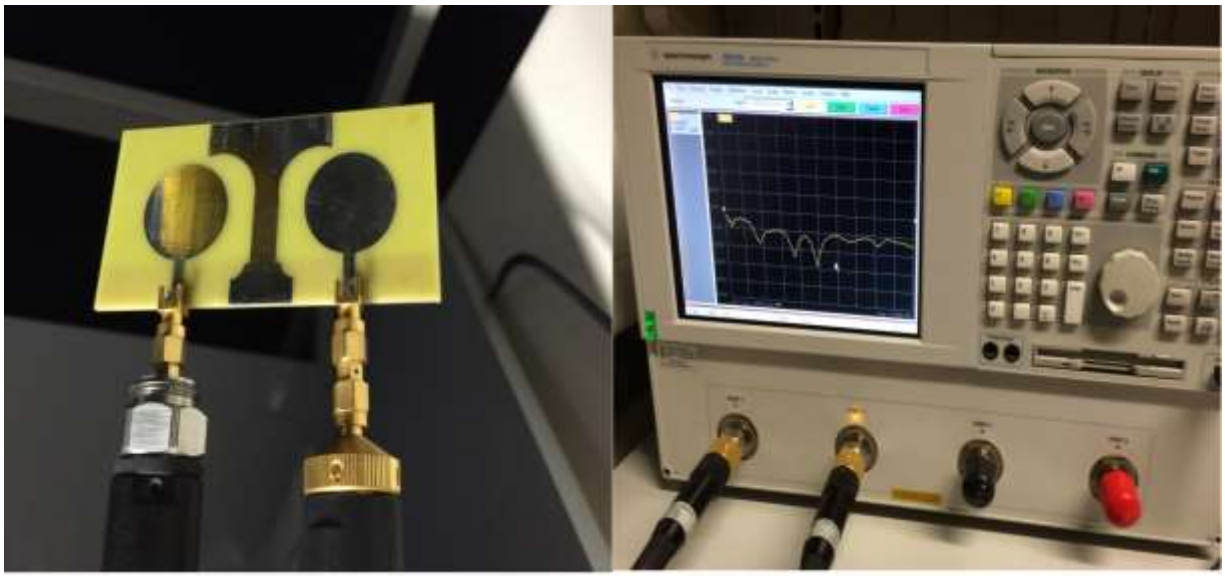

Figure 5.14: Photograph of the proposed UWB-MIMO antennas measured using a network analyser

After calibration with the network analyser, both a return loss and transmission losses have been measured and recorded. Figure 5.15(a) shows the measured and simulated return losses of the impedance bandwidth (S_{11} < -10 dB) comparatively between the dual UWB-MIMO antennas with and without the proposed wideband decoupling structure.

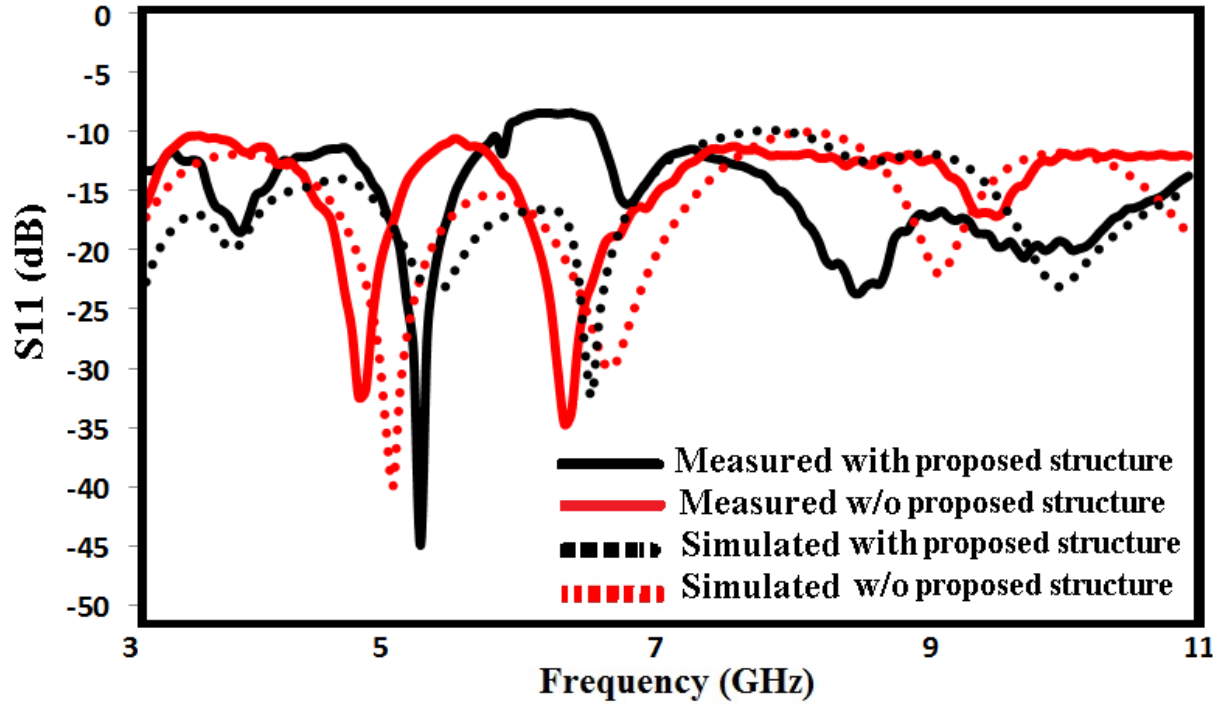

(a)

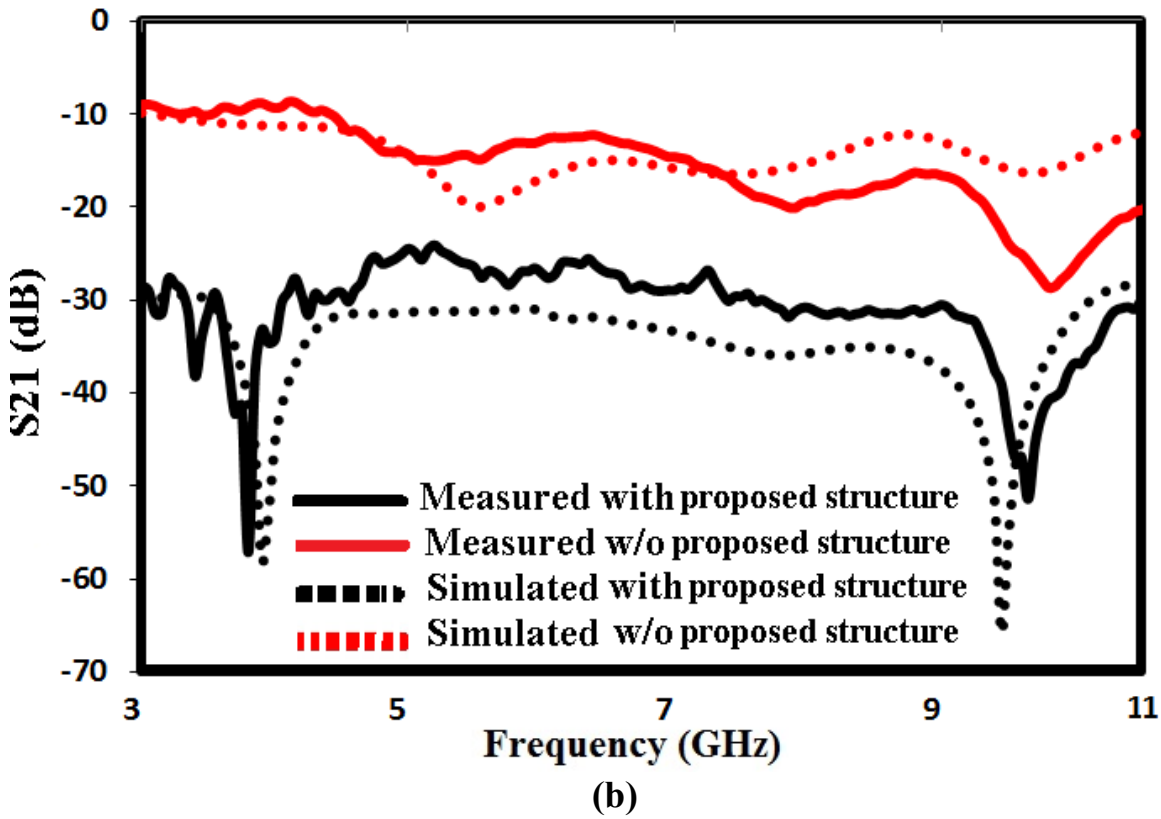

(b)

Figure 5.15: Comparison of simulated and measured scattering parameters without and with a decoupling structure. **(a)** Reflection coefficient (S_{11}) and **(b)** Transmission coefficient (S_{21})

It is observed that the proposed MIMO antennas has a wide measured bandwidth 7.5 GHz and covers the whole UWB band ranging 3.1–10.6 GHz with a return loss better than -10 dB that satisfy the requirements of UWB operation.

They are in a reasonable agreement between the measured and simulated plots while a slight difference between these results can be noticed. That may be attributed to minor factors such as an inaccuracy in the fabrication process, variation in the quality of the substrate, and the mismatch effect of SMA connectors.

Figure 5.15(b) shows the measured and the simulated mutual coupling comparatively between dual UWB antennas with and without the proposed decoupling structure.

The prototyped MIMO antenna has wide frequency range covers from 3 to 11 GHz with the measured isolation less than -27 dB.

These measured results agree well with the simulated results obtained before as presented previously in Figure 5.6.

A slight deviation can be attributed to the fabrication tolerances. From this experimental verification, it can be concluded that the proposed wideband decoupling structure can effectively reduce the mutual coupling between array elements.

In all these measurements, one port is excited and the other terminated by standard 50 Ω load.

5.3.4.2 Radiation patterns characteristics

The radiation patterns of the proposed UWB-MIMO antennas were measured at various frequencies (e.g. 4 GHz, 6 GHz and 8 GHz).

The measurements of radiation patterns are carried out in an anechoic chamber (inside University of Greenwich campus).

The measured radiation patterns data obtained from the anechoic chamber were relatively small. Hence, relative radiation patterns were employed for comparison. These values were normalised to the maximum co-pol for comparison with the simulation results.

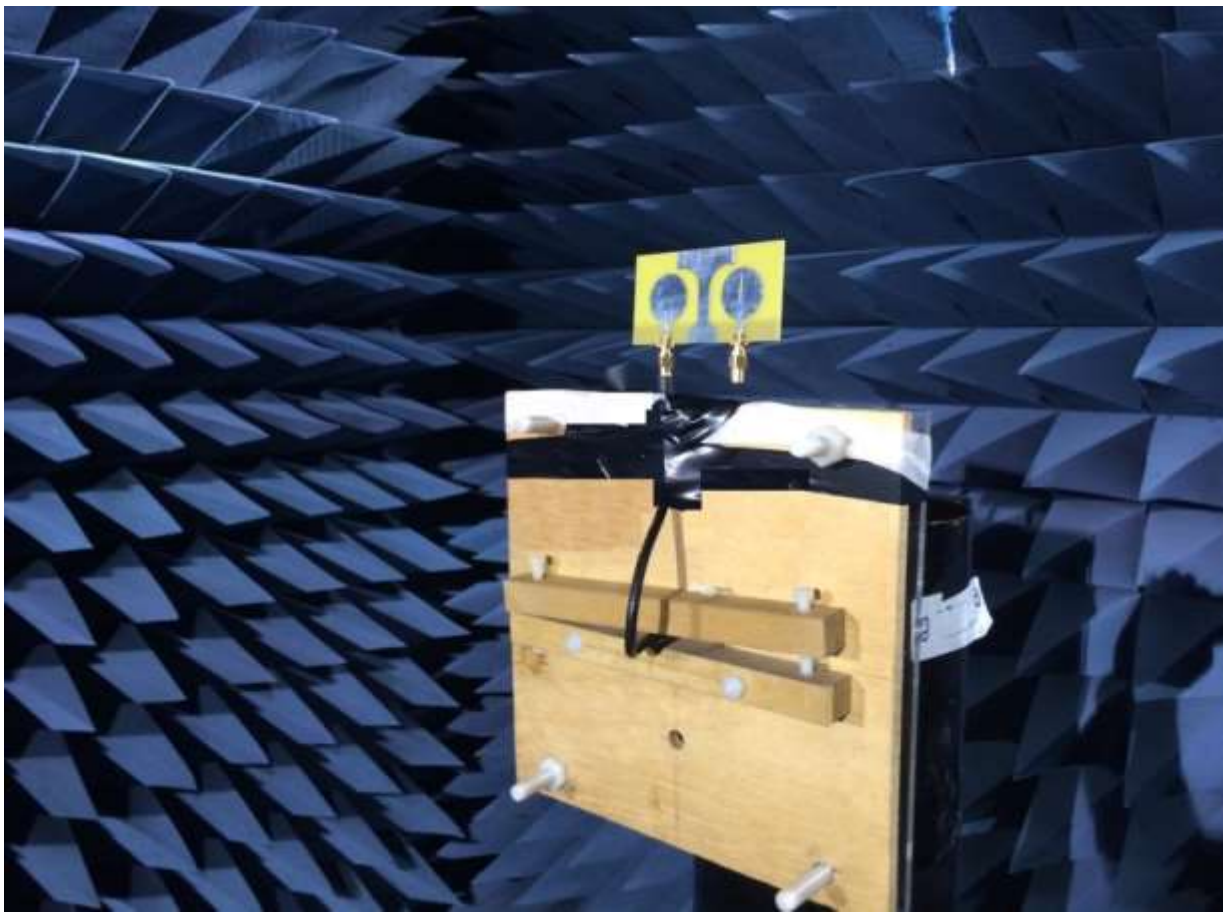

Figure 5.16: Photograph of the AUT mounted inside an anechoic chamber

The measured and simulated far-field radiation patterns are normalised with respect to the realised gain without and with the proposed wideband decoupling structure are presented in Figure 5.17 and Figure 5.18; respectively:

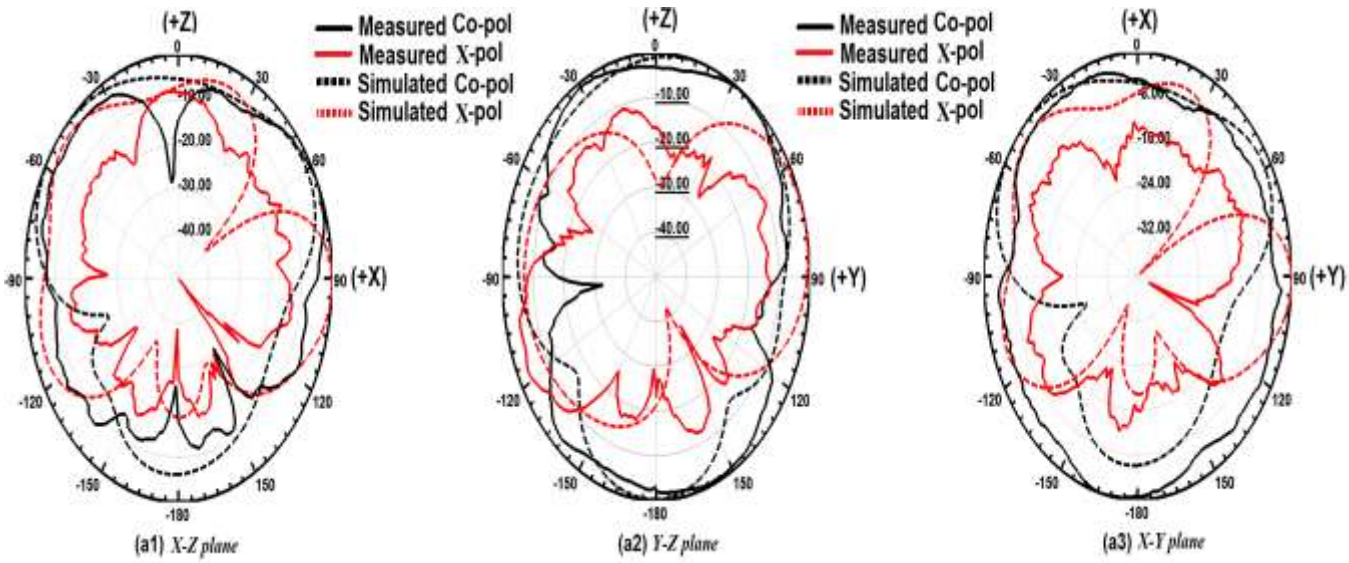

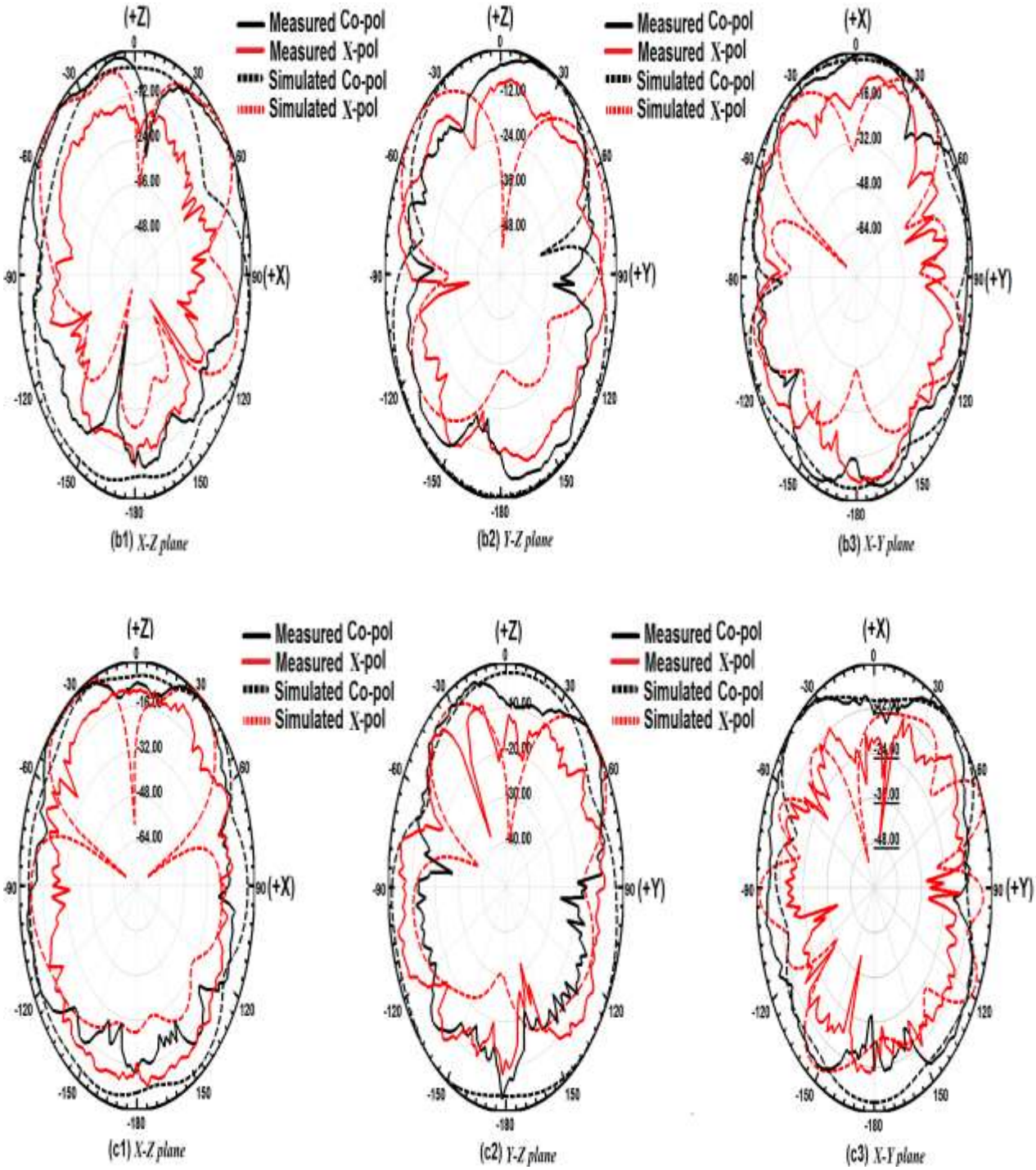

Figure 5.17: Measured versus simulated radiation patterns (normalised) without the proposed wideband decoupling structure: **(a1)** XZ plane, **(a2)** YZ plane, and **(a3)** XY plane at 4 GHz; **(b1)** XZ plane, **(b2)** YZ plane, and **(b3)** XY plane at 6 GHz; and **(c1)** XZ plane, **(c2)** YZ plane, and **(c3)** XY plane at 8 GHz; respectively, with port 1 excited. (Solid line: measured, broken line: simulated, black colour: co-pol, and red colour: cross-pol)

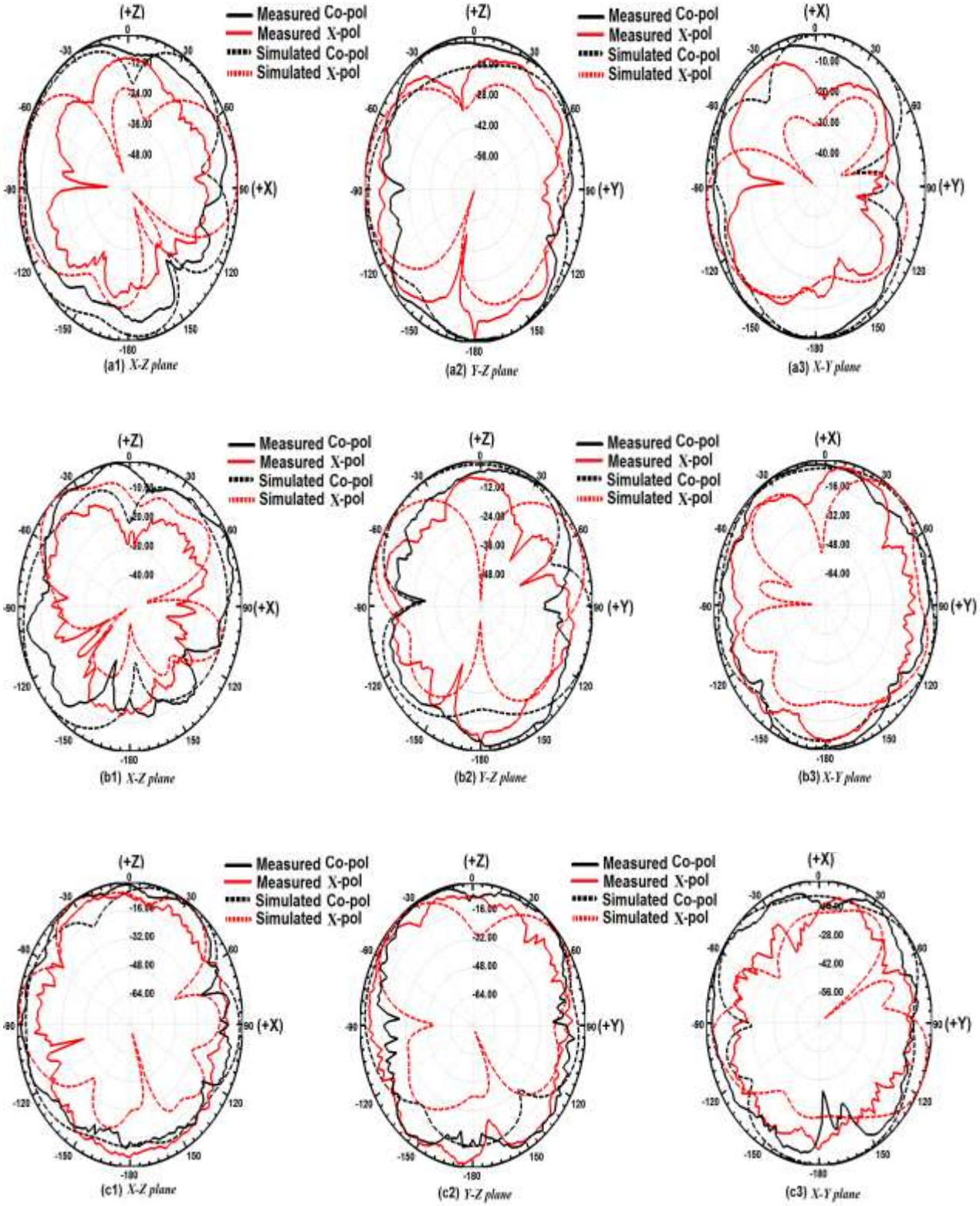

Figure 5.18: Measured versus simulated radiation patterns (normalised) with the proposed wideband decoupling structure: **(a1)** XZ plane, **(a2)** YZ plane, and **(a3)** XY plane at 4 GHz; **(b1)** XZ plane, **(b2)** YZ plane, and **(b3)** XY plane at 6 GHz; and **(c1)** XZ plane, **(c2)** YZ plane, and **(c3)** XY plane at 8 GHz; respectively, with port 1 excited. (Solid line: measured, broken line: simulated, black colour: co-pol, and red colour: cross-pol)

During the measurement, one of the input ports was excited, and the other was terminated with a 50 Ω load. In general; no significant difference is observed between the different co-polarisation and cross polarisation patterns of the measured and the simulated results. The radiation patterns have good omnidirectional in the major planes (i.e. YZ and XY planes). However, some nulls appear after inserting the proposed decoupling structure, especially in the measured cross-polarised. Moreover, there are some slight discrepancies between the measured and simulated results in a different frequency band of interest, which are probably due to the effect of the SMA connectors, cables and implementation imperfections.

5.3.5 Comparison with other Approaches and Published works

Table 5.3 presents a summarised comparison of our proposed UWB-MIMO antennas against other array works previously reported and recently published in the open literature. The UWB-MIMO antennas are tabulated concerning various criteria such as bandwidth, mutual coupling level (S_{21}), antennas geometric size and complexity, and utilisation of the isolation techniques. Therefore the proposed UWB-MIMO antennas presented in this chapter has some outstanding characteristics because of the compact size, geometric simplicity, broad bandwidth, low correlation and good diversity performance. However; the main advantage gained here is simplicity of the design process that make this technique very attractive for designing MIMO-UWB antennas with high isolation characteristics.

Table 5.3: Comparison with previous works of UWB-MIMO antennas designs

Ref. No.	BW GHz	Coupling −dB	Volume mm^3	Space λ_0	Isolation technique	Geometric complexity	Main antenna geometry
[137]	3-6	-21	4650	0.5	EBG structure	Complex	Dual radiating monopoles
[153]	2.8-8	-17	5429	0.4	Separated ground plane	Simple	Dual circular shaped monopoles radiator
[232]	3.1-10.6	-20	1120	0.4	Stub Insertion	Complex	Dual monopole elements
[284]	2.2-10.2	-20	3072	0.5	Stub Insertion	Medium	Dual monopoles elements
[285]	1.8-6.5	-20	29768	0.5	Placement and orientation	Medium	Circular slot antenna with stepped ground
[286]	3-12	-15	5120	0.5	Resonator slot in between	Medium	Dual identical rectangular with a circular slot
[287]	3.1-10.6	-18	1920	0.5	DGS structure	Complex	Printed fractal antenna
[386]	3.1-5	-22	1120	0.5	NL	Complex	Dual circular monopole
This work	3.1-10.6	-31	6992	0.35	Planar decoupling structure	Simple	Dual circular monopole UWB-MIMO antenna

5.4 Chapter Summary

In this chapter, a novel MIMO antenna with high isolation characteristics was designed and developed for UWB application. Many antennas array designs presented in the open literature have reported excellent designs with UWB operation. However, some of these multiple UWB antennas suffer from large size, high profile, not cover a wide isolation BW, utilised of complicated decoupling structures that can affect the fabrication cost. All of the above issues have been tackled in this chapter. Specifically, all the multiple antennas presented in this chapter are small (total antenna dimensions are: $93\times47\times1.6$ mm^3), thin (fabricated on FR_4 substrate) and cover the entire UWB band) which makes them attractive for compact wireless devices. In section 5.3, printed multiple antennas were designed to operate in the UWB range. First, the coupling mechanism was identified as being mainly through the reactive near-field coupling and direct space wave radiation. Then, a coupling reduction was achieved by adding an appropriate decoupling solution. Moreover, simple, but highly efficient, isolation technique was proposed. Design and simulations were conducted using HFSS software version 17.0 and there was a precise performance study involving isolation, radiation patterns, and surface current density distribution. The effectiveness of the proposed wideband decoupling structure has been shown to be useful in achieving compactness, and better isolation of less than -31 dB is obtained through the entire UWB frequency range for an antenna spacing less than 0.35 λ_0 of the lowest frequency. The simulations agree well with the measurements including both the scattering parameters and far-field radiation pattern properties. Moreover, analysis results (theoretically and practically) have shown that the proposed UWB-MIMO antenna guarantees the entire UWB operation with high isolation and almost keeps omnidirectional radiation performance. Finally, the proposed antennas were compared in detail with other previous UWB design works regarding bandwidth, mutual coupling level, geometric size and implementation complexity. All the measured and simulated results indicate that the proposed MIMO antenna array has more advantages than other works in points of criteria, thus being suitable for deployment in some portable devices, such as mobile handsets or laptops using UWB technology combined with MIMO techniques. The major content of this chapter has been a manuscript published as a full-length journal paper in the International Journal of Microwave and Wireless Technologies (JMWT) [R2] and also as a full-length conference paper for IEEE MTT-S International Microwave Workshop Series on Advanced Materials and Processes for RF and THz Applications (2017 IMWS-AMP) [R4]. The introduction and other sections of this chapter have been rewritten to create a better flow and to prevent a repetition of the materials already presented in other chapters.

Chapter 6: Development of Multiple Antenna with High Isolation for Multi-band Applications

6.1 Introduction

In recent years, the interest for multi-band multiple-antennas systems has been growing for multi-standard wireless terminals. Many wireless technologies are consolidated together in a single device that requires being as multi-functionality antennas with multi-service (multi-bands) on a given printed circuit board.

Furthermore, there are many situations where a user will use several wireless devices simultaneously using different services via multi-frequency bands.

Nowadays, to eliminate the need to use separate microstrip antennas for each application, a single multi-band antenna it is possible being used, multi-band antennas can simultaneously operate on multiple frequencies, covering all desirable wireless communication applications [1].

Table 6.1 below shows some most popular different wireless communication bands and their applications that will be interested in the research.

Table 6.1: Frequency bands for different feasible wireless services

Application		Frequency Range
LTE		700 MHz
GSM		890 - 915 MHz & 935 - 960 MHz
DCS		1.71 – 1.88 GHz
PCS		1.85 – 1.99 GHz
UMTS		1.92 - 2.17 GHz
GPS		1575 MHz & 1227 MHz
Wi-Fi -Wireless Local Area Networks	IEEE 802.11 b/g/n IEEE 802.11 a/n	2.40- 2.48 GHz 5.15-5.85 GHz
WiMAX	IEEE 802.16 b/g/n	2.3 - 2.4 GHz & 2.5 – 2.7 GHz & 3.3 – 3.8 GHz
UWB		3.1 – 10.6 GHz

6.2 Multi-band Technology

Recent developments in wireless communication systems have increased the demand for multi-band MIMO antennas that can operate at multiple frequencies with sufficient

bandwidth.

For example, Multi-band PIFAs have been widely used as built-in antennas by most of the mobile handset manufacturers.

Here; more attractive and accessible method to make PIFA can work at multi-band operation i s by etching slots \ slits with different shapes on the radiating planar element. The planar radia tor may contain one or several slots\slits to produce multiple resonant modes. For instance; the popular Nokia PCB phones shown in Figure 6.1 use a multi-band PIFA to operate in the GSM band and Bluetooth band [34, 16].

(a) **(b)**

Figure 6.1: Photograph of multi-band PIFA in **(a)** Nokia 6030 **(b)** Nokia 1110 [34]

Moreover; another popular handset Sony Ericsson T68 shown in Figure 6.2 has used a multi-band PIFA to operate at GSM 900/1800/1900 [42, 54].

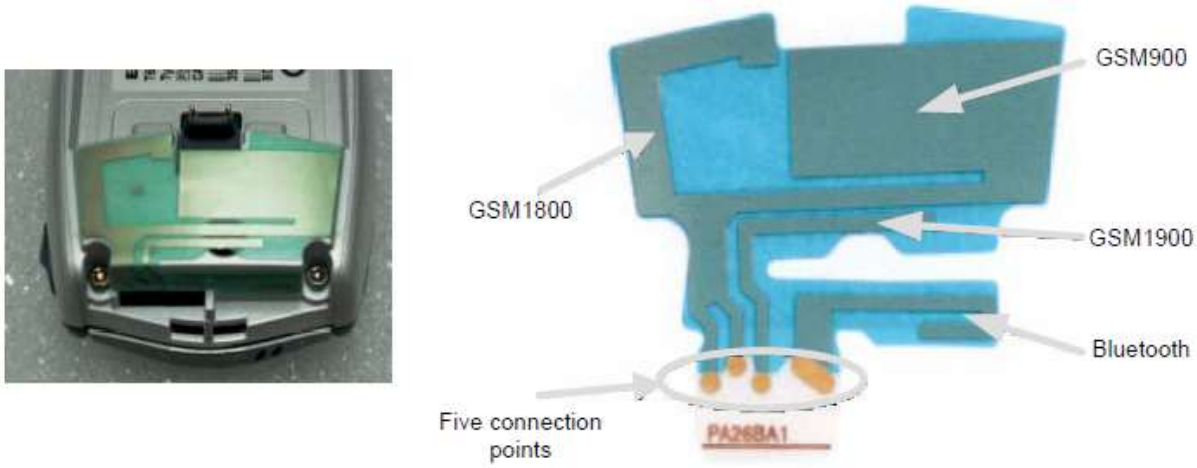

Figure 6.2: Photograph of the multi-band antenna in Sony Ericsson T68 handset [42]

Different methods or techniques have been used in the printed microstrip antennas arrays to achieve multi-band or wideband operation. Some of these methods are pointed here:

1- Modifying the radiators shape: the radiators can take different shapes, as mentioned before in chapter one (Figure 1.3), and hence multi-band can be easily obtained.

2- Slotted radiators: the slot can disturb the current path on the radiators and hence change the performance of the microstrip antennas. Slots technique is employed in the design of many microstrip antennas, and it became the most commonly used technique when a multi-band operation is an aim [6, 8, 7, 55].
3- Using a foam layer between the radiator and the substrate can generate multi-band and wideband performance [1, 2]
4- Shorting walls: If the shorting-wall is properly placed, the area of the resonating element can be substantially shrunk and this allows surface currents to travel longer distance where a wide BW can be obtained, and the antenna size can be minimised. [11].
5- Shorting pins: Inserting shorting pins to microstrip antennas can improve the antenna BW by a few more percentages; it is one of the popular size-reduction techniques for mobile antennas [77].
6- Stacked multi-layers [147], also can be used to generate multi-band operation.
7- Fractals shapes; recently, instead of making slots with different shapes in the planar radiator of the antenna, fractal geometry has been applied to provide multi-band operation, performance enhancement and to meet the other miniaturisation requirements of wireless terminals. As mentioned before; fractals are comprised of elements patterned after self-similar designs to maximise the length, or increase the physical path of the current [246]. The beneficial gives useful applications in mobile terminals and microwave communications. Furthermore, it has been found a little adjustment of the shape can make it work in the demanded resonance frequencies.

In such multi-band antennas arrays, achieving high isolation between the radiating elements is a challenging task, and also it is difficult to control the isolation over the desired multiple bands. So it gives a real challenge to antenna designers to produce efficient MIMO systems with high isolation multi-band characteristics. Although there is an extensive literature (as presented before) on multi-band antennas arrays embedded with different decoupling or isolation techniques for various wireless applications, the following vital issues need to be addressed:

1- Obtaining a significant coupling reduction level and better performances of the operating multi-bands by implementing appropriate decoupling mechanisms, in same time maintaining on acceptable impedance matching characteristics.

2- Low profile (compactness) and planar decoupling structures always desirable to suit modern antenna array designs.
3- The isolation\decoupling method complexity of the antennas array circuits and other fabrication costs to be more reasonable to use in real practical applications (e.g. handsets).

This chapter addresses the above issues with a new applicable multi-band MIMO design. A high isolation antenna array for quad-band applications is presented. The isolation is achieved through a combination of hybrid isolation enhancement mechanisms. The antennas performances and MIMO characteristics are investigated and also verified both numerically and experimentally. The simulation results presented in this chapter were performed using HFSS ver 17.0, as presented in section 6.3.

6.3 Multiple Antennas with High Isolation for Multi-band Applications

6.3.1 Antenna Layout and Design Procedure

Annular ring slot antennas have been of great interest to numerous researchers and antenna engineers in recent decades [1]. Moreover, ring-slot antennas are easy to design; they have a relatively wide bandwidth and can be flexibly tuned by slight changes in their dimensions. In this work, we propose a simple design of a quad-frequency annular ring slot antenna fed by a microstrip line. Furthermore, the quad frequency characteristics of the annular ring slot antenna are also investigated.

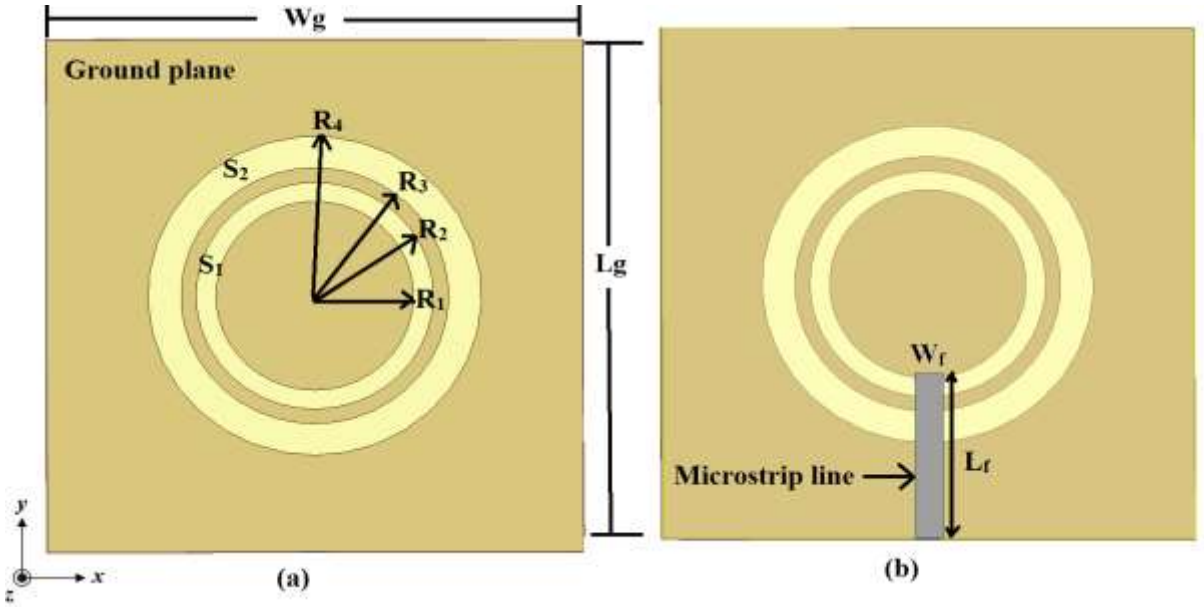

Figure 6.3: Schematic antenna element layout. **(a)** Front view and **(b)** Back view.

Figure 6.3 illustrates the geometry of the initial design of the single antenna element. Several optimisations of the proposed antennas by using Ansoft HFSS software version 17.0 have been performed, and the results present that the number of multi-band, the centre of a frequency of each band and bandwidth can be controlled by the dimensions optimisation of these ring-slots. It should also be noted that the dimensions of the ground plane can affect bandwidths of the four modes [1]. Figure 6.3(a) and (b) shows the schematic diagram of a single antenna element, two annular-ring slots (denoted by S_1 and S_2) with different radii (Figure 6.1(a)) were introduced for quad-bands operation with a copper ground plane printed on the same side of FR_4 substrate. On the other side of the square substrate, a 50 -Ω- microstrip line has adhered below the ground plane (the shaded area in Figure 6.1(b)). The antenna dimensions obtained after optimization are as the following: substrate height (h) = 1.6 mm, ground plane length (L_g) = 65 mm, ground plane width (W_g) = 65 mm, feedline length (L_f) = 21 mm, feed line width (W_f) = 3.4 mm and radius R_1 = 12 mm, R_2 = 14 mm, R_3 = 16 mm and R_4 = 20 mm, space (S) = 40 mm and measured from element centre to centre (approximately equal 0.25 λ_0 of the lowest frequency band.

6.3.2 Multiple Antennas with Hybrid Isolation Mechanisms

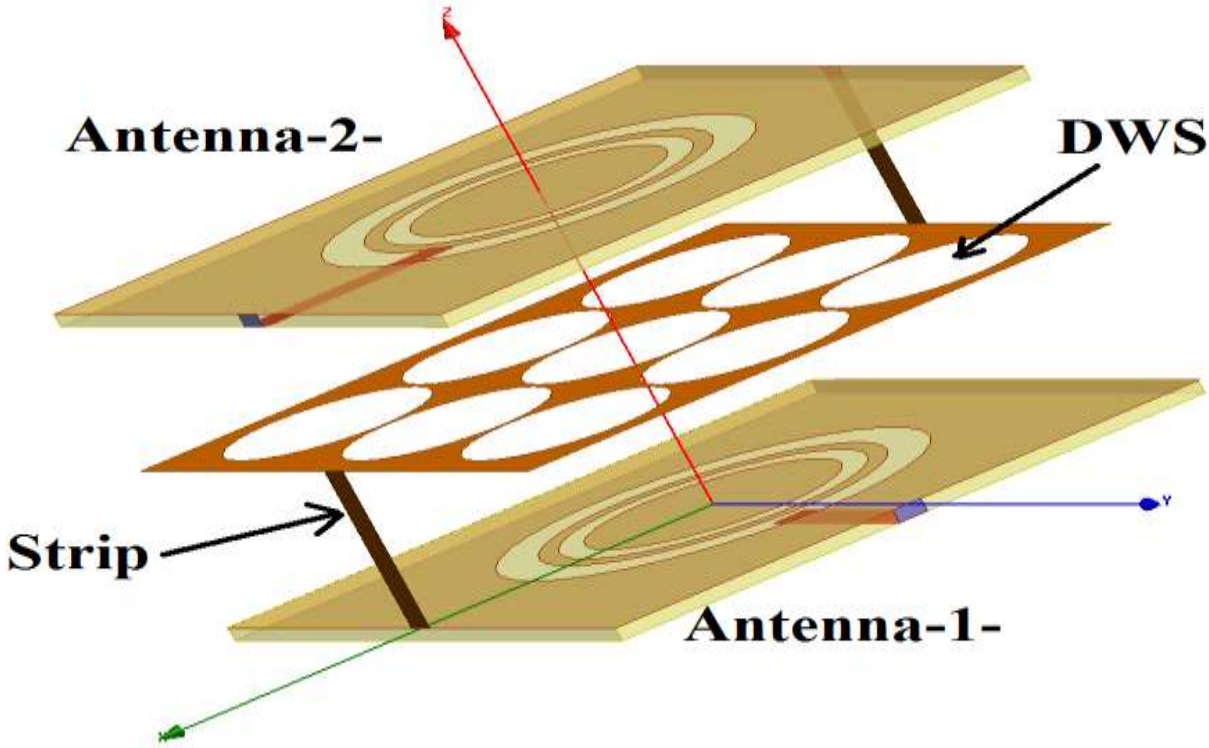

Figure 6.4: 3D Perspective view showing the configuration of the proposed antennas array using hybrid methods: Thin DWS inserted in middle and two strips embedded from sides to reduce the near-field coupling. The antenna orientation of the microstrip line feeds also shown.

In this work; the MIMO antennas (referred to as Antenna-1- and Antenna-2-) is fabricated on an inexpensive FR_4 substrate with a thickness of 1.6 mm and relative permittivity of 4.4.

The identical antennas were designed and separated (back to back) by 40 mm ($\lambda_0/4$ at the lowest frequency, where λ_0 is the free space wavelength). Figure 6.4 shows the proposed multi-band MIMO antennas.

Here; hybrid isolation enhancement mechanisms are combined and efficiently utilised to reduce the mutual coupling between the proposed antennas.

Firstly; antenna orientation is achieved by arranging antenna microstrip line feeds orthogonally locating to each other to improve multi-band isolation.

Then; a very thin wall defected with metallic lattice pattern composes 3×3 circular slots (as shown in Figure 6.4) to form a planner Defected Wall Structure (DWS) in between.

However; the proposed defected wall has been optimised and intended for mutual coupling suppression; it can block the direct space wave propagation from the antenna elements and reflect part of the fields of specific bands.

Finally; isolation enhanced by introducing additional non-radiating shorting strips linking the ground plane of each antenna. This solution has been shown to act like neutralisation lines withdrawing an amount of the signal on one antenna and bringing it back to the other so that the mutual coupling is reduced effectively.

6.3.3 Theoretical Analysis

6.3.3.1 Scattering parameters performances

The return loss (reflection coefficient) and the transmission loss (mutual coupling) for the dual MIMO antennas without and with the proposed decoupling structures are plotted in Figure 6.5(*a*) and Figure 6.5(*b*);

Here; Figure 6.5(a) illustrates the reflection coefficient performance; First; From the simulated return loss parameters; It is observed that the proposed antenna array have a good response for quad resonance to operate in many applications such as DCS mobile communication, Higher GSM band (1.7-1.8 GHz), LTE band (2.55-2.7 GHz), WiMAX band (3.3-3.5 GHz) and intended HiperLAN (4.8-5.2 GHz) with a return loss of -19 dB, -15 dB, -20 dB and -16 dB; respectively.

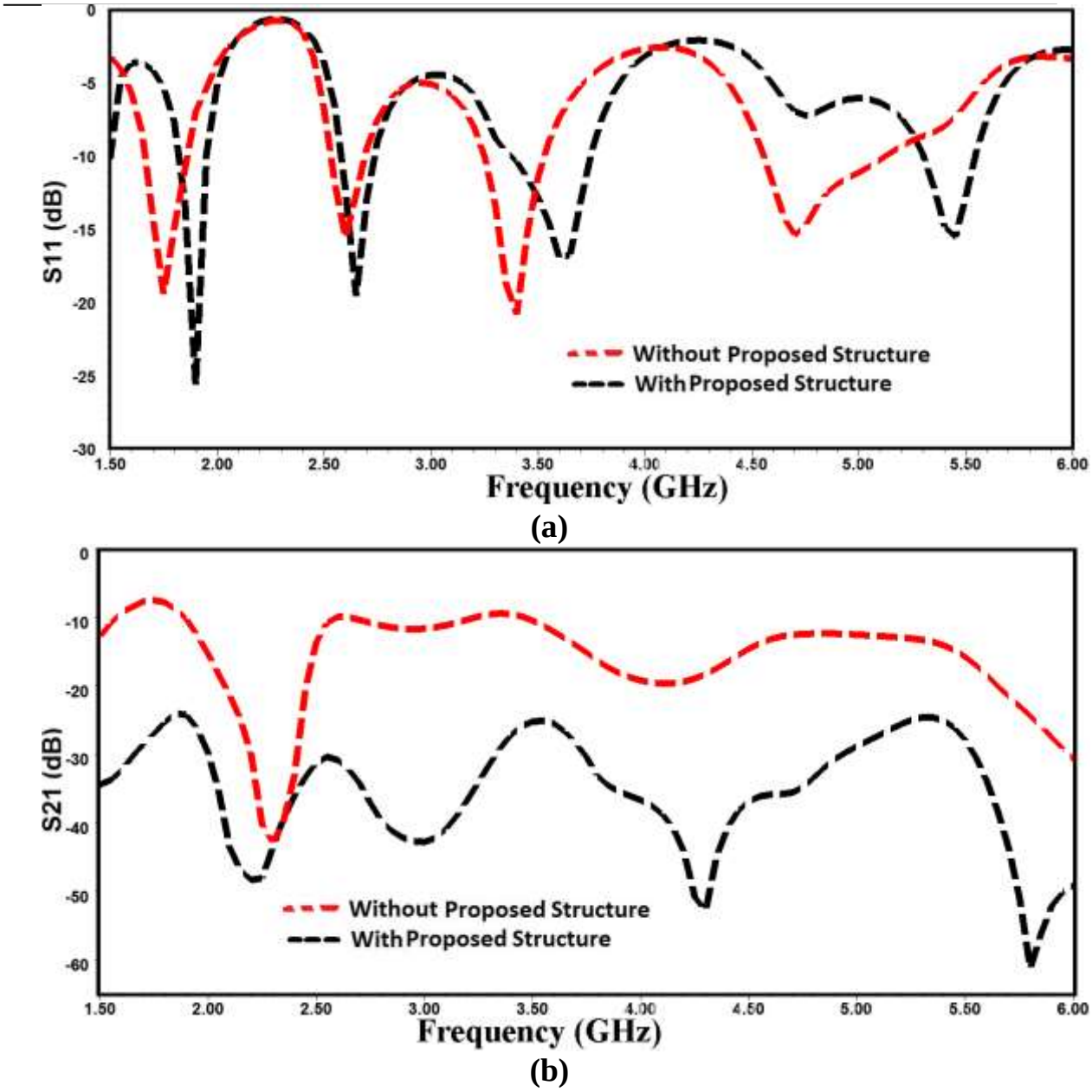

Figure 6.5: The simulated scattering parameters of the proposed multi-band antennas without (dashed line-red colour) and with decoupling structure (dashed line-black colour). **(a)** Reflection coefficient (S_{11}) and **(b)** Transmission coefficient (S_{21})

However; for the proposed case (with hybrid decoupling structures) and due to the lossy nature of these structure, return loss decreased from -19 dB to -25 dB and from -15 dB to -19 dB for the first, second band; respectively but increased from -20 dB to -16 dB for the third band and still maintain -15 dB at fourth band for the proposed case. It is observed an increment shift in each band can be noticeable for the proposed antenna (after inserting the hybrid decoupling proposed structures). Hence, a slight shifting almost occurs at the first and second resonance whereas more shifting towards higher frequencies occurs at the third and fourth resonance.

Meanwhile; it can be seen that the -10 dB |S11| bandwidth is sensitive and slightly affected after the insertion of the proposed hybrid decoupling structures between the MIMO antenna elements. Table 6.2 presents the simulated -10 dB bandwidths and the reflection coefficient parameters of the multi-band (quad-band) antennas before and after insertion of the proposed hybrid decoupling structures

Table 6.2: simulated -10 dB bandwidths of the multi-band antennas in both cases

Parameters	Band I	Band II	Band III	Band IV
BW (GHz) Without Case	0.15 (1.7-1.85 GHz)	0.15 (2.55-2.7 GHz)	0.2 (3.3-3.5 GHz)	0.5 (4.75-5.25 GHz)
BW (GHz) With Case	0.12 (1.83-1.95 GHz)	0.15 (2.57-2.72 GHz)	0.25 (3.4-3.65 GHz)	0.45 (5.1-5.55 GHz)

However; this shifting can be compensated by slightly adjusting the width of the slots to keep the resonance frequency identical in both cases. This shift is caused by the capacitive coupling, and extra inductance may be added that associated with the proposed wall (DWS) and short strips. Secondly; the coupling between the proposed antenna elements can be determined from the transmission coefficients (S_{21} and S_{12} parameters); it is observed a significant reduction in mutual coupling have been achieved when hybrid isolation mechanisms are combined. The simulated mutual coupling recorded in terms of S_{21}, is -7 dB, -9 dB, -10.5 dB and -11 dB at approximately: 1.75 GHz, 2.6 GHz, 3.3 GHz and 5 GHz; respectively compared to -27 dB,-30.5 dB, -31 dB and -28 dB at same mentioned centre frequencies for the proposed array, as shown in Figure 6.5(*b*). However; excellent isolation (S_{21}) of better than -27 dB has been achieved and more than 17 dB improvement over the reference antenna can be obtained in each band.

6.3.3.2 Effectiveness of the hybrid isolation mechanism

In this section; four different scenarios (models) are investigated that given in Figure 6.6 (a-d), to further inspect the performance of the proposed multi-band MIMO antenna and investigate the various decoupling mechanisms to be effectively utilised for isolation enhancement in multi-band MIMO applications.

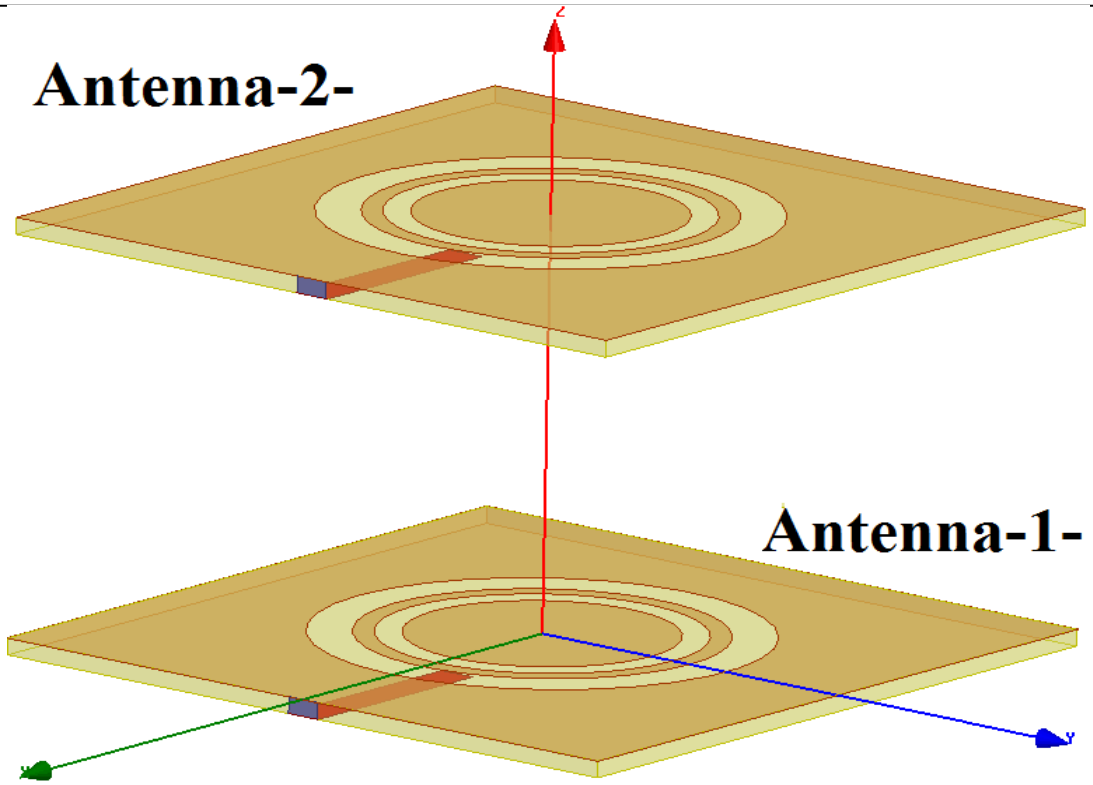

(a)

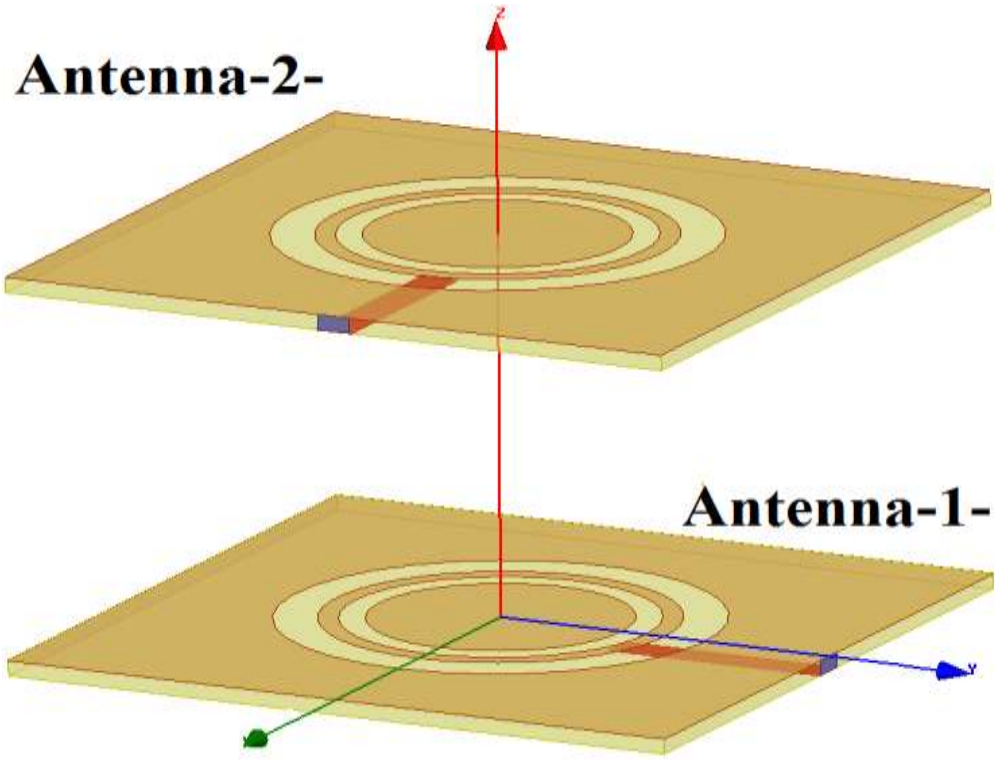

(b)

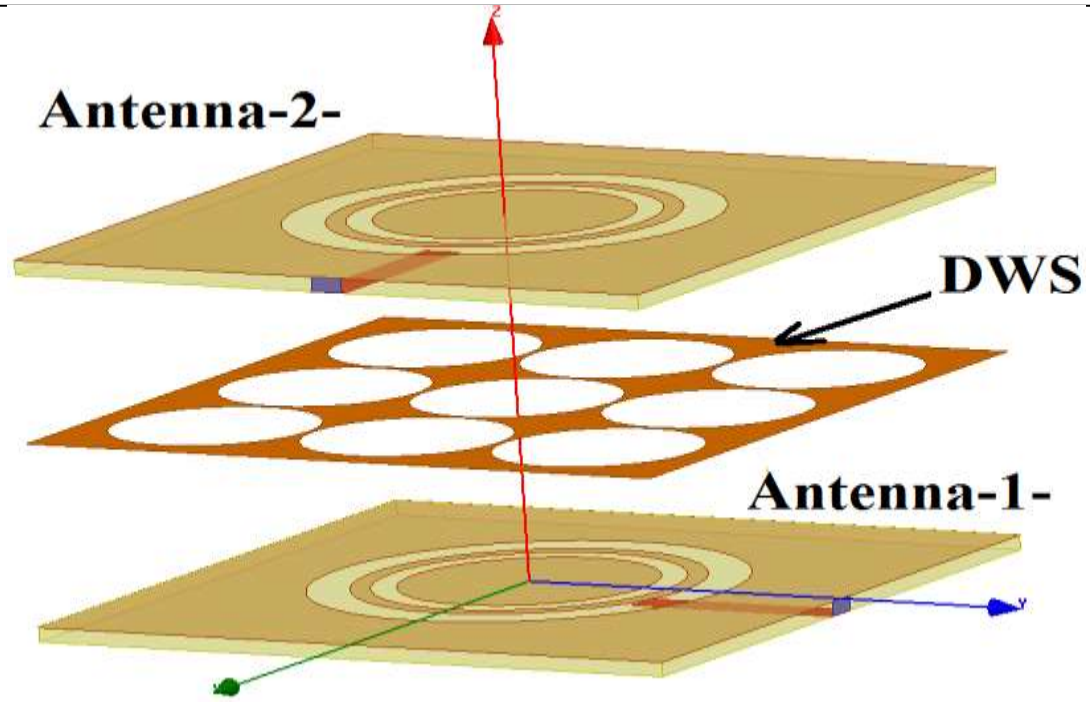

(c)

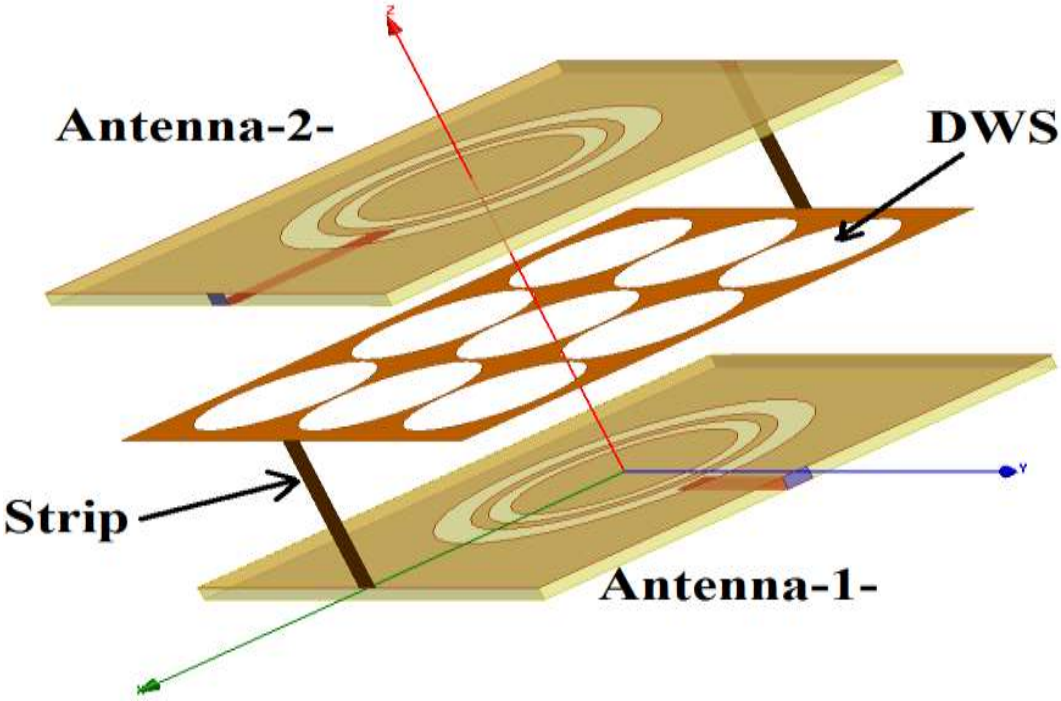

(d)

Figure 6.6: Multi-band MIMO antennas with different scenarios or models: **(a)** Reference antennas (Model I), **(b)** Antenna orientation (Model II), **(c)** Antenna orientation and DWS (Model III), and **(d)** Proposed antennas with hybrid (antenna orientation, DWS and strips) decoupling mechanisms (Model IV).

Here; individual simulated S_{11} and S_{21} parameter variations plot for these mentioned scenarios are presented in Figure 6.7(a) and Figure 6.7(b); respectively:-

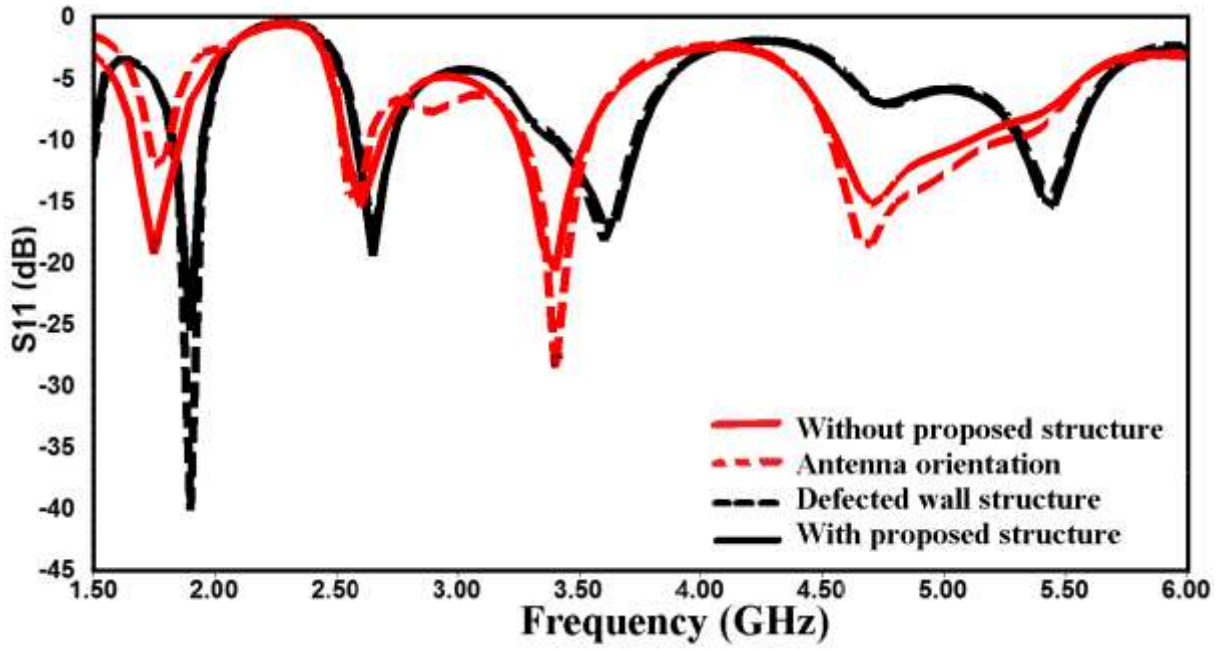

(a)

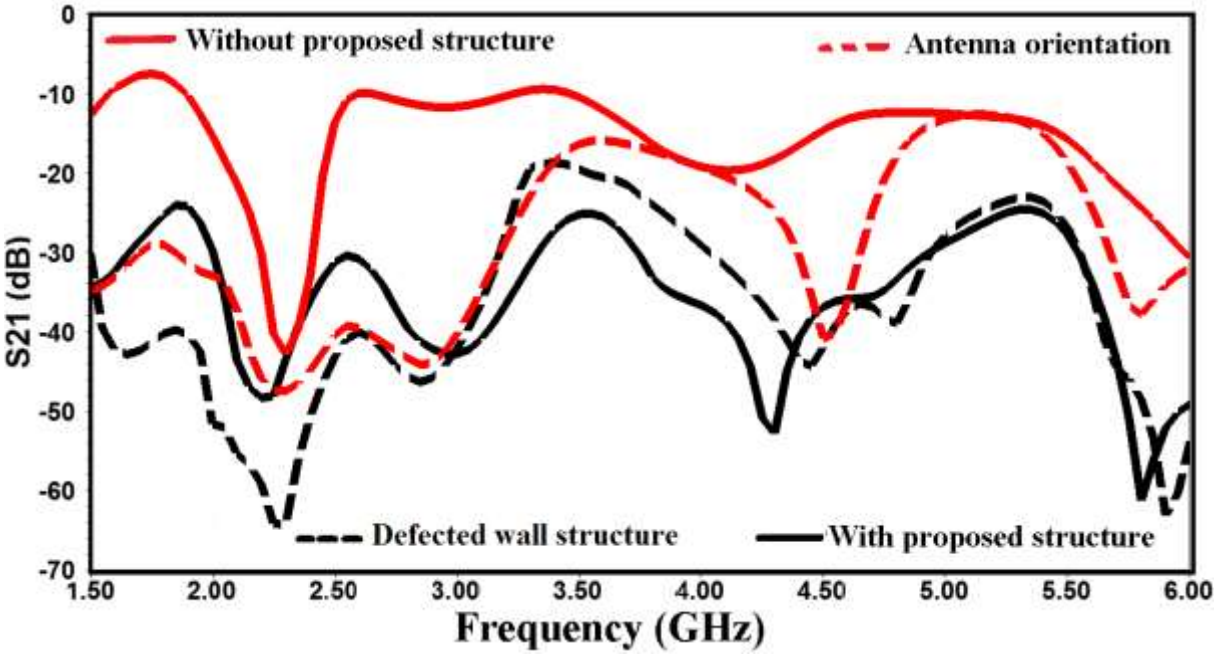

(b)

Figure 6.7: Simulated scattering parameters for different models of multi-band antennas **(a)** Reflection coefficient (S_{11}) and **(b)** Transmission coefficient (S_{21})

However, applying antenna orientation (Model II) as seen in Figure 6.6(*b*), help to improve isolation between the MIMO antennas array but not for the entire multi-band range, only a real enhancement, $S_{21} \leq -28$ dB can be seen in the first lower band frequency (i.e. 1.75 GHz), as presented in Figure 6.7(*b*). Then; a defected wall structure had been inserted (Model III) as seen in Figure 6.6(*c*), here; a better isolation in both lower bands (≤ −39 dB) and higher bands (≤ −24 dB) but still no significant isolation was obtained in middle band (i.e. 3.3 GHz), as shown in Figure 6.7(*b*). Finally; to further increase the isolation between MIMO antennas in all frequencies range of the multi-band operation; a hybrid decoupling mechanisms (including antenna orientation, DWS and strips insertion) have been proposed, it is noticed by introducing this model (Model IV) as shown in Figure 6.6(*d*), an excellent isolation (S_{21}) of better than -27 dB has been achieved, and more than 17 dB improvement over the reference antenna can be obtained in each band, as illustrated in Figure 6.7(*b*). Therefore, the proposed antennas embedded with hybrid decoupling mechanisms can be employed to reduce mutual coupling between the multi-band MIMO antenna elements effectively.

6.3.3.3 Radiation patterns, gain and radiation efficiency

This section presents the study performed on the effect of far-field radiation patterns as a comparison between both cases (without and with inserting decoupling structures). The two orthogonal-plane patterns of the MIMO antennas are demonstrated in Figure 6.8 corresponding to the XZ and YZ principal planes. Overall antenna radiation patterns are relatively stable across the multi-band frequencies. However; no significant degradation of the radiation patterns are noticed for both cases and still nearly omni-directional patterns at various multi-band frequencies.

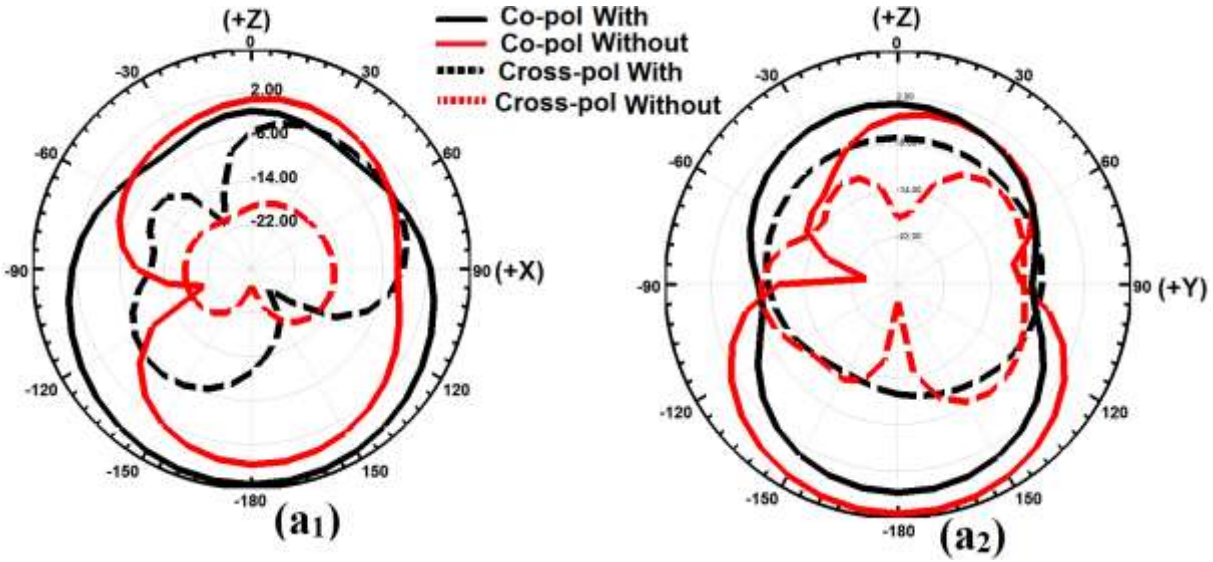

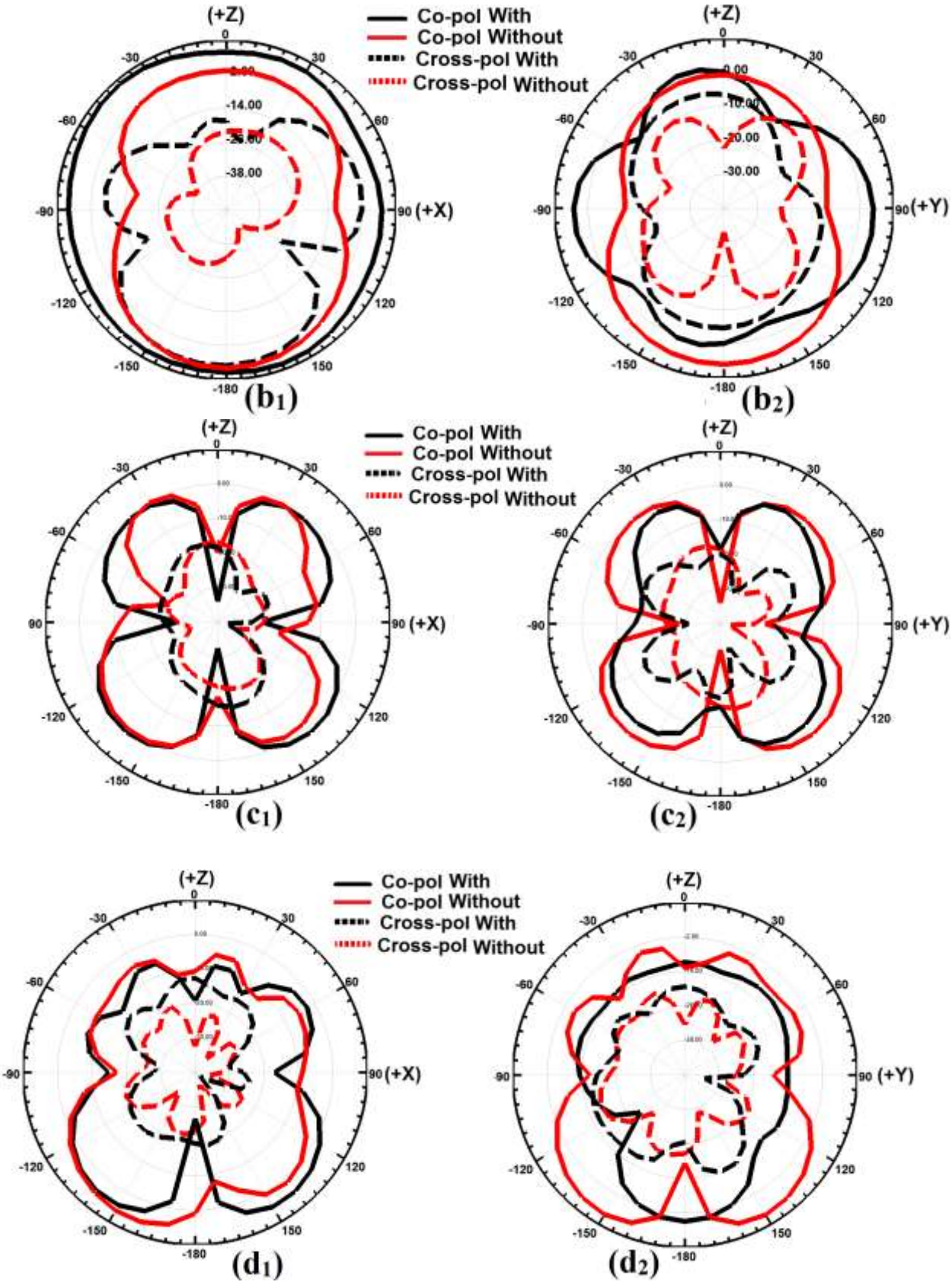

Figure 6.8: The simulated radiation patterns: **(a1)** XZ plane, and **(a2)** YZ plane at 1.75 GHz; **(b1)** XZ plane, and **(b2)** YZ plane at 2.6 GHz; **(c1)** XZ plane, and **(c2)** YZ plane at 3.4 GHz; **(d1)** XZ plane, and **(d2)** YZ plane at 5 GHz; respectively. (Solid line: co-pol, dashed line: cross-pol, black colour: with, and red colour: without)

These plots were obtained with one antenna port excited and other port terminated with matched impedance, i.e. 50 Ω load. Meanwhile, the simulated peak gain and antenna radiation efficiency at multi-band frequencies are plotted in Figure 6.9.

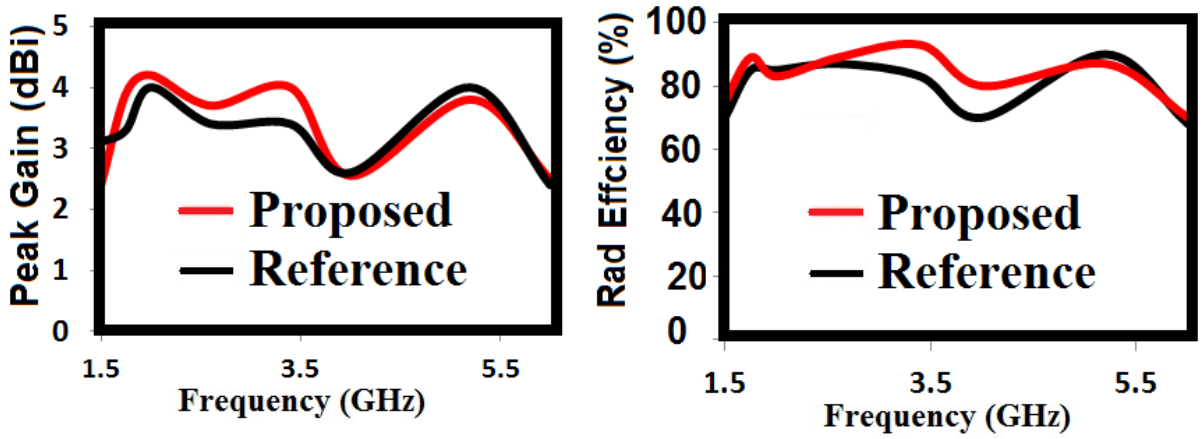

Figure 6.9: Simulated peak gains **(Left)** and radiation efficiencies **(Right)** of the proposed antenna.

The achieved peak gain for the proposed MIMO antennas varies between range 3.4–4.2 dBi, It is also observed that the radiation efficiency of the proposed antennas array is still high (more than 80%) in the entire multi-bands frequencies which certify that the proposed hybrid isolation methods do not have any noticeable effect on radiation characteristics.

6.3.3.4 Simulated surface currents distribution

To further elaborate the effectiveness of these proposed decoupling structures (DWS and shorting strips), the degree of isolation in the proposed antenna can be observed by presenting surface currents distribution.

HFSS ver 17.0 software was used to generate images of the surface current distributions at multi-bands frequencies when the first antenna is excited while the other is terminated with a matched load (50 Ω).

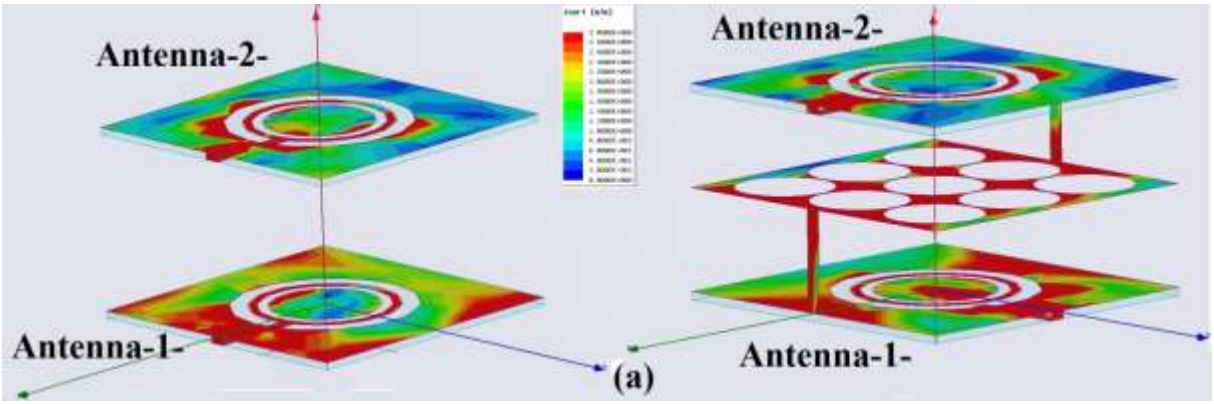

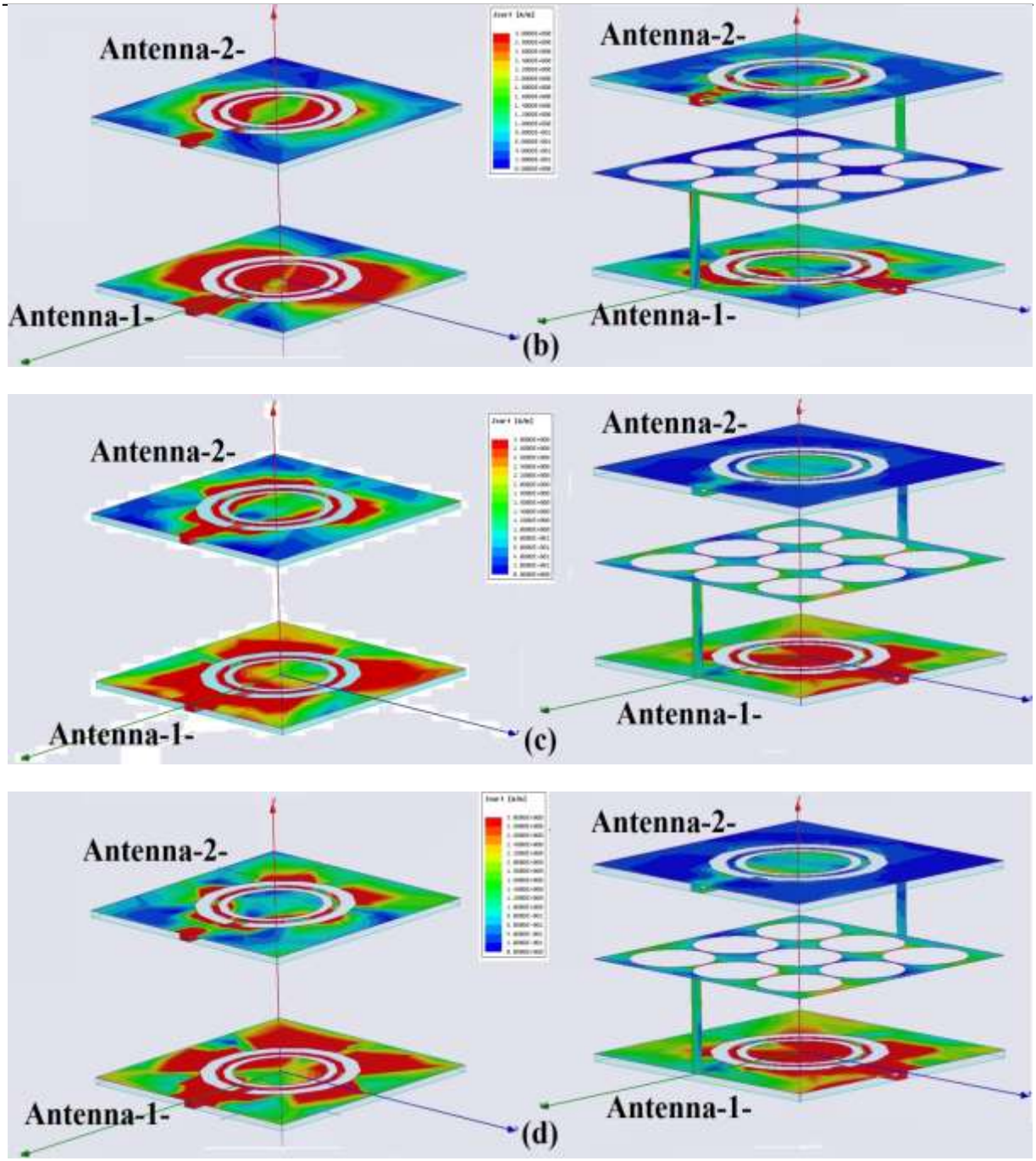

Figure 6.10: Simulation of surface currents distribution on the reference antenna array (left side) and the proposed antenna array (right side), when first antenna is excited and second antenna is terminated with a 50 Ω load. at a frequency: **(a)** 1.75 GHz, **(b)** 2.6 GHz, **(c)** 3.4 GHz, and **(d)** 5 GHz.

Here; Figure 6.10 illustrates the surface current distributions at the four operating frequency bands. It is observed that most of the currents are concentrated on the wall (DWS) and the shorting strips, and thus it ameliorates the ports isolation between antennas. However; these decoupling structures play a significant role in providing the high isolation by preventing induced currents to reach the unexcited antenna.

6.3.3.5 MIMO Characteristics

In general; the correlation between any two antennas within a MIMO system should be kept as low as possible to improve the performance and capacity of these MIMO systems. In this work, ECC (ρ_{12}) can be calculated using S-parameters of the MIMO system as defined before in Eq. (2.13), which assumed an ideal and uniform propagation multipath environment, antenna system is lossless, and one of the antenna elements is excited separately while keeping the other antennas matched terminated. However; from the simulated results, the envelope correlation coefficient of the proposed antenna array is smaller (< -20 dB) compared that shown in the reference case (as presented in Figure 6.11). This observation satisfies the diversity criteria and indicates for better behaviour over the entire multi-band frequencies.

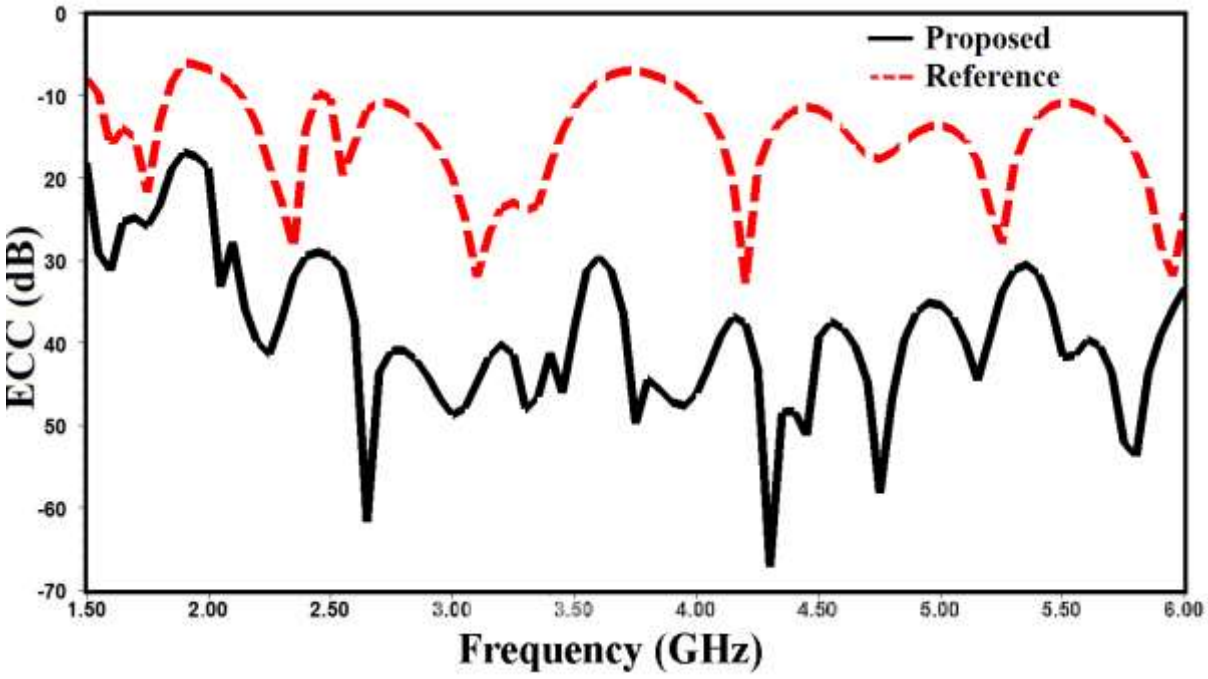

Figure 6.11: Simulated envelope correlation coefficient of the reference antenna (dashed line-red colour) and proposed (solid line-black colour).

6.3.4 Fabrication and Experimental Demonstration

To validate the simulation results, the proposed antenna array had been fabricated, tested, measured and then compared with simulated results. Photograph of the fabricated multi-band antenna element is illustrated in Figure 6.12. The proposed antennas were fabricated via the PCB etching process of an inexpensive FR_4 substrate having a thickness of 1.6 mm, dielectric permittivity constant of 4.4 (with a loss tangent of 0.017).

The microstrip lines were fed through 50 Ω SMA. Finally; the antenna element is made up of copper sheet with a thickness of 0.2 mm.

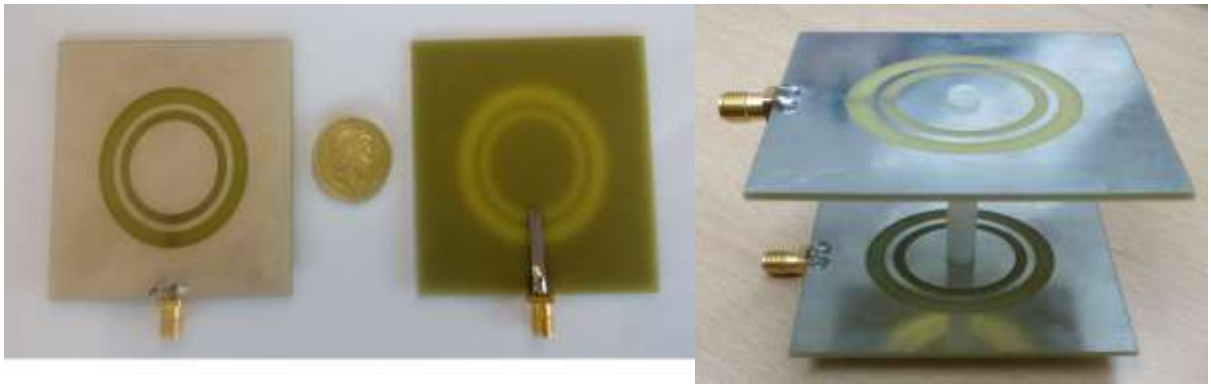

Figure 6.12: A prototype of the antenna. (a) fabricated single element (Top and back view), (b) fabricated MIMO antennas

The performance of the proposed multi-band antennas array has been verified through accurate measurements performed using Agilent Technologies N5230A PNA–L a vector network analyser (as shown in Figure 6.13) inside Brunel University London allowing measurements of the reflection coefficients of microwaves in 300 KHz −20 GHz range.

Figure 6.13: Photograph of the proposed multi-band antennas measured using a network analyser

After calibration with the network analyser, both a return loss and transmission losses have be en measured and recorded accurately.

The measured and simulated scattering parameter plots (return and transmission losses) for both the reference and the proposed antenna are presented in Figure 6.14(a) and (b);

respectively.

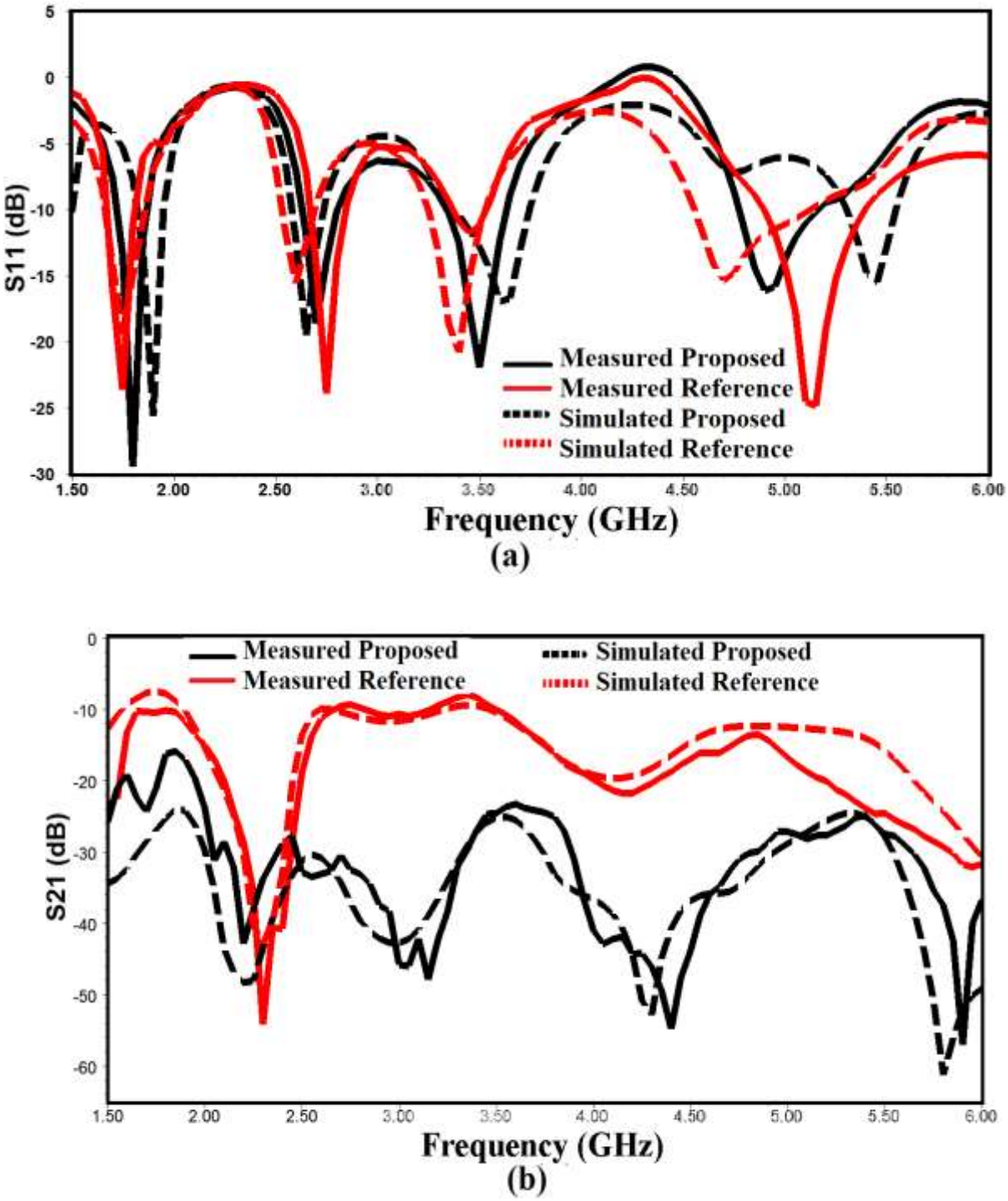

Figure 6.14: Comparison of the simulated and the measured scattering parameters for both reference and proposed antenna array. **(a)** Reflection coefficient (S_{11}) and **(b)** Transmission coefficient (S_{21})

Figure 6.14(*a*) shows the measured and the simulated return loss of impedance bandwidth (S_{11} < -10 dB) comparatively between multi-band antennas array. The mutual coupling measured in terms of S_{21}, is -10 dB, -11 dB, -10.75 dB and -14.5 dB at approximately: 1.75 GHz, 2.6 GHz, 3.3 GHz and 5 GHz; respectively compared to -16 dB, -33 dB, -32 dB and -28 dB at

same mentioned centre frequencies for the proposed array, as shown in Figure 6.14(*b*). Moreover; a reasonably good agreement can be noticed between the measured and the simulated plots although a slight difference between these results can be noticed. That may be attributed to some common factors such as an inaccuracy in the fabrication process, variation in the quality of the substrate, and the mismatch effect of SMA connectors. In all these measurements, one port is excited and the other terminated by the standard 50 Ω load. Finally; from this experimental verification, it can be concluded that the proposed MIMO antennas with hybrid isolation mechanisms can be utilised to reduce the mutual coupling in multi-band applications.

6.3.5 Comparison with Other Approaches and Published works

As mentioned before; other methods have also been applied to reduce mutual coupling between various multi-band antenna arrays such as: Defected or slotted ground plane technique, insertion of EBG structures, spatial and angular variations, and the inclusion of resonators or stubs. In this section; Table 6.3 presents a summarised comparison of our proposed antenna array against other works previously reported and recently published in the open literature; the proposed antennas show excellent isolation maintaining on good compactness with reduced physical separation between antenna arrays.

Table 6.3: Performance comparison for different multi-band antennas designs

Ref. No	No. of Bands	S_{21} (dB)	Dimensions (W×L×H)	Volume mm^3	Space (λ_0)	Design Complexity	Decoupling Technique
[104]	Four	≤-12	60×100×0.8	4800	0.5	Medium	DGS
[165]	Four	≤-15	125×85×0.8	8500	0.097	Complex	Combination
[277]	Four	≤-16	100×60×5.8	34800	0.25	Simple	Separation
[342]	Four	≤-15	100×50×5.8	29000	0.3	Medium	Orientation
[353]	Four	≤-12	100×60×5.8	34800	0.2	Medium	Orientation
[356]	Four	≤-22	118×52×1.6	9817	0.4	Medium	Orientation
[365]	Four	≤-14	60×100×1.6	9600	0.4	Medium	Orientation
Proposed	Four	≤-27	65×65×1.6	6760	0.25	Simple	Hybrid

6.4 Chapter Summary

In this chapter, a new high isolation quad-band slots antenna array has been presented. Many antenna array designs presented in the open literature have reported excellent designs with multi-frequency bands. However, some of these multiple microstrip antennas suffer from large size, high profile, a limited number of bands (almost only dual bands) as well as complicated decoupling structures that can affect the fabrication cost. All of the above issues have been tackled in this chapter. All the multiple antennas presented in this chapter are small (total antenna dimensions of 65×65×1.6 mm^3) and thin (fabricated on FR_4 substrate), which makes them attractive for compact wireless devices. In section 6.3, printed multiple antennas were designed to operate in four-bands. The MIMO antennas can be used to serve most of the mobile and wireless applications, including DCS mobile communication, Higher GSM band (1.7-1.8 GHz), LTE band (2.55 -2.7 GHz), WiMAX band (3.3 - 3.5 GHz), intended HiperLAN (4.8 - 5.2 GHz) and many more. First, the coupling mechanism was identified being mainly through the reactive near-field coupling and direct space wave radiation. Then, a coupling reduction was achieved by adding a hybrid decoupling solution. Moreover, a combination of isolation enhancement mechanisms has been proposed for reducing the mutual coupling effects between the closely packed antenna elements, which is relatively straightforward and uncomplicated in terms of its implementation. Design and simulations were conducted using HFSS software version 17.0, with a precise performance study involving isolation, radiation patterns, and surface current density distribution also being performed. A good isolation of more than 17 dB improvement over the reference antenna has been obtained in each band, for an antenna spacing less than a quarter wavelength of the lowest operating frequency. A prototype of the proposed antenna array has been fabricated, measured and the idea has been verified. A good agreement has been observed between the measured and the simulated results, thus that demonstrating the success of the suggested design topology. Finally, the proposed antennas were favourably compared with other previous works regarding antenna size, isolation level and implementation complexity. All the measured and simulated results indicate that the proposed MIMO antenna array has more advantages than other works in points of criteria and hence, it could prove to be an excellent candidate in multiband antenna applications for some portable devices using MIMO systems. The contents of this chapter form a manuscript published in the European Conference on Antennas and Propagation (EuCAP 2018) [R3]. The introduction and other sections of this chapter have been rewritten to create a better flow and to prevent a repetition of the materials already presented in other chapters.

Chapter 7: Conclusions and Future Work Directions

7.1 Overview of the thesis

Microstrip antennas arrays are extensively used in various wireless applications. The rapid growth and continuous commercial interest in wireless communication systems, especially in mobile communication systems, has significantly increased the demand for compact in size, low cost, high isolation and better diversity performance multiple antennas, which are the critical components used in any such system.

Extensive analysis of the mutual coupling effects in different applications in this thesis has demonstrated that the choice of appropriate coupling reduction approaches is strongly linked to various crucial parameters, including multiple antenna geometry, operating frequency, bandwidth, integration platform, and the device form factor. This shows the importance of the guidelines provided herein to identify the underlying coupling mechanisms and to devise effective coupling reduction approaches for the considered applications. The thesis was aimed at developing multiple compact antennas with high isolation performance that are easy to design and cheap to fabricate. Other objectives, were to investigate the coupling mechanisms and to devise new decoupling methods operating on the various wireless applications that follow simple design guidelines.

A study of various state-of-the-art antennas and their MC represented the initial phase of this research. During the literature review and analysis of the previously published work, some issues regarding the sources of coupling problems were identified. It was pointed out how identification of these coupling mechanisms requires a deep understanding of the way that different antennas radiate EM waves and the interaction between them. Next, the classification of different coupling reduction techniques based on the coupling mechanisms were comprehensively studied, it is more beneficial to suggest appropriate solutions according specific application's requirements. For instance, to suppress the significant substrate coupling (surface waves) between the two antennas focused upon in Chapter 4, an applicable fractal based EBG structure was designed to act as a band-stop filter.

On the other hand, for suppression of antenna coupling through space-wave radiation, depending on the application requirement and restrictions, different isolation techniques, such as insertion of a parasitic decoupling structure (as presented in Chapter 5), or antennas reorientation (as presented in Chapter 6) were effectively adopted.

In specific geometries, a combination of several of the coupling reduction techniques (including hybrid isolation approaches) has been successfully adopted and operationalised in this work for overcoming the issues discussed above and thus, provide the best antenna isolation (as presented in Chapter 6). In this thesis, the proposed designs were implemented and tested using HFSS ver 17.0 software. Moreover, the performance of these designs was compared with that found in recently published works.

Finally, the obtained results were comprehensively analysed and explained. Based on the investigations of various multiple-antenna systems conducted for this Ph.D. research, preliminary guidelines have been put forward for assisting antenna designers when devising strategies for antenna isolation. Specifically, a spacing of a quarter wavelength (0.25 λ_0) was chosen as an empirical separation of different multiple antennas to start this thinking process, which is illustrated graphically in the following flow-chart in Figure 7.1.

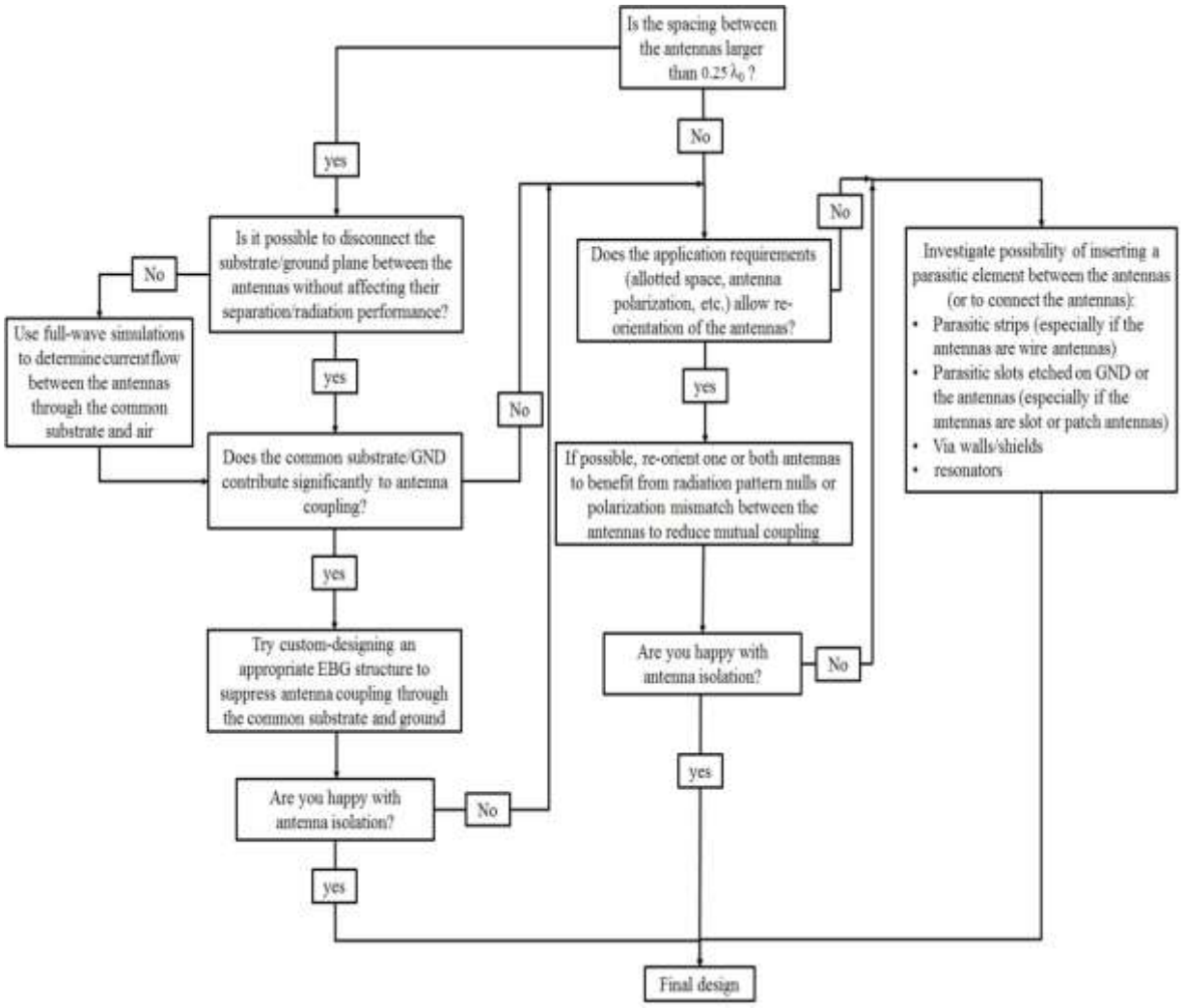

Figure 7.1: Flow-chart showing the design process for isolation enhancement in multiple-antenna systems

7.2 Conclusions

The proposed multiple microstrip antennas in this thesis are all compact, which makes it easy to integrate any of them into mobile handsets or other wireless devices. Different multiple microstrip antennas with new isolation approaches were developed under three categories: narrow-band**,** UWB and multi-band. All the designs reported in this thesis have been fabricated and measured, with the measured results being compared with the simulated ones and these agreed well in most cases.

Multiple antenna elements with high isolation for narrow-band applications

In Chapter 4, in relation to the narrow-band design, a novel planar fractal-based EBG structure was proposed for mutual coupling (MC) reduction between dual microstrip antenna (PIFA) elements. The proposed antenna can operate at approximately 2.65 GHz for a wireless Long Term Evolution (LTE) application with compact design dimensions. A second iterative order FEBG with a bandgap filter characteristic was employed to reduce MC between dual PIFA elements due to its capability of suppressing surface waves propagation in a given frequency range. The FEBG structure without any shorting pins builds on a well-known fractal structure called the Sierpinski carpet, where two iterations have been applied as a uniplanar EBG between dual PIFA elements to increase the isolation performance.

Moreover, the proposed antenna with a Fractal-based EBG structure (FEBG) has been shown to be useful for low-frequency narrow-band MIMO applications. In the narrow-band antenna array design work, fractal structures were utilised for MC reduction between microstrip multiple antennas operating in a MIMO environment. FEBG structures have a unique property of compactness with long current paths and they can work efficiently in a low-frequency range due to space-filling features. Besides this, these fractal structures can provide a band-stop effect, because of their self-similarity features for a particular frequency band, these filtering effects being due to the combination of inductance and capacitance. Fractal geometry is considered to be an appropriate technique when designing multiband and low-profile antennas. These fractal structures can also be utilised for MC reduction between different microstrip antennas operating in a MIMO environment.

Multiple antenna elements with high isolation for UWB applications

In Chapter 5, in regards to the UWB designs, a new monopole MIMO antenna with high isolation and a compact size was designed and developed for UWB application.

The proposed multiple antennas operate over the frequency band from 3.1 to 10.6 GHz for this application. A simple but highly efficient isolation technique was proposed, with this being achieved through a novel planar decoupling structure inserted between dual MIMO antennas. Moreover, a centre slot is etched on the common ground to increase isolation further. The effectiveness of the proposed wideband decoupling structure has been shown to be useful in achieving compactness, and better isolation of less than -31 dB is obtained through the entire UWB frequency range for an antenna spacing less than 0.35 λ_0 of the lowest frequency.

In the approach utilised, by placing and adding a non-resonating and parasitic decoupling structure between multiple antennas, other active coupling paths can be created. Moreover, the coupled radiation introduces induced currents on the neighbouring antenna. The proposed wideband decoupling structure can also capture the near coupling fields and converts them into surface currents to be shorted with a ground plane and such that multiple coupling paths reduce the strong direct coupling between ports, hence reducing the MC. In this work, the dimensions of the proposed decoupling structure were optimised to obtain a maximum surface currents pickup strategy.

Moreover, the analysis results have shown that the proposed UWB-MIMO antenna guarantees an entire UWB bandwidth with high isolation and almost keeps omnidirectional radiation performance. All the results (theoretically and practically) indicate that the proposed antenna array has more advantages than other works in points of the criteria (regarding size, geometric complexity, BW and isolation level). The proposed array has been demonstrated as being suitable for some portable devices, such as mobile handsets or laptops using UWB technology combined with MIMO techniques.

Multiple antenna elements with high isolation for multi-band applications

In Chapter 6, in the context of multi-band design, high isolation quad-band multiple antennas were presented for different applications, including: DCS; higher GSM; LTE2500; WiMAX; and HiperLAN bands.

A combination of isolation enhancement mechanisms was proposed for reducing the MC effects between the closely packed antenna elements, which is relatively straightforward and easy to implement. A good isolation of more than 17 dB improvement over the reference antenna can be obtained in each band, for an antenna spacing of less than 0.25 λ_0 of the lowest frequency.

Hybrid isolation enhancement mechanisms have been combined and efficiently utilised to reduce the MC between the proposed multiple antennas.

Firstly, antenna orientation has been achieved by arranging antenna microstrip line feeds orthogonally located to each other to improve multiband isolation. Then, a very thin wall defected with a metallic lattice pattern was utilised to form a planner Defected Wall Structure (DWS) in between. Moreover, the proposed defected wall was optimised and intended for MC suppression, for it can block the space wave propagation from the antenna elements and reflect part of the fields of specific bands.

Finally, isolation was enhanced by introducing additional non-radiating shorting strips linking the ground plane of each antenna. This solution has been shown to act like neutralisation lines withdrawing a certain amount of the signal on one antenna and bringing it back to the other, so that the MC is reduced.

The proposed antenna has some outstanding characteristics, such as a geometric simplicity, compact size and low correlation, which give the antenna an excellent diversity performance and makes it a good candidate for multiband applications for some portable devices using MIMO systems.

7.3 Future Work Directions

Only some aspects of coupling problems and suppression have been considered in this thesis and hence, this work is by no means complete.

However; this research can be easily extended in a number of ways and proposed future avenues to this end are provided in what follows.

1- The material used in the MIMO antennas proposed in this thesis was an inexpensive FR_4, which is considered as a lossy material. In fact, a substrate material is also imperative for radiation patterns and BW of the antenna.

Hence, the efficiency of the multiple antennas could be further enhanced by using other expensive lossless materials.

2- In this thesis, only dual multiple antennas were proposed in different wireless applications (narrow-band, UWB and multi-band). Similar simulations could be further carried out that extended to (n x m) array (e.g. 3x3 or 4x4 array).

Moreover; experimental implementations of these larger arrays could be used to verify the strength of the simulated values.

3- In relation to chapter 4, the capability of the proposed fractal based EBG structure (Sierpinski carpet) to suppress the surface currents on a common ground plane of multiple PIFAs was demonstrated.

Alternatively, other linear fractal types such as a Koch curve, Hilbert curve or a Cantor set could be utilised. Moreover, other multiple antenna types (e.g. monopolies or slots) could also be used instead of PIFAs to study the performance of this fractal based EBG structure.

4- Mutual coupling reduction with fractal structures remains to be a very topical matter that requires more investigation. For instance, it is possible combine these attractive geometries with already existing decoupling techniques, such as DGS or EBG, that consequently, could lead to more satisfactory high isolation characteristics and better MIMO performance.

5- Nevertheless, reducing MC in MIMO based on fractal geometry still an active topic. Regarding which, no significant contribution has been made in the coupling reduction over a wideband or UWB frequency range using this concept.

6- In this thesis, all of the proposed antennas measurements were carried out inside an anechoic chamber. However, in the future wireless communication systems, multiple antennas might be embedded inside laptops or other wireless devices and hence, their effects on antenna performance need to be investigated.

When multiple antennas are built on portable devices, the impact from a human body or user's effect should also be considered and studied. Meanwhile, the SAR (Specific Absorption Rate) value of these multiple antennas on the user should also be considered.

7- In this thesis, as the dimensions of the proposed MIMO antennas are feasible to be used in handset. However; it could be applicable for use on base station. Hence, more space would be allowed and simpler isolation solutions can be effectively introduced.

8- Performing field measurements campaign for the proposed MIMO antennas, for instance; assess the performance under a real-world environment including specific propagation environments (e.g. indoor or outdoor).

Moreover, other scenarios (e.g. rural or urban environment) could be taken into consideration, thus providing practical multiple antennas with better diversity performance.

9- In relation to chapter 2, the process of the multiple antennas was obtained in the PCS applications (working at 1.9 GHz approximately) and as a result, it is recommended that designers could move on other wireless applications, such as GSM, DCS, LTE, UMTS, WLAN or even UWB frequencies.

In addition, the work could be extended to be cover multi-band or UWB designs. It needs to be borne in mind that this requires repeating the theoretical calculations to elicit the proper antenna dimensions, according to those new bands requirements.

List of References and Bibliography

[1] Constantine A. Balanis, “Antenna theory: analysis and design” Third edition, Hoboken, New Jersey, United States of America: John Wiley & Sons, New York, 2005.

[2] J. L. Volakis, Antenna Engineering Handbook, 4th ed., McGraw-Hill Companies, 2007.

[3] M. C. Liang et al., “The effect of finite ground on a rectangular C-patch antenna,” in IEEE Antennas and Propagation Soc. International. Symposium., Columbus, OH, pp. 732-735, 2003.

[4] F. H. Chu and K. L. Wong, “Folded monopole slot antenna for penta-band clamshell mobile phone application,” IEEE Trans. Antennas and Propagation. Vol. 57, No.11, 2009.

[5] O. T. Meng and T. K. Geok, “A dual-band omnidirectional microstrip antenna,” Progress In Electromagnetics Research, vol. 106, pp. 363–376, 2010.

[6] J. Volakis, "Antenna Engineering Handbook," McGraw Hill, Ch. 13, 2007.

[7] Yi Huang, and Kevin Boyle, "Antennas: From Theory to Practice", John Wiley & Sons, ISBN: 978-0-470-510"' published on 28-5, 2008.

[8] F.R. Terman,” Electronic Radio and Engineering” MacGraw-Hill.

[9] Stutzman, W.L. and Thiele, G.A., Antenna Theory and Design, John Wiley & Sons, Inc,1998.

[10] Retrieved online from PIFA Antenna ttarl.org. ’’http://ttarl.org/attachments/PIFA_Planar_Inverted_F_Antenna.pdf ’’

[11] J. Volakis, "Antenna Engineering Handbook," McGraw Hill, Ch. 36, 2007.

[12] Z. N. Chen and Y. W. Chia, ‘’Broadband Planar Antennas Design and Applications’’, John Wiley & Sons Ltd. 2006.

[13] W. Kwak, S. O. Park, and J. S. Kim, “A folded planar inverted-F antenna for GSM/DCS/Bluetooth triple-band application,” IEEE Antennas Wireless Propagation. Letter., vol. 5, 2006.

[14] S. Tondare and V. Navale, "Meander Line Antenna for LTE Communications,"

[15] R. Garg et al., ‘’Microstrip Antenna Design Handbook’’, Norwood, MA: Artech House, 2001.

[16] Z. Ying and J. Andersson, ‘’Multi band, multi antenna system for modern mobile terminal," in 6th International Symposium on Antennas, Propagation and EM Theory, pp. 287-290, 2003.

[17] Dhande, Pramod. "Antennas and its Applications," DRDO Science Spectrum, pp. 66-78, 2009.

[18] H. Wang, X. B. Huang and D. G. Fang, "A Single Layer Wideband U-Slot Microstrip Patch Antenna Array", IEEE Antennas and Wireless Propagation Letters, vol.7, pp. 9-12, 2008.

[19] G. Augustin, P.Bybi, V.Sarin, P. Mohanan, C. Aanandan and K. Vasudevan, "A Compact Dual-Band Planar Antenna for DCS-1900/PCS/PHS,WCDMA/IMT-2000, and WLAN Applications", IEEE Antennas and Wireless Propagation Letters, vol.7, pp.108-111, 2008.

[20] Retrieved online from ’’http://www.antenna-theory.com’’

[21] R. Vaughan and J. B. Andersen, ‘’Channels, Propagation and Antennas for Mobile Communications’’. Institution of Engineering and Technology, 2003.

[22] H. Wang, D. Fang, Y. Xi, C. Luan, and B. Wang, ‘’On the mutual coupling of the finite microstrip antenna arrays," International Symposium on Electromagnetic Compatibility, pp. 10 -14, 2007.

[23] P. Fletcher, M. Dean, and A. Nix, ‘’Mutual coupling in multi-element array antennas and its influence on MIMO channel capacity," Electronics Letters, vol. 39, pp. 342-344, 2003.

[24] M. Ozdemir, E. Arvas, and H. Arslan, ‘’Dynamics of spatial correlation and

implications on MIMO systems," IEEE Communications Magazine, vol. 42, pp. S14 -S19, 2004.

[25] R. Janaswamy, ‘’Effect of element mutual coupling on the capacity of fixed length linear arrays," IEEE Antennas and Wireless Propagation Letters, vol. 1, no. 1, pp. 157-160, 2002.

[26] H. Morishita, Y. Kim, and K. Fujimoto, ‘‘Design Concept of Antennas for Small Mobile Terminals and the Future Perspectives,’’ IEEE Antenn. Propag. Mag., Vol. 44, No. 5, pp. 30–42, 2002.

[27] F. Yang and Y. Rahmat-Samii, ‘’Microstrip antennas integrated with electromagnetic band-gap (EBG) structures: a low mutual coupling design for array applications," IEEE Transactions on Antennas and Propagation, vol. 51, pp. 2936-2946, 2003.

[28] F. Elek, R. Abhari, and G. V. Eleftheriades, ‘’A uni-directional ring-slot antenna achieved by using and electromagnetic band-gap surface," IEEE Transactions on Antennas and Propagation, vol. 53, pp. 181-190, 2005.

[29] D. Sievenpiper, D. Sievenpiper, Lijun Zhang, R. F. J. Broas, N. G. Alexopolous and E. Yablonovitch, "High-impedance electromagnetic surfaces with a forbidden frequency band," IEEE Trans. Microwave Theory Tech., vol. 47, pp. 2059-2074, 1999.

[30] F. Yang and Y. Rahmat-Samii, "Reflection phase characterizations of the EBG ground plane for low profile wire antenna applications," IEEE Transactions on Antennae and Propagation, vol. 51, pp. 2691-2703, 2003.

[31] M. Schwartz, W. R. Bennett, and S. Stein, Eds., ‘’Communication Systems and Techniques’’. McGARW-HILL, 1966.

[32] S. Mohanna, A. Farahbakhsh, and S. Tavakoli, “Mutual coupling reduction in two-dimensional array of microstrip antennas using concave rectangular patches,” Journal of telecommunications, Vol. 2, No. 2, 2010.

[33] Z. Ying and D. Zhang, “Study of the Mutual Coupling, Correlations and Efficiency of Two PIFA Antennas on a Small Ground Plane”, IEEE Antennas Propagation. Society International Symposium, vol. 3B, 2005.

[34] Z. Ying, ‘’Some important antenna innovations in the mobile terminal industry in the last decade," in Antenna 06 Nordic antenna symposium, Sweden, 2006.

[35] Q. Teruel, O. I. Sanchez, L. R. Iglesias, “Soft surface for reducing mutual coupling between loaded PIFA antennas”, IEEE Antennas Wireless Propag. Lett., vol. 9, 2010.

[36] Y. Hajilou, H. R. Hassani, and B. Rahmati, “Mutual coupling reduction between microstrip patch antennas,” 2012 6th European Conference on Antennas and Propagation (EUCAP), 2012.

[37] Y. Chung, S.-S. Jeon, S. Kim, D. Ahn, J.-I. Choi, and T. Itoh, "Multifunctional microstrip transmission lines integrated with defected ground structure for RF front-end application," IEEE Transactions on Microwave Theory and Techniques, Vol. 52, No. 5, pp. 1425–1432, 2004.

[38] Yang, F. and Y. Rahmat Sami, "The effects of an electromagnetic bandgap (EBG) structure on two element microstrip patch antenna array," IEEE Transactions Antennas and Propagation, Vol. 51, No. 10, pp. 2936–2946, 2003.

[39] Sievenpiper, D. F., "High-impedance electromagnetic surfaces," Ph.D. dissertation, UCLA, 1999.

[40] Zheng, Q.R.; Fu, Y.Q.; Yuan, N.Ch. ''A novel compact spiral electromagnetic band-gap structure'', IEEE Trans. Antennas Propag., Vol. 56, No. 6, pp.1656–1660, 2008.

[41] Gao, Y., Chen, X., Ying, Z. and Parini, C., ''Design and performance investigation of a dual-element PIFA array at 2.5 GHz for MIMO terminal'', IEEE Transactions on Antennas and Propagation, Vol. 55, No.12, pp.3433-3441, 2007.

[42] C.D. Nallo, A. Faraone, M. Maddaleno and T. Galia, "Principles and applications of the folded inverted conformal antenna (FICA) technology," Milan, Italy, 2005.

[43] Karaboikis, M., Soras, C., Tsachtsiris, G. and Makios, V., ''Compact dual-printed inverted-F antenna diversity systems for portable wireless devices'', IEEE Antennas and Wireless Propagation Letters, Vol.3, No.1, pp.9-14, 2004.

[44] V. Voipio, P. P. Vainikainen, and T. A. Toropainen, ''Wideband patch antenna array techniques for mobile communications," 1998.

[45] Sharawi, Mohammad S. "Printed MIMO antenna systems: performance metrics, implementations and challenges." Forum for Electromagnetic Research Methods and Application Technologies (FERMAT). Vol. 1. 2014.

[47] A. Salim, A. Ahmad and R. Fyath. ''MIMO Fractal Antennas '', LAP Lambert Academic Publishing, 2013.

[48] K. Ogawa, J. Takada, "Concept of diversity antenna gain," COST 273, TD Vol. 03,No.142, 2003.

[49] Vaughan, R. G. and J. B. Anderson, ''Antenna diversity in mobile communications," IEEE Trans. Veh. Tech., Vol. 36, No. 4, pp. 149-172, 1987.

[50] H. L. Xiao, S. Ouyang, Z. P. Nie, "Cross polar discrimination of MIMO antenna configurations", Wireless communications, networking and mobile computing (WiCOM), 2008.

[51] R. Glogowski and C.Peixeiro, "Multiple printed antennas for integration into small multistandard handsets," IEEE Antennas Wireless Propag. Lett., vol. 7, 2008.

[52] K. Fujimoto, Mobile Antenna Systems Handbook, 3rd ed., Artech House, Inc. 2008.

[53] G. Tsachtsiris, C. Soras, M. Karaboikis, and V. Makios, "A printed folded Koch monopole antenna for wireless devices," Microw. Opt. Technol. Lett. ,vol. 40, no. 5, 2004.

[54] Z. Yong and J. Andersson, "Multi band, multi antenna system for modern mobile terminal," 6th International Symposium on Antennas, Propagation and EM Theory Proceedings (ISAPE'03), pp. 287-290, Beijing, China, 2003.

[55] J. D. Kraus," The Helical Antennas", Antennas, Chapter 7. McGraw-Hill: New York, 1950.

[56] G. Tsoulos, ‘’MIMO System Technology for Wireless Communications’’, Taylor & Francis Group, LLC, 2006.

[57] H. Li, B. K. Lau, Y. Tan, S. He, and Z. Ying, “Impact of current localization on the performance of compact MIMO antennas,” in Proc. 5th Eur. Conf., Antennas Propag. (EuCAP’2011), Rome, Italy, pp. 11-15, 2011.

[58] D. Gesbert, M. Shafi, D. Shiu, P. J. Smith, and A. Naguib, “From theory to practice: an overview of MIMO space–time coded wireless systems,” IEEE Journal on Selected Areas in Communications, Vol. 21, No. 3, 2003.

[59] Salehi, M., Motevasselian, A., Tavakoli, A. and Heidari, T., ‘’Mutual coupling reduction of microstrip antennas using defected ground structure’’ In Communication systems, ICCS 2006. 10th IEEE Singapore International Conference on pp. 1-5, 2006.

[60] Salehi, M. and Tavakoli, A., ‘’A novel low mutual coupling microstrip antenna array design using defected ground structure’’, AEU-International Journal of Electronics and Communications, Vol. 60, No. 10, pp.718-723, 2006.

[61] Zainud-Deen, S. H., M. F. Badr, E. El-Deen, K. H. Awadalla, and H. A. Sharshar, “Microstrip antenna with defected ground plane structure as a sensor for landmines detection,” Progress In Electromagnetics Research B, Vol. 4, pp. 27–39, 2008.

[62] F. Zhu, J. Xu and Q. Xu, “Reduction of Mutual Coupling Between Closely-Packed Antenna Elements Using Defected Ground Structure,” Electronic Letters, Vol. 45, No.12, pp. 601-602, 2009.

[63] Zhu, Fuguo, et al. “Reduction of Mutual Coupling between Closely-Packed Antenna Elements Using Defected Ground Structure.” 2009 3rd IEEE International Symposium on Microwave, Antenna, Propagation and EMC Technologies for Wireless Communications, 2009.

[64] S. Xiao, M.-C. Tang, Y.-Y. Bai, S. Gao, and B.-Z. Wang, “Mutual coupling suppression in microstrip array using defected ground structure,” IET Microwaves, Antennas & Propagation, Vol. 5, No. 12, p. 1488, 2011.

[65] Arya, A.K., Patnaik, A. and Kartikeyan, M.V., ’’A compact array with low mutual coupling using defected ground structures’’. In Applied Electromagnetics Conference (AEMC), pp. 1-4, 2011.

[66] M. I. Ahmed, A. Sebak, E. A. Abdallah, and H. El-hennawy, “Mutual coupling reduction using defected ground structure (DGS) for array applications,” 15 International Symposium on Antenna Technology and Applied Electromagnetics, 2012.

[67] P. C. nirmal, A. Nandgaonka, and S. Nalbalwar, “Mutual Coupling Reduction between H Shaped Compact MIMO Antenna for WLAN Application,” International Journal of Wireless and Microwave Technologies, Vol. 7, No. 6, pp. 46–57, 2017.

[68] C. V. Antuna, G. Hotopan, S. V. Hoeye, M. F. Garcia, L. F. H. Ontanon, and F. L.-H. Andres,“Defected Ground Structure for Coupling Reduction between Probe Fed Microstrip Antenna Elements,” PIERS Online, Vol. 6, No. 6, pp. 542–546, 2010.

[69] Zulkii, Fitri Yuli, and Eko Tjipto Rahardjo. "Compact MIMO Microstrip Antenna with Defected Dround for Mutual Coupling suppression." PIERS Draft Proc., Marrakesh, Morocco International conference, pp. 20-23, 2011.

[70] Habashi, A., Nourinia, J. and Ghobadi, C., ‘’A rectangular defected ground structure (DGS) for reduction of mutual coupling between closely-spaced microstrip antennas’’, In Electrical Engineering (ICEE), 2012 20th Iranian Conference on pp. 1347-1350, 2012.

[71] A. A. Ibrahim, M. A. Abdalla, A. B. Abdel-Rahman, and H. F. A. Hamed, "Compact MIMO antenna with optimized mutual coupling reduction using DGS," International Journal of Microwave and Wireless Technologies, Vol. 6, No. 02, pp. 173–180, 2013.

[72] Abdalla, M.A. and Mohamed, I.S., ''Mutual coupling reduction in integrated transmit-receive array antennas using high order DGS filter'', In Antennas and Propagation & USNC/URSI National Radio Science Meeting, 2015 IEEE International Symposium on (pp. 432-433), 2015.

[73] Tu, D.T.T., Van Hoc, N., Quan, H. and Van Yem, V., ''Compact MIMO antenna with low mutual coupling using defected ground structure'', In Communications and Electronics (ICCE), 2016 IEEE Sixth International Conference on (pp. 242-247), 2016.

[74] Chung, Y., Jeon, S.S., Ahn, D., Choi, J.I. and Itoh, T., ''High isolation dual-polarized patch antenna using integrated defected ground structure'', IEEE Microwave and Wireless Components Letters, 14(1), pp.4-6, 2004.

[75] K. Wei, J.-Y. Li, L. Wang, and R. Xu, "Microstrip antenna array mutual coupling suppression using coupled polarisation transformer," IET Microwaves, Antennas & Propagation, Vol. 11, No. 13, pp. 1836–1840, 2017.

[76] K. Wei, L. Wang, Z. Xing, R. Xu, and J. Li, "S-shaped periodic defected ground structures to reduce microstrip antenna array mutual coupling," Electronics Letters, Vol. 52, No. 15, pp. 1288–1290, 2016.

[77] David M. Pozar, "Microwave Engineering", Third Edition (Intl. Ed.); John Wiley & Sons, ISBN 0-471-44878-8, pp 170-174, 2005.

[78] L. Gupta and A. D. D. Dwivedi, "Suppression of coupling in a microstrip antenna array by grounded defective strips in Bluetooth devices," Journal of Computational Electronics, Vol. 17, No. 1, pp. 436–441, 2017.

[79] C. G. Kakoyiannis and P. Constantinou, "Compact Printed Arrays with Embedded Coupling Mitigation for Energy-Efficient Wireless Sensor Networking," International Journal of Antennas and Propagation, pp. 1–18, 2010.

[80] Chen, Yong-Zhong. "Novel fractal DGS based on MEMS and its application in miniaturization of microstrip antenna array," Journal of Electronic Science and Technology, Vol. 9 , No. 3, pp. 250-255, 2011.

[81] Wei, Kun, et al. "Mutual coupling reduction by novel fractal defected ground structure bandgap filter", IEEE Transactions on Antennas and Propagation, Vol. 64, No. 10, pp. 4328-4335, 2016.

[82] Wei, Kun, et al. "Defected ground structures for mutual coupling suppression and XP level improvement", Applied Computational Electromagnetics International Society Symposium (ACES), 2017.

[83] C.-M. Luo, J.-S. Hong, and L.-L. Zhong, "Isolation Enhancement of a Very Compact UWB-MIMO Slot Antenna with Two Defected Ground Structures," IEEE Antennas and Wireless Propagation Letters, vol. 14, pp. 1766–1769, 2015.

[84] J. Tao, Q. Feng, and D. Tian, "Compact coplanar waveguide-fed Ultra-wideband MIMO antenna with half slot structure," 2016 Progress in Electromagnetic Research Symposium (PIERS), 2016

[85] Kang, L., Li, H., Wang, X.H. and Shi, X.W., ''Miniaturized band-notched UWB MIMO antenna with high isolation'', Microwave and Optical Technology Letters, Vol. 58, No. 4, pp.878-881, 2016.

[86] Bhattacharya, D. and Joshi, M., ‘’DGS based mutual coupling reduction in an ultra wideb and microstrip patch antenna array’’, In Innovations in Information, Embedded and Communication Systems (ICIIECS), 2017 International Conference on (pp.1-4), 2017.

[87] Giri, A.K., Pahadsingh, S. and Sahu, S., ‘’Compact MIMO antenna system with high isolation for ultra-wideband applications’’, In Wireless Communications, Signal Processing and Networking (WiSPNET), pp. 2496-2498), 2017.

[88] J.-F. Li, Q.-X. Chu, and T.-G. Huang, ‘’A compact wideband mimo antenna with two novel bent slits," IEEE Transactions on Antennas and Propagation, Vol. 60, pp. 482-489, 2012.

[89] Y. Li, W. Li, C. Liu, and T. Jiang, “A printed diversity Cantor set fractal antenna for ultra-wideband communication applications,” ISAPE, 2012.

[90] F. Latif, F. A. Tahir, and M. U. Khan, “Compact UWB-MIMO antenna with band-rejection in WLAN,” 2016 16th Mediterranean Microwave Symposium (MMS), 2016.

[91] K. Trivedi and D. Pujara, “Mutual coupling reduction in wideband tree shaped fractal dielectric resonator antenna array using defected ground structure for MIMO applications,” Microwave and Optical Technology Letters, Vol. 59, No. 11, pp. 2735–2742, 2017.

[92] Chung, Y., S. Jeon, D. Ahn, J. Choi, and T. Itoh, ‘’High isolation dual polarized patch antenna using integrated defected ground structure," IEEE Microw. Component Lett., Vol. 14, pp. 4-6, 2004.

[93] Zulki, F. Y., E. T. Rahardjo, and D. Hartanto, ‘’Radiation properties enhancement of triangular patch microstrip antenna array using hexagonal defected ground structure," Progress In Electromagnetic Research M, Vol. 5, pp. 101-109, 2008.

[94] H. Zhai, Z. Ma, Z. Li and C. Liang, "Reduction of Mutual Coupling Between PIFA Antennas for Dual-Band WiMAX Operations," Microwave Opt Technol Lett, Vol. 55, pp. 2321-2324, 2013.

[95] M. S. Sharawi, A.B. Numan, M. U. Khan and D. N. Aloi, “A Dual-Element Dual-Band MIMO Antenna System With Enhanced Isolation for Mobile Terminals,” IEEE Antennas andWireless Propagation Letters, Vol. 11, pp. 1006-1009, 2012.

[96] Ahmed, F., Feng, Y. and Li, R., ‘’Dual wide-band four-unit MIMO antenna system for 4G/LTE and WLAN mobile phone applications’’, In Antennas and Propagation Conference (LAPC), 2013 Loughborough (pp. 202-207), 2013.

[97] Dhar, S.K. and Sharawi, M.S., ‘’A multi-band isolation enhanced loaded semi-ring MIMO antenna’’, In Microwave Conference (EuMC), 44th European, pp. 386-389, 2014.

[98] Yi, L., Yu, Y., Liu, X., Chen, S., Rizka, N.M. and Gu, Z., ‘’Compact printed dual-band monopole array with high port isolation’’, In Antennas and Propagation (ISAP), 2014 International Symposium, pp. 463-464, 2014.

[99] Zheng, F., Deng, J., Yi, L., Yu, Y. and Chen, S., ‘’Compact dual-band printed monopole array with high port isolation’’, In Microwave Conference (APMC), Asia-Pacific, Vol. 3, pp. 1-3, 2015.

[100] Mahmoud, S., Swelam, W. and El Azeem, M.H.A., ‘’A compact highly isolated two ports microstrip antenna based on Defected Ground Structure for WLAN/WiMAX applications’’. In Progress in Electromagnetic Research Symposium (PIERS), pp. 4380-438, 2016.

[101] Babu, M.S., Rajesh, A., Shankar, T., Nakkeeran, R. and Idayachandran, G., ‘’Design of Dual-Element Tri-Band (DETB) MIMO antenna with improved isolation’’, In Electronics and

Communication Systems (ICECS), 2nd International Conference on, pp. 47-50, 2015.

[102] Zulkifli, F.Y., Rahardjo, E.T. and Hartanto, D., ‘’Mutual coupling reduction using dumbbell defected ground structure for multiband microstrip antenna array’’, Progress In Electromagnetics Research, 13, pp.29-40, 2010.

[103] Abdelwahab, Khaled A., Esmat A. Abdallah, and Mohamed Aboul-Dahab. "Compact Quad-band PIFA Antenna for LTE Handsets with MIMO and Low Mutual Coupling." PIERS Proceedings, 2013.

[104] M. K. Meshram, R. K. Animeh, A. T. Pimpale and N. K. Nikolova, "A novel quad-band diversity antenna for LTE and Wi-Fi applications with high isolation," Antennas and Propagation, IEEE Transactions on, Vol. 60, No. 9, pp. 4360-4371, 2012.

[105] F. Yang and Y. Rahmat-Samii, “Mutual coupling reduction of microstrip antennas using electromagnetic band-gap structure,” IEEE Antennas and Propagation Society International Symposium, 2001

[106] Jibrael, F.J., ‘’Multiband cross dipole antenna based on the triangular and quadratic fractal Koch curve’’, International Journal of Engineering (IJE), Vol. 4, No.3, pp.201, 2007.

[107] Yang, L., Feng, Z., Chen, F. and Fan, M., ‘’A novel compact electromagnetic band-gap (EBG) structure and its application in microstrip antenna arrays’’,In Microwave Symposium Digest, IEEE MTT-S International, Vol. 3, pp. 1635-1638), 2004.

[108] Yang, Li, et al. "A novel compact electromagnetic-bandgap (EBG) structure and its applications for microwave circuits", IEEE Transactions on Microwave Theory and Techniques, Vol. 53, No. 1 , pp.183-190, 2005.

[109] Q.-R. Zheng, Y.-Q. Fu, and N.-C. Yuan, "A Novel Compact Spiral Electromagnetic Band-Gap (EBG) Structure," IEEE Transactions on Antennas and Propagation, vol. 56, pp. 1656-1660, 2008.

[110] B. Bhuvaneswari, K. Malathi, and A. Shrivastav, “Effect of placing mushroom electromagnetic bandgap structures at the inset feedline of microstrip patches,” IET Microwaves, Antennas & Propagation, Vol. 6, No. 13, pp. 1487–1497, 2012.

[111] S. Abushamleh, H. Al-Rizzo, A. A. Kishk, and H. Khaleel, “Miniaturized thin soft surface structure using metallic strips with ledge edges,” IEEE Antennas and Propagation Society International Symposium (APSURSI), 2013.

[112] Z. Liu, Y. Shi, D. Shi, and Y. Gao, “Mutual coupling reduction of a 2.6 GHz Dual-Element MIMO Antenna System with EBG structures,” URSI General Assembly and Scientific Symposium (URSI GASS), 2014.

[113] J. Kumar, S. S. Shirgan, and D. B. Patil, “Miniature wideband 1×2 micro-strip antenna for 4G application,” 2014 IEEE Global Conference on Wireless Computing & Networking (GCWCN), 2014.

[114] Jiang, T., Jiao, T. and Li, Y., ‘’Array mutual coupling reduction using L-loading E-shaped electromagnetic band gap structures’’, International Journal of Antennas and Propagation, 2016.

[115] E. Rajo-Iglesias, Ó. Quevedo-Teruel, and L. Inclan-Sanchez, “Mutual Coupling Reduction in Patch Antenna Arrays by Using a Planar EBG Structure and a Multilayer Dielectric Substrate,” IEEE Transactions on Antennas and Propagation, Vol. 56, No. 6, pp. 1648–1655, 2008.

[116] Y. Su, L. Xing, Z. Z. Cheng, J. Ding, and C. J. Guo, “Mutual coupling reduction in microstrip antennas by using dual layer uniplanar compact EBG (UC-EBG) structure,” 2010

International Conference on Microwave and Millimeter Wave Technology, 2010.

[117] H. S. Farahani, M. Veysi, M. Kamyab, and A. Tadjalli, "Mutual Coupling Reduction in Patch Antenna Arrays Using a UC-EBG Superstrate," IEEE Antennas and Wireless Propagation Letters, Vol. 9, pp. 57–59, 2010.

[118] Mavridou, M., Feresidis, A.P., Gardner, P. and Hall, P.S., ''Tunable Electromagnetic Band Gap slits for mutual coupling reduction''. In European Microwave Conference (EuMC), pp. 207-210), 2013.

[119] S. Ghosh, T.-N. Tran, and T. Le-Ngoc, "Dual-Layer EBG-Based Miniaturized Multi-Element Antenna for MIMO Systems," IEEE Transactions on Antennas and Propagation, Vol. 62, No. 8, pp. 3985–3997, 2014.

[120] Li, Q. and Feresidis, A.P., ''Miniaturised two-layer slit-patch structure for compact decoupling printed antenna array'', In Wireless Symposium (IWS), IEEE International (pp. 1-4), 2014.

[121] Phuong, H.N.B., Van Phi, H., Kiem, N.K., Dinh, D.N., Tuan, T.M. and Chien, D.N., ''Design of compact EBG structure for array antenna application'', In Advanced Technologies for Communications (ATC), 2015 International Conference on (pp. 178-182).

[122] Cho, T.J., Kim, J.K. and Lee, H.M., ''Mutual coupling reduction between two microstrip patch antennas using isolated soft surface structures'', In Antennas and Propagation Society International Symposium, (pp. 1-4), 2009.

[123] Quevedo-Teruel, Ó., Inclan-Sanchez, L. and Rajo-Iglesias, E., ''Soft surfaces for reducing mutual coupling between loaded pifa antennas'', IEEE Antennas and Wireless Propagation Letters, 9, pp.91-94, 2010.

[124] Wang, Haiming, et al. "A high isolation MIMO antenna used a fractal EBG structure" Antennas & Propagation (ISAP), Proceedings of the International Symposium on. Vol. 1. IEEE, 2013.

[125] Abedin, M.F. and Ali, M., 2005, July. ''Reducing the mutual-coupling between the elements of a printed dipole array using planar EBG structures'', In Antennas and Propagation Society International Symposium IEEE (Vol. 2, pp. 598-601).

[126] R. Mäkinen, V. Pynttäri, J. Heikkinen, and M. Kivikoski, "Improvement of antenna isolation in hand-held devices using miniaturized electromagnetic band-gap structures," Microwave and Optical Technology Letters, Vol. 49, No. 10, pp. 2508–2513, 2007.

[127] H. F. Shaban, H. A. Elmikaty, and A. A. Shaalan, "Study The Effects Of Electromagnetic Band-Gap (EBG) Substrate on two Patch Microstrip Antenna," Progress In Electromagnetics Research, Vol. 10, pp. 55–74, 2008.

[128] Z. Z. Abidin, R. A. Abd-Alhameed, N. J. Mcewan, and M. B. Child, "Analysis of the effect of EBG on the mutual coupling for a two-PIFA assembly," 2010 Loughborough Antennas & Propagation Conference, 2010.

[129] S. D. Assimonis, T. V. Yioultsis, and C. S. Antonopoulos, "Design and Optimization of Uniplanar EBG Structures for Low Profile Antenna Applications and Mutual Coupling Reduction," IEEE Transactions on Antennas and Propagation, Vol. 60, No. 10, pp. 4944–4949, 2012.

[130] M. Islam and M. S. Alam, "Design of High Impedance Electromagnetic Surfaces for Mutual Coupling Reduction in Patch Antenna Array," Materials, Vol. 6, No. 1, pp. 143–155, 2013.

[131] Naser-Moghadasi, Mohammad, et al. "Compact EBG structures for reduction of mutual

coupling in patch antenna MIMO arrays", Progress in Electromagnetics Research Vol. 53 , pp.145-154, 2014.

[132] E. Beiranvand, M. Afsahy, and V. Sharbati, “Reduction of the mutual coupling in patch antenna arrays based on EBG by using a planar frequency-selective surface structure,” International Journal of Microwave and Wireless Technologies, Vol. 9, No. 02, pp. 349–355, 2015.

[133] Lee, J.Y., Kim, S.H. and Jang, J.H., ‘’Reduction of mutual coupling in planar multiple antenna by using 1-D EBG and SRR structures’’, IEEE Transactions on Antennas and Propagation, Vol. 63, No. 9, pp.4194-4198, 2015.

[134] B. Mohamadzade and M. Afsahi, “Mutual coupling reduction and gain enhancement in patch array antenna using a planar compact electromagnetic bandgap structure,” IET Microwaves, Antennas & Propagation, Vol. 11, No. 12, pp. 1719–1725, 2017.

[135] Haraz, O.M. and Sebak, A.R., ‘’On the mutual coupling of UWB antenna arrays using EBG layers’’, In Antennas and Propagation Society International Symposium (APSURSI), (pp. 1-2). 2012.

[136] B. Kasi, Y. E. Jalil, and C. K. Chakrabarty, “A low mutual coupling design of UWB array,” 2014 IEEE Asia-Pacific Conference on Applied Electromagnetics (APACE), 2014.

[137] Q. Li, A. P. Feresidis, M. Mavridou, and P. S. Hall, “Miniaturized Double-Layer EBG Structures for Broadband Mutual Coupling Reduction Between UWB Monopoles,” IEEE Transactions on Antennas and Propagation, Vol. 63, No. 3, pp. 1168–1171, 2015.

[138] M. Mavridou, A. P. Feresidis, and P. Gardner, “Tunable Double-Layer EBG Structures and Application to Antenna Isolation,” IEEE Transactions on Antennas and Propagation, Vol. 64, No. 1, pp. 70–79, 2016.

[139] M. S. Alam, M. T. Islam, and N. Misran, “A Novel Compact Split Ring Slotted Electromagnetic Bandgap Structure For Microstrip Patch Antenna Performance Enhancement,” Progress In Electromagnetics Research, Vol. 130, pp. 389–409, 2012.

[140] Yang, L., Fan, M. and Feng, Z., ‘’A spiral electromagnetic bandgap (EBG) structure and its application in microstrip antenna arrays’’, In Microwave Conference Proceedings, 2005. APMC 2005. Asia-Pacific Conference Proceedings (Vol. 3, pp. 4-pp), 2005.

[141] Y. Wang, J. Huang, and Z. Feng, “A novel fractal multi-band ebg structure and its application in multi-antennas,” IEEE Antennas and Propagation International Symposium, 2007.

[142] Soliman, Ahmed M., et al. "Design of planar inverted F antenna over uniplanar EBG structure for laptop mimo applications." Microwave and Optical Technology Letters Vol. 57, No.2, pp.277-285, 2015.

[143] H. Li, J. Xiong, and S. He, “A compact planar MIMO antenna system of four elements with similar radiation Characteristics and isolation structure,” IEEE Antennas Wireless Propagation. Letter. Vol. 8, 2009

[144] A. Neyestanak, F. Jolani, and M. Dadgarpour, ‘’Mutual coupling reduction between two microstrip patch antennas," Canadian Conference on Electrical and Computer Engineering, pp. 739-742, 2008.

[145] Chiu, Chi-Yuk, et al. "Reduction of mutual coupling between closely-packed antenna elements", IEEE Transactions on Antennas and Propagation Vol. 55, No.6, pp. 1732-1738, 2007.

[146] Jolani, F., Dadgarpour, A.M. and Dadashzadeh, G, ‘’Reduction of mutual coupling

between dual-element antennas with new PBG techniques'', In Antenna Technology and Applied Electromagnetics and the Canadian Radio Science Meeting, 2009. ANTEM/URSI 2009. 13th International Symposium on (pp. 1-4), 2009.

[147] J Choma & WK Chen. "Feedback networks: theory and circuit applications". Singapore: World Scientific. ISBN 981-02-2770-1, Chapter 3, p. 225, 2007.

[148] T. Fukusako and Y. Harada, "A Comprehensive Study On Decoupling Between Inverted-F Antennas Using Slitted Ground Plane," Progress In Electromagnetics Research C, Vol. 37, pp. 199–209, 2013.

[149] A. Feresidis and Q. Li, "Miniaturised slits for decoupling PIFA array elements on handheld devices," Electronics Letters, Vol. 48, No. 6, pp. 310-312, 2012.

[150] S. Zuo, Y.-Z. Yin, W.-J. Wu, Z.-Y. Zhang, and J. Ma, "investigations of reduction of mutual coupling between two planar monopoles using two λ/4 slots," Progress In Electromagnetics Research Letters, Vol. 19, pp. 9–18, 2010.

[151] Sonkki, Marko, and Erkki Salonen., "Low Mutual Coupling between Monopole Antennas by Using Two Slots" IEEE Antennas and Wireless Propagation Letters Vol. 9 ,pp.138-141, 2010.

[152] Najam, Ali Imran, Yvan Duroc, and Smail Tedjini. "Design & characterization of antenna system for UWB-MIMO communications systems." Antennas and Propagation (EuCAP), 2010.

[153] M. Jusoh, M. F. Jamlos, M. R. B. Kamarudin, and M. F. B. A. Malek, "A MIMO Antenna Design Challenges For UWB Application," Progress In Electromagnetics Research B, Vol. 36, pp. 357–371, 2012.

[154] L. Liu, H. Zhao, T. S. P. See, and Z. N. Chen, "A printed ultra-wideband diversity antenna," in The 2006 IEEE 2006 International Conference on Ultra-Wideband'', pp. 351-356, 2006.

[155] C. Yong, L. Wen-jun, and C. Chong-hu, "Printed diversity antenna for ultra-wideband applications," in IEEE International Conference on Ultra-Wideband (ICUWB), 2010, pp. 1-4, 2010

[156] Y. Liu and C. Sun, "A compact printed MIMO antenna for UWB application with WLAN band-rejected," 2016 11th International Symposium on Antennas, Propagation and EM Theory (ISAPE), pp. 95-97. 2016.

[157] Singh, P. and Purohit, R.V., ''Compact MIMO Antenna for UWB Applications'', International Journal of Advanced Research in Electronics and Communication Engineering (IJARECE) Vol. 5, No. 11, 2016.

[158] L. Liu, S. W. Cheung, and T. I. Yuk, "Compact multiple-input–multiple-output antenna using quasi-self-complementary antenna structures for ultrawideband applications," IET Microwaves, Antennas & Propagation, Vol. 8, No. 13, pp. 1021–1029, 2014.

[159] Kong, Y., Li, Y. and Yu, W., ''High isolation multi-input multi-output ultra-wideband antenna with a WLAN rejection band'', In Microwave Conference (APMC), 2015 Asia-Pacific, Vol. 2, pp. 1-2, 2015.

[160] Zhang, Y., Wu, X., Li, Y. and Liu, Z., ''A compact printed UWB MIMO antenna with WLAN band rejection'', In Progress in Electromagnetic Research Symposium (PIERS), pp. 2464-2466, 2016.

[161] Ahmed, F., Hasan, N. and Rahman, A.M.A.,'' A compact planar multiple-input multiple-output (MIMO) antenna for ultra-wideband applications'', In Electrical Information and

Communication Technology (EICT), 2017 3rd International Conference on (pp. 1-5), 2017.

[162] P. S. Rao, K. J. Babu, and A. M. Prasad, "Compact Multi-Band Mimo Antenna With Improved Isolation," Progress In Electromagnetics Research M, Vol. 62, pp. 199–210, 2017.

[163] W. Yu, S. Yang, A. Tang, and M.-H. Cho, "A new dual-band diversity antenna used for mobile phone," 2009 IEEE Antennas and Propagation Society International Symposium, 2009.

[164] H. S. Singh, G. K. Pandey, P. K. Bharti, and M. K. Meshram, "Compact penta-band coupled-fed printed monopole MIMO/diversity antenna for smart mobile phone," 2013 International Conference on Microwave and Photonics (ICMAP), 2013.

[165] S. Shoaib, I. Shoaib, N. Shoaib, X. Chen, and C. G. Parini, "Design and Performance Study of a Dual-Element Multiband Printed Monopole Antenna Array for MIMO Terminals," IEEE Antennas and Wireless Propagation Letters, Vol. 13, pp. 329–332, 2014.

[166] C. Arnold and M. El-Shenawee,"Design of multi-band uniplanar MIMO antenna for mobile devices with LTE/WLAN operation," IEEE International Symposium on Antennas and Propagation & USNC/URSI National Radio Science Meeting, 2015.

[167] Sahu, N.K., Das, G. and Gangwar, R.K., ''Dual polarized triple-band dielectric resonator based hybrid MIMO antenna for WLAN/WiMAX applications'', Microwave and Optical Technology Letters, Vol. 60, No.4, pp.1033-1041, 2018.

[168] C. Rowell and E. Y. Lam, "Multiple Frequency Band and High Isolation Mobile Device Antennas Using a Capacitive Slot," IEEE Transactions on Antennas and Propagation, Vol. 60, No. 8, pp. 3576–3582, 2012.

[169] M. M. Morsy and A. M. Morsy, "Dual-band meander-line MIMO antenna with high diversity for LTE/UMTS router," IET Microwaves, Antennas & Propagation, Vol. 12, No. 3, pp. 395–399, 2018.

[170] Chi, G., Li, B. and Qi, D, ''Dual-band printed diversity antenna for 2.4/5.2 GHz WLAN application'', Microwave and optical technology letters, Vol. 45, No. 6, pp.561-563, 2005.

[171] Han, J., Ding, W. and Liu, P., ''November. Two-element diversity printed antenna for 2.4/5GHz dual-band WLAN application'', In Microwave, Antenna, Propagation, and EMC Technologies for Wireless Communications (MAPE), 2011 IEEE 4th International Symposium on (pp. 730-732), 2011.

[172] Park, J.W. and Lee, H.M., ''Isolation improvement of two-port multiple-input-multiple-output antenna using slits and split ring resonators on the ground plane'', In Antenna Technology (iWAT), 2011 International Workshop on (pp. 392-395), 2011.

[173] J. Lee, K. Lee, N. Park and J. Park, "Design of Dual-Band MIMO Antenna with High Isolation for WLAN Mobile Terminal," ETRI J., Vol. 35, pp. 177-187, 2013.

[174] Wu, Y.T., Chu, Q.X. and Yao, S.J., ''A dual-band printed slot diversity antenna for wireless communication terminals'', In Wireless Symposium (IWS), 2013 IEEE International (pp. 1-3), 2013.

[175] Qin, H. and Liu, Y.F., ''Compact dual-band MIMO antenna with high port isolation for WLAN applications'', Progress In Electromagnetics Research, 49, pp.97-104, 2014.

[176] Jiang, W., Yang, L., Wang, B. and Gong, S., ''A high isolation dual-band MIMO antenna for WLAN application'', In Antennas and Propagation (ISAP), 2017 International Symposium on (pp. 1-2), 2017.

[177] Nandi, S. and Mohan, A., ''A Compact Dual-Band MIMO Slot Antenna for WLAN Applications'', IEEE Antennas and Wireless Propagation Letters, 16, pp. 2457-2460, 2017.

[178] X. Zhou, X. Quan, and R. Li, "A Dual-Broadband MIMO Antenna System for GSM/UMTS/LTE and WLAN Handsets," IEEE Antennas and Wireless Propagation Letters, vol. 11, pp. 551–554, 2012.

[179] K.-J. Kim, W.-G. Lim, and J.-W. Yu, "High Isolation Internal Dual-Band Planar Inverted-F Antenna Diversity System with Band-Notched Slots for MIMO Terminals," 2006 European Microwave Conference, 2006.

[180] Kim, K.J. and Ahn, K.H., ''The high isolation dual-band inverted F antenna diversity system with the small N-section resonators on the ground plane'', Microwave and Optical Technology Letters, Vol. 49, No. 3, pp.731-734, 2007.

[181] Cui, S., Liu, Y., Jiang, W. and Gong, S.X., ''Compact dual-band monopole antennas with high port isolation'', Electronics Letters, Vol.47, No.10, pp.579-580, 2011.

[182] Soltani, S., Lotfi, P. and Murch, R.D., ''Design of compact dual-band dual-port WLAN MIMO antennas using slots'', In Antennas and Propagation & USNC/URSI National Radio Science Meeting, 2015 IEEE International Symposium on (pp. 924-925), 2015.

[183] Singh, H.S. and Meshram, M.K., '' Printed Monopole Diversity Antenna for USB Dongle Applications'', Wireless Personal Communications, Vol. 86, No. 2, pp.771-787, 2016.

[184] Abidin, Z. Z., et al. "Four element antenna array working at 2.4/5.2 GHz for wireless USB dongle applications", Electro technical Conference (MELECON), 16th IEEE Mediterranean, 2012.

[185] Li, Y., Luo, Y. and Yang, G., ''Multi-Band 10-Antenna Array for Sub-6 GHz MIMO Applications in 5G Smartphones'', IEEE Access, 2018.

[186] Y. Ding, Z. Du, K. Gong, and Z. Feng, "A four-element antenna system for mobile phones", IEEE Antennas Wireless Propag. Lett., Vol. 6, 2007.

[187] Li, Z., Du, Z. and Gong, K., ''A novel wideband printed diversity antenna for mobile phone application'', In Antennas and Propagation Society International Symposium, AP-S 2008. IEEE (pp. 1-4), 2008.

[188] Chou, H.T., Cheng, H.C., Hsu, H.T. and Kuo, L.R., ''Investigations of isolation improvement techniques for multiple input multiple output (MIMO) WLAN portable terminal applications'', Progress In Electromagnetics Research, 85, pp.349-366, 2008.

[189] C.-C. Hsu, K.-H. Lin, and H.-L. Su, "Implementation of Broadband Isolator Using Metamaterial-Inspired Resonators and a T-Shaped Branch for MIMO Antennas," IEEE Transactions on Antennas and Propagation, Vol. 59, No. 10, pp. 3936–3939, 2011.

[190] Z. Jin, "Small-Size and High-Isolation MIMO Antenna for WLAN," ETRI Journal, Vol. 34, No. 1, pp. 114–117, 2012.

[191] S. Hong, J. Lee, and J. Choi, "Design of UWB Diversity Antenna for PDA Applications," 2008 10th International Conference on Advanced Communication Technology, 2008.

[192] Yahya, R. and Denidni, T.A.," Design of a new dual-polarized ultra-wideband planar CPW fed antenna'', In Antennas and Propagation (APSURSI), 2011 IEEE International Symposium on (pp. 1770-1772), 2011.

[193] M. Gallo, E. Antonino-Daviu, M. Ferrando-Bataller, M. Bozzetti, J. M. Molina-Garcia-Pardo, and L. Juan-Llacer, "A broadband pattern diversity annular slot antenna," IEEE Trans. on Antennas and Propagation, Vol. 60, pp. 1596-1600, 2012.

[194] Liu, Li, S. W. Cheung, and T. I. Yuk. "Compact MIMO antenna for portable devices in UWB applications." IEEE Transactions on Antennas and Propagation Vol. 61, No.8 , pp.4257-

4264, 2013.

[195] B. P. Chacko, G. Augustin, and T. A. Denidni, "Compact uni-planar antenna with polarization diversity for UWB applicaton in portable devices," 2014 IEEE Antennas and Propagation Society International Symposium (APSURSI), 2014.

[196] R.-J. Xiao, X.-B. Wei, and L. Jin, "A band-notched UWB MIMO antenna with high notch-band-edge selectivity," 2015 Asia-Pacific Microwave Conference (APMC), Vol. 1, pp. 1-3, 2015.

[197] S. Tripathi, A. Mohan, and S. Yadav, "A Compact Koch Fractal UWB MIMO Antenna With WLAN Band-Rejection," IEEE Antennas and Wireless Propagation Letters, vol. 14, pp. 1565–1568, 2015.

[198] S. Kareemulla and V. Kumar, "A novel compact MIMO antenna for ultra-wideband applications," 2015 IEEE International Conference on Signal Processing, Informatics, Communication and Energy Systems (SPICES), 2015.

[199] Y. Wu and Y. Long, "A design of compact 2-port UWB MIMO antenna," 2015 IEEE 4th Asia-Pacific Conference on Antennas and Propagation (APCAP), 2015

[200] Syedakbar, S., Ramesh, S. and Deepa, J.," Ultra-wide band monopole planar MIMO antenna for portable devices",In Electrical, Instrumentation and Communication Engineering (ICEICE), 2017 IEEE International Conference on (pp. 1-4), 2017.

[201] Khan, M.S., Capobianco, A.D., Asif, S.M., Anagnostou, D.E., Shubair, R.M. and Braaten, B.D., " A compact CSRR-enabled UWB diversity Antenna", IEEE Antennas and Wireless Propagation Letters, Vol. 16, pp.808-812, 2017.

[202] Lamsoge, A. and Khade, S.S., " Compact MIMO antenna for UWB application", In Futuristic Trends in Research and Innovation for Social Welfare (Startup Conclave), World Conference on (pp. 1-4), 2016.

[203] Antonino-Daviu, E., Gallo, M., Bernardo-Clemente, B. and Ferrando-Bataller, M., 2010, ''Ultra-wideband slot ring antenna for diversity applications'', Electronics letters, Vol. 46, No.7, pp.478-480.

[204] Li, Y., xing Li, W., Liu, C. and Jiang, T.," Two UWB-MIMO antennas with high isolation using sleeve coupled stepped impedance resonators" In Antennas and Propagation (APCAP), 2012 IEEE Asia-Pacific Conference on (pp. 21-22), 2012.

[205] C.-X. Mao and Q.-X. Chu, "Compact Coradiator UWB-MIMO Antenna with Dual Polarization," IEEE Transactions on Antennas and Propagation, Vol. 62, No. 9, pp. 4474–4480, 2014.

[206] Patre, S.R. and Singh, S.P., ''MIMO antenna using castor leaf-shaped quasi-self-complemetary elements for broadband applications'', In International Microwave and RF Conference (IMaRC), 2015 IEEE MTT-S (pp. 140-142), 2015.

[207] Patre, S.R. and Singh, S.P., ''Broadband multiple-input–multiple-output antenna using castor leaf-shaped quasi-self-complementary elements'', IET Microwaves, Antennas & Propagation, Vol. 10, No. 15, pp.1673-1681, 2016.

[208] Zhu, J., Li, S., Feng, B., Deng, L. and Yin, S., ''Compact dual-polarized UWB quasi-self-complementary MIMO/diversity antenna with band-rejection capability'', IEEE Antennas and Wireless Propagation Letters, Vol. 15, pp.905-908, 2016.

[209] Zhou, F., Qian, Z., Liu, T., Han, J. and Peng, C., ''Design of diversity antenna for ultra-wideband applications'', In Ultra-Wideband (ICUWB), 2010 IEEE International Conference on Vol. 1, pp. 1-4, 2010.

[210] Chacko, B.P., Augustin, G. and Denidni, T.A., ‘’Uniplanar polarisation diversity antenna for ultra-wideband systems’’, IET Microwaves, Antennas & Propagation, Vol. 7, No. 10, pp.851-857, 2013.

[211] Zhao, Hui, et al. ‘’A compact UWB diversity antenna’’, International Journal of Antennas and Propagation, 2014.

[212] Gao, Peng, et al. "Compact printed UWB diversity slot antenna with 5.5-GHz band-notched characteristics", IEEE Antennas and Wireless Propagation Letters , Vol.13, pp. 376-379, 2014.

[213] Kharche, Shilpa, et al. "Mutual coupling reduction using variable length SRR like structure in ultra-wideband MIMO antennas." International Microwave and RF Conference (IMaRC), 2015 IEEE MTT-S , 2015.

[214] Gao, Y., Chiau, C.C., Chen, X. and Parini, C.G., ‘’A compact dual-element PIFA array for MIMO terminals’’, In Loughborough Antennas Propagation conference, 2005.

[215] M. Nikolic, A. Djordjevic, and A. Nehorai, ‘’Microstrip antennas with sup- pressed radiation in horizontal directions and reduced coupling," Antennas and Propagation, IEEE Transactions on, Vol. 53, pp. 3469-3476, 2005.

[216] Dhanvijay, M., Pattekar, A. and Gupta, R.K., ‘’Compact circular ring shaped monopole UWB MIMO antenna’’, In Sensing, Signal Processing and Security (ICSSS), 2017 Third International Conference on (pp. 104-107), 2017.

[217] Wong, Kin Lu, Saou Wen Su, and Yen Liang Kuo. "A printed ultra wideband diversity monopole antenna" , Microwave and optical technology letters Vol. 38, No.4, pp.257-259, 2003.

[218] Cheng, Y., Lu, W.J., Cheng, C.H., Cao, W. and Li, Y., ‘’Compact diversity antenna with T shape stub for ultra-wideband applications’’, In Microwave Conference, 2008, APMC 2008. Asia-Pacific (pp. 1-4), 2008.

[219] M. S. Khan, M. F. Shafique, A. D. Capobianco, E. Autizi, and I. Shoaib, “Compact UWB-MIMO antenna array with a novel decoupling structure,” Proceedings of 10th International Bhurban Conference on Applied Sciences & Technology (IBCAST), 2013.

[220] S. Kharche, G. S. Reddy, B. Mukherjee, R. Gupta, and J. Mukherjee, “Mimo Antenna For Bluetooth, Wi-Fi, Wi-Max and UWB Applications,” Progress In Electromagnetics Research C, Vol. 52, pp. 53–62, 2014.

[221] Tang, T.C. and Lin, K.H., ‘’an ultrawideband MIMO antenna with dual band-notched function’’, IEEE Antennas and wireless propagation letters, Vol. 13, pp.1076-1079, 2014.

[222] Huang, H.F. and Xiao, S.G., ‘’Compact triple band-notched UWB MIMO antenna with simple stepped stub to enhance wideband isolation’’, Progress in Electromagnetics Research, Vol. 56, pp.59-65, 2015.

[223] Chandel, R., Gautam, A.K. and Rambabu, K.,’ Design and Packaging of an Eye-Shaped Multiple-Input–Multiple-Output Antenna With High Isolation for Wireless UWB Applications’’, IEEE Transactions on Components, Packaging and Manufacturing Technology, Vol. 8, No. 4, pp.635-642, 2018.

[224] Chandel, R. and Gautam, A.K., ‘’Compact MIMO/diversity slot antenna for UWB applications with band-notched characteristic’’, Electronics Letters, Vol. 52, No. 5, pp.336-338, 2016.

[225] C. Yong, L. Wen-jun, C. Chong-hu, C. Wei, and L. Yong, “Printed diversity antenna with cross shape stub for ultra-wideband applications,” 11th IEEE Singapore International

Conference on Communication Systems, ICCS 2008, pp. 813-816, 2008.

[226] B. P. Chacko, G. Augustin, and T. A. Denidni, "Uniplanar slot antenna for ultra-wideband polarization-diversity applications," IEEE Antennas and Wireless Propagation Letters, Vol. 12, pp. 88-91, 2013.

[227] Kumar, R. and Pazare, N.," A Printed Semi-Circular Disc UWB MIMO/Diversity Antenna with Cross Shape Slot Stub'', Wireless Personal Communications, Vol. 91, No. 1, pp.277-291, 2016.

[228] K. M. Prasanna and S. K. Behera, "Compact two-port UWB MIMO antenna system with high isolation using a fork-shaped structure," 2013 International Conference on Communication and Signal Processing, 2013.

[229] Dhar, Sagar K., and Mohammad S. Sharawi. "An isolation enhanced ultra-wideband semi-ring monopole MIMO antenna", Antennas and Propagation & USNC/URSI National Radio Science Meeting, 2015 IEEE International Symposium.

[230] D. D. Katre and R. P. Labade, "Higher isolated dual band notched UWB MIMO antenna with fork stub," 2015 IEEE Bombay Section Symposium (IBSS), 2015.

[231] Kumar, R. and Pazare, N., ''Compact printed ultra-wideband diversity monopole antenna with slant inverted tree-shaped stub'', IET Microwaves, Antennas & Propagation, Vol. 9, No. 14, pp.1595-1604, 2015..

[232] S. Zhang, Z. N. Ying, J. Xiong, and S. L. He," Ultrawideband MIMO/diversity antennas with a tree-like structure to enhance wideband isolation'', IEEE Antennas and Wireless Propagation Letters, Vol.8, pp.1279-1282, 2009.

[233] Iqbal, A., Saraereh, O.A., Ahmad, A.W. and Bashir, S., ''Mutual Coupling Reduction Using F-Shaped Stubs in UWB-MIMO Antenna'', IEEE Access, 6, pp.2755-2759, 2018.

[234] Najam, Ali Imram, Yvan Duroc, and Smail Tedjni. "UWB-MIMO antenna with novel stub structure." Progress in Electromagnetics Research Vol. 19 pp.245-257, 2011.

[235] Tripathi, Shrivishal, Akhilesh Mohan, and Sandeep Yadav, ''A compact octagonal fractal UWB MIMO antenna with WLAN band rejection'', Microwave and Optical Technology letters Vol.57, No.8 , pp. 1919-1925, 2015.

[236] Lee, J.M., Kim, K.B., Ryu, H.K. and Woo, J.M., ''A compact ultrawideband MIMO antenna with WLAN band-rejected operation for mobile devices'', IEEE Antennas and wireless propagation letters, Vol. 11, pp.990-993, 2012.

[237] K. Chhabilwad, G. Reddy, A. Kamma, B. Majumder, and J. Mukherjee, "Compact dual band notched printed UWB MIMO antenna with pattern diversity," 2015 IEEE International Symposium on Antennas and Propagation & USNC/URSI National Radio Science Meeting, 2015.

[238] Kiem, Nguyen Khac, Huynh Nguyen Bao Phuong, and Dao Ngoc Chien. "Design of compact 4× 4 UWB-MIMO antenna with WLAN band rejection." International Journal of Antennas and Propagation, 2014.

[239] Chi, G., Li, B. and Qi, D., ''Dual-band printed diversity antenna for 2.4/5.2 GHz WLAN application'', Microwave and optical technology letters, Vol. 45, No. 6, pp.561-563, 2005.

[240] Y. Ding, Z. Du, K. Gong, and Z. Feng, "A Novel Dual-Band Printed Diversity Antenna for Mobile Terminals," IEEE Transactions on Antennas and Propagation, Vol. 55, No. 7, pp. 2088–2096, 2007.

[241] X. Wang, Z. Du, and K. Gong, "A compact wideband planar diversity antenna covering

UMTS and 2.4GHz WLAN bands," IEEE Antennas Wireless Propag. Lett., vol. 7, 2008.

[242] Li, Yingsong, Wenxing Li, and Wenhua Yu. "A Multi-Band/UWB MIMO/Diversity Antenna with an Enhanced Isolation Using Radial Stub Loaded Resonator", Applied Computational Electromagnetics Society Journal Vol.28, No.1 , 2013.

[243] Y. K. Choukiker, S. K. Behera, and S. K. Sharma, "Hybrid fractal shape planar monopole antenna with MIMO implementation covering multiband wireless communications for handheld devices," 2013 IEEE Antennas and Propagation Society International Symposium (APSURSI), 2013.

[244] Y. K. Choukiker, S. K. Sharma, and S. K. Behera, "Hybrid Fractal Shape Planar Monopole Antenna Covering Multiband Wireless Communications With MIMO Implementation for Handheld Mobile Devices," IEEE Transactions on Antennas and Propagation, Vol. 62, No. 3, pp. 1483–1488, 2014.

[245] Toktas, A. and Akdagli, A., 2014, ''Wideband MIMO antenna with enhanced isolation for LTE, WiMAX and WLAN mobile handsets'', Electronics Letters, 50(10), pp.723-724.

[246] K. Singh, V. Grewal and R. Saxena, "Fractal antennas: A novel miniaturization technique for wireless communications," International Journal of Recent Trends in Engineering, vol. 2, No. 5, 2009.

[247] Sarrazin, J., Mahé, Y., Avrillon, S. and Toutain, S., ''Four co-located antennas for MIMO systems with a low mutual coupling using mode confinement'', In Antennas and Propagation Society International Symposium, 2008. AP-S 2008. IEEE (pp. 1-4), 2008.

[248] Shoaib, S., Shoaib, I., Shoaib, N., Chen, X. and Parini, C.G.,'' MIMO antennas for mobile handsets'', IEEE Antennas and Wireless Propagation Letters, 14, pp.799-802, 2015.

[249] Kakkar, A., Tripathy, M.R. and Singh, A.K.,'' A novel compact two element MIMO antenna with pie shaped slot structure for dual band applications'', In Progress in Electromagnetics Research Symposium-Fall (PIERS-FALL), pp. 336-341 ,2017.

[250] Sharawi, M.S.,'' A dual-band dual element compact MIMO antenna system for mobile 4G terminals'', Microwave and Optical Technology Letters, 55(2), pp.325-329, 2013.

[251] Chen, Z., Yang, S. and Zhu, Q.,''A compact WLAN MIMO antenna with improved isolation for portable devices''. In Communication Problem-Solving (ICCP), 2014 IEEE International Conference on (pp. 489-491), 2014.

[252] Chaudhari, A.A., Jadhav, V., Kharche, S.U. and Gupta, R.K.,'' Compact dual-band MIMO antenna with high isolation for 3/4G, Wi-Fi, bluetooth, Wi-MAX and WLAN applications'', In Progress in Electromagnetic Research Symposium (PIERS), pp. 112-115, 2016.

[253] Y. Gao, C. Chiau, X. Chen, and C. Parini, "Modified PIFA and its array for MIMO terminals," IEE Proceedings - Microwaves, Antennas and Propagation, vol. 152, no. 4, p. 255, 2005.

[254] Gao, Yue, Xiaodong Chen, Clive Parini, and Zhinong Ying. "Study of a dual-element PIFA array for MIMO terminals", In Antennas and Propagation Society International Symposium IEEE, pp. 309-312, 2006.

[255] Pan, J., Zhang, L., Liu, C., Liu, H. and Okuno, Y.,'' A novel compact Printed Inverted-F MIMO antenna operating at 5.8 GHz for WiFi applications'', In Progress in Electromagnetic Research Symposium (PIERS), pp. 1323-1326, 2016.

[256] Wang, Lili, Chongyu Wei, and Weichen Wei. "Design of a high isolation dual-band MIMO antenna for LTE terminal." Antennas & Propagation (ISAP), 2013 Proceedings of the

International Symposium on. Vol. 2, 2013.

[257] El Bakouchi, Raefat Jalila, et al. "Broadband MIMO antenna for HiperLAN/2, WLAN, and WiMAX applications with high isolation." International Journal of Microwave and Wireless Technologies, vol. 8, No.2, pp.309-317, 2016.

[258] H. Hui, "Practical dual-helical antenna array for diversity/MIMO receiving antennas on mobile handsets," IEE Proceedings - Microwaves, Antennas and Propagation, vol. 152, no. 5, p. 367, 2005.

[259] M. A. Razzaq, J.-G. Rhee, S.-I. Yang, and M. S. Khalid, "A novel T-shaped slot PIFA for MIMO applications," 2009 IEEE 13th International Multitopic Conference, 2009.

[260] N. Yousefzadeh, C. Ghobadi, and M. Kamyab, "Consideration Of Mutual Coupling In A Microstrip Patch Array Using Fractal Elements," Progress In Electromagnetics Research, vol. 66, pp. 41–49, 2006.

[261] Gao, Y., Chiau, C.C., Chen, X. and Parini, C.G., ''Design of diversity antenna array for Galileo/GPS receivers'', In Antennas and Propagation, 2006. EuCAP 2006. First European Conference on (pp. 1-5) 2006.

[262] Q. Wang, D. Plettemeier, H. Zhang, K. Wolf, and E. Ohlmer, "Design and diversity performance of optimized dual-element PIFA antennas for MIMO handsets," 2010 International Workshop on Antenna Technology (iWAT), 2010.

[263] N. H. Noordin, A. O. El-Rayis, N. Haridas, B. Flynn, A. T. Erdogan, and T. Arslan, "Triangular lattices for mutual coupling reduction in patch antenna arrays," 2011 Loughborough Antennas & Propagation Conference, 2011.

[264] Fitri Yuli Zulki°i and Eko Tjipto Rahardjo "Compact MIMO Microstrip Antenna with Defected Ground for Mutual Coupling Suppression," 201 Progress In Electromagnetics Research Symposium Proceedings, Marrakesh, Morocco, pp 20-23, 2011.

[265] B. Aouadi and J. Belhadj Tahar, "Requirements Analysis of Dual-Band MIMO Antenna," Wireless Personal Communications, vol. 82, no. 1, pp. 35–45, 2014.

[266] Y. Sung, "Multi-band reconfigurable antenna for mobile handset applications," IET Microwaves, Antennas & Propagation, vol. 8, no. 11, pp. 864–871, 2014.

[267] O. Ahmed and A.-R. Sebak, "Mutual Coupling Effect on Ultrawideband Linear Antenna Array Performance," International Journal of Antennas and Propagation, vol. 2011, pp. 1–11, 2011.

[268] T. Phairat and T. Chanchai, "Design of an UWB quasi rhomboid shaped element bowtie antenna for MIMO applications," Proceedings of the World Congress on Engineering, vol. 2, 2011.

[269] Jusoh, M., Jamlos, M.F., Malek, M.F., Kamarudin, M.R. and Harun, H., ''Analysis of radiation efficiency effects on UWB MIMO tree-antenna positioning'', In Electromagnetic Compatibility (APEMC), 2012 Asia-Pacific Symposium, pp. 897-900, 2012.

[270] H. S. Singh, G. K. Pandey, P. K. Bharti, and M. K. Meshram, "Design of low profile ultra-wide-band PIFA for MIMO applications," 2014 IEEE Region 10 Symposium, 2014.

[271] J. Guterman, A. A. Moreira, and C. Peixeiro, "Microstrip fractal antennas for multistandard terminals," IEEE Antennas Wireless Propag. Lett, vol. 3, 2004.

[272] A. A. L. Neyestanak, A. Danideh, and R. Sadeghifakhr, "Compact size microstrip array MIMO antenna operable in multiband," 2008 24th Biennial Symposium on Communications, 2008.

[273] R. S. Fakhr, A. A. L. Neyestanak, and M. Naser-Moghadasi, "Compact Size And Dual Band Semicircle Shaped Antenna For Mimo Aplications," Progress In Electromagnetics Research C, vol. 11, pp. 147–154, 2009.

[274] A. Jamil, M. Z. Yusoff, N. Yahya, and M. A. Zakariya, "Design and parametric study of multiple element MIMO antennas for WLAN," 2012 4th International Conference on Intelligent and Advanced Systems (ICIAS2012), 2012.

[275] Salim, Ali J., et al. "A new fractal based PIFA antenna design for MIMO dual band WLAN applications." PIERS Proceedings. 2012.

[276] S. Xiao, T. Sun, C. Wang and W. Wang, "A compact and dual-band microstrip MIMO antenna for LTE mobile terminals," in Communications in China (ICCC), 2014 IEEE/CIC International Conference On, pp. 474-478, 2014.

[277] Singh, H.S., Agarwal, M., Pandey, G.K. and Meshram, M.K., ''A quad-band compact diversity antenna for GPS L1/Wi-Fi/LTE2500/WiMAX/HIPERLAN1 applications'', IEEE Antennas and Wireless Propagation Letters, 13, pp.249-252, 2014.

[278] G. Dadashzadeh, A. Dadgarpour, F. Jolani, and B. Virdee, "Mutual coupling suppression in closely spaced antennas," IET Microwaves, Antennas & Propagation, vol. 5, no. 1, pp. 113-125, 2011.

[279] G. Zhai, Z. N. Chen, and X. Qing, "Mutual coupling reduction of compact four-element MIMO slot antennas using metamaterial mushroom structures," 2015 International Workshop on Antenna Technology (iWAT), 2015.

[280] G. Zhai, Z. N. Chen, and X. Qing, "Enhanced Isolation of a Closely Spaced Four-Element MIMO Antenna System Using Metamaterial Mushroom," IEEE Transactions on Antennas and Propagation, vol. 63, no. 8, pp. 3362–3370, 2015.

[281] Zhai, G., Chen, Z.N. and Qing, X., ''Isolation-enhanced four-element MIMO antenna system using mushroom'', In Antennas and Propagation (APCAP), 2015 IEEE 4th Asia-Pacific Conference, pp. 16-17, 2015.

[282] H. Qi, X. Yin, and H. Zhao, "A hybrid solution for mutual coupling reduction between closely spaced microstrip antennas," 2015 Asia-Pacific Microwave Conference (APMC), 2015.

[283] Cao, P., ''UWB antennas for wireless communications'', Doctoral dissertation, University of Liverpool, 2013.

[284] S. Hong, K. Chung, J. Lee, S. Jung, S.-S. Lee, and J. Choi, "Design of a diversity antenna with stubs for UWB applications," Microwave and Optical Technology Letters Microw. Opt. Technol. Lett., vol. 50, no. 5, pp. 1352–1356, 2008.

[285] S.-Y. Lin and H.-R. Huang, "Ultra-wideband MIMO antenna with enhanced isolation," Microwave and Optical Technology Letters, vol. 51, no. 2, pp. 570–573, 2009.

[286] C.-X. Mao, Q.-X. Chu, Y.-T. Wu, and Y.-H. Qian, "Design And Investigation Of Closely-Packed Diversity Uwb Slot-Antenna With High Isolation," Progress In Electromagnetics Research C, vol. 41, pp. 13–25, 2013.

[287] Y. Li, W. Li, C. Liu, and T. Jiang, "A printed diversity Cantor set fractal antenna for ultra wideband communication applications," Isape2012, 2012.

[288] Choi, S. H., J. K. Park, S. K. Kim, and J. Y. Park, "A new ultrawideband antenna for UWB applications," Microwave and Optical Technology Letters, Vol. 40, No. 5, pp.399-401, 2004.

[289] Chung, K. and Yoon, J.H., ''Integrated MIMO antenna with high isolation characteristic'', Electronics letters, 43(4), pp.199-201, 2007.

[290] Qi, H., L. Liu, X. Yin, H. Zhao, and W. J. Kulesza, "Mutual coupling suppression between two closely spaced microstrip antennas with an asymmetrical coplanar strip wall," IEEE Antennas and Wireless Propagation Letters, Vol. 15, 2016

[291] M. Suwailam, M. Boybay, and O. Ramahi, ''Single-negative (SNG) meta-mate

rials for mutual coupling reduction in high-prole antennas," IEEE Antennas and Propagation Society International Symposium, pp. 1-4, 2009.

[292] M. M. Bait-Suwailam, M. S. Boybay, and O. M. Ramahi, "Electromagnetic Coupling Reduction in High-Profile Monopole Antennas Using Single-Negative Magnetic Metamaterials for MIMO Applications," IEEE Transactions on Antennas and Propagation, vol. 58, no. 9, pp. 2894–2902, 2010.

[293] Chiau, C. C., X. Chen, and C. G. Parini. "A compact four-element diversity-antenna array for PDA terminals in a MIMO system", Microwave and Optical Technology Letters, Vol. 44, No.5, pp. 408-412, 2005.

[294] S. B. Yeap, X. Chen, J. A. Dupuy, C. C. Chiau and C. G. Parini, "Low profile diversity antenna for MIMO applications," Electron. Lett., vol. 42, no. 2, 69–71, 2006.

[295] J.-B. Yan, C.-Y. Chiu, and R. Murch, ''Handset 4-port mimo antenna using slit separated pifa and quarterwave-slot antenna pair," IEEE Antennas and Propagation Society International Symposium, pp. 1-4, 2008.

[296] A. R. Mallahzadeh, S. Es'haghi, and A. Alipour, "Design of an E-shaped mimo antenna using iwo algorithm for wireless application at 5.8GHz," Progress In Electromagnetics Research, PIER 90, 187-203, 2009.

[297] Bhuiyan, R. H., R. Dougal, and M. Ali. "A novel multi-element fractal PIFA with wide pattern coverage for 915 MHz RFID wireless sensors." Antennas and Propagation Society International Symposium, 2009. APSURSI'09. IEEE. IEEE, 2009.

[298] Azremi, A. A. H., Kyro, M., Ilvonen, J., Holopainen, J., Ranvier, S., Icheln, C., & Vainikainen, P. ''Five-element inverted-F antenna array for MIMO communications and radio direction finding on mobile terminal'', In Antennas & Propagation Conference, LAPC 2009. Loughborough, pp. 557-560, 2009.

[299] Bae, Hongpyo, et al. "Compact mobile handset MIMO antenna for LTE700 applications", Microwave and Optical Technology Letters, Vol. 52, No.11 pp.2419-2422, 2010.

[300] Z. Li, M. S. Han, X. Zhao and J. Choi, "MIMO Antenna with Isolation Enhancement for Wireless USB Dongle Application at WLAN Band," Proceedings of Asia-Pacific Microwave Conference, pp. 758-761, 2010.

[301] S. Zhang, P. Zetterberg and S. He, "Printed MIMO antenna system of four closely-spaced elements with large bandwidth and high isolation," Electron. Lett. Vol, 46 no. 15, 2010

[302] Yue Li, Zhijun Zhang, Wenhua Chen, Zhenghe Feng, Iskander, M.F., "A Dual-Polarization Slot Antenna Using a Compact CPW Feeding Structure," Antennas and Wireless Propagation Letters, IEEE, vol. 9, pp. 191-194, 2010.

[303] Z. N. Chen, T. See, and X. N. ''Low Configuration optimization of suspended plate antennas for reduction of mutual coupling'', International Workshop on Antenna Technology (iWAT), pp. 441-444, 2011.

[304] Al-Nuaimi, M.K.T., ''Mutual coupling evaluation of dual-miniaturized PIFA antenna array for MIMO terminals'', In Wireless Conference 2011-Sustainable Wireless Technologies (European Wireless), 11th European, pp.1-4, 2011.

[305] S.-W. Su and C.-T. Lee, "Printed two monopole-antenna system with a decoupling neutralization line for 2.4-GHz MIMO applications," Microwave and Optical Technology Letters, vol. 53, no. 9, pp. 2037–2043, 2011.

[306] Y. Lee, D. Ga and J. Choi, "Design of a MIMO Antenna with Improved Isolation Using MNG Metamaterial," International Journal of Antennas and Propagation, Vol.2012, pp.1-7.

[307] H. T. Chattha, Y. Huang, S. J. Boyes, and X. Zhu, "Polarization and Pattern Diversity-Based Dual-Feed Planar Inverted-F Antenna," IEEE Transactions on Antennas and Propagation, vol. 60, no. 3, pp. 1532–1539, 2012.

[308] Noordin, N.H., Wong, Y.C., Erdogan, A.T., Flynn, B. and Arslan, T., ''Meandered inverted-F antenna for MIMO mobile devices'', In Antennas and Propagation Conference (LAPC), 2012 Loughborough (pp.1-4), 2012.

[309] Malik, J., Patnaik, A. and Kartikeyan, M.V., ''Novel compact MIMO antenna for WLAN application'', In Applied Electromagnetics Conference (AEMC), pp. 1-2, 2013.

[310] Ghosh, S., Tran, T.N. and Le-Ngoc, T., Miniaturized four-element diversity PIFA. IEEE Antennas and Wireless Propagation Letters, 12, pp.396-400, 2013.

[311] Lin, S.Y. and Liu, I.H., ''Small inverted-U loop antenna for MIMO applications'', Progress In Electromagnetics Research, 34, pp.69-84, 2013.

[312] Chung, K.L. and Kharkovsky, S., ''Mutual coupling reduction and gain enhancement using angular offset elements in circularly polarized patch array.'', IEEE Antennas and Wireless Propagation Letters, 12(9), pp.1122-1124, 2013.

[313] Marzudi, W.N.N.W., Abidin, Z.Z., Muji, S.Z.M., Ma, Y. and Abd-Alhameed, R.A., ''Minimization of Mutual Coupling Using Neutralization Line Technique for 2.4 GHz Wireless Applications''. International Journal of Innovation in the Digital Economy (IJIDE), Vol.6, No.3, pp.1-15, 2015.

[314] Haraz, Osama M., Mohammad Ashraf, and Saleh Alshebeili. "Single-band PIFA MIMO antenna system design for future 5G wireless communication applications" In Wireless and Mobile Computing, Networking and Communications (WiMob), 2015 IEEE 11th International Conference on, pp. 608-612. , 2015.

[315] Anitha, R., Mathew, S., Vinesh, P.V., Mohanan, P. and Vasudevan, K.,''Compact 4 port MIMO antenna using polarization and pattern diversity'', In Wireless and Microwave Technology Conference (WAMICON), 2015 IEEE 16th Annual, pp. 1-4, 2015.

[316] K. L. Wong, S. W. Su, and Y. L. Kuo, "A printed ultra-wideband diversity monopole antenna," Microwave and Optical Technology Letters, vol. 38, pp. 257-259, 2003.

[317] T See, T.S. and Chen, Z.N.,'' An ultrawideband diversity antenna. IEEE Transactions on Antennas and Propagation'', 57(6), pp.1597-1605, 2009.

[318] Najam, A.I., Duroc, Y., Leao, J.F. and Tedjini, S., ''A novel co-located antennas system for UWB-MIMO applications'', In Radio and Wireless Symposium, 2009. RWS'09. pp. 368-371, 2009.

[319] Najam, Ali Imran, Yvan Duroc, and Smail Tedjini. "Design and analysis of MIMO antennas for UWB communications", Antennas and Propagation (EuCAP), 2010 Proceedings of the Fourth European Conference on, 2010.

[320] (chapter 11: application and technologies, short – range wireless communication: fundamentals of RF system design and application, second edition by alan bensky)

[321] S. Mohammad, A. Nezhad, H. R. Hassani, and A. Foudazi, "A dual-band WLAN/UWB printed wide slot antenna for mimo/diversity applications," Microwave and Optical

Technology Letters, vol. 55, no. 3, pp. 461–465, 2013.

[322] OSKOUEI, Hamid Reza Dalili. "Design of New Compact Ultra-Wideband Microstrip Antenna for MIMO application," International Journal of Natural & Engineering Sciences Vol.7, No.2 , 2013.

[323] Li, J.F., Chu, Q.X., Li, Z.H. and Xia, X.X., ‘’Compact dual band-notched UWB MIMO antenna with high isolation’’, IEEE transactions on antennas and propagation, Vol.61, No.9, pp.4759-4766, 2013.

[324] Pazare, Neha, et al. "Design of asymmetric CPW fed slot antennas for pattern and polarization diversity", Wireless Computing and Networking (GCWCN), 2014 IEEE Global Conference on, 2014.

[325] A. Toktas and A. Akdagli, “Compact multiple-input multiple-output antenna with low correlation for ultra-wide-band applications,” IET Microwaves, Antennas & Propagation, 2015.

[326] Khan, M.S., Capobianco, A.D., Naqvi, A., Ijaz, B., Asif, S. and Braaten, B.D., ‘’Planar, compact ultra-wideband polarisation diversity antenna array’’, IET Microwaves, Antennas & Propagation, Vo.9 , No.15, pp.1761-1768, 2015.

[327] Sarrazin, J., Y. Mah´e, S. Avrillon, and S. Toutain, “Collocated microstrip antennas for MIMO systems with a low mutual coupling using mode confinement,” IEEE Trans. Antennas Propag.,Vol. 58, No. 2, 589–592, 2010.

[328] S. Kareemulla and V. Kumar, “A novel compact MIMO antenna for ultra-wide-band applications,” 2015 IEEE International Conference on Signal Processing, Informatics, Communication and Energy Systems (SPICES), pp. 1-5, 2015.

[329] Kang, L., Li, H., Wang, X. and Shi, X., ‘’Compact offset microstrip-fed MIMO antenna for band-notched UWB applications’’, IEEE Antennas and Wireless Propagation Letters, Vol.14, pp.1754-1757, 2015.

[330] Roshna, T.K., Deepak, U., Sajitha, V.R. and Mohanan, P., 2015, December. ‘’A 3-port UWB MIMO antenna with enhanced isolation’’, In Applied Electromagnetics Conference (AEMC), pp. 1-2, 2015.

[331] Khan, M.S., Capobianco, A.D., Iftikhar, A., Asif, S. and Braaten, B.D., ‘’A compact dual polarized ultrawideband multiple-input-multiple-output antenna’’, Microwave and Optical Technology Letters, 58(1), pp.163-166, 2016.

[332] Srivastava, G. and Mohan, A., ‘’Compact MIMO slot antenna for UWB applications’’, IEEE Antennas and Wireless Propagation Letters, Vo.15, pp.1057-1060, 2016.

[333] Ling, X. and Li, R., 2011. A novel dual-band MIMO antenna array with low mutual coupling for portable wireless devices. IEEE antennas and wireless propagation letters, 10, pp.1039-1042.

[334] Roshna, T.K., Deepak, U. and Mohanan, P., ‘’A compact Coplanar 4-port MIMO antenna for high-speed UWB applications’’, In Antennas and Propagation in Wireless Communications (APWC), 2016 IEEE-APS Topical Conference on (pp. 106-109), 2016.

[335] Huang, H.F. and Xiao, S.G., ‘’A Compact Polarization Diversity UWB MIMO Antenna with a Fork-Shaped Decoupling Structure’’, Progress In Electromagnetics Research, 69, pp.87-92, 2017.

[336] Sipal, D., Abegaonkar, M.P. and Koul, S.K., ‘’easily extendable compact planar UWB MIMO antenna array’’, IEEE Antennas and Wireless Propagation Letters, 16, pp.2328-2331, 2017.

[337] Kakkar, A. and Tripathy, M.R., ‘’A compact four element MIMO slot antenna for ultra-wideband application’’, In Progress in Electromagnetics Research Symposium-Fall (PIERS-FALL), pp. 3036-3041, 2017.

[338] Mathur, Rohit, and Santanu Dwari. "Compact 4-Port MIMO/Diversity Antenna with Low Correlation for UWB Application", Frequenz 2018.

[339] Chi, G., Li, B. and Qi, D., ‘’Dual-band printed diversity antenna for 2.4/5.2GHz WLAN application’’, Microwave and optical technology letters, 45(6), pp.561-563, 2005.

[340] Manteghi, M. and Rahmat-Samii, Y.,’’ Novel compact tri-band two-element and four-element MIMO antenna designs’’, In Antennas and Propagation Society International Symposium 2006, IEEE, pp. 4443-4446, 2006.

[341] M. Manteghi and Y. Rahmat-Samii, “A novel miniaturized triband PIFA for MIMO applications,” Microwave. Optical. technology. Letter. vol. 49, no. 3, 2007.

[342] Bhatti, R.A., Choi, J.H. and Park, S.O., ‘’Quad-band MIMO antenna array for portable wireless communications terminals,’’ IEEE antennas and wireless propagation letters, Vol.8, pp.129-132, 2009.

[343] S. Nezhad and H. R. Hassani, "A novel triband E-shaped printed monopole antenna for MIMO application," Antennas and Wireless Propagation Letters, vol. 9, pp. 576-579, 2010.

[344] S. W. Su, “High-gain dual-loop antennas for MIMO access points in the 2.4/5.2/5.8 GHz bands,” IEEE Trans. Antennas Propagation., vol. 58, no. 7, 2010.

[345] Shin, Bong-Gyu, et al. "Diversity and MIMO antenna for multi-band mobile handset applications", Antennas and Propagation (APSURSI), 2011 IEEE International Symposium on, 2011.

[346] J. R. Costa, E. B. Lima, C. R. Medeiros, and C. A. Fernandes, “Evaluation of a New Wideband Slot Array for MIMO Performance Enhancement in Indoor WLANs,” IEEE Transactions on Antennas and Propagation, vol. 59, no. 4, pp. 1200–1206, 2011.

[347] Su, S.W. and Lee, C.T.,’’ Low-cost dual-loop-antenna system for dual-WLAN-band access points’’, IEEE Transactions on Antennas and Propagation, 59(5), pp.1652-1659, 2011.

[348] Su, S.W. and Lee, C.T., ‘’Printed, low-cost, dual-polarized dual-loop-antenna system for 2.4/5 GHz WLAN access points’’. In Antennas and Propagation (EUCAP), Proceedings of the 5th European Conference on (pp. 1253-1257), 2011.

[349] Mallahzadeh, A.R., Seyyedrezaei, S.F., Ghahvehchian, N. and Mallahzadeh, S., ‘’Tri-band printed monopole antenna for WLAN and WiMAX MIMO systems’’, In Antennas and Propagation (EUCAP), Proceedings of the 5th European Conference on (pp. 548-551), 2011.

[350] Kulkarni, A.N. and Sharma, S.K., ‘’ A compact multiband antenna with MIMO implementation for USB Size 4G LTE wireless devices’’, In Antennas and Propagation (APSURSI), 2011 IEEE International Symposium on (pp. 2215-2218), 2011.

[351] Su, S.W., Lee, C.T. and Chang, F.S.,’’ Dual-polarized dual-loop-antenna system for 2.4/5 GHz WLAN access points’’ In Electromagnetics, Applications and Student Innovation (iWEM), 2011 IEEE International Workshop on (pp. 24-28), 2011.

[352] Kulkarni, A.N. and Sharma, S.K., ‘’A multiband antenna with MIMO implementation for USB dongle size wireless devices’’, Microwave and Optical Technology Letters, 54(8), pp.1990-1994, 2012.

[353] Singh, H.S., Pandey, G.K., Bharti, P.K., Agarwal, M. and Meshram, M.K., ‘’Simulation study of Four Element MIMO Antenna System with Pattern and Polarization Diversity’’.

[354] Karimian, R., Soleimani, M. and Hashemi, S.M.,'' Tri-band four elements MIMO antenna system for WLAN and WiMAX application,'' Journal of Electromagnetic Waves and Applications, Vol.26, No.(17-18), pp.2348-2357, 2012.

[355] Yao, Y., Wang, X. and Yu, J., ''Multiband planar monopole antenna for LTE MIMO systems,'' International Journal of Antennas and Propagation, 2012.

[356] M. Darvish and H. R. Hassani, "Quad band CPW-Fed monopole antenna for MIMO applications," 2012 6th European Conference on Antennas and Propagation (EUCAP), 2012.

[357] Darvish, M. and Hassani, H.R ''Multiband uniplanar monopole antenna for MIMO applications'', In Electrical Engineering (ICEE), 2012 20th Iranian Conference on (pp. 1125-1128), 2012.

[358] Li, J.F., Chu, Q.X. and Li, Z.H., ''Compact conventional phone antenna integrated with wideband multiple input multiple output antenna'', Microwave and Optical Technology Letters, 54(8), pp.1958-1962, 2012.

[359] J. Guo, J. Fan, L. Sun and B. Sun, "A four-antenna system with high isolation for mobile phones," Antennas and Wireless Propagation Letters, IEEE, vol. 12, pp. 979-982, 2013.

[360] Karimian, R., Oraizi, H., Fakhte, S. and Farahani, M.,'' Novel F-shaped quad-band printed slot antenna for WLAN and WiMAX MIMO systems'', IEEE Antennas and Wireless Propagation Letters, 12, pp.405-408, 2013.

[361] MoradiKordalivand, A., Rahman, T.A. and Khalily, M., ''Common elements wideband MIMO antenna system for WiFi/LTE access-point applications'', IEEE Antennas and Wireless Propagation Letters, Vol.13, pp.1601-1604, 2014.

[362] Li, G., Zhai, H., Ma, Z., Liang, C., Yu, R. and Liu, S., ''Isolation-improved dual-band MIMO antenna array for LTE/WiMAX mobile terminals,'' IEEE Antennas and Wireless Propagation Letters, 13, pp.1128-1131, 2014.

[363] Chattha, H.T., Nasir, M., Jamal, Y., Sharif, A., Huang, Y. and Alja'afreh, S.S., ''MIMO antenna using modified planar inverted-F antennas,'' Antennas and Propagation Society International Symposium (APSURSI), pp. 390-391, 2014.

[364] Cheng, Y., Sun, Z., Lu, W. and Zhu, H., ''A novel compact dual-band MIMO antenna'', In Antennas and Propagation (APCAP), 2014 3rd Asia-Pacific Conference on (pp. 157-160), 2014.

[365] H. S. Singh, G. K. Pandey, and M. K. Meshram, "Internal coupled-fed four-element multi-wideband diversity antenna for LTE mobile handsets," 2015 IEEE Applied Electromagnetics Conference (AEMC), 2015.

[366] O. M. Arabi, N. Ali, P. S. Excell, A. M. Altimimi, and R. A. Abd-Alhameed, "Multipolarized/Multi-Band orthogonal MIMO antenna for WiFi and WiMax applications," 2015 IEEE International Symposium on Antennas and Propagation & USNC/URSI National Radio Science Meeting, 2015.

[367] W.-J. Liao, C.-Y. Hsieh, B.-Y. Dai, and B.-R. Hsiao, "Inverted-F/Slot Integrated Dual-Band Four-Antenna System for WLAN Access Points," IEEE Antennas and Wireless Propagation Letters, vol. 14, pp. 847–850, 2015.

[368] Zhekov, S.S., Tatomirescu, A. and Fr, G., ''Compact multiband sensing MIMO antenna array for cognitive radio system'', In Antennas & Propagation Conference (LAPC), 2015 Loughborough (pp. 1-5), 2015.

[369] Peristerianos, A., Theopoulos, A., Koutinos, A.G., Kaifas, T. and Siakavara, K., ''Dual-

band fractal semi-printed element antenna arrays for MIMO applications'', IEEE Antennas and Wireless Propagation Letters, 15, pp.730-733, 2016.

[370] Li, L., Zhang, X., Yin, X. and Zhou, L., ''A compact triple-band printed monopole antenna for WLAN/WiMAX applications'', IEEE Antennas and Wireless Propagation Letters, 15, pp.1853-1855, 2016.

[371] Peng, B., Hong, W., Zhang, Q., Gao, Y., Zhu, J., Deng, L., Li, S. and Zeng, Q., ''CPW-fed dual-band MIMO antenna based on harmonic resonance with high isolation'' In Antennas and Propagation (APSURSI), 2016 IEEE International Symposium on (pp. 57-58), 2016.

[372] Sarkar, D., Saurav, K. and Srivastava, K.V., ''A compact four element CSRR-loaded antenna for dual band pattern diversity MIMO applications'', In Microwave Conference (EuMC), 2016 46th European (pp. 1315-1318), 2016.

[373] Sim, C.Y.D., Chen, C.C. and Lee, Y.L., ''A dual-band antenna design for MIMO LTE applications with reduced ground effects''. International Journal of RF and Microwave ComputerAided Engineering, 26(1), pp.80-87, 2016.

[374] Menon, S.K., ''Microstrip Patch Antenna Assisted Compact Dual Band Planar Crossover'', Electronics, 6(4), p.74, 2017.

[375] Chithradevi, R. and Sreeja, B.S., ''A novel dual band square patch antenna with better isolation and low correlation'', In Inventive Systems and Control (ICISC), 2017 International Conference on (pp. 1-4), 2017.

[376] S. Ranvier, C. Luxey, P. Suvikunnas, R. Staraj and P Vainikainen, "Capacity Enhancement by Increasing Both Mutual Coupling and Efficiency: a Novel Approach," Antennas and Propagation Society International Symposium, pp. 3632-3635, 2007.

[377] Marzudi, W.N.N.W., Abidin, Z.Z., Muji, S.Z., Yue, M. and Abd-Alhameed, R.A., ''Minimization of mutual coupling using neutralization line technique for 2.4 GHz wireless applications,'' International Journal of Digital Information and Wireless Communications (IJDIWC), Vol.4, No.3, pp.292-298, 2014.

[378] Baek, J. and Choi, J., ''The design of a LTE/MIMO antenna with high isolation using a decoupling network'', Microwave and Optical Technology Letters, 56(9), pp.2187-2191, 2014.

[379] M. Ezzat and C. S. Lee, "A simple optimization technique for reducing mutual coupling between two coupled antennas," 2015 IEEE International Symposium on Antennas and Propagation & USNC/URSI National Radio Science Meeting, 2015.

[380] A. Diallo, C. Luxey, P. L. Thuc, R. Staraj, and G. Kossiavas, ''Enhanced di- versity antennas for umts handsets,'' First European Conference on Antennas and Propagation, pp. 1-5, 2006.

[381] A. Chebihi, C. Luxey, A. Diallo, P. Le Thuc, and R. Staraj, "A novel isolation technique for closely spaced PIFAs for UMTS mobile phones," IEEE Antennas and Wireless Propagation Letters, vol. 7, pp. 665-668, 2008.

[382] Diallo, A., et al. "Diversity performance of multiantenna systems for UMTS cellular phones in different propagation environments." International journal of antennas and propagation, 2008.

[383] S. W. Su, C. T. Lee and F. S. Chang ,"Printed MIMO-Antenna System Using Neutralization-Line Technique for Wireless USB-Dongle Applications," IEEE Transactions on Antennas and Propagation, Vol. 60, No.2, pp. 456-463, February, 2012.

[384] See, C.H., Hraga, H.I., Noras, J.M., Abd-Alhameed, R.A. and McEwan, N.J., 2013.

Compact multiple input and multiple output/diversity antenna for portable and mobile ultra-wideband applications. IET Microwaves, Antennas & Propagation, Vol.7, No.6, pp.444-451.

[385] See, Chan H., et al. "Compact MIMO/diversity antenna for portable and mobile UWB terminals." Microwave Conference (APMC), Asia-Pacific, 2014.

[386] S. Zhang and G. F. Pedersen, “Mutual Coupling Reduction for UWB MIMO Antennas With a Wideband Neutralization Line,” IEEE Antennas and Wireless Propagation Letters, vol. 15, pp. 166–169, 2016.

[387] A. Diallo, C. Luxey, P. L. Thuc, R. Staraj, and G. Kossiavas, “Study and Reduction of the Mutual Coupling Between Two Mobile Phone PIFAs Operating in the DCS1800 and UMTS Bands,” IEEE Transactions on Antennas and Propagation, vol. 54, no. 11, pp. 3063–3074, 2006.

[389] See, Chan Hwang, et al. "Wideband printed MIMO/diversity monopole antenna for WiFi/WiMAX applications." IEEE transactions on antennas and propagation Vol.60, No.4, pp. 2028-2035, 2012.

[390] Zhanmeng, L., Chunlan, L., Luqu, Y., Jianxin, J. and Jie, Y., 2012, May. A novel compact dual-band MIMO antenna for WLAN application. In Microwave and Millimeter Wave Technology (ICMMT), 2012 International Conference on (Vol. 3, pp. 1-4).

[391] Wang, Y. and Du, Z., ‘’A wideband printed dual-antenna system with a novel neutralization line for mobile terminals,’’ IEEE Antennas and Wireless Propagation Letters, Vol.12, pp.1428-1431, 2013.

[392] H. S. Singh, B. R. Meruva, G. K. Pandey, P. K. Bharti and M. K. Meshram, "Low mutual coupling between MIMO antennas by using two folded shorting strips," Progress in Electromagnetics Research B, vol. 53, pp. 205-221, 2013.

[393] Wang, Y. and Du, Z., ‘’A wideband printed dual-antenna with three neutralization lines for mobile terminals’’. IEEE Transactions on Antennas and Propagation, Vol.62, No.3, pp.1495-1500, 2014.

[394] S.-C. Chen, Y.-S. Wang, and S.-J. Chung, “A Decoupling Technique for Increasing the Port Isolation Between Two Strongly Coupled Antennas,” IEEE Transactions on Antennas and Propagation, vol. 56, no. 12, pp. 3650–3658, 2008.

[395] Coetzee, J.C. and Yu, Y., ‘’Port decoupling for small arrays by means of an eigenmode feed network’’, IEEE Transactions on Antennas and Propagation, 56(6), pp.1587-1593, 2008.

[396] R. Bhatti, S. Yi, and S.-O. Park, “Compact Antenna Array With Port Decoupling for LTE-Standardized Mobile Phones,” IEEE Antennas and Wireless Propagation Letters, vol. 8, pp. 1430–1433, 2009.

[397] S. Zuo, Y.-Z. Yin, Z.-Y. Zhang, W.-J. Wu, and J.-J. Xie, “Eigenmode Decoupling For Mimo Loop-Antenna Based On 180Â° Coupler,” Progress In Electromagnetics Research Letters, vol. 26, pp. 11–20, 2011.

[398] N. Nakajima, Tomoko Yamazaki, and Wei Ni, “Mutual coupling cancellation for compact MIMO antenna with 3 dB hybrid,” Proce. 2nd International Conf. on Wireless VITAE, pp. 1-4, 2011.

[399] Liu, X., Yu, Y., Tang, C., Li, M. and Li, T., ‘’A novel design of microstrip decoupling network for two-element antenna arrays’’, In Applied Computational Electromagnetics Society Symposium (ACES), 2017 International (pp. 1-2), 2017.

[400] Zhang, X.Y., Xue, C.D., Cao, Y. and Ding, C.F., ‘’Compact MIMO antenna with embedded decoupling network’’, In Computational Electromagnetics (ICCEM), 2017 IEEE

International Conference on (pp. 64-66), 2017.

[401] J. C. Coetzee, "Dual-Frequency Decoupling Networks for Compact Antenna Arrays," International Journal of Microwave Science and Technology, vol. 2011, pp. 1–3, 2011.

[402] B. Wu and K. M. Luk, "A 4-port diversity antenna with high isolation for mobile communications," IEEE Trans. Antennas Propag., vol. 59, no. 5, pp. 1660–1667, 2011.

[403] Sato, Hiroshi, et al. "A Method of Dual-frequency Decoupling for Two-element MIMO Antenna." PIERS Proceedings. 2013.

[404] H. L. Peng, R. Tao, W. Y. Yin, and J. F. Mao, "A novel compact dualband antenna array with high isolations realized using the neutralization technique," IEEE Trans. Antennas Propag., vol. 61, no. 4, pp. 1958–1962, 2013

[405] Liu, P., Sun, D., Wang, P. and Gao, P., ''Design of a Dual-Band MIMO Antenna with High Isolation for WLAN Applications'', Progress In Electromagnetics Research, 74, pp.23-30, 2018.

[406] Saleh, A.M., Sayidmarie, K.H., Abd-Alhameed, R.A., Jones, S., Noras, J.M. and Excell, P.S., ''Compact tri-band MIMO antenna with high port isolation for WLAN and WiMAX applications'', In Antennas & Propagation Conference (LAPC), 2016 Loughborough (pp. 1-4), 2016.

[407] Min, K.S., Kim, D.J. and Moon, Y.M.," Improved MIMO antenna by mutual coupling suppression between elements'', In Wireless Technology, 2005. The European Conference on (pp. 125-128), 2005.

[408] Ghosh, C.K. and Parui, S.K., ''Reduction of mutual coupling between E-shaped microstrip antennas by using a simple microstrip I-section'', Microwave and Optical Technology Letters, 55(11), pp.2544-2549, 2013.

[409] K. J. Babu, R. W. Aldhaheri, M. Y. Talha, and I. S. Alruhaili, "Design Of A Compact Two Element Mimo Antenna System With Improved Isolation," Progress In Electromagnetics Research Letters, vol. 48, pp. 27–32, 2014.

[410] Zhang, Q.C., Zhang, J. and Wu, W., ''Reduction of mutual coupling between cavity-backed slot antenna elements'', Progress In Electromagnetics Research, 53, pp.27-34, 2014.

[411] Sun, X.B. and Cao, M.Y.," Low mutual coupling antenna array for WLAN application'', Electronics Letters, 53(6), pp.368-370, 2017.

[412] Cheng, Y.F., Ding, X., Shao, W. and Wang, B.Z., ''Reduction of mutual coupling between patch antennas using a polarization-conversion isolator'', IEEE Antennas and Wireless Propagation Letters, 16, pp.1257-1260, 2017.

[413] Farsi, Saeed, et al. "Mutual coupling reduction between planar antennas by using a simple microstrip U-section." IEEE antennas and wireless propagation letters 11 (2012): 1501-1503.

[414] Wang, H., Fang, D.G. and Ge, P., '' Mutual coupling reduction between two conformal microstrip patch antennas'',. In Environmental Electromagnetics, 2009. CEEM 2009. 5th Asia-Pacific Conference on (pp. 176-179), 2009.

[415] Z. Li, Z. Du, M. Takahashi, K. Saito, and K. Ito, ''Reducing mutual cou- pling of mimo antennas with parasitic elements for mobile terminals'', IEEE Transactions on Antennas and Propagation, vol. 60, pp. 473-481, 2012.

[416] B. K. Lau and J. Andersen, ''Simple and efficient decoupling of compact arrays with parasitic scatterers," IEEE Transactions on Antennas and Propagation, vol. 60, pp. 464-472,

2012.

[417] Payandehjoo, K. and Abhari, R., ‘’Investigation of parasitic elements for coupling reduction in multiantenna handset devices’’, International Journal of RF and Microwave Computer Aided Engineering, Vol.24, No.1, pp.1-10. 2014.

[418] Syed, Avez, and Rabah W. Aldhaheri. "A compact ultra-wideband MIMO antenna with improved isolation." Antennas and Propagation & USNC/URSI National Radio Science Meeting, 2015 IEEE International Symposium on. IEEE, 2015.

[419] S. Rajkumar, K. T. Selvan, and P. H. Rao, “Compact two-element UWB fractal monopole MIMO antenna using T-shaped reflecting stub for high isolation,” 2015 IEEE MTT-S International Microwave and RF Conference (IMaRC), 2015.

[420] M. S. Khan, I. Shoaib, E. Autizi, A.-D. Capobianco, A. I. Najam, and M. F. Shafique, “Compact ultra-wideband diversity antenna with a floating parasitic digitated decoupling structure,” IET Microwaves, Antennas & Propagation, vol. 8, no. 10, pp. 747–753, 2014.

[421] Rakluea, Paitoon, Peuv Poch "Development of circular ring antennas for mobile broadband systems", Information Technology and Electrical Engineering (ICITEE), 2015 7th International Conference on IEEE, 2015.

[422] Quddus, A., Saleem, R., Shabbir, T., ur Rehman, S. and Shafique, M.F., ‘’Dual port UWB-MIMO antenna with ring decoupling structure’’, In Progress in Electromagnetic Research Symposium (PIERS) (pp. 116-119), 2016.

[423] Alfakhri, A., Ashraf, M.A., Alasaad, A. and Alshebeili, S., ‘’A compact size ultra-wideband MIMO antenna with simple decoupling structure’’, In Antenna Technology and Applied Electromagnetics (ANTEM), 2016 17th International Symposium on (pp. 1-2), 2016.

[424] Chuang, Ching-Song, Wu-Tung Hsu, and Lin Ming Chun, "A compact multi band MIMO antenna", Electrical and Electronics Engineering (ELECO), 2013 8th International Conference on IEEE, 2013.

[425] C. K. Ghosh, B. Mandal, and S. K. Parui, “Mutual Coupling Reduction Of A Dual-Frequency Microstrip Antenna Array By Using U-Shaped Dgs And Inverted U-Shaped Microstrip Resonator,” Progress In Electromagnetics Research C, vol. 48, pp. 61–68, 2014.

[426] Zhai, Huiqing, et al. "A high isolation dual-band MIMO antenna array for multiaccess mobile terminals", Microwave and Optical Technology Letters 57.3 (2015): 672-677.

[427] Yu, Y., Yi, L., Liu, X., Gu, Z. and Li, J., ‘’Mutual coupling reduction of dual-frequency patch antennas using a simple microstrip H-Section’’, In Antennas and Propagation & USNC/URSI National Radio Science Meeting, 2015 IEEE International Symposium on (pp. 388-389), 2015.

[428] Khade, S.S. and Badjate, S.L., ‘’Printed multiband monopole antenna for MIMO wireless applications’’, In Microwave, Optical and Communication Engineering (ICMOCE), 2015 International Conference on (pp. 272-275), 2015.

[429] Reddy, P.N.K. and Anuradha, S., A Compact Four Element UWB MIMO Antenna., International Conference on Trends in Electronics and Informatics ICEI, 2017.

[430] Najam, Ali Imran, Yvan Duroc, and Smail Tedjini. "Design & characterization of an antenna system for UWB-MIMO communications systems." Antennas and Propagation (EuCAP), 2010 Proceedings of the Fourth European Conference on. IEEE, 2010.

[431] Zhang, L., Liu, W. and Jiang, T., ‘’A compact UWB MIMO antenna with high isolation’’, In Antennas and Propagation (APSURSI), 2016 IEEE International Symposium on (pp. 913-914), 2016.

[432] Avendal, Johan, Zhinong Ying, and Buon Kiong Lau. "Multiband diversity antenna performance study for mobile phones" Antenna Technology: Small and Smart Antennas Metamaterials and Applications, 2007. IWAT'07 International Workshop on. IEEE, 2007.

[433] Hsu, Chih-Chun, et al. "Design of MIMO antennas with strong isolation for portable applications" Antennas and Propagation Society International Symposium, 2009. APSURSI'09. IEEE. IEEE, 2009.

[434] Aouadi, Belgacem, and Jamel Belhadj Tahar. "Four-element MIMO antenna with refined isolation thanks to spiral resonators" Multimedia Computing and Systems (ICMCS), 2014 International Conference on IEEE, 2014.

[435] K. Sarabandi and Y. J. Song, "Subwavelength Radio Repeater System Utilizing Miniaturized Antennas and Metamaterial Channel Isolator," IEEE Transactions on Antennas and Propagation, vol. 59, no. 7, pp. 2683–2690, 2011.

[436] M. M. B. Suwailam, M. S. Boybay, and O. M. Ramahi, "Mutual coupling reduction in MIMO antennas using artificial magnetic materials," 2009 13th International Symposium on Antenna Technology and Applied Electromagnetics and the Canadian Radio Science Meeting, 2009.

[437] Lihao, Huang, et al. "Reduction of mutual coupling between closely-packed antenna elements with split ring resonator (SRR)." Microwave and Millimeter Wave Technology (ICMMT), 2010 International Conference on. IEEE, 2010.

[438] Pan, Bai Cao, et al. "Reduction of the spatially mutual coupling between dual-polarized patch antennas using coupled metamaterial slabs." Scientific reports 6 (2016): 30288.

[439] M. M. B. Suwailam, M. S. Boybay, and O. M. Ramahi, "Single-negative (SNG) metamaterials for mutual coupling reduction in high-profile antennas," 2009 IEEE Antennas and Propagation Society International Symposium, 2009.

[440] D. A. Ketzaki and T. V. Yioultsis, "Metamaterial-Based Design of Planar Compact MIMO Monopoles," IEEE Transactions on Antennas and Propagation, Vol.61, No.5, pp. 2758-2766, May, 2013.

[441] Bhende, Saish, Sanket Shah, Sufyan Mukri, and Meet Vaidya. "Isolation Improvement between Closely Spaced Microstrip Loop Antennas using Metamaterial Structure." International Journal of Computer Applications 123, no. 15 (2015).

[442] M. M. Bait-Suwailam, O. F. Siddiqui, and O. M. Ramahi, "Mutual Coupling Reduction Between Microstrip Patch Antennas Using Slotted-Complementary Split-Ring Resonators", IEEE Antennas and Wireless Propagation Letters, vol. 9, pp. 876–878, 2010.

[443] Lee, Y., Chung, H., Ha, J. and Choi, J., ''Design of a MIMO antenna with improved isolation using meta-material'', In Antenna Technology (iWAT), 2011 International Workshop on (pp. 231-234), 2011.

[444] Torabi, Y., Bahri, A. and Sharifi, A.R., ''A novel metamaterial MIMO antenna with improved isolation and compact size based on LSRR resonator'', IETE Journal of Research, Vol.62, No.1, pp.106-112, 2016.

[445] Zhu, Jianfeng, et al. "Ultrawideband MIMO/diversity antenna using CSRR structure for isolation enhancement" Antennas and Propagation (APCAP), 2015 IEEE 4th Asia-Pacific Conference on. IEEE, 2015.

[446] Zhu, X., Yang, X., Song, Q. and Lui, B., ''Compact UWB-MIMO antenna with metamaterial FSS decoupling structure'', EURASIP Journal on Wireless Communications and Networking, 2017(1), p.115, 2017.

[447] M. S. Sharawi, A. B. Numan and D. N. Aloi, “Isolation Improvement in a Dual-Element MIMO Antenna System Using Capacitively Loaded Loops,” Progress In Electromagnetics Research, Vol. 134, pp. 247-266, 2013.

[448] H. R. Khaleel, H. M. Al-Rizzo, D. G. Rucker, Y. A. Rahmatallah, and S. Mohan, “Mutual coupling reduction of dual-band printed monopoles using MNG metamaterial,” 2011 IEEE International Symposium on Antennas and Propagation (APSURSI), 2011.

[449] A. A. Gheethan, P. A. Herzig, G. Mumcu, “Compact 2x2 Coupled Double Loop GPS Antenna Array Loaded With Broadside Coupled Split Ring Resonators,” IEEE Transactions on Antennas and Propagation, vol. 61, no. 6, pp. 3000-3008, 2013

[450] B. Aouadi and J. Belhadj Tahar, “Requirements Analysis of Dual Band MIMO Antenna,” Wireless Personal Communications, vol. 82, no. 1, pp. 35–45, 2014.

[451] M. S. Sharawi, “Printed multi-band MIMO antenna systems: Techniques and Isolation mechanisms,” The 8th European Conference on Antennas and Propagation (EuCAP 2014), 2014.

[452] Kumar, A., Ansari, A.Q., Kanaujia, B.K. and Kishor, J., ‘’High Isolation Compact Four-Port MIMO Antenna Loaded with CSRR for Multiband Applications’’, 2018.

[453] Marzudi, W.N.N.W., Abidin, Z.Z., Muji, S.Z., Yue, M. and Abd-Alhameed, R.A., ‘’Minimization of mutual coupling using neutralization line technique for 2.4 GHz wireless applications’’, International Journal of Digital Information and Wireless Communications (IJDIWC), 4(3), pp.292-298, 2014.

[454] Wong, K.L., Su, S.W. and Kuo, Y.L., ‘’A printed ultra-wideband diversity monopole antenna’’, Microwave and optical technology letters, 38(4), pp.257-259, 2003.

[455] Ren, J., Hu, W., Yin, Y. and Fan, R., ‘’Compact printed MIMO antenna for UWB applications’’, IEEE Antennas and Wireless Propagation Letters, 13, pp.1517-1520, 2014.

[456] Su, S.W. and Chang, F.S., "High-gain dual-WLAN-band dual-loop antennas for MIMO access-points", In Antennas and Propagation (EuCAP), 2010 Proceedings of the Fourth European Conference on (pp. 1-5), 2010.

[457] Byun, J., Jo, J.H. and Lee, B.,’’ Compact dual band diversity antenna for mobile handset applications’’, Microwave and Optical Technology Letters, 50(10), pp.2600-2604, 2008.

[458] Li, J.F., Chu, Q.X. and Li, Z.H., ‘’Compact conventional phone antenna integrated with wideband multiple input multiple output antenna’’, Microwave and Optical Technology Letters, 54(8), pp.1958-1962, 2012.

[459] Imani, A., Nourinia, J. and Ghobadi, C., ‘’A Novel Dual-Band Printed Diversity Antenna for 2.4/5.2 GHz WLAN Applications’’, 2011.

[460] Chi, G., Li, B. and Qi, D., ‘’Dual band printed diversity antenna for 2.4/5.2GHz WLAN application’’, Microwave and optical technology letters, 45(6), pp.561-563, 2005.

[461] Sahu, N.K., Das, G., Sharma, A. and Gangwar, R.K., 2017, December. Design of a dual-polarized triple-band hybrid MIMO antenna for WLAN/WiMAX applications.

[462] T. Michalski, V. Wienstroer, and R. Kronberger, ‘’Beam forming capabilities of smart antennas on mobile terminals," 3rd European Conference on Antennas and Propagation, pp. 1608-1611, 2009.

[463] Mak, A.C., Rowell, C.R. and Murch, R.D., ‘’Isolation enhancement between two closely packed antennas’’, IEEE Transactions on Antennas and Propagation, 56(11), pp.3411-3419, 2008.

[464] Lee, C.H., Chen, S.Y. and Hsu, P., ‘’Integrated dual planar inverted-F antenna with enhanced isolation’’, IEEE Antennas and Wireless Propagation Letters, 8, pp.963-965, 2009.

[465] Ghosh, J., Ghosal, S., Mitra, D. and Bhadra Chaudhuri, S.R, ‘’Mutual coupling reduction between closely placed microstrip patch antenna using meander line resonator’’, Progress In Electromagnetics Research, 59, pp.115-122., 2016.

[466] L. Minz and R. Garg, “Reduction of mutual coupling between closely spaced PIFAs”, Electronics Letters, vol. 46, no. 6, p. 392, 2010.

[467] Kang, D.G., Tak, J. and Choi, J., ‘’MIMO antenna with high isolation for WBAN applications’’, International Journal of Antennas and Propagation, 2015.

[468] Park, C.H., Yang, E.S. and Son, H.W., ‘’Reduction of mutual coupling between closely spaced microstrip antennas with H-shaped isolation wall’’, In Progress in Electromagnetic Research Symposium (PIERS) (pp. 5055-5055), 2016.

[469] Zhang, S., Lau, B.K., Sunesson, A. and He, S., Closely located dual PIFAs with T-slot induced high isolation for MIMO terminals. In Antennas and Propagation (APSURSI), 2011 IEEE International Symposium on (pp. 2205-2207), 2011.

[470] J. Pei, A. Wang, and X. Cai, "A novel dual-band printed antenna with a defected ground plane for WLAN applications," 9th International Symposium on Antennas Propagation and EM Theory (ISAPE), pp. 185-188, 2010.

[471] S. Zhang, B. K. Lau, Y. Tan, Z. Ying, and S. He, ‘’Mutual coupling reduction of two pifas with a t-shape slot impedance transformer for mimo mobile terminals’’, IEEE Transactions on Antennas and Propagation, vol. 60, pp. 1521-1531, 2012.

[472] Yao, Y., Wang, X., Chen, X., Yu, J. and Liu, S., ‘’Novel diversity/MIMO PIFA antenna with broadband circular polarization for multimode satellite navigation’’, IEEE Antennas and Wireless Propagation Letters, 11, pp.65-68, 2012.

[473] S. Zhang, S. Khan, and S. He, ‘’Reducing mutual coupling for an extremely closely-packed tunable dual-element pifa array through a resonant slot antenna formed in-between’’, IEEE Transactions on Antennas and Propagation, vol. 58, pp. 2771 -2776, 2010

[474] J. Ouyang, F. Yang, and Z. M. Wang, “Reducing Mutual Coupling of Closely Spaced Microstrip MIMO Antennas for WLAN Application,” IEEE Antennas and Wireless Propagation Letters, vol. 10, pp. 310–313, 2011.

[475] J. Park, J. Choi, J.-Y. Park, and Y.-S. Kim, “Study of a T-Shaped Slot With a Capacitor for High Isolation Between MIMO Antennas,” IEEE Antennas and Wireless Propagation Letters, vol. 11, pp. 1541–1544, 2012.

[476] M. A. Abdalla and A. A. Ibrahim, “Compact and Closely Spaced Metamaterial MIMO Antenna With High Isolation for Wireless Applications,” IEEE Antennas and Wireless Propagation Letters, vol. 12, pp. 1452–1455, 2013.

[477] Habashi, A., Nourinia, J. and Ghobadi, C., ‘’Mutual coupling reduction between very closely spaced patch antennas using low-profile folded split-ring resonators (FSRRs)’’, IEEE Antennas and Wireless Propagation Letters, 10, pp.862-865, 2011.

[478] X. M. Yang, X. G. Liu, X. Y. Zhou, and T. J. Cui, “Reduction of Mutual Coupling Between Closely Packed Patch Antennas Using Waveguided Metamaterials,” IEEE Antennas and Wireless Propagation Letters, vol. 11, pp. 389–391, 2012.

[479] Xue, C.D., Zhang, X.Y., Cao, Y.F., Hou, Z. and Ding, C.F., ‘’MIMO Antenna Using Hybrid Electric and Magnetic Coupling for Isolation Enhancement’’, IEEE Transactions on Antennas and Propagation, Vol.65, No.10, pp.5162-5170, 2017.

[480] Ma, X.Z., Zhao, M.Y., Zhang, D.F. and Liu, P.J.,''Mutual Coupling Reduction between Very Closely Spaced Microstrip Antennas Using CPW Structure'', In MATEC Web of Conferences, Vol. 75, p. 06001, EDP Sciences, 2016.

[481] Jafri, S.I., Saleem, R., Shafique, M.F. and Brown, A.K., ''Compact reconfigurable multiple-input-multiple-output antenna for ultra-wideband applications'', IET Microwaves, Antennas & Propagation, Vol.10, No.4, pp.413-419, 2016.

[482] W. L. Chen and G. M. Wang, "Small Size Edge–fed Sierpinski carpet microstrip patch antenna," Progress in Electromagnetics Research, vol. 3, pp. 195–202, 2008.

[483] L. Habib. "Fractal monopole antenna," U.S. Patent, No. 7, 248, 223, B2, 2007.

[484] S. D. Assimonis, T. V. Yioultsis, and C. S. Antonopoulos, "Design and Optimisation of Uniplanar EBG Structures for Low Profile Antenna Applications and Mutual Coupling Reduction," IEEE Transactions on Antennas and Propagation, Vol. 60, No. 10, pp. 4944–4949, 2012.

[485] K. Q. Costa and V. Dmitriev, "Theoretical analysis of a modified Koch monopole with reduced dimensions," IEE Proc. Microwave. Antennas Propagation. vol. 153, No. 5, 2006.

[486] B. Manimegalai and S. Raju, "A multifractal cantor antenna for multiband wireless applications," IEEE Antennas Wireless Propagation. Lett. vol. 8, 2009.

[487] Tunable metamaterial – Wikipedia Available online:
https://en.wikipedia.org/wiki/Tunable_metamaterial

[488] Long Li; Bin Li; Hai-Xia Liu; Chang-Hong Liang; "Locally resonant cavity cell model for electromagnetic band gap structures", IEEE Transactions on Antennas and Propagation, Vol. 54, No. 1, PP. 90 – 100, 2006.

[489] J.-Y. Pang, S.-Q. Xiao, Z.-F. Ding, and B.-Z. Wang, "Two-Element PIFA Antenna System With Inherent Performance of Low Mutual Coupling," Antennas Wirel. Propag. Lett. IEEE Antennas and Wireless Propagation Letters, vol. 8, pp. 1223–1226, 2009.

[490] J. Byun, J.-H. Jo, and B. Lee, "Compact dual-band diversity antenna for mobile handset applications," Microwave and Optical Technology Letters, vol. 50, no. 10, pp. 2600–2604, 2008.

[491] J. Guterman, A. Moreira, and C. Peixeiro, "Two-element multi-band fractal PIFA for MIMO applications in small size terminals," IEEE Antennas and Propagation Society Symposium, 2004.

[492] C. Kittel, ''Introduction to Solid State Physics.'' New Jersey: John Wiley & Sons, 2005.

[493] F. Yang and Y. Rahmat-Samii, "Electromagnetic Band Gap Structures in Antenna Engineering," 2008.

[494] Ansoft Corporation, Ed., ''Left-Handed Metamaterial Design Guide.'' Pittsburgh, PA 15219, USA: Ansoft LLC, 2007.

[495] P. Kovacs, T. Urbanec "Electromagnetic Bandgap Structures: Practical Tips and Advice for Antenna Engineers," Radio engineering, Vol. 21, No. 1, pp. 414-421, 2012.

[496] Rajagopalan A., Gupta G., Konanur A.S., Hughes B., Lazzi G.''Increasing channel capacity of an ultra-wideband MIMO system using vector antennas'', IEEE Trans. Antennas and Propagation, vol. 55, no.10, 2880-2887, 2007.